D - Science and Technology

Page

Science and Technology

Page

Science and Technology

GeoStream: Design and Implementation of a Flood Information Management System for Urban Flood Risk Management

Angel Bien N. Casañares*, Gracien T. Esmeralda, Carlo A. Sayson, Cennedy Jay O. Timola, Brian Steven G. Pajarillo
College of Information and Communications Technology, STI West Negros University, Bacolod City, Philippines
*Email: angel.casanares@wnu.sti.edu.ph

Abstract

Floods remain one of the most destructive natural disasters in the Philippines, disproportionately affecting communities with limited access to localized, real-time disaster information. This study presents GeoStream, a flood information management system consisting of a mobile application for residents and a web-based dashboard for administrators, developed for Victorias City, Negros Occidental, Philippines. The system integrates an interactive GIS-based flood map, real-time flood status reporting, evacuation center tracking, heatmap indicators, and emergency hotline access, built using React Native, Firebase Realtime Database, PHP Laravel, and MySQL. Development followed the Agile Scrum methodology to ensure iterative refinement based on stakeholder feedback. The system was evaluated by 41 participants 10 Disaster Risk Reduction and Management Office (DRRMO) officers, 2 IT experts, and 30 residents using the PIECES evaluation framework across six dimensions: Performance, Information, Control, Efficiency, and Service. Results yielded an overall weighted mean of 4.70 (Strongly Agree), indicating high system effectiveness and user satisfaction across all dimensions. These findings demonstrate that GeoStream successfully bridges the information gap in localized flood management, enabling faster data-driven decision-making for both local authorities and community members. The system provides a scalable model for integrating geospatial technology into urban disaster preparedness in flood-prone Philippine cities.

Keywords: Flood; Mapping; Routing; Evacuation; Emergency Hotlines

1. Introduction

The most frequently occurring natural disasters are floods, earthquakes, cyclones, and famine. These events cause thousands of deaths, injuries, and incur billions of dollars in economic losses annually, as stated by (Goosman 2022). Some communities may struggle to recover infrastructure, others their health or jobs sectors. Every local crisis requires specific responses to guide recovery according to (Rienne 2021). Currently, residents in the Philippines often rely on PAGASA satellites for general weather forecasts, but they lack a way to view real-time conditions in specific flood-prone areas. Our system aims to bridge this gap by leveraging rapid technological advances to pinpoint flood zones on a map, enabling both the government and residents to prepare effectively before a disaster strikes.

The article published by Nanette Guadalquiver et al. (2021) stated that flash floods brought by torrential rains hit at least four localities in northern Negros Occidental, particularly those in the third district, early morning on New Year's Day. In Victorias City, waters rose in 12 villages, including five considered "critically" affected: Barangays 1, 7, 9, 13, and 19A. Councilor Francis Frederick Palanca said some 1,508 persons were affected in the 12 villages. By noon, more than 400 families had been evacuated to the barangay halls, transport terminal, cultural center, and coliseum. (Guadalquiver et al. 2021). In one of the cities in the Philippines where we conducted our study, floodwaters reached waist-deep levels in several "critically" affected villages, forcing the evacuation of over 400 families (Palanca 2021). This sudden rise caught many off guard, highlighting the danger of relying on general forecasts without localized, real-time information.

To address this, we developed a comprehensive mobile application tailored for the city where we conducted our research. The application features a "Guest mode" that allows users to easily view emergency hotlines and the locations of evacuation centers. By fostering individual awareness and enabling local authorities to make faster decisions during a crisis, this project highlights how mobile technology can empower communities and build a safer urban environment.

2. Related Work

2.1 Flood Disasters in Urban and Philippine Context

Flooding continues to rank among the most frequently occurring and economically devastating natural disasters worldwide. In the Philippine context, urban flooding presents a particularly acute challenge due to the country's geographic exposure to typhoons and the rapid, unplanned expansion of low-lying urban communities. Fauzi (2021) documented the complexity of coastal flood responses in Manila Bay, noting that centralized government systems frequently fail to reach community-level stakeholders in time to enable effective evacuation. Similarly, Tabios (2023) examined the Pasig-Marikina River Basin in Metro Manila, arguing that effective flood risk management requires not only infrastructure investment but also real-time data integration across local government units. These studies collectively highlight a systemic gap: existing disaster response frameworks in the Philippines rely heavily on top-down information dissemination, leaving residents with limited access to localized, actionable flood data.

At the local level, this gap was evident in Victorias City, Negros Occidental, where flash floods on New Year's Day 2021 affected 12 barangays, critically impacting five, and forced the evacuation of over 400 families (Guadalquiver et al., 2021). The absence of a localized flood monitoring system contributed to delayed community response, underscoring the need for city-specific, technology-driven solutions.

2.2 GIS and Geospatial Approaches to Flood Management

Geospatial technologies have increasingly been applied to flood risk management, offering the ability to visualize, analyze, and communicate flood data in an accessible format. Bolanio et al. (2023) demonstrated the utility of GIS in mapping and assessing flood evacuation sites in Las Nieves, Agusan del Norte, Philippines, establishing that spatial data integration significantly improves evacuation planning accuracy. Their work affirmed that GIS-based platforms can bridge the gap between raw flood data and actionable community guidance. Building on this, González-Villa et al. (2022) proposed a structured evacuation management system for large-scale disasters, emphasizing that geospatial routing and real-time status updates are critical components of any modern disaster response platform. These findings directly inform GeoStream's design, which integrates interactive flood mapping, heatmap indicators, and evacuation center tracking as core features.

2.3 Mobile and Web-Based Disaster Management Systems

The proliferation of smartphones has prompted researchers to develop mobile-based platforms as frontline tools for disaster communication and response. Montefalcon et al. (2021) developed IRespondPH, a mobile and web-based application for post-disaster needs assessment in the Philippines, demonstrating that dual-platform systems significantly improve data collection and coordination between residents and government agencies. Similarly, Rey et al. (2022) introduced Mamamayan, an Android-based community emergency reporting and notification system, which enabled real-time incident reporting at the barangay level. Baltazar et al. (2022) extended this approach with a disaster and crime reporting system for Hagonoy, Bulacan, incorporating a decision support mechanism to assist local government units in prioritizing responses. Traya et al. (2022) further contributed a mobile tsunami alert system with integrated evacuation routing, illustrating the viability of combining geographic data with emergency notifications in a single mobile interface. Across these studies, a recurring design principle emerges: effective disaster management platforms must integrate real-time data, role-based access, and community participation — all of which are central to GeoStream's architecture.

2.4 Crowdsourced and Community-Driven Flood Monitoring

A growing body of research highlights the value of community-generated data in supplementing official flood monitoring efforts. Helmrich et al. (2021) explored opportunities for crowdsourcing in urban flood monitoring, finding that citizen-reported data can substantially increase the spatial and temporal resolution of flood information, particularly in areas where sensor infrastructure is limited. However, Fan et al. (2020) cautioned that crowdsourced data from social media tends to concentrate around populous areas, introducing spatial biases that can skew disaster response priorities. Abbasi et al. (2022) addressed this reliability concern by proposing a trustable

mobile crowdsourcing framework for flooded smart areas, incorporating verification mechanisms to filter inaccurate reports. Sharma (2021) reinforced the community angle from a governance perspective, arguing that local knowledge and actor involvement are essential components of sustainable flood risk management in developing countries. These findings informed GeoStream's community reporting feature, which allows residents to submit flood status updates while administrators retain validation authority to ensure data integrity.

2.5 Technology as an Enabler of Disaster Resilience

Beyond individual system designs, broader research supports the role of technology in transforming disaster preparedness at scale. Abid et al. (2024) examined community-based flood mitigation in Malaysia, finding that digital platforms substantially enhance public participation in disaster policy implementation when designed with accessibility in mind. Radu (2020) similarly argued that technology, when properly deployed, can fundamentally improve disaster detection, communication, and recovery. These perspectives affirm GeoStream's positioning as both a technical tool and a governance instrument — one that empowers both residents and local authorities to collaborate more effectively during flood events.

2.6 Research Gap

Despite the breadth of existing work, a notable gap persists in the literature: few systems have been designed and deployed for mid-sized Philippine cities with context-specific flood data, community-level participation mechanisms, and integrated evaluation frameworks. Existing Philippine-focused systems such as IRespondPH and Mamamayan address broader disaster reporting but do not offer city-specific GIS flood mapping, heatmap visualization, or real-time evacuation center availability tracking. GeoStream directly addresses this gap by offering a comprehensive, locally tailored flood information management system evaluated through a structured PIECES framework in Victorias City, providing a replicable model for similar flood-prone urban communities in the Philippines.

3. Objectives

The primary objective of this study is to increase flood awareness and enhance disaster response through geospatial technology and real-time data dissemination. In one of the cities in the Philippines where we conducted our study, the system uses an interactive GIS interface to provide residents and local authorities with accurate information on flood-prone areas. By using a common data-sharing framework, the system ensures access to essential data, including historical flood patterns, intensity measures, and evacuation channels, in a clear, interactive format. Through cloud storage and a mobile-friendly design, this implementation maximizes accessibility and efficiency, making the city where we conducted our research more resilient against flooding.

Specifically, the study aimed to:

- To provide the residents with an interactive, user-friendly mapping tool that allows residents to identify the flood-prone areas within the city;
- To implement a guest mode that provides limited access, allowing users to view general flood information and emergency hotlines.
- To integrate community-driven information by enabling them to report flood status within the area;
- To provide residents a real-time status of the evacuation center within the city;
- To integrate the heatmap indicator technology as a status of the affected area
- And to develop a verification method of user registration, ensuring data integrity that accounts are being created;

4. Materials and Methods

4.1 System Development and Architecture

The system was developed using the latest technologies to ensure efficiency, accessibility, and reliability. A dual-platform solution, consisting of a web application for the administrators and a

mobile application for the residents. The goal is to improve urban flood monitoring and data analysis while enabling residents to view flood zones, access emergency hotlines, and track the availability of evacuation centers.

Development was performed using the following tools and technologies:

- Operating System – Windows 10 and 11 were used as the main development environments.
- Collaboration Tools – File sharing has been facilitated using Google Drive, Microsoft Teams, and Messenger.
- Documentation – The documentation was managed using Microsoft Word and Google Docs.
- Development Platforms – The system was built and tested using Visual Studio Code, Sublime, and XAMPP for Local Server Implementation and Back-End Testing.
- Front-end – React, HTML, CSS, and Bootstrap.
- Back-end – PHP Laravel and Firebase.
- Mobile Development – React Native.
- Database – MySQL and Firebase Realtime Database.

This architecture ensured the system could effectively handle user registrations, real-time flood data synchronization, and web application analytics visualization.

4.2 System Methodology

The proponents chose the agile scrum model as the software development methodology. It is based on the idea of incremental development in which requirements and solutions evolve naturally through teamwork among self-organizing cross-functional teams. An important benefit of agile development is its ability to deliver value quickly, as well as to improve overall quality and reliability. In addition, agile methodologies provide teams with the agility and flexibility to respond effectively to changing requirements and shifting project situations. By emphasizing close teamwork and ongoing improvement, agile development practices create a dynamic, responsive work environment that enables teams to simplify processes, maximize productivity, and deliver effective solutions quickly.

The Agile Model is an iterative and incremental approach to software development that emphasizes flexibility, collaboration, and client satisfaction. It focuses on delivering small, functional software quickly, enabling frequent adjustments based on feedback and changing requirements.

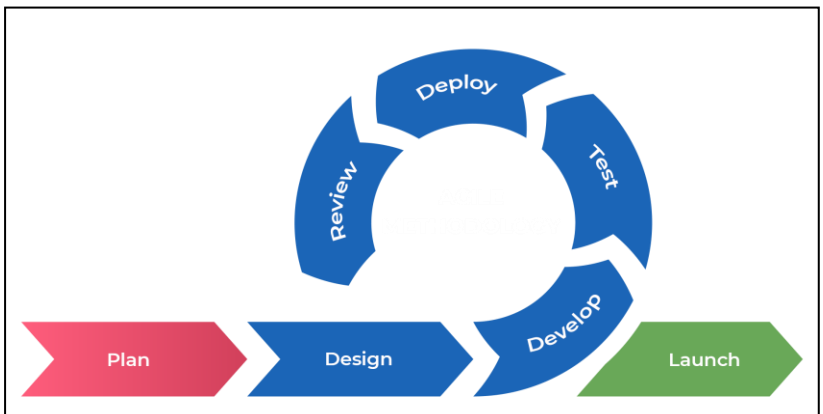

Figure 1 Agile Software Development (System Development Life Cycle)

4.3 Location and Participants

The study was conducted in the City of Victorias, which served as the pilot location for the deployment and testing of the system. A total of 41 participants were involved in the evaluation phase. This included:

- 10 Officers from the Disaster Risk Reduction Management Office
- 1 IT expert each in Fire Station and Barangays

- 30 Local Residents

The officers, local residents, and IT expert were involved through purposive sampling to evaluate the application and technical functions of the system.

4.4 System Testing with each beneficiary

The system was conducted through an on-site visit to each barangay, specifically Barangay 6 and Barangay 2, also with the Police Station, Fire Station and lastly at the office of the City Disaster Risk Reduction and Management Office (CDRRMO). This aims to evaluate the usability, functionality, and the overall user experience of both systems in a real-use scenario:

- Web Application:
- Mobile Application:

The requirements gathering for the GeoStream focused on core functionalities essential for risk mitigation and community safety. Key components including interactive flood maps, user accounts, post-flood evaluations, and emergency hotlines were prioritized to simplify communication with the CITY DISASTER RISK REDUCTION AND MANAGEMENT OFFICE (CDRRMO). By utilizing historical data and specific flood-zone coordinates provided by local authorities, the system ensures high accuracy in its response operations and in the relevance of its data.

To ensure long-term effectiveness, the project used the PIECES Evaluation Framework to assess the platform across Performance, Information, Economics, Control, Efficiency, and Service. This structured approach allowed the team to measure response times, data security, and overall service reliability. By aligning technical requirements with this rigorous evaluation model, the system ensures a high-quality user experience and a sustainable tool for long-term disaster management.

5. Results

The development and implementation of the GeoStream successfully met its objectives of improving disaster preparedness and data accessibility. By integrating real-time flood data synchronization and an intuitive interface, the system supports core functions, including identifying flood-prone areas, planning evacuations, and reporting. These features have significantly reduced response delays, enabling the CDRRMO and residents to make data-driven decisions that enhance community resilience and safety.

A comprehensive evaluation using the PIECES Framework confirmed the system's reliability and efficiency. The platform demonstrated high performance, handling substantial data loads with minimal latency, and provided robust data management through seamless synchronization across all modules. Beyond operational improvements, the system achieved significant cost efficiencies by automating manual data entry and monitoring processes. Security was also a primary focus, with strict encryption protocols and role-based access controls to protect sensitive disaster management information.

User feedback consistently highlighted the system's user-friendly design and swift response times, particularly in high-pressure emergency scenarios. While the platform has successfully fulfilled both functional and non-functional requirements across all PIECES dimensions, including Performance, Control, and Efficiency, it remains a dynamic tool. Ongoing optimizations based on user input will continue to refine its service quality, ensuring the system remains a transformative and dependable resource for urban flood risk management.

Table 1 Likert's Scale Mean for GeoStream System Evaluation

Rating	Weighted Mean	Verbal Description
5	4.21-5.00	Strongly Agree
4	3.41-4.20	Agree
3	2.61-3.40	Neutral
2	1.81-2.60	Disagree
1	1.00-1.80	Strongly Disagree

The formula for LSM is:

$$x = \frac{5 *fi+4 *+3 *fi+2 *fi+1 *fi}{N}$$

Where: x=weighted mean
fi=frequency if the 1 score
N = total number of respondents
The effectiveness, efficiency, and usability of GeoStream for VCDRRMO as assessed and evaluated by end-users and IT (Information Technology) Experts.

5.1 User Evaluation Based on the PIECES Framework

The evaluation of the system, conducted using the PIECES Framework, garnered exceptional feedback from both end users and IT experts. With an overall weighted mean of 4.70, the results fall within the Strongly Agree range, reflecting the system's high effectiveness across key dimensions such as performance, information accuracy, security, and service delivery. These findings confirm that the platform successfully fulfills user expectations by providing a secure, dependable, and highly responsive digital environment tailored for organizational operations.

Table 2 End-Users and IT Experts on PIECES Software Evaluation in terms of Performance Throughout and Response Time

Indicator	**Weighted Mean**	**Interpretation**
Performance (throughput & response time)	4.68	Strongly Agree
Information (Input, Output, Data Storage)	4.68	Strongly Agree
Control & Security	4.71	Strongly Agree
Efficiency	4.73	Strongly Agree
Service	4.74	Strongly Agree
Total	**4.70**	**Strongly Agree**

LSM Formula:

$$x = \frac{5 *fi+4 *+3 *fi+2 *fi+1 *fi}{N}$$

$$= \frac{4.68 + 4.68 + 4.71 + 4.73 + 4.74}{5}$$

$$= \frac{23.54}{5}$$

Total = **4.70**

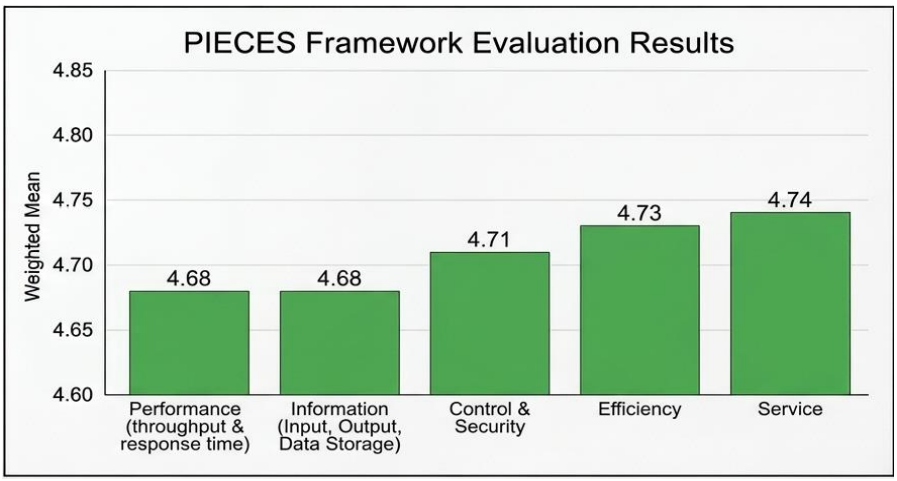

Figure 2 Bar graph representation of PIECES Framework Evaluation results

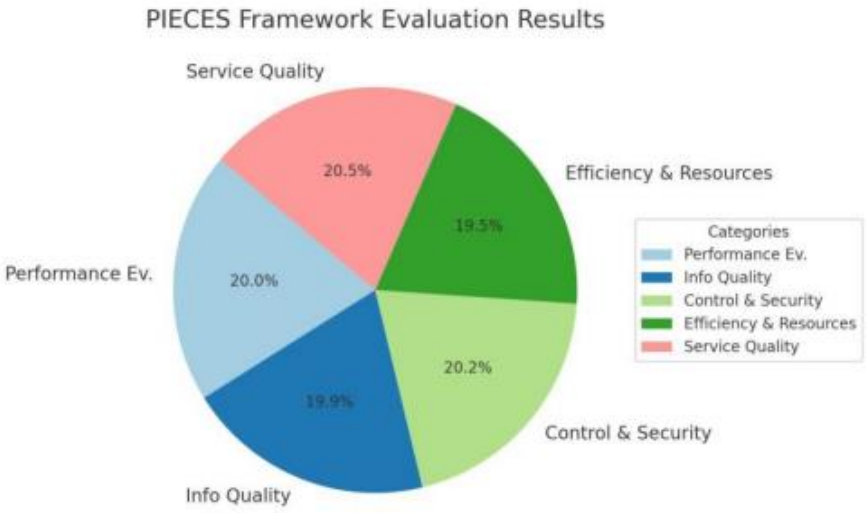

Figure 3 Pie chart representation of PIECES Framework Evaluation results

6. Discussion

The discussion of the research findings highlights how the GeoStream successfully fulfilled its primary objectives by modernizing disaster preparedness and response in Victorias City. By integrating real-time flood data synchronization and interactive mapping, the platform bridged the information gap that often hampers emergency services during a crisis. The findings suggest that transitioning from manual, paper-based workflows to an automated digital environment not only improved the accuracy of flood-prone area identification but also significantly reduced the time required for evacuation planning and real-time reporting, thereby directly contributing to the safety and resilience of the local community.

Central to this success was the rigorous evaluation using the PIECES Framework, which served as a blueprint for optimizing the system's performance and reliability. The discussion reveals that the platform's architecture can handle substantial data loads with minimal latency, a critical factor during peak user activity in emergency scenarios. This technical stability, combined with the seamless flow of information across all modules, established a robust foundation for the City Disaster Risk Reduction and Management Office (CDRRMO) to execute swift, data-driven decisions while ensuring that residents had access to the same high-quality information.

Operational and economic factors further distinguish the platform's impact, as the automation of monitoring and reporting processes led to significant cost efficiencies. By reducing manual workload, the CDRRMO boosted overall productivity and enabled human resources to focus on more complex response tasks. Furthermore, the implementation of stringent security protocols—including role-based access, audit trails, and encryption—ensured that sensitive disaster management data remained protected, meeting the high standards required for government-level information systems.

Ultimately, the overwhelmingly positive user feedback underscores the value of the system's intuitive design and navigation. The discussion concludes that GeoStream has surpassed traditional disaster management methods by offering unparalleled reliability and speed, making it an essential resource for the city. While the system currently meets all functional and non-functional requirements, the findings advocate for a strategy of continuous optimization. By staying responsive to evolving user needs and environmental shifts, GeoStream can remain a cornerstone of Victorias City's long-term strategy for disaster flexibility and urban resilience.

7. Conclusion

The development and implementation of GeoStream is a significant milestone in disaster preparedness and response for Victorias City, positioning it as a vital enabler for both the CDRRMO and residents. By integrating core functions such as flood-prone area identification, real-time data synchronization, and evacuation planning, the system successfully bridges critical information

management gaps. Its user-friendly platform not only enhances operational efficiency but also fosters greater community engagement through interactive mapping and emergency communication tools, creating a more cohesive approach to disaster risk management.

Evaluated through the PIECES framework, GeoStream has proven its excellence in providing timely, accurate information while reducing administrative burdens and optimizing resource allocation. The system facilitates data-driven decision-making, allowing local authorities to coordinate more effectively with the public during high-pressure emergency scenarios. Its success highlights the transformative potential of technology-based solutions in flood-prone regions, demonstrating how modern data analytics can be paired with citizen participation to significantly improve urban resilience.

Looking forward, GeoStream's sustainability is supported by its capacity for continuous evolution driven by user feedback and the implementation of comprehensive training programs. As climate change and rapid urbanization increase the complexity of disaster risks, the system serves as a prime example of how modernizing infrastructure can lead to swifter, more effective mitigation strategies. Ultimately, GeoStream has established a safer and more resilient urban environment in Victorias City, providing a scalable model for integrating modern technology into long-term disaster flexibility efforts.

Acknowledgements

We extend our sincere gratitude to Dr. Mae B. Lodana for seeing the potential in this study. We are deeply thankful to Ms. Orville Balangue, Mr. Bobby Rodriguez, and Mr. Feliciano Santiago, our Capstone Study Review Panel, for their invaluable guidance, patience, expertise, and encouragement throughout this research. Their support has been instrumental in the successful completion of this project.

We also wish to express our appreciation to Mr. Brian Steven G. Pajarillo, our Capstone Project Consultant, for his expertise, constructive feedback, and unwavering support; his insights greatly shaped the direction and quality of our work. Our profound thanks also go to the City Disaster Risk Reduction Management Office (CDRRMO) for their cooperation during the data-gathering process, specifically Mr. Rodolfo Retirado III and the entire staff whose expertise contributed significantly to this study.

References

Abbasi, S., et al. (2022). Trustable Mobile Crowd Sourcing for Acquiring Information from a Flooded Smart Area. ArXiv (Cornell University), 1–3. Retrieved from https://doi.org/10.1109/sciot56583.2022.9953706. January 1, at 10:00 A.M.

Abid, S. K., Sulaiman, N., Al-Wathinani, A. M., & Goniewicz, K. (2024). Community-based flood mitigation in Malaysia: Enhancing public participation and policy effectiveness for sustainable resilience. Journal of Global Health, 14, 04290. Retrieved from https://doi.org/10.7189/jogh.14.04290. January 1, at 11:00 A.M.

Baltazar, John, et al. (2022, December 1). Disaster and Crime Reporting and Monitoring System for Hagonoy Bulacan with Decision Support Mechanism. IEEE Xplore. Retrieved from https://doi.org/10.1109/HNICEM57413.2022.10109571. January 1, at 4:00 P.M.

Bolanio, et al. (2023, February 23). MAPPING AND ASSESSMENT OF FLOOD EVACUATION SITES IN A GEOSPATIAL ENVIRONMENT: A CASE IN LAS NIEVES, AGUSAN DEL NORTE, PHILIPPINES. Isprs-Archives.copernicus.org; Copernicus GmbH. Retrieved from https://doi.org/10.5194/isprs-archives-XLVIII-4-W6-2022-473-2023. January 1, at 4:00 P.M.

Fan, C. et al. (2020). Spatial biases in crowdsourced data: Social media content attention concentrates on populous areas in disasters. Computers, Environment and Urban Systems, 83, 101514. Retrieved from https://doi.org/10.1016/j.compenvurbsys.2020.101514. December 23, at 4:00 P.M.

Fauzi, D. (2021). Coastal Flood Responses in Manila Bay, the Philippines. Case Studies in the Environment, 5(1). Retrieved from https://online.ucpress.edu/cse/article-abstract/5/1/1438458/118423/Coastal-Flood-Responses-in-Manila-Bay-the?redirectedFrom=fulltext. November 22, 2024, at 6:00 P.M.

Gomez et al. (2024, December 27). Javi cancels New Year's Day event to focus on Victorias flood prevention - Digicast Negros. Digicast Negros. Retrieved from https://digicastnegros.com/javi-cancels-new-years-day-event-to-focus-on-victorias-flood-prevention/?_sc=ODA5ODUxNSM2NTc%3D. January 6, at 2:00 P.M.

González-Villa, J., Cuesta, A., Alvear, D., & Balboa, A. (2022). Evacuation management system for major disasters. Applied Sciences, 12(15), 7876. Retrieved from https://www.mdpi.com/2076-3417/12/15/7876. November 22, 2024, at 5:00 P.M.

Helmrich et al. (2021). Opportunities for crowdsourcing in urban flood monitoring. Environmental Modelling & Software, 143, 105124. Retrieved from https://doi.org/10.1016/j.envsoft.2021.105124. December 23, at 3:00 P.M.

Montefalcon, et al. (2021). IRespondPH: A Mobile and Web-based Application for Post Disaster Needs Assessment and Response in the Philippines. 2021 5th International Conference on E-Society, E-Education and E-Technology. Retrieved from https://doi.org/10.1145/3485768.3485784. January 1, at 3:00 P.M.

Protecting people and communities from the risk of floods in Metro Manila. (2021, May 19). Retrieved from https://www.preventionweb.net/news/protecting-people-and-communities-risk-floods-metro-manila. March 25, 2024, at 3:00 P.M.

Rey, W,. et al. (2022, March 7). Mamamayan: An Android mobile Community-based Emergency Reporting and Notification System. Index.ieomsociety.org; IEOM Society. Retrieved from https://index.ieomsociety.org/index.cfm/article/view/ID/455. January 1, at 2:00 P.M.

Sharma, R. (2021). Community Based Flood Risk Management: Local Knowledge and Actor's Involvement Approach from Lower Karnali River Basin of Nepal. Journal of Geoscience and Environment Protection, 09(06), 35–65. Retrieved from https://doi.org/10.4236/gep.2021.96003. January 1, at 12:00 P.M.

Sintia Radu. (2020, January 15). How Technology Can Battle Natural Disasters. US News & World Report; U.S. News & World Report. Retrieved from https://www.usatoday.com/videos/tech/columnist/saltzman/2023/08/15/how-tech-can-help-protect-against-natural-disasters/8351495001/. March 27, 2024, at 6:00 P.M.

Tabios, G. Q., III. (2023). Urban dimensions of floodings and holistic flood risk management: case of Pasig-Marikina River Basin in Metro Manila. In Urban dimensions of floodings and holistic flood risk management (pp. 347–370). Retrieved from https://link.springer.com/chapter/10.1007/978-981-19-7804-3_11. November 22, 2024, at 6:00 P.M.

The City of Manila Could be Underwater by 2050 if Climate Change Isn't Stopped. (2019). Esquiremag.ph. Retrieved from https://www.esquiremag.ph/politics/news/manila-underwater-climate-change-a00304-20191105?s=truhjr2v4dndv8fugsorroickq. March 24, 2024, at 3:00 P.M.

Traya, Romel, et al. (2022) Android Mobile Application: Tsunami Alert System with an Escape Route for Evacuation in Municipal Disaster Risk Reduction and Management Office | IEEE Conference Publication | IEEE Xplore. (n.d.). Ieeexplore.ieee.org. Retrieved from https://ieeexplore.ieee.org/abstract/document/9930386. January 1, at 1:00 P.M.

Understanding poverty and children's health before natural disasters strike. (2021, October 13). EHN. Retrieved from https://pubmed.ncbi.nlm.nih.gov/18579887/. March 27, 2024, at 7:00 P.M.

Real-Time Single-Phase Generator Fault and Protection System

Cyrus Y. Bigcas
STI West Negros University, Bacolod City, Philippines
Email : cyrus.bigcas@wnu.sti.edu

Abstract

This study presents the design, implementation, and evaluation of a Real-time Single-Phase Generator Fault and Protection System to automate the monitoring process, provide an immediate response, and improve the safety and efficiency of generators. The device integrates the following features: real-time measurements of current, voltage, power, power factor, and percent load; automatic shutdown under fault conditions (overload, over-voltage, under-voltage); and remote monitoring via SMS. The specific objective of the study is to evaluate the performance of the device based on the aforementioned features, with emphasis on the following criteria: data monitoring accuracy of current, voltage, power, power factor, and percent load; content accuracy of SMS features and correct protective response upon fault detection. Performance evaluations for current monitoring yielded an overall accuracy of 99.46%, while power monitoring demonstrated a negligible 0.97% error rate. Although voltage monitoring faced an "Acceptable" interpretation due to an aggregate 2.24% error, it remained "Highly Accurate" during no-load states. The power factor monitoring effectively identified unique electrical signatures across 13 load types, maintaining stable readings for inductive and mixed loads. Safety features were proven reliable, with the SMS alert feature delivering accurate notifications in an average of 1.15 seconds. Physical protection was equally decisive; the RCBO isolated ground and short-circuit faults with an average response time of 1.53 seconds. Voltage protection via the VMR maintained a consistent 3-second trip time, while current-based relay protection achieved near-instantaneous isolation at 2 milliseconds. These technical benchmarks were mirrored by the user acceptability study, with an overall mean score of 4.68. Usability emerged as the strongest qualitative metric at 4.70, underscoring the system's practical operational effectiveness. The evaluation instrument itself was statistically validated with a Cronbach’s alpha of 0.825, ensuring the reliability of these assessments. Overall, the evaluation indicates excellent performance and acceptance, confirming the device’s accuracy, effectiveness, reliability, and practical applicability in improving the stability, efficiency, and safety of single-phase generators.

Keywords: single-phase generator; protection system; remote monitoring

1. Introduction

Electric power generators play a crucial role in maintaining a continuous and reliable electricity supply for industries, households, and commercial establishments. In areas with frequent power interruptions or unstable power grids, generators serve as essential backup power sources. The reliability and efficiency of these generators are vital in preventing operational disruptions and ensuring the safe operation of critical infrastructures such as hospitals, manufacturing plants, and data centers (Kumar et al., 2021).

Despite their importance, generators are susceptible to several electrical faults, including overvoltage, undervoltage, overload, short circuits, and ground faults. These faults may lead to equipment damage, operational downtime, financial losses, and hazardous situations such as electrical fires and electric shocks (Gupta & Singh, 2019). Traditional generator monitoring and protection systems commonly rely on manual inspections and basic protective devices such as circuit breakers. Although these devices provide protection, they typically operate only after a fault has occurred, limiting their ability to detect faults early and enable preventive actions (Ahmed et al., 2020).

Single-phase generators are commonly used in residential and small commercial applications. These generators operate on a single alternating current waveform and are typically used to power small appliances or provide backup power during power interruptions. However, compared with three-phase generators, single-phase generators produce less stable power output due to the fluctuating nature of their alternating current waveform. The generated waveform continuously oscillates between positive and negative peak values, making large-scale power generation more challenging with a single current path (Kim, 2024).

Recent technological advancements in embedded systems have enabled the development of intelligent monitoring and protection systems. Microcontrollers are programmable devices capable of interacting with sensors and other electronic components to control and monitor system operations. One widely used microcontroller platform is Arduino, which is known for its affordability, open-source environment, and ease of programming (Arduino Documentation, 2021). Microcontroller-based systems allow developers to collect real-time data from sensors, process electrical parameters, and activate protective mechanisms automatically.

Energy management is another important aspect of generator operation. Parker and Lee (2021) reported that improved energy management strategies in backup generators can increase fuel efficiency by up to 25%. Automated load balancing and adaptive control systems help regulate power demand, reduce fuel consumption, and extend generator lifespan.

Electrical faults remain one of the major causes of generator malfunction. According to Kumar and Roy (2018), automated protection systems can prevent up to 90% of major electrical failures by rapidly isolating faulty components and activating shutdown mechanisms. The integration of microcontroller-based fault detection systems significantly improves the accuracy and response time of protective devices (Gonzalez & Chen, 2022).

Communication technologies such as Global System for Mobile Communications (GSM) have also been widely used in monitoring systems. GSM modules enable devices to communicate via cellular networks and transmit notifications via Short Message Service (SMS). According to EFY Bureau (2024), GSM modules can transmit operational data and system alerts through AT command communication protocols. A study published in *Computers and Electronics in Agriculture* demonstrated the effectiveness of GSM technology for remote data acquisition, achieving 100% data accuracy with a data loss rate of only 0.66%. SMS notifications were typically delivered within 10 to 15 seconds, while command-response communication required approximately 30 seconds.

Accurate monitoring of electrical parameters is essential in generator protection systems. The PZEM-004T sensor module is widely used to measure electrical parameters, including voltage, current, power, and energy consumption, in single-phase electrical systems. Ridwan and Hafit (2025) reported that the sensor achieved an average measurement error of only 1.19% relative to calibrated reference instruments, demonstrating its reliability for real-time energy monitoring.

Protective devices also play a critical role in ensuring electrical safety. One commonly used device is the Residual Current Circuit Breaker with Overcurrent Protection (RCBO), which protects electrical circuits from earth leakage currents, overload conditions, and short circuits. RCBO devices automatically disconnect the electrical supply when abnormal current conditions are detected, thereby reducing the risk of electric shock and equipment damage.

Another protective device frequently used in electrical systems is the Voltage Monitoring Relay (VMR). This device continuously monitors voltage levels and disconnects the load when the voltage exceeds or falls below safe operating limits. Voltage monitoring relays help protect electrical equipment from both overvoltage and undervoltage conditions.

Real-time monitoring systems significantly improve generator performance and reliability. Mendez and Carter (2021) found that real-time power-quality monitoring improved generator efficiency by approximately 15% while reducing harmonic distortion by 30% (Mendez and Carter, 2021). Similarly, Liu et al. (2020) demonstrated that dynamic load balancing algorithms enhance generator performance by distributing electrical loads more efficiently.

Generator reliability is also closely related to overall power system stability. Nguyen et al. (2020) emphasized that frequent generator failures can affect the stability of microgrid systems and may lead to widespread power interruptions. These findings highlight the need for effective monitoring and protection systems capable of detecting abnormal conditions early.

A study by Martinez et al. (2020) developed an automated generator protection system that integrates microcontrollers and relay-based protection mechanisms. The study reported that the automated system successfully reduced generator downtime by approximately 40% and improved operational efficiency.

Despite these technological advancements, many small-scale generator systems still rely on conventional protection methods that lack real-time monitoring capabilities and remote notification features. This gap highlights the need for a more integrated monitoring and protection system capable

of detecting electrical faults, providing immediate protective responses, and notifying operators of abnormal conditions.

In response to these challenges, this study proposes the development of a **Real-Time Single-Phase Generator Fault and Protection System**. The system is designed to monitor key electrical parameters, including voltage, current, power, power factor, frequency, and percent load. It can also detect electrical faults such as overvoltage, undervoltage, overload, short circuits, and ground faults. In addition, the system incorporates GSM-based SMS notification to alert operators whenever abnormal conditions occur.

By integrating microcontroller technology, sensor-based monitoring, protective relays, and wireless communication, the proposed system aims to improve generator reliability, reduce operational downtime, and enhance electrical safety in residential and small commercial power applications.

2. Objectives of the Study

The objective of this study is to design and develop a Real-Time Single-Phase Generator Fault and Protection System.

Specifically, this study aims to:

1. Develop and fabricate a real-time monitoring system with the following features:
   a. Load (current) monitoring
   b. Voltage monitoring
   c. Power monitoring
   d. Power factor monitoring
   e. Percent load monitoring
   f. SMS alert notification upon fault detection
2. To determine whether the developed Real-Time Single-Phase Generator Monitoring and Protection System achieved its intended performance, the following success criteria were established prior to testing:
   a. Monitoring Accuracy:
      The load (current), voltage, power, and percent load monitoring functions were considered successful if the percentage error between the actual measured value and the displayed value did not exceed 5%.
   a. Power Factor Monitoring:
      The power factor monitoring function was considered successful if the system consistently displayed power factor values corresponding to the characteristics of the connected load with stable readings across repeated trials.
   a. SMS Notification Performance:
      The SMS notification feature was considered successful if fault messages were transmitted with 100% message content accuracy and delivered within 1–10 seconds after fault detection.

3. Materials and Methods

3.1 Research Design

This study employed a **descriptive–developmental research design** to design, construct, and evaluate the *Real-Time Single-Phase Generator Fault and Protection System*. The research focused on prototype development, controlled laboratory testing, performance validation, and user acceptability assessment.

The study aimed to:

- Develop a functional prototype capable of real-time monitoring.
- Evaluate monitoring accuracy (voltage, current, power, power factor, percent load).
- Test protection mechanisms (overvoltage, under voltage, overcurrent, undercurrent, ground fault, short circuit).
- Assess SMS notification reliability.
- Determine system acceptability based on features, functionality, and usability.

Prototype Design and System Architecture

Major Components

The prototype consists of:

- Arduino Uno Microcontroller
- GSM Module
- Circuit Breaker (MCB)
- PZEM-004T Energy Monitoring Module
- Residual Current Breaker with Overcurrent Protection (RCBO)
- Voltage Monitoring Relay (VMR)
- Relay Module
- LCD Display
- LED Light Indicator

Physical Dimensions

- Enclosure: 9.8 in × 5.7 in × 11 in (453 sq. in area)
- LCD: 2 in × 1 in
- RCBO, VMR, MCB: 1.8 in × 2.7 in × 2.4 in

System Operation

When connected to a single-phase generator:

1. The circuit breaker energizes the system.
2. The Voltage Monitoring Relay activates after a 10-second delay.
3. The PZEM-004T measures:
    - Voltage
    - Current
    - Power
    - Energy
    - Frequency
    - Power Factor
4. Data is processed by the Arduino.
5. Real-time readings are displayed on the LCD.
6. Upon fault detection:
    - Relay disconnects load.
    - RCBO trips (for ground/short faults).
    - GSM module sends SMS notification.

Fabrication and Construction

The prototype was assembled inside a secured metal enclosure with:

- Cut-outs for LCD and LED indicator
- Mounted internal protection devices
- Proper wiring using THHN 12 AWG conductors
- Socket outlet connection for load testing

Existing laboratory tools were used (soldering iron, tester, drill, pliers, etc.), which were not included in project cost.

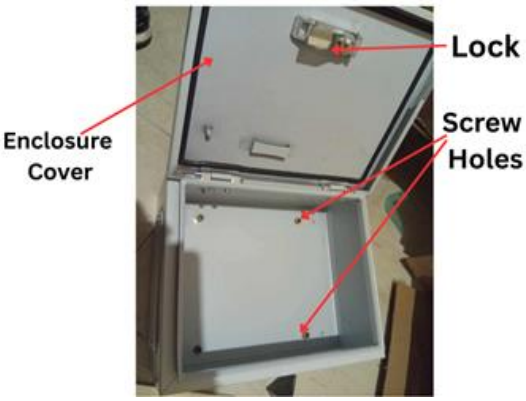

Figure 1 shows the preparation of materials, wiring connections, component assembly, and installation of the protection devices during the fabrication stage of the prototype.

Cost Analysis

Total Project Cost: **₱3,827.00**

- Materials: ₱3,777.00 (98.69%)
- Labor: ₱50.00 (1.31%)

The majority of expenses were allocated to materials and protection components.

Prototype Testing

Device Testing Procedures

Load Monitoring Tests

The system was tested under five load categories:

- No Load
- Pure Resistive Load
- Inductive Load
- Mixed Load
- Dynamic Load

Each load condition was tested three times.

A calibrated-grade digital multimeter (SANWA Model CD800a), purchased in 2023, was used as the reference instrument for the validation tests. At the time of the study, the instrument had not yet undergone external calibration because it was newly acquired and was operated within the manufacturer's specified accuracy as indicated in the product specifications and compared with LCD-displayed values.

Voltage Monitoring

Voltage readings were measured using an AC multimeter and compared against displayed values.

Power Monitoring

- Actual Power was calculated using:
- Power (W) = Voltage × Current
- Displayed power was obtained from LCD readings.

Power Factor Monitoring

- Power factor values were obtained directly from LCD display.

Percent Load Monitoring

- Generator rated capacity: **2800 W**
- Formula used:
- Actual % Load = (Actual Power / 2800 W) × 100
- Two test conditions:
    - Greater than 30% load
    - Less than 30% load

SMS Performance Testing

Faults simulated:

- Overload
- Underload
- Overvoltage
- Under voltage

Time delay was measured using a stopwatch.

Message content accuracy was verified through received SMS.

Ground Fault and Short Circuit Testing

- Faults were simulated using low-resistance conductor.
- Trip time was measured.
- RCBO response was recorded.

Voltage Protection Testing

Voltage levels were varied using a VARIAC:

- +5%, +10%, +15% (Overvoltage)
- −5%, −10%, −15% (Under voltage)

Trip response time recorded.

- Nominal Voltage: 230V
- Tolerance based on Philippine Electrical Code (±5%)

Current Protection Testing

Current thresholds tested:

- Overcurrent: >125%, >150%, >175%
- Undercurrent: <30%, <60%, <90%

Trip time recorded.

The overload test levels were established at 125%, 150% and175% of the rated current. The initial threshold of 125% was selected based on the National Electrical Code (NEC) requirement for continuous loads, which requires overcurrent protective devices to be rated at not less than 125% of the continuous load. The succeeding overload levels (150% and 175%) were adopted to simulate progressively increasing overload conditions and to evaluate the responsiveness, fault detection capability, and SMS alert performance of the developed real-time monitoring system under varying fault severities. These test levels were intended for system performance evaluation and were not intended to validate compliance with standardized circuit breaker tripping curves such as IEC or NEMA standards.

The undercurrent detection thresholds were predetermined at less than 30%, 60%, and 90% of the rated current. These thresholds were selected to simulate different levels of current reduction and to assess the sensitivity and reliability of the developed monitoring system in identifying abnormal operating conditions. The selected values do not represent NEC requirements, as the NEC primarily addresses overcurrent protection. Instead, they were established as design criteria for the experimental evaluation of the prototype under controlled testing conditions.

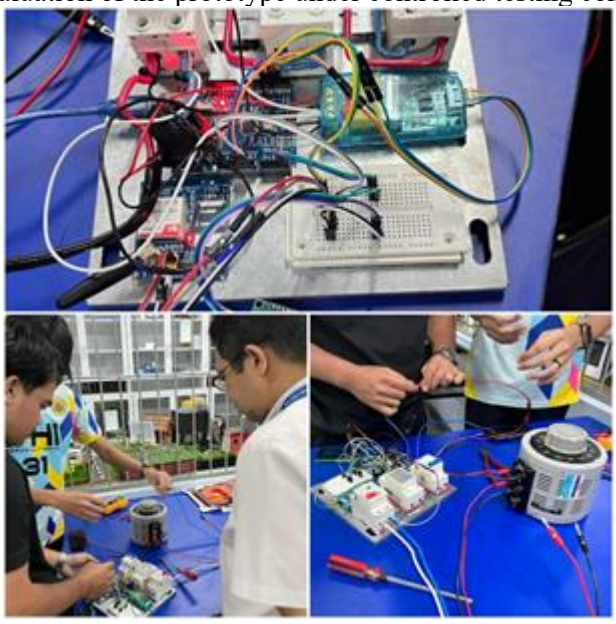

Following fabrication, a series of laboratory and field tests were conducted to evaluate system performance under different operating conditions as shown in Figure 2.

Reliability Assessment

Cronbach's Alpha Formula:

$\alpha = (N / (N - 1)) \times [1 - (\Sigma\sigma^2_i / \sigma^2_t)]$

Results:

- Number of Items: 11
- Cronbach's Alpha: 0.825
- Interpretation: Good Reliability

Validity Assessment

Content validity was evaluated using Lawshe's CVR method.

- All items obtained CVR = 1.00
- Interpretation: Excellent Validity

Acceptability Assessment

Respondents: 30 Electrical Engineering Students
Weighted Mean Results:

- Features: 4.68
- Functionality: 4.67
- Usability: 4.70
- Overall: 4.68 (Highly Acceptable)

Data Analysis

Mean Interpretation Scale

4.50–5.00 = Highly Acceptable
3.50–4.49 = Acceptable
2.50–3.49 = Moderately Acceptable
1.50–2.49 = Poor
1.00–1.49 = Not Acceptable

Percent Error Formula

% Error = (Actual − Expected / Expected) × 100

Error Interpretation:

<1% = Highly Accurate
1–5% = Acceptable
5–10% = Fair
10–20% = Marginal
20% = Inaccurate

4. Results

4.1 Prototype Description

The system was designed as a compact, integrated monitoring and protection unit suitable for both laboratory and operational environments.

The device's enclosure is constructed from a metal casing to improve structural durability and protect internal electrical components from external damage. The enclosure measures 25 cm × 30 cm × 15 cm and features a locking mechanism to prevent unauthorized access.

A 2 × 1-inch LCD display is installed at the upper middle portion of the enclosure to present real-time electrical parameters such as voltage, current, power, and power factor. A 16 mm LED indicator is mounted on the upper left portion to indicate system status. A 40 × 60 mm outlet opening is installed at the bottom portion for load connection.

Internally, the prototype integrates both monitoring and protection components. The monitoring section utilizes the PZEM-004T energy monitoring module connected to an Arduino microcontroller to acquire real-time measurements of voltage, current, power, and energy from the generator.

The protection system consists of the following components:

- Voltage Monitoring Relay (VMR)
- Residual Current Breaker with Overcurrent Protection (RCBO)
- Relay Module
- GSM Module

The circuit breaker is connected to the generator and serves as the device's main switch. Its output terminal is connected to the input terminal of the Voltage Monitoring Relay (VMR). The VMR output is then connected to the RCBO, which provides protection against ground-fault and short-circuit conditions.

The RCBO is connected to the relay module, which is controlled by the Arduino. When a fault condition is detected, the Arduino sends a signal to the relay to disconnect the load from the generator.

Additionally, the GSM module is connected to the Arduino to send SMS notifications to the user whenever a fault condition occurs. When connected to a 220-V generator, the system automatically activates the relay within 1–3 seconds to establish a connection between the device and the power source.

4.2 Performance Evaluation

a. Load (Current) Monitoring

The results of load current monitoring under different load conditions, including no load, pure resistive load, inductive load, mixed load, and dynamic load.

Under no-load conditions, the system recorded zero current in both actual and displayed measurements across all trials, resulting in 0% error, indicating high accuracy.

For pure resistive loads, the light bulb recorded a 4.44% error, while the coffee maker and rice cooker showed 2.25% and 2.10% error, respectively. These values fall within the acceptable accuracy range.

In the inductive load category, the ceiling fan obtained a 0.92% error, interpreted as highly accurate, while the electric fan and electric drill recorded 2.04% and 3.4% error, respectively, which were rated as acceptable.

Mixed load conditions consisting of resistive and inductive appliances also demonstrated acceptable monitoring accuracy, with percentage errors ranging from 2.6% to 3.3%.

For dynamic loads, the laptop and tablet produced acceptable errors of 3% and 1.2%, respectively, while the cellphone recorded 5.3%, interpreted as fair.

Overall, the monitoring system achieved a combined percent error of only 0.54%, indicating high accuracy in measuring load current.

These results support the findings of the study by Ridwan and Hafit (2025), which reported an average error rate of 1.19% for the PZEM-004T sensor when compared with calibrated reference meters.

b. Voltage Monitoring

Under no-load conditions, the system recorded an actual voltage of 225.30 V and a displayed voltage of 225.20 V, resulting in a minimal 0.04% error, which is interpreted as highly accurate.

For resistive, inductive, and mixed loads, the monitoring system recorded percentage errors ranging from 2.1% to 3%, which fall within the acceptable accuracy range.

Under dynamic load conditions, voltage monitoring remained stable, with errors ranging from 2.1% to 2.6%, indicating reliable voltage measurement performance.

The overall monitoring results show that the system can accurately monitor generator voltage under various operating conditions.

c. Power Monitoring

For no-load conditions, both actual and displayed power values were zero, resulting in 0% error.

Among resistive loads, the rice cooker and coffee maker demonstrated high accuracy with errors of 0.26% and 0.12%, respectively. The light bulb showed a 6.7% error, which was interpreted as fair.

For inductive loads, including the ceiling fan, electric fan, and electric drill, the system recorded errors ranging from 0.23% to 0.71%, which indicates high monitoring accuracy.

Mixed load configurations also produced acceptable error values ranging from 0.8% to 2.1%.

The overall system recorded a combined percent error of 0.97%, indicating high accuracy.

These findings align with the study of Mendez and Carter (2021), which demonstrated that real-time power monitoring systems improve generator efficiency and operational stability.

d. Power Factor Monitoring

The results show that power factor values varied depending on the load type. Resistive loads produced power factors close to unity, while inductive loads exhibited lower power factors due to reactive power components.

Dynamic loads such as laptops, cellphones, and tablets recorded lower power factors ranging from 0.49 to 0.84, which is expected due to switching power supply characteristics.

The overall mean power factor recorded by the system was 0.81, indicating a generally stable balance between real and apparent power under different operating conditions.

e. Percent Load Monitoring

When the generator load exceeded 30%, the system maintained normal operation without disconnecting the supply. The recorded percent load showed a minimal 0.01% error, indicating high accuracy.

When the generator load was below 30%, the system automatically disconnected the supply, demonstrating the proper functioning of the under-load protection feature. The overall percent load monitoring achieved an error of 0.3%, confirming the monitoring system's accuracy.

4.3 SMS Notification Performance

The average message transmission delay was 1.15 seconds, and all messages were successfully received with 100% accuracy. This result confirms that the GSM module provides reliable real-time fault notification.

4.4 Ground Fault and Short Circuit Protection

For both fault conditions, the RCBO successfully tripped in all trials, achieving 100% response accuracy. The average trip time recorded was approximately 1.53 seconds, demonstrating reliable fault isolation performance.

4.5 Voltage Protection

The system successfully detected overvoltage and undervoltage conditions at deviation levels of 5%, 10%, and 15% from the nominal voltage of 230 V. The Voltage Monitoring Relay (VMR) consistently tripped within 3 seconds, ensuring protection of connected loads.

4.6 Current Protection

The relay successfully responded to all simulated faults, tripping within 2 milliseconds for both overcurrent and undercurrent conditions. These results demonstrate the system’s capability to quickly isolate abnormal current conditions and protect the generator from damage.

4.7 Acceptability Test Results

Thirty Electrical Engineering students evaluated the system based on features, functionality, and usability.

Results show that:

- Features obtained a mean of 4.68
- Functionality obtained 4.67
- Usability obtained 4.70

The overall mean of 4.68 indicates that the system is Highly Acceptable. This confirms that the developed Real-Time Single-Phase Generator Fault and Protection System is suitable for practical monitoring and protection applications.

5. Discussions

The following are the major findings of the study:

1. The study successfully designed and fabricated the Real-Time Single-Phase Generator Monitoring and Protection System with all specified components. The device incorporated an Arduino Uno microcontroller for sensor data processing, a GSM module for sending SMS notifications about the generator's current and voltage conditions, and a PZEM-004T energy monitoring module for measuring AC RMS voltage, current, and power. The system also utilized a Residual Current Breaker with Overcurrent Protection (RCBO) for protection against short-circuit and earth-leakage faults, a relay module for current protection control, and a Voltage Monitoring Relay (VMR) for overvoltage and under-voltage protection. All components were properly integrated according to the design specifications, and the device operated as intended during assembly and initial testing, confirming the successful fabrication of a fully functional prototype.
2. The performance evaluation of the device was conducted based on the following features: monitoring of electrical parameters such as load (current), voltage, power, power factor, and percent load; SMS alert performance; and protection features including ground fault and short circuit protection, overvoltage and under voltage protection, and overcurrent and undercurrent protection.
    a. The load (current) monitoring achieved a total percentage error of 0.54%, resulting in a “Highly Accurate” interpretation. Under no-load conditions, the system recorded 0% error, while pure resistive and inductive loads maintained acceptable to highly accurate performance. The ceiling fan demonstrated the highest precision among active loads with 0.92% error, while the cellphone produced the highest percent error of 5.3%. Across 13 load configurations and 39 trials, the system maintained stable readings, with a mean actual current

of 656.59 mA and a mean displayed current of 660.17 mA, confirming highly accurate monitoring.

b. The voltage monitoring system demonstrated high accuracy under no-load conditions with only 0.04% error. Under resistive, inductive, mixed, and dynamic load conditions, the system recorded acceptable error rates of 2.1% to 3%. However, the combined difference between the mean actual voltage (219.82 V) and the mean displayed voltage (224.82 V) resulted in an overall 2.27% error, which falls within the "Acceptable" accuracy category according to the adopted error interpretation scale.

c. The power monitoring function recorded an overall mean actual power of 1930.75 W and a mean displayed power of 1952.62 W, producing a total percentage error of 0.97%, which is interpreted as "Highly Accurate." No-load and inductive load conditions yielded the highest precision, with error values of 0% and 0.23%, respectively. Pure resistive loads showed more variation, with errors ranging from 0.26% for rice cookers to 6.7% for light bulbs.

d. The power factor monitoring recorded an overall mean power factor of 0.81 across five test conditions. No-load conditions maintained a stable reading of 0.95, while inductive and mixed loads exhibited consistent values reaching 0.94. Pure resistive loads produced a wider range of power factor values, while dynamic loads such as tablets and cellphones showed lower power factors due to switching power supply characteristics.

e. The percent load monitoring demonstrated high accuracy with an overall mean accuracy of 99.7% and a total error of only 0.3%. Loads exceeding 30% of generator capacity maintained continuous power supply with 0.01% error, while loads below 30% consistently triggered automatic supply disconnection.

f. The SMS notification feature was evaluated through 12 trials under four simulated fault conditions: overload, underload, overvoltage, and under voltage. All trials achieved 100% message accuracy, with an overall average response delay of 1.15 seconds, confirming reliable real-time alert capability. The recorded overall average SMS delay of 1.15 seconds represents the total end-to-end response time from fault detection until successful receipt of the SMS notification on the recipient's mobile phone. This duration includes the processing time of the Arduino controller, GSM module command execution, transmission through the GSM network, and message delivery to the receiving device. Since all simulated fault conditions consistently produced accurate SMS notifications within approximately one to two seconds, the developed system demonstrated prompt remote fault notification suitable for real-time generator monitoring applications.

g. The ground fault and short circuit protection system demonstrated reliable performance with 100% successful RCBO tripping in all trials. The average trip time recorded was 1.53 seconds, ensuring rapid disconnection of hazardous electrical conditions.

h. The voltage protection system successfully detected both overvoltage and undervoltage conditions within 5% to 15% deviation from the rated voltage. The Voltage Monitoring Relay (VMR) consistently triggered disconnection with an average trip time of 3 seconds.

i. The current protection system achieved consistent and reliable fault isolation across all simulated conditions. Both overcurrent and undercurrent faults triggered relay disconnection with an extremely fast response time of 2 milliseconds.

3. The system acceptability evaluation was conducted based on three key criteria:
   - Features: Mean score of 4.68
   - Functionality: Mean score of 4.67
   - Usability: Mean score of 4.70

   Among these criteria, usability received the highest rating, indicating that respondents found the system easy to use and effective at monitoring generator conditions.
4. Overall, the findings confirm that the developed Real-Time Single-Phase Generator Fault and Protection System is accurate, reliable, effective, and highly acceptable to users, demonstrating its potential application as an improved monitoring and protection solution for single-phase generators.

6. Conclusions

Based on the study's results, the developed Real-Time Single-Phase Generator Monitoring and Protection System successfully achieved its intended objectives by providing accurate, real-time

monitoring of critical electrical parameters, including current, voltage, power, power factor, and percent load under varying load conditions.

The system demonstrated reliable protection capabilities by effectively detecting abnormal conditions, including overvoltage, undervoltage, ground faults, short circuits, overcurrent, and undercurrent, thereby improving the generator's operational safety and reducing the risk of equipment damage.

The SMS notification feature performed consistently, enabling prompt communication of system faults to the user. Additionally, the evaluation conducted by the respondents revealed high user acceptance, particularly in terms of system functionality, usability, and effectiveness in real-time monitoring and automated protection.

Overall, the results confirm that integrating microcontroller-based monitoring, real-time data acquisition, and automated protection mechanisms can significantly enhance the safety, reliability, and efficiency of single-phase generator operations.

Based on the findings of the study, the following recommendations are proposed:

1. **For the Energy and Power Industry**, the developed system may be adopted as a cost-effective monitoring and protection solution for small-scale generator installations. The system supports the growing demand for smart, automated power management technologies.
2. **For Generator Operators and End-Users**, the adoption of the system is encouraged to improve generator safety and operational efficiency. Real-time monitoring and automatic fault detection can help prevent equipment damage, reduce maintenance costs, and minimize unexpected power interruptions.
3. **For Industrial and Commercial Establishments**, the system may be implemented to enhance generator reliability, particularly in facilities that rely heavily on backup power systems, such as hospitals, data centers, and manufacturing plants.
4. **For Future Researchers**, it is recommended to further improve the system by expanding its capability to support three-phase generators, integrating Internet of Things (IoT) technologies, and incorporating additional sensors such as temperature and vibration monitoring to detect mechanical generator faults.

Acknowledgment

The completion of this study would not have been possible without the valuable contributions of several individuals and groups.

The author would like to acknowledge the efforts of the former student-researchers who initially conducted and completed this study. Their dedication and hard work in the design, development, and data-gathering phases served as the foundation for this research.

Sincere appreciation is extended to the panel members for their constructive comments, insightful suggestions, and professional guidance, which significantly improved the quality of this study.

The author also expresses gratitude to the administration and faculty of the College of Engineering for their continued support and for providing the necessary facilities and resources essential to the completion and presentation of this research.

Special thanks are given to the respondents, particularly the Electrical Engineering students, for their participation and valuable feedback during the system evaluation.

The author is deeply grateful to his family for their unwavering support, understanding, and encouragement throughout the completion and presentation of this study.

Above all, the author offers his utmost gratitude to Almighty God for His guidance, wisdom, and strength in accomplishing this endeavor.

The Author

References

ABB (2003). Power generator protection and control. Retrieved from https://new.abb.com/medium-voltage/digital-substations/protection-relays/power-generator-protection-and-control

ABB (2008). Measuring and monitoring relays. Retrieved from https://new.abb.com/low-voltage/products/electronicrelays/monitors

Accuenergy. (2018). Current transformers (CTs). retrieved from https://www.accuenergy.com/products/current-transformers/

Agil, F., Wibowo, N. C. H., & Mustofa, H. (2025). Design and evaluation of an IoT-based real-time energy monitoring system using NodeMCU and PZEM-004T. Digital System and Computing, 1(1), 13–18. doi.org

Ahmed, M. (2023, August 24). Understanding Mean Absolute Error (MAE) in Regression: A Practical Guide. Retrieved December 20, 2025, from https://medium.com/@m.waqar.ahmed/understanding-mean-absolute-error-mae-in-regression-a-practical-guide-26e80ebb97df

Alexander, C. K., & Sadiku, M. N. O. (2017). Fundamentals of electric circuits (6th ed.). McGraw-Hill Education.

Aman, M. A., Abbasi, M. Z., Khan, A., Jan, W., & Munir, M. (2018). *Power generator automation, monitoring and protection system*.

Bender Inc. (2021.). *Electrical safety solutions for generator monitoring*.

Blanchard, B. S., & Fabrycky, W. J. (2011). Systems engineering and analysis (5th ed.). Pearson Education.

Boylestad, R. L., & Nashelsky, L. (2013). Electronic devices and circuit theory (11th ed.). Pearson Education.

Chapman, S. J. (2012). Electric machinery fundamentals (5th ed.). McGraw-Hill Education.

Control Theory | Applied Mathematics | University of Waterloo. (2012.).

Dewesoft. (2024, February 26). *Current transducers vs current transformers: What are the differences?* Dewesoft.

Dewesoft. (2024, July 1). *Volts, currents, and the basic concepts of electricity*. Dewesoft.

EFY Bureau. (2023, August 29). *GPRS and GSM modules: Applications, AT commands, and interface*. Electronics For You.

EFY Bureau. (2024, October 24). *GPRS/GSM module made easy: working, AT commands, and uses 101 explained.*

Electronics For You. (2017). *LCD – Liquid crystal display types, working, uses, pros-cons*.

Energy Education. (2020, April 28). Electrical wire.

GEYA Electrical. (2003). *What is the voltage monitoring relay working principle?*

Glover, J. D., Sarma, M. S., & Overbye, T. J. (2012). Power system analysis and design (5th ed.). Cengage Learning.

Hasibuan, A. (2023). *Control and monitoring of 1 phase generator automatic voltage regulator internet of things.*

Hitachi Energy. (2004). *Generator circuit-breaker monitoring system GMS600*.

IEEE. (2018). IEEE guide for protective relaying. Institute of Electrical and Electronics Engineers.

International Electrotechnical Commission. (2018). IEC standards on voltage characteristics.

Kim, D. (2024, November 27). *Single-phase vs. Three-phase Power Explained*. Woodstock Power.

Li, Z., et al. (2025). Life prediction of residual current circuit breaker with overcurrent protection based on Wiener process with random effects. Journal of Electrical Engineering & Technology, 20(4551).

Mouly, M., & Pautet, M. B. (2009). The GSM system for mobile communications. Telecom Publishing.

Mustapha, I., Balami, & Muhammad, U. (2023). Microcontroller. *Engineering Research Journal, 3*(8), 25–35. Retrieved April 10, 2025, from https://www.openjournals.ijaar.org/index.php/erj/article/view/126

National Electrical Manufacturers Association. (2007). Electrical enclosures (NEMA standards).

National Electrical Manufacturers Association. (n.d.). *Enclosures*.

National Fire Protection Association. (2023). NFPA 70: National Electrical Code (NEC).

Peacefair. (2004). PZEM-004T AC power monitoring module datasheet.

Rojo, J. (2024, July). Basics of solid-state relays (Application note SLVAFU8). *Texas Instruments*. Retrieved April 25, 2025, from https://www.ti.com/lit/an/slvafu8/slvafu8.pdf

Schneider Electric. (2006). Residual current circuit breakers with overcurrent protection (RCBO).

Sheng, H., Wang, F., & Tipton IV, C. W. (2011). A Fault Detection and Protection Scheme for Three-Level DC–DC Converters Based on Monitoring Flying Capacitor Voltage. *IEEE*, *27*(2). 10.1109/TPEL.2011.2161333

Soderby, K. (2021, November 18). Liquid crystal displays (LCD) with Arduino. *Arduino*. Retrieved April 25, 2025, from https://docs.arduino.cc/learn/electronics/lcd-displays/

Stallings, W. (2018). Computer networking with Internet protocols and technology. Pearson Education.

TechTarget. (2005). Electric current. Retrieved from https://www.techtarget.com/whatis/definition/current

The Spruce. (2008.). *Electrical circuit overload problems and prevention*.

VASUMURUGAN, R. (20013). *Generator protection functions and test methods*.

What is an Embedded System? *Definition and FAQs | HEAVY.AI. (2012).*

William. (2024, July 3). *What is Voltage Monitoring Relay and What Does it Do? GEYA Electrical Equipment Supply*

Earthquake Safety of Concrete Hollow Blocks (CHB) Buildings in Naguilian, La Union

Reintjie L. Dizon*, Jayvi Bryan C. Gutierrez, Reynald P. Lucero, Zhean Gwyneth B. Macagba, Benedict R. Ong, James Alfred D. Viluan
Saint Louis College of San Fernando, La Union, Philippines
*Email : reintjied@gmail.com

Abstract

This study assessed the earthquake safety of Concrete Hollow Block (CHB) buildings in Naguilian, La Union, addressing concerns on their structural vulnerability and preparedness against seismic events. Specifically, it aimed to determine the building profiles in terms of use and model type, evaluate their level of vulnerability to common failure patterns, and identify repair practices undertaken by residents. A descriptive-quantitative research design was employed using a 12-point checklist questionnaire adapted from the PHIVOLCS–JICA "How Safe is My House? Self-check for Earthquake Safety." Data were collected through checklist-based interviews and analyzed using frequency and thematic analysis. The study focused on five barangays with the highest concentration of CHB buildings: Bimmotobot, Casilagan, Lioac Norte, San Antonio, and Suguidan Norte. Results revealed that many CHB structures exhibit moderate to high vulnerability due to inadequate construction practices, lack of structural reinforcements, and non-compliance with minimum building standards. Common failure risks include wall cracking, poor material quality, and improper connections, while repairs are often temporary and non-engineered. These findings highlight the urgent need for improved construction awareness and stricter implementation of building codes. The study provides a basis for developing informational brochures and vulnerability maps to guide residents and assist local government units in disaster risk reduction planning and policy formulation.

Keywords: Concrete Hollow Blocks; Earthquake Safety; Structural Vulnerability; Building Assessment; Disaster Risk Reduction

1. Introduction

Earthquakes are among the most destructive natural hazards, posing significant threats to human life, infrastructure, and economic stability. Globally, seismic events have caused extensive damage, particularly in regions where buildings are not designed to withstand ground shaking. Earthquakes between 1998 and 2017 resulted in nearly 750,000 deaths, with a large proportion attributed to structural collapse. This highlights the critical role of proper construction practices and adherence to engineering standards in mitigating earthquake-related risks. Studies have shown that poorly designed and non-engineered buildings are more susceptible to failure, emphasizing the importance of structural integrity in earthquake-prone areas (Keim, 2021; USGS, n.d.).

Recent global events further demonstrate the consequences of inadequate construction. The 2023 Türkiye earthquake revealed that even reinforced concrete structures can fail due to poor material quality, insufficient reinforcement, and improper detailing (Temblor, 2023; Moore, 2023). In contrast, countries like Chile have significantly reduced earthquake damage through the continuous improvement of building codes and construction practices (Shine, 2023). These contrasting cases highlight an ongoing discussion in the field: while engineering advancements can greatly enhance structural resilience, their effectiveness largely depends on strict implementation and public compliance.

In the Philippines, earthquake risk remains a major concern due to its location along the Pacific Ring of Fire. Efforts to update the National Building Code reflect the need to adapt to evolving hazards and construction technologies (Romero, 2023). However, despite these initiatives, many structures—particularly in rural areas—remain non-compliant with established standards. The impact of this issue was evident during the 2022 Abra earthquake, where thousands of houses were reported damaged across Northern Luzon (IFRC, 2023). This situation underscores the persistent vulnerability of residential buildings, especially those constructed using traditional and cost-driven methods.

Concrete Hollow Blocks (CHB) are widely used in the Philippines due to their affordability and ease of construction. While they offer practical advantages, CHB structures are inherently weak against lateral forces unless properly reinforced (Bueno, 2022). Research indicates that non-engineered masonry buildings, often constructed without professional supervision, exhibit higher vulnerability to seismic events due to poor materials and lack of structural detailing (Novelli et al., 2019). Furthermore, although retrofitting techniques have been proven effective in improving seismic performance, they are not widely practiced due to cost constraints and limited awareness (Multazam et al., 2023). This creates a gap between available engineering solutions and actual construction practices in communities. An important distinction in earthquake safety is the difference between repair and retrofitting. Repair refers to the restoration of damaged structural or non-structural components to their original condition after deterioration or damage. Typical repair practices include patching cracks, replacing damaged masonry units, and restoring surface finishes. While repairs may improve the appearance or functionality of a structure, they do not necessarily increase its capacity to resist future seismic forces. In contrast, retrofitting involves the modification or strengthening of an existing structure to improve its seismic performance and structural resilience. Common retrofitting techniques include the addition of reinforced concrete jackets, steel bracing systems, fiber-reinforced materials, and other structural enhancements designed to increase strength, stiffness, and ductility. Previous studies have shown that retrofitting is generally more effective than conventional repair methods in reducing earthquake vulnerability and preventing structural failure during future seismic events. Understanding this distinction is essential in evaluating the adequacy of post-earthquake interventions applied to CHB buildings and in assessing whether existing practices contribute to long-term structural safety.

La Union, identified as a high-risk seismic zone by hazard assessment tools, presents a critical case for evaluating building safety (GFDRR, n.d.). Specifically, the municipality of Naguilian is located near active fault systems, increasing the likelihood of experiencing damaging ground motion. Despite this, many residential structures in the area are constructed using CHB without strict adherence to building codes or engineering supervision. This condition raises concerns about the preparedness and resilience of these buildings in the event of a strong earthquake. Given these conditions, this study aims to assess the earthquake safety of Concrete Hollow Block (CHB) buildings in Naguilian, La Union. Specifically, it seeks to evaluate the building profiles in terms of use and model type, determine their level of vulnerability to earthquake-induced failure patterns, and examine the repair practices employed by residents. Ultimately, the study intends to provide a basis for developing an informational brochure and vulnerability maps to enhance community awareness and support local government efforts in disaster risk reduction.

Conceptual Framework: Earthquake Vulnerability of Concrete Hollow Block (CHB) Buildings in Naguilian, La Union

This conceptual framework explores the relationship between the profile of the Concrete Hollow Blocks (CHB) buildings and their vulnerability, with their profile and building information from the 12-point checklist questionnaire as independent variables. Other use of the facility is categorized into residential and commercial, acquiring the variations in occupancy patterns. The model type is classified based on the PHIVOLCS masonry housing typology as Model A, Model B, or Other. Model A generally represents structures that comply with recommended construction standards, whereas Model B and Other structures exhibit varying degrees of non-compliance and potential vulnerability to seismic hazards. The dependent variable is the level of vulnerability, which varies based on independent variables. It is hypothesized that non-code compliant CHB buildings may exhibit higher vulnerability levels, given potential deviations from established safety standards. The study aimed to provide insights into the specific vulnerabilities associated with non-compliance, informing regulatory practices and proposed measures for non-compliant buildings to enhance earthquake safety. A vulnerability map is incorporated into the report, which shows the level of vulnerability in each of the barangays. Also, this study aimed to raise awareness of employing minimum construction standards and the importance of earthquake safety through informational brochure.

The input consists of the profile of the building in terms of other use of the facility, and model type of the building; vulnerability of the different buildings to failure pattern; and evaluation of CHB buildings' vulnerability to strong earthquakes. The process will be analysis and evaluation of the profile of the buildings, utilization of 12-point checklist questionnaire assessment tool, and formulation and validation of the Informational Brochure and Vulnerability Map. A detailed report specific to the assessed barangay, outlining the vulnerability of CHB buildings to earthquakes and recommended measures for non-compliant Concrete Hollow Block (CHB) buildings in Naguilian, La Union will be presented together with Vulnerability Maps. Moreover, information about construction standards and earthquake safety will be presented through an informational brochure. By examining these factors and their interrelationships, this research provides valuable insights and recommendations to enhance and raise awareness on earthquake safety of concrete hollow blocks (CHB) buildings in Naguilian, La Union, ultimately contributing to the safety and resilience of the local community in the face of seismic hazards.

The initial result verifies whether a structure was properly built under appropriate construction procedures and recommended measures, or whether it will require necessary strengthening. This allows the residents and occupants to understand and realize that the earthquake risk is their own concern on which the researchers will be able to recommend measures through the outputs.

2. Objectives

Aligned with the objective of strengthening disaster resilience and community safety in earthquake-prone areas, this study pursues four key objectives: (1) to assess the profile of Concrete Hollow Block (CHB) buildings in Naguilian, La Union in terms of their use and structural model type; (2) to evaluate the level of vulnerability of these CHB buildings to earthquake-induced failure using a standardized assessment tool; (3) to examine the repair practices employed by residents on damaged CHB buildings and determine their adequacy in enhancing structural safety; and (4) to develop evidence-based outputs, including an informational brochure and vulnerability maps, that will guide residents and local government units in improving earthquake preparedness and structural resilience. These objectives are anchored in the need to promote safe construction practices, strengthen compliance with building standards, and reduce the risks associated with non-engineered masonry structures.

The contributions of this study are both theoretical and practical. For local government units (LGUs), it provides empirical data to support policy formulation, hazard mitigation planning, and targeted interventions for vulnerable communities. For disaster risk reduction and management offices, it offers a basis for improving assessment tools, preparedness programs, and community-based awareness initiatives. For civil engineering practitioners and students, the study contributes to the body of knowledge on seismic vulnerability of CHB structures and highlights the importance of engineering involvement in construction. Institutionally, the findings serve as a reference for developing extension programs focused on earthquake safety and structural awareness. Ultimately, the study envisions safer and more resilient communities in which informed construction practices and proactive risk reduction measures minimize the impact of earthquakes on lives and properties.

3. Materials and Methods

This study employed a descriptive–quantitative research design to systematically evaluate the earthquake safety of Concrete Hollow Block (CHB) buildings in Naguilian, La Union, Philippines. The study area was selected due to its proximity to active fault systems, particularly the Tubao Fault, making it vulnerable to seismic hazards. Five barangays—Bimmotobot, Casilagan, Lioac Norte, San Antonio Norte, and Suguidan Norte—were purposively selected based on an initial ocular survey identifying the highest concentration of CHB structures. A total of 47 buildings were included in the study, with inclusion criteria limited to one- to two-storey CHB-based residential or mixed-use structures that were accessible for inspection and whose occupants consented to participate.

The sample size of 47 CHB buildings was considered adequate for the objectives of this study because it covered the five barangays identified through an initial ocular survey as having the highest concentration of CHB structures in Naguilian, La Union. A purposive sampling approach was adopted

to ensure that the selected buildings possessed characteristics relevant to the assessment of earthquake vulnerability. Since the study aimed to describe existing conditions and identify common vulnerability patterns rather than estimate population parameters through inferential statistics, the inclusion of 47 buildings provided sufficient coverage of the target structures within the selected barangays. Furthermore, the sample captured variations in building use, construction characteristics, and observed structural conditions, allowing meaningful comparisons and analysis of earthquake-related vulnerabilities within the study area.

Data were collected using a 12-point earthquake safety checklist adapted from the Philippine Institute of Volcanology and Seismology (PHIVOLCS) and the Japan International Cooperation Agency (JICA) tool titled *"How Safe is My House? Self-check for Earthquake Safety."* No modifications were made to the assessment criteria, scoring system, or interpretation of results. However, the instrument was supplemented with building profile information, such as occupancy type, model classification, and repair history, to provide additional context relevant to the CHB buildings assessed in Naguilian, La Union. These supplementary data did not alter the original checklist structure and were used solely to support the analysis and interpretation of findings. The checklist assesses key structural components such as wall configuration, reinforcement detailing, mortar quality, roof framing, and visible structural defects. Each item was scored using a binary system (1 for compliant/safe and 0 for non-compliant/unsafe), with total scores ranging from 0 to 12. Prior to data collection, permission was secured from the local government unit, and the researchers conducted an orientation to standardize the use of the assessment tool. Data gathering involved a combination of ocular inspections and structured interviews with building occupants or owners to verify construction details, repair history, and modifications. Observations were recorded systematically, and photographic documentation was taken when permitted.

To further characterize the structural condition of the assessed buildings, each CHB structure was classified according to the PHIVOLCS model typology for masonry houses. Model A refers to CHB buildings that generally comply with recommended construction standards, including the use of 150-mm-thick (6-inch) CHB walls, 10-mm-diameter vertical reinforcing bars spaced at approximately 40 cm, 10-mm horizontal reinforcing bars installed every three layers of CHB, a properly compacted 1:4 cement-to-sand mortar mix, and adequately constructed roof framing and roofing systems. In contrast, Model B refers to CHB buildings with lower levels of structural compliance, typically characterized by 100-mm-thick (4-inch) CHB walls, 6-mm-diameter vertical reinforcing bars spaced at approximately 90 cm, 6-mm horizontal reinforcing bars every three CHB layers, non-compacted mortar mixtures, and substandard roof construction details. Buildings that did not conform to the specifications of either Model A or Model B were categorized as "Other" and were considered non-standard or non-engineered structures for the purpose of this study. This classification was used to assess the relationship between building type and earthquake vulnerability.

The collected data were encoded and analyzed using frequency distribution and percentage analysis to determine the profile and vulnerability levels of the buildings. The total checklist scores were categorized into three levels of vulnerability: high (0–7), medium (8–10), and low (11–12), based on PHIVOLCS guidelines. In addition, thematic analysis was applied to qualitative responses to identify common repair practices and construction behaviors among residents. Based on the results, an informational brochure and a vulnerability map were developed to communicate earthquake safety measures and visualize the distribution of at-risk structures across the selected barangays. These outputs were subjected to validation by local government representatives, including the Municipal Disaster Risk Reduction and Management Office (MDRRMO). Ethical considerations were strictly observed, including the use of informed consent, voluntary participation, and confidentiality of all respondent information, ensuring that all collected data were used solely for academic purposes.

4. Results

This section presents the results of the study using thematic analysis, the interpretation of the raw data and their discussions. The data gathered are presented according to the statement of the problem.

A. Profile of the CHB Buildings

Table 1 reveals the results of the residents' profiles categorized as residential, commercial, and other. Among the CHB buildings, a significant majority of 75% falls under the residential category. This differs from the commercial and other categories, which tally for only 25% of the total residents. This data indicates that the majority of CHB buildings in the five surveyed barangays of Naguilian, La Union, are primarily used for residential purposes.

According to the International Code Council (ICC), a residential building is defined as "any building or portion thereof designed or used for normal sleeping and living quarters by human occupants."

As mentioned, Naguilian, La Union, is considered primarily residential for several reasons. Firstly, Table 1 shows that 75% of CHB buildings in five surveyed barangays are classified as residential, significantly exceeding other categories. This suggests a dominant focus on housing residents. Secondly, the prevalence of single-family homes and apartments listed for sale or rent, along with Naguilian's official description as a peaceful and laid-back town, indicates a majority of land allocated for residential purposes. Additionally, the high population density, limited commercial activity, and historical context as a haven for migrants further support the notion that Naguilian's primary function is to provide housing for its residents.

Table 1. Other Use of the Facility

Other Use of the Facility	Frequency	Percentage
Residential	35	75%
Commercial	9	19%
Others	3	6%
TOTAL	47	100%

Table 2 indicates that most CHB structures in the study area fall under the “Other” category, comprising 87% of total residences. Model A accounts for 0%, while Model B represents 13%. This suggests that the majority of CHB buildings in Naguilian, La Union do not conform to either PHIVOLCS-defined Model A or Model B classifications.

However, these findings may not fully represent actual conditions in the study area due to non-response from some participants and the presence of abandoned houses during data collection.

CHB structures are generally evaluated based on five specifications: CHB wall, vertical steel bars, horizontal steel bars, mortar mix, and roof frame/roofing. According to PHIVOLCS (2021), Model A consists of thicker CHB walls (6”–400×200×150 mm), 10 mm vertical bars spaced at 40 cm, 10 mm horizontal bars spaced at 60 cm every three layers, compacted 1:4 mortar mix, and properly constructed roofing. Model B uses thinner CHB walls (4”–400×200×100 mm), 6 mm vertical bars spaced at 90 cm, 6 mm horizontal bars spaced at 60 cm every three layers, non-compacted 1:4 mortar mix, and substandard roofing construction.

The “Other” category includes structures that do not meet either Model A or Model B standards. These are considered non-compliant as they were generally not designed by licensed engineers and often fail to conform to building codes, increasing vulnerability to seismic hazards. Typical characteristics include 4” CHB walls, 10 mm vertical bars spaced at 1 meter, 10 mm horizontal bars every three layers, non-compacted mortar mix, and improperly constructed roofing systems.

Despite established construction standards, DIY or non-engineered housing remains prevalent. Professional design is recommended to ensure safety and compliance (Baum, 2022), yet self-built housing persists due to cost limitations, autonomy, and customization preferences.

Non-engineered housing poses significant structural risks. Proper engineering guidance is critical to ensure stability and compliance with building codes. Nevertheless, hollow-block construction without columns remains common in many developing regions due to affordability and construction simplicity (United Nations Human Settlements Programme, 2022). However, this approach raises safety concerns, particularly in earthquake-prone and climate-vulnerable areas (Global Earthquake Model, 2023).

In conclusion, the study underscores the need to strengthen awareness of proper residential construction practices, including CHB classification standards and building code compliance. Improving understanding of structural risks associated with non-engineered housing may support safer construction decisions and enhance community resilience..

Table 2. Model Type of the Building

Model Type	Frequency	Percentage
Model A	0	0%
Model B	6	13%
Others	41	87%
TOTAL	47	100%

Table 3 represents the level of vulnerability of the CHB buildings in Naguilian, La Union with score ranges 0-7, 8-10, and 11-12 points wherein these score ranges correspond to the respondents' building being highly vulnerable, medium vulnerable, and low vulnerable to earthquake. The descriptive equivalent rating correlates with the interpretation of highly vulnerable as unsafe and requires immediate consultation from experts, medium vulnerable as requires strengthening and consultation from experts, and low vulnerable as safe for now but needs confirmation from experts. This interpretation is adapted from the Self-check for earthquake safety of Concrete Hollow Block (CHB) Houses Assessment from PHIVOLCS.

In terms of the scores of the respondents using the 12-point questionnaire from PHIVOLCS it appears that a greater percentage of the buildings fall under the score ranges 0-7 with a percentage of 87% which indicates high vulnerability, while other CHB buildings fall under score ranges 8-10 with percentage of 13% which equivalents to the CH buildings being medium vulnerable to earthquake, and none of the respondents' CHB buildings falls under the low vulnerable to earthquake.

There are a lot of factors that lead the CHB buildings to become highly vulnerable to earthquakes such as the designer of the structure, code compliancy, age of construction, and location. This factor applies to those respondents' CHB buildings found in Naguilian, La Union which is why vulnerability assessment of houses is needed especially in earthquake prone areas as it gives knowledge on the impacts of earthquake and helps create mitigation plans to reduce damages on building as well as fatalities. (Zakir, et al. 2023).

Overall, this shows that the majority of the CHB buildings indicates high vulnerability to earthquakes therefore it is unsafe and there is need for an immediate touch or consultation from experts. The high level of vulnerability observed among the assessed CHB buildings supports the findings of Zakir et al. (2023), who reported that non-engineered residential structures exhibit greater susceptibility to earthquake-induced damage due to deficiencies in structural detailing and reinforcement. Likewise, Novelli et al. (2019) found that masonry buildings constructed without adequate engineering design are significantly more vulnerable to seismic forces. The present study therefore reinforces existing evidence that non-compliance with recommended construction standards increases earthquake risk in residential communities.

Table 3. Level of Vulnerability of the CHB Buildings

Score Range	Frequency	Percentage
0 – 7	41	87%
8 – 10	6	13%
11-12	0	0%
TOTAL	47	100%

Table 4 reveals the results of the number of CHB buildings repaired and not repaired after past earthquakes. The results were taken from the third question on the 12-point checklist questionnaire wherein ten (10) CHB buildings were found to be damaged by past earthquakes. Among the ten (10) buildings, only 20% had undergone repair works while the remaining 80% were not repaired. The repair works that were employed include patching of cement on the cracked parts of the

building and restoring the CHB walls by inserting CHB pieces on holes caused by earthquakes. This is not recommended especially that the CHB walls were load-bearing and require strengthening techniques after they have been damaged.

While house repairs may address immediate issues, they often do not improve or enhance the overall resilience of a structure. Simple repairs may solve visible damages however they do not guarantee structural safety needed to withstand future disasters such as earthquakes. On the other side, Retrofitting surpasses repairs since it integrates new features into the existing structure which enhance the structure's resilience to seismic activities or other natural forces, increasing their strength, resistance, and lifespan. (Theerkadharshini, et al. 2018).

Seismic retrofitting is required for homes that are vulnerable to failures and damage by seismic forces. Construction techniques are greatly advanced now and the effects of earthquakes on different structures are better understood today than 20 or 30 years ago. At that time, building codes were a little less stringent compared to modern-day standards. (J.A.M. Concept Remodeling, 2019).

The findings regarding post-earthquake interventions are consistent with the work of Theerkadharshini et al. (2018), who emphasized that conventional repair methods often restore appearance or functionality but do not necessarily improve structural resistance to future earthquakes. Similarly, Multazam et al. (2023) demonstrated that retrofitting measures can significantly enhance the seismic performance of CHB masonry structures. The absence of retrofitting practices among the assessed buildings highlights a gap between available engineering solutions and actual practices within the community.

Overall, the residents of Naguilian did not use any retrofitting technique on their damaged buildings. However, it is highly recommended for them to adapt any seismic retrofitting technique to strengthen the buildings and prevent further damages during seismic activities.

Table 4. Post-Earthquake Damaged CHB Buildings Condition

Condition	Frequency	Percentage
Repaired	2	20%
Not Repaired	8	80%
TOTAL	10	100%

The informational brochure as the output of the study was based from the findings on the ocular inspection and checklist-based interview that seeks to evaluate the level of vulnerability of the CHB buildings. The purpose of the informational brochure is to raise awareness on employing minimum construction standards and the importance of earthquake safety. The overall impact of the output will help enhance awareness of residents in Naguilian, on earthquake safety of Concrete Hollow Block (CHB) buildings in Naguilian, La Union and disaster mitigation awareness.**Figure 1.** Informational Brochure

The vulnerability map as the output of the study was based from the findings on the ocular inspection and checklist-based interview that seeks to evaluate the level of vulnerability of the CHB buildings. The purpose of the vulnerability map with the integrated recommendations will provide insights into the specific vulnerabilities associated with non-compliance, informing regulatory practices and proposed measures for non-compliant buildings to enhance earthquake safety. The

overall impact of the output will inform the Municipal Disaster Risk Reduction and Management Office (MDRRMO) and other Local Government Unit officials, including the building official of Naguilian, on earthquake safety of Concrete Hollow Block (CHB) buildings in Naguilian, La Union and disaster mitigation awareness.

Figure 2. Barangay Lioac Norte Vulnerability

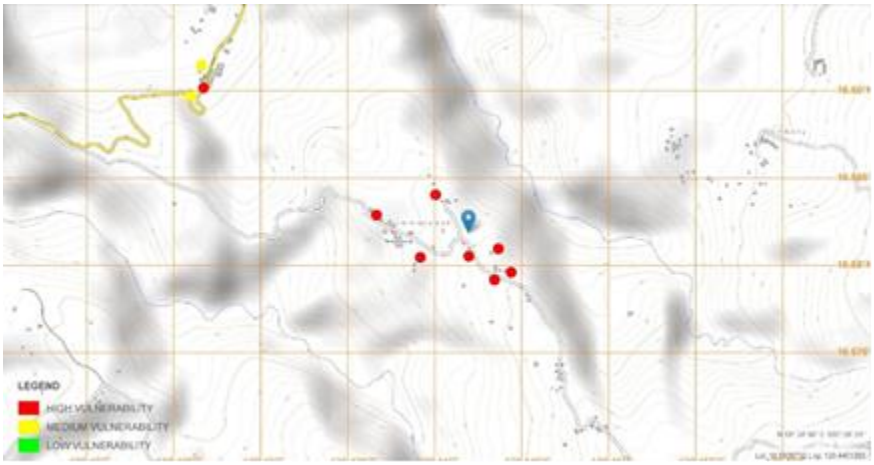

Figure 3. Barangay Bimmotobot Vulnerability Map

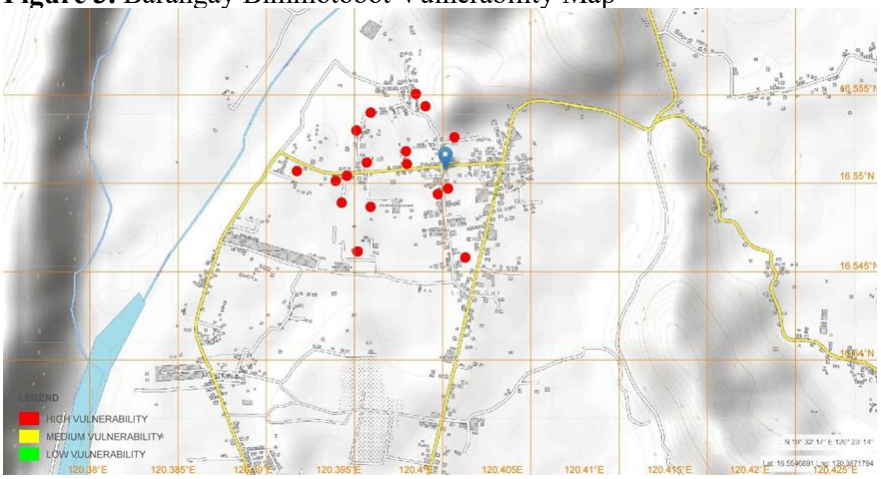

Figure 4. Barangay Casilagan Vulnerability Map

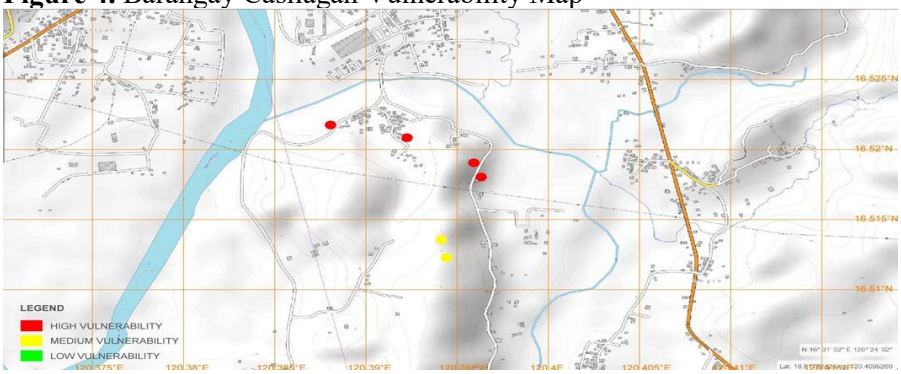

Figure 5. Barangay San Antonio Vulnerability Map

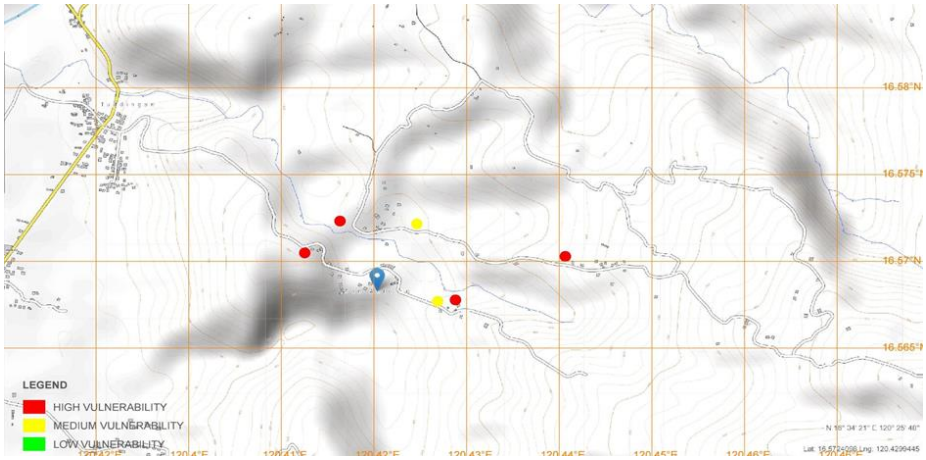

Figure 6. Barangay Suguidan Norte Vulnerability Map

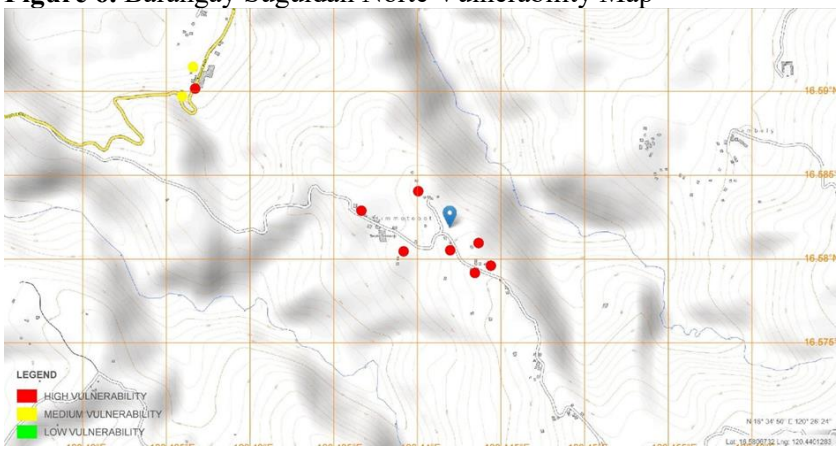

5. Discussion

The findings of this study indicate that the majority of CHB residential structures in Naguilian, La Union fall under the "Other" category (87%), with only 13% classified as Model B and none as Model A. This result strongly suggests that most existing CHB housing in the study area does not conform to PHIVOLCS-defined engineered standards for Model A and Model B construction. This is a key empirical conclusion directly supported by the data.

A major implication of this result is that current assumptions regarding residential CHB housing compliance may not reflect actual field conditions. While PHIVOLCS models assume standardized reinforcement, material spacing, and proper construction practices, the dominance of "Other" structures indicates widespread deviation from these standards. This challenges the assumption that low-rise CHB housing in rural or semi-urban settings generally follows minimum engineering guidelines. Instead, the findings suggest that non-engineered or partially engineered construction is the prevailing practice.

The characteristics of the "Other" category—such as inadequate reinforcement spacing, non-compacted mortar, and improper roofing systems—further support the conclusion that these structures are likely non-compliant with established building codes. This is also a directly supported conclusion based on observed structural attributes. Consequently, these buildings may exhibit increased vulnerability to seismic and environmental hazards, particularly in earthquake-prone regions such as the Philippines.

The findings are consistent with the study of Novelli et al. (2019), which reported that non-engineered masonry buildings are common in developing countries and often fail to comply with

recommended construction standards due to the absence of professional engineering supervision. Similarly, the predominance of structures classified under the "Other" category in this study suggests that many CHB buildings in Naguilian were constructed outside the standard PHIVOLCS classifications. These findings support previous observations that informal or partially engineered construction practices remain prevalent despite the existence of building regulations and technical guidelines.

Interview responses from several homeowners provided additional insight into the prevalence of structures classified under the "Other" category. Many respondents indicated that financial constraints influenced their construction decisions, leading them to prioritize affordability over compliance with recommended building standards. Some homeowners reported relying on local masons and experienced builders rather than licensed engineers or architects due to budget limitations, while others cited limited awareness of specific structural requirements for earthquake-resistant construction. These responses suggest that economic considerations and limited access to professional engineering services may have contributed to the observed deviations from PHIVOLCS-recommended construction practices.

From a theoretical standpoint, the findings suggest that existing housing classification models (e.g., PHIVOLCS Model A and B) may require expansion or refinement to better capture the diversity of real-world construction practices. The emergence of a large "Other" category indicates a classification gap that limits the explanatory power of current models. Future frameworks should consider incorporating gradations of non-engineered or semi-compliant structures to improve hazard assessment accuracy.

Future research should focus on structural performance validation of "Other" category buildings, particularly through experimental testing such as shake-table simulations, load resistance analysis, and material strength assessments. Comparative studies between Model A, Model B, and "Other" structures under controlled stress conditions are also necessary to quantify differences in structural resilience. Additionally, socio-economic studies examining decision-making factors in self-built housing could further explain the persistence of non-engineered construction practices.

In summary, this study conclusively establishes that most CHB structures in the study area fall outside standard engineered classifications. It supports the hypothesis that non-engineered housing is dominant in the locality and suggests a significant gap between building code standards and actual construction practices. It further speculates that economic and contextual factors drive this deviation. These findings highlight the need for improved enforcement of building standards, expanded classification models, and further empirical testing of structural vulnerability in informal housing systems.

6. Conclusion

Based on the findings of the study, the researchers concluded that most of the buildings assessed are residential in type and are predominantly classified under the "Other" model category. This indicates that a large proportion of CHB structures do not conform to the prescribed Model A and Model B standards. Moreover, the majority of CHB buildings across the five barangays were found to be highly vulnerable to earthquake hazards, suggesting an urgent need to improve their structural resilience. It was also determined that residents commonly apply non-strengthening repair techniques when addressing damaged CHB structures, which do not enhance the overall safety or integrity of the buildings.

In response to these conditions, the informational brochure developed by the researchers was found to be effective in increasing residents' awareness of the vulnerability of CHB buildings to earthquakes. Likewise, the vulnerability map produced in the study was effective in assisting the local government unit (LGU) in identifying the seismic risk levels of CHB structures. These outputs may support the implementation of appropriate regulatory measures and targeted interventions aimed at improving compliance with building standards and strengthening the resilience of non-engineered CHB buildings.

Furthermore, residents should be encouraged to conduct regular maintenance and inspection of their homes and to consult qualified professionals when structural damages are observed in order to prevent potential accidents. Disaster preparedness initiatives, such as seminars on pre-earthquake,

during earthquake, and post-earthquake safety measures, should also be conducted to enhance community awareness and readiness. Capacity-building activities such as seismic safety workshops for local officials are likewise recommended to strengthen understanding of CHB-related seismic risks and appropriate safety interventions.

In addition, the development of community-specific emergency response plans, including coordination with emergency services and regular earthquake drills, is strongly recommended to improve disaster response effectiveness. Finally, structural strengthening measures such as retrofitting techniques—like the installation of plywood wall panels for lateral stability and the application of steel bands around CHB structures—are recommended to enhance resistance against seismic forces and reduce potential structural failure during earthquakes.

Acknowledgements

The researchers sincerely express their heartfelt gratitude to Engr. Reynald P. Lucero for his invaluable guidance, patience, and unwavering support throughout the conduct of this study. His expertise, insightful advice, and continuous encouragement greatly contributed to the completion and improvement of this research.

Deep appreciation is also extended to Engr. Ron Jake V. Uy, Engr. Michael Velonza, and Dr. Niño Randy C. Flores for their meaningful insights, constructive comments, and generous sharing of time and knowledge during the evaluation of this study. Their suggestions significantly enriched the quality and direction of the research.

The researchers likewise acknowledge Engr. Froilan S. Florendo, Jr., Municipal Engineer of Naguilian, for his assistance, valuable recommendations, and time devoted to supporting the conduct of this study, as well as the Local Government Unit (LGU) of Naguilian for granting permission and cooperation during data gathering. Above all, the researchers are deeply grateful to God Almighty, the source of wisdom, strength, and guidance, and to their families and friends for their constant prayers, encouragement, and support throughout the completion of this research.

References

ACI Committee 318. (2019). *Building code requirements for structural concrete (ACI 318-19) and commentary*. American Concrete Institute. https://www.concrete.org

Ammon, C. J. (2019). *Earthquake effects*. Pennsylvania State University. http://eqseis.geosc.psu.edu/cammon/HTML/Classes/IntroQuakes/Notes/earthquake_effects.html

Bueno, F. G. (2022, September 23). *CHB laying: The basics of common masonry in the Philippines*. Pinoy Builders. https://pinoybuilders.ph/chb-laying-the-basics-of-common-masonry-in-the-philippines/

Civil Lead. (2021, October 22). *Load bearing structure: Components, advantages and disadvantages*. https://www.civillead.com/load-bearing-structure-and-frame-structure/

Global Facility for Disaster Reduction and Recovery. (n.d.). *ThinkHazard!: La Union earthquake hazard assessment*. https://www.thinkhazard.org/en/report/24213-philippines-region-ii-ilocos-region-la-union/EQ

International Federation of Red Cross and Red Crescent Societies. (2023). *Philippines: Earthquake emergency response update*. https://www.ifrc.org

Keim, M. (2021, June 28). *When buildings collapse*. DisasterDoc. https://disasterdoc.org/when-buildings-collapse/

Moore, A. (2023, February 23). *Why the Turkey-Syria earthquakes were so destructive*. NC State University College of Natural Resources. https://cnr.ncsu.edu/news/2023/02/turkey-syria-earthquakes/

Multazam, Z., Yamamoto, K., Timsina, K., Gadagamma, C. K., & Meguro, K. (2023). *Shaking table tests of the one-quarter scale model of concrete hollow blocks masonry houses retrofitted with fiber-reinforced paint*. Research Square. https://doi.org/10.21203/rs.3.rs-2983732/v1

Novelli, V., Ngoma, I. N., Kloukinas, P., Kafodya, I., De Risi, R., Macdonald, J. H. G., & Goda, K. (2019). *Seismic vulnerability assessment of non-engineered masonry buildings in Malawi*. ResearchGate. https://www.researchgate.net/publication/334721551

Philippine Institute of Volcanology and Seismology. (n.d.). *How safe is my house? Self-check for earthquake safety of concrete hollow block (CHB) houses in the Philippines*. Department of Science and Technology. https://www.phivolcs.dost.gov.ph

Romero, P. (2023, February 13). *Senate seeks amendments to 50-year-old building code*. Philstar Global. https://www.philstar.com/headlines/2023/02/13/2244509/senate-seeks-amendments-50-year-old-building-code

Shine, I. (2023, March 10). *This is how we can make buildings earthquake-proof*. PreventionWeb. https://www.preventionweb.net/news/how-we-can-make-buildings-earthquake-proof

Temblor. (2023, February 28). *A preliminary report on the February 6, 2023 earthquakes in Türkiye*. PreventionWeb. https://www.preventionweb.net/news/preliminary-report-february-6-2023-earthquakes-turkiye

United Nations Human Settlements Programme. (2023). *Annual report 2022*. UN-Habitat. https://unhabitat.org/annual-report-2022

United States Geological Survey. (n.d.). *Earthquake hazards program*. https://www.usgs.gov/programs/earthquake-hazards

Zakir, R. F., et al. (2023). *Vulnerability assessment of non-engineered houses related to earthquake in West Pasaman District*. IOP Conference Series: Earth and Environmental Science, 515(1), 012075. https://doi.org/10.1088/1755-1315/515/1/012075

VISCANE: An Edge-Based AI System for Sugarcane Quality Grading and Maturity Detection Using RGB-HSV Imaging

Faye N. Cuevas*, Windy D. Elipse, John Rolo C. Flores, Lynol I. Ibarra, Raymart B. Abella
College of Information and Communications Technology, STI West Negros University, Bacolod City, Philippines
*Email: cuevas.247492@wnu.sti.edu.ph

Abstract

In the Philippines, particularly in the agricultural municipality of Isabela, Negros Occidental, smallholder farmers sustain the sugarcane industry but face unstable yields and market fluctuations due to reliance on traditional grading methods. To address these challenges, this study introduces VISCANE, an edge-based AI system for non-destructive sugarcane quality grading and maturity detection using RGB-HSV imaging. Developed under the Agile-Scrum Methodology, it integrates a computer vision pipeline with a deterministic backend model. Two models, ResNet-18 and YOLOv8, were trained on 10,229 images of three sugarcane cultivars (VMC 84-524, VMC 84-947, and MAURITIO RC888) across three maturity stages. YOLOv8 attained 97.68% accuracy, while ResNet-18 achieved 97.54%. The system fuses visual predictions with farmer-reported data, such as disease severity, weeding, fertilizer application, and ratoon stage, to scale Sugar Regulatory Administration (SRA) baselines into actionable yield forecasts (LKG/TC and LKG/HA). This study builds on prior computer vision applications in agriculture, where YOLO-based models achieved over 91% accuracy in fruit maturity detection (Yuan et al., 2025; Sun & Wang, 2025). Similarly, Seo and Sim (2024) showed that a hybrid YOLOv8–ResNet50 model outperformed single-model approaches in diagnosing pepper crop diseases, underscoring the complementary strengths of YOLO-based and ResNet-based deep learning models in agricultural image analysis. It aligns with AI-driven decision-support systems that integrate agronomic data to guide farmer decisions on irrigation, fertilization, and harvest scheduling (Vamsi et al., 2026). VISCANE extends these approaches to localized sugarcane contexts. Despite strong performance, limitations include restricted validation to three cultivars and classification errors in MAURITIO RC888 Mature samples. Future work should expand validation across regions, cultivars, field conditions, camera devices, integrate IoT-based agronomic data, and enhance model transparency.

Keywords: Sugarcane maturity detection; Edge-based AI; Image classification; Decision support system

1. Introduction

Sugarcane (Saccharum officinarum) is one of the world's most important crops. It produces over 1.9 billion metric tons annually, and is a major source of sugar, bioethanol, and biomass energy (Food and Agriculture Organization of the United Nations, 2025). According to Rose and Chilvers (2018), farmers face challenges such as climate change, resource scarcity, and market instability, which have led to the adoption of digital tools, such as artificial intelligence and precision farming, to improve productivity and sustainability.

In Southeast Asia, sugarcane supports rural employment and regional growth, however, it still faces pressures from changing weather, labor shortages, and weak supply chains (Solomon et al., 2024). Countries such as Thailand, the Philippines, and Indonesia are adopting technologies, such as, satellite imaging, mobile advisory services, and blockchain systems, to improve transparency (Diyanah, Kozono, and Hazmi, 2024). But, despite these advances, rural adoption remains low because of poor infrastructure and limited digital skills (Montesclaros and Teng, 2023).

In the Philippines, sugarcane covers more than 400,000 hectares of land, with 85% of farmers cultivating plots of five hectares or less (Sugar Regulatory Administration [SRA], 2019). This smallholder dominance leaves the industry vulnerable to unstable yields and market price volatility. Programs like block farming and digital agriculture have shown potential to increase productivity and incomes (Pantoja et al., 2019; Briones et al., 2023). However, adoption remains limited due to the need for inclusive policies and cooperative systems (Oñal, Junitilla, and Ortega, 2021).

Negros Occidental, known as the "Sugar Bowl of the Philippines," produces more than half of the country's sugar. Yet smallholder farmers, particularly in agricultural municipalities like Isabela,

Negros Occidental, which serves as the primary scope of this study, continue to struggle with declining yields, rising costs, and climate risks (Briones, Galang, and Latigar, 2023). Reliance on traditional practices and limited access to digital tools reduce competitiveness, which makes technology adoption essential to sustain livelihoods and protect the province's role in the national sugar industry (SRA, 2019).

To address these challenges, this study introduces VISCANE: An Edge-Based AI System for Sugarcane Quality Grading and Maturity Detection Using RGB-HSV Imaging. VISCANE integrates farmer-reported inputs with image-based maturity classification to generate real-time predictions of sugar content. Specifically, the system employs YOLOv8 for stalk detection and ResNet-18 for maturity classification. Prior studies have demonstrated YOLO's effectiveness in fruit maturity detection, achieving over 91% accuracy in blueberry ripeness classification (Yuan et al., 2025; Sun & Wang, 2025). Similarly, Vamsi et al. (2026) showed that AI-driven decision-support systems can integrate agronomic data to guide farmer decisions on irrigation, fertilization, and harvest scheduling. Most notably, Seo and Sim (2024) found that a hybrid YOLOv8–ResNet50 model outperformed single-model approaches in diagnosing pepper crop diseases, highlighting the complementary strengths of YOLO in object detection and ResNet in feature extraction. Grounded in the principles of precision agriculture (Rose & Chilvers, 2018), VISCANE extends these proven approaches to localized sugarcane contexts.

By means of offering a low-cost, non-destructive, and accessible tool, the system empowers smallholder farmers, guides them in assessing sugarcane quality before and after harvest, and strengthens their participation in the sugarcane value chain. Furthermore, this research contributes to inclusive digital transformation and aligns with national and ASEAN priorities for resilience and competitiveness.

Conceptually, the study is anchored on precision agriculture and AI-based decision-support, where image-derived maturity predictions and farmer-reported agronomic inputs are combined to support localized harvest and yield decisions.

2. Objectives

The main objective of this study is to develop VISCANE, an edge-based AI system for sugarcane quality grading and maturity assessment using RGB-HSV imaging. The system is designed to provide smallholder farmers with a non-destructive, accessible decision-support tool that improves grading accuracy and guides farmers in evaluating the quality of sugarcane before and after harvesting.

Specifically, the study aims to:

- Design and implement an edge-based AI architecture capable of processing RGB-HSV imaging data for sugarcane quality grading, maturity detection, and variety classification across the three target cultivars (VMC 84-524, VMC 84-947, and Mauritius RC888/ Mauritio RC888).
- Establish a non-destructive imaging methodology that guarantees transparency, operational reliability, and ease of use for smallholder farmers operating in rural environments.
- Integrate beneficiary-centered features into the system to support equitable valuation and reliable crop assessment, specifically through:
    a. Inclusion of essential agronomic inputs, such as crop variety, total land area, and infestation severity;
    b. Application of computer vision for maturity detection to facilitate objective crop grading (e.g., classifying stalks as "Mature");
    c. Utilization of model-based yield calculations anchored on baseline LKG/TC and LKG/HA data from the Sugar Regulatory Administration (SRA), mathematically adjusted for agronomic penalties (e.g., a localized penalty for RSSI infestation);
    d. Computation of area-weighted LKG/TC and LKG/HA averages to project realistic, farm-level production outcomes;

e. Generation of predictive estimated yield outputs that translate the user's input land area (in hectares) into actionable Total LKG forecasts (e.g., 25 tons × 1.87 LKG/TC = 46.75 LKG); and
f. Development of transparent reporting interfaces that display these calculations in a clear, accessible format to guide farmer evaluation during pre- and post-harvest stages.

- Evaluate the system's effectiveness and efficiency in both pre-harvest and post-harvest settings, ensuring alignment with local realities, improved decision-making, and farmer empowerment through accessible and actionable insights.

3. Materials and methods

3.1 Research Design

The study developed and evaluated VISCANE, an edge-based AI system for sugarcane quality grading and maturity detection. The system combined image-based classification with farmer-provided agronomic inputs to support harvest-readiness assessment, estimated yield computation, and recommendation generation. The work followed an applied system-development design, where the mobile application, backend services, image-classification model, and yield-estimation workflow were built and tested as one integrated prototype.

The development process followed an iterative Agile-Scrum approach. Each development cycle focused on a specific system function, such as image capture, model training, maturity classification, agronomic input collection, yield calculation, and report generation. This process allowed the system to be refined based on implementation testing and model-evaluation results.

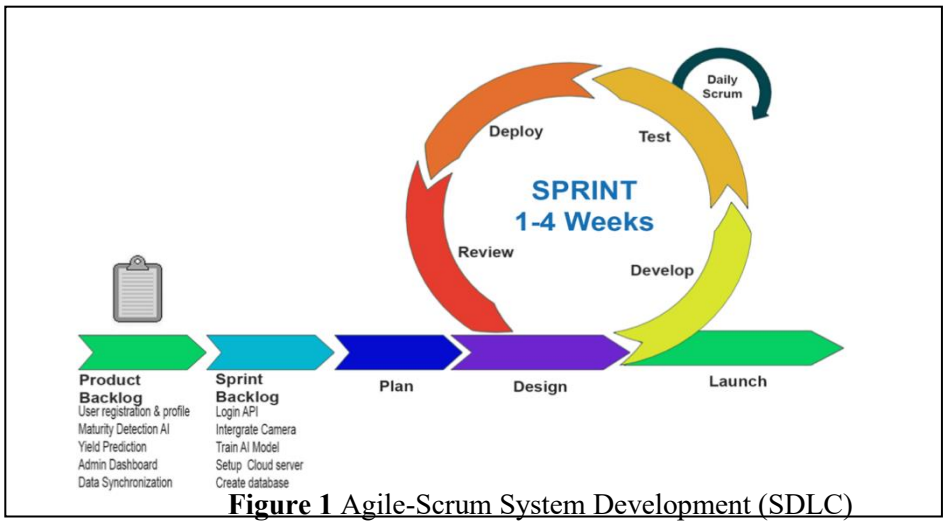

Figure 1 Agile-Scrum System Development (SDLC)

3.2 System Workflow

The VISCANE workflow began with the farmer capturing a sugarcane image through the mobile application. The system then processed the image for maturity and variety classification. The classification result was combined with farmer-entered agronomic data, including sugarcane variety, farm size, RSSI infestation severity, weeding frequency, fertilizer application frequency, ratoon stage, and plowing frequency.

After receiving these inputs, the system applied a deterministic yield-estimation process. The selected variety determined the baseline values and weighting factors used in the computation. The maturity classification affected the final estimate through maturity-based penalties. A Mature classification applied no maturity penalty, while Not Mature and Over Mature classifications reduced the estimated output according to the predefined variety-specific penalty values.

The final output included estimated LKG/TC, estimated LKG/HA, and farmer-facing recommendations. These recommendations were generated based on the predicted maturity status and the agronomic conditions entered by the user.

3.3 Dataset Preparation

The image dataset was prepared according to the sugarcane variety and the maturity condition. The supported varieties were VMC 84-524, VMC 84-947, and MAURITIO RC888 / Mauritius RC888. The maturity classes were Not Mature, Mature, and Over Mature. For model training, each image was assigned to a combined variety-and-maturity category. This allowed the model to learn both the sugarcane variety and the maturity condition from the same image. The implemented categories included the following nine classes:

Table 1 Categories and Classes of Datasets

Variety and Maturity Category	Variety	Maturity Class
VMC 84-524, Mature	VMC 84-524	Mature
VMC 84-524, Not Mature	VMC 84-524	Not Mature
VMC 84-524, Over Mature	VMC 84-524	Over Mature
VMC 84-947, Mature	VMC 84-947	Mature
VMC 84-947, Not Mature	VMC 84-947	Not Mature
VMC 84-947, Over Mature	VMC 84-947	Over Mature
MAURITIO RC888/Mauritius RC888, Mature	MAURITIO RC888/ Mauritius RC888	Mature
MAURITIO RC888/Mauritius RC888, Not Mature	MAURITIO RC888/ Mauritius RC888	Not Mature
MAURITIO RC888/Mauritius RC888, Over Mature	MAURITIO RC888/ Mauritius RC888	Over Mature

The dataset preparation followed a classification-based structure. Images were first organized by sugarcane variety and maturity status. The system then verified whether each image file could be opened properly. Corrupt or unreadable images were excluded from the prepared dataset. Exact duplicate files were grouped during preprocessing to reduce direct duplicate leakage, while near-duplicate captures were reviewed through the split-audit process.

After validation and grouping, the images were divided into training, validation, and testing sections. The training section was used to fit the classification models, the validation section was used to monitor model performance during training, and the testing section was reserved for final evaluation. In the documented training run, the prepared dataset contained 10,229 images: 3,416 for training, 3,404 for validation, and 3,409 for testing.

Table 2 Datasets

Sugarcane Varieties and Maturity	Sample Images	Training Images	Testing Images	Validation Images	Total Images
VMC 84-524 (Not Mature)		357	357	356	1,070
VMC 84-524 (Mature)		329	328	327	984
VMC 84-524 (Over Mature)		232	231	231	694
VMC 84-947 (Not Mature)		421	421	420	1,262
VMC 84-947 (Mature)		436	434	433	1,303
VMC 84-947 (Over Mature)		462	461	461	1,384
MAURITIO RC888/Mauritius RC888 (Not Mature)		381	380	381	1,142
MAURITIO RC888/Mauritius RC888 (Mature)		442	441	440	1,323
MAURITIO RC888/Mauritius RC888 (Over Mature)		356	356	355	1,067
TOTAL		3,416	3,409	3,404	10,229

Table 3 Dataset Distribution

Dataset Section	Purpose	Number of Images	Dataset Percentage
Training Set	Used to train the image-classification models	3,416	33.39%
Validation Set	Used to monitor model performance during training	3,404	33.28%
Testing Set	Used for final model evaluation	3,409	33.33%
Total Prepared Dataset	Complete dataset used in the study	10,229	100%

3.4 Image Preparation and Augmentation

Before training, images were checked and prepared to ensure that the models received consistent inputs. For ResNet-18 classification, each training image was first resized to 256 x 256 pixels and then randomly cropped using RandomResizedCrop with a scale range of 0.95 to 1.00 and an aspect-ratio range of 0.95 to 1.05. The cropped image was then resized to the model input size of 320 x 320 pixels.

Data augmentation was applied only to the training set to improve the model's ability to handle field-image variation. Because the dataset contains sugarcane stalk images, the augmentation settings were kept conservative to prevent distortion of the stalk shape, rind texture, and color cues. The ResNet-18 training transform used random horizontal flipping with a probability of 0.30, random rotation up to 3 degrees, and light color jitter with brightness 0.06, contrast 0.06, saturation 0.04, and no hue shift. Images were then converted to tensors and normalized using ImageNet mean values of [0.485, 0.456, 0.406] and standard deviation values of [0.229, 0.224, 0.225]. Validation and testing images were not augmented; they were resized directly to 320 x 320 pixels, converted to tensors, and normalized with the same ImageNet values. No random crop, random rotation, ColorJitter, or flipping was applied to the validation and testing sets.

For YOLOv8 classification, conservative augmentation settings were used or recommended to avoid unrealistic geometric and color changes: hsv_h=0.001, hsv_s =0.10, hsv_v=0.10, degrees=2, translate=0.02, scale=0.10, shear=0.0, perspective=0.0, fliplr=0.3, flipud=0.0, mosaic=0.10, mixup=0.0, copy_paste=0.0, and close_mosaic=10. The augmentation design avoided vertical flipping, 90-degree rotation, significant hue or saturation changes, heavy cropping, strong perspective transformation, heavy blurring, heavy mosaicking, and mix-up.

The image workflow used RGB images as the main input representation. HSV-related adjustments were applied as part of the color augmentation process, particularly in the YOLOv8 classification training. In this implementation, HSV was used to support color variation during training rather than as a separate hand-crafted feature-extraction method.

3.5 Image-Classification Models

Two image-classification model families, ResNet-18 and YOLOv8 classification, were trained and evaluated. The suggested ResNet-18 setup employs a single output head that directly predicts the combined variety-maturity class. YOLOv8 was configured for classification and trained on the same dataset.

The deployed YOLOv8 component was used for image classification purposes. The evaluated project did not employ YOLOv8 as a bounding-box detector or for region localization. Therefore, the computer vision task assessed in this study was a combined variety-maturity image classification.

Both models were trained for 45 epochs using a batch size of 32. ResNet-18 used a 320 x 320 input after the training transform described above. The learning rate was 0.0002, and the weight decay was 0.001. ResNet-18 also employed class-weighted loss to mitigate the impact of class imbalance during training. Balanced batch sampling was maintained as an optional diagnostic configuration. The

objective of training both model families was to determine which classifier yielded superior performance within the VISCANE maturity-assessment workflow.

3.6 Maturity Interpretation

The system interpreted each predicted category according to its variety and maturity components. For example, a prediction of VMC 84-524, Mature was interpreted as the VMC 84-524 variety with a Mature maturity status. The maturity component was then used by the recommendation and yield-estimation workflow.

When the model produced probability scores across the combined classes, the system determined the ultimate maturity status by aggregating the probabilities in accordance with the maturity classes. The maturity class with the highest aggregated probability was designated as the definitive maturity outcome. This methodology enabled the system to employ a combined variety-maturity classification while still producing a straightforward maturity output for farmers.

3.7 Agronomic Parameterization and Deterministic Modeling

The predictive engine ensures reliable yield forecasts by using a deterministic, weighted-baseline approach parameterized with localized metrics from the Sugar Regulatory Administration (SRA) for common sugarcane varieties in Isabela, Negros Occidental (VMC 84-524, VMC 84-947, MAURITIO RC888).

In the backend, a Linear Regression model (fit_intercept = False) implemented in scikit-learn maps five key agronomic inputs, RSSI pest severity, weeding frequency, fertilizer frequency, ratoon stage, and plowing frequency, to variety-specific weights. When farmers submit scans, their field inputs are evaluated against these weights to compute a continuous agronomic adjustment variable (A), which refines yield predictions to actual farm conditions.

3.7.1 Yield Prediction and Quality Grading Algorithms

The final algorithmic grading relies on the mathematical fusion of the edge-derived visual features and the cloud-computed agronomic variables. First, the mean Visual Grade is calculated from the computer vision output array:

$$Visual\ Grade = \frac{1}{n}\sum_{i=1}^{n} Visual\ Feature_i$$

The regression engine computes the raw Agronomic Adjustment (A) while isolating negative field-management practices into an Agronomic Penalty (P). A variety-specific maturity penalty, derived from computer vision classification, is incorporated to enforce yield deductions from issues such as sucrose inversion in over-mature cane or excess moisture in under-mature cane.

$$\mathrm{A} = \sum_{k}(w_k \times x_k)$$

$$P = \sum_{k}(0, w_k \times x_k) + w_{maturity(v)}$$

To prevent the computation of negative theoretical yields, the penalty is converted into a bounded Agronomic Multiplier (M):

$$M = \max(0, 1 + P)$$

The final predictive yield outputs ($\hat{y}$) are computed by scaling the official SRA Baselines *(B)* using the multiplier *(M)*. These functions strictly bound the predictions, ensuring they do not exceed the theoretical maximums for the selected variety *(v)*, ratoon stage *(s)*, and farm size in hectares *(h)*:

$$\hat{y}_{LKGTC} = max\left(0, min\left(B_{LKGTC(v,s)}, B_{LKGTC(v,s)\times} M\right)\right)$$

$$\hat{y}_{TCHA} = max\left(0, min\left(B_{TCHA(v,s)\times} h, B_{TCHA(v,s)\times} h \times M\right)\right)$$

Ultimately, the system outputs the final Predicted Quality Grade by directly fusing the AI visual assessment with the regression-based agronomic adjustment:

$$Predicted\ Quality\ Grade\ =\ Visual\ Grade\ +\ A$$

3.7.2 Varietal Parameterization and Agronomic Weighting Algorithms

The predictive engine is parameterized for three dominant sugarcane cultivars commonly grown within the study scope, Isabela Negros Occidental, each with distinct agronomic responses and penalty structures. VMC 84-524 benefits strongly from frequent weeding and precise fertilizer application but is moderately sensitive to ratoon aging, with penalties for both premature and delayed harvests. VMC 84-947, a fast-growing variety, requires less weeding and plowing and shows resilience across ratoon stages, yet it incurs a severe penalty when over-mature due to rapid sucrose inversion. In contrast, MAURITIO RC888 responds only moderately to standard cultivation practices but is highly vulnerable to foliar diseases, resulting in stronger penalties under RSSI infection, and suffers heavily if harvested prematurely because of its slow Brix accumulation. Together, these varietal parameterizations ensure that yield predictions account for the unique biological resilience, cultivation requirements, and maturity risks of the most prevalent cultivars in the region.

3.7.3 Summary of Agronomic Weights

Table 4 outlines the comparative distribution of the predefined agronomic weights (w_k) assigned to field inputs, as well as the dynamic maturity penalties $(w_{maturity(v)})$ triggered by the computer vision classification across the supported cultivars.

Table 4 Distribution of Variety-Specific Agronomic Weights *(w)*

Agronomic Input Variable *(x)*	VMC 84-524 Weight (*w*)	VMC 84-947 Weight *(w)*	MAURITIO RC888 Weight *(w)*
RSSI (Disease Severity)	-0.45	-0.45	-0.55
Weeding Frequency	0.35	0.28	0.28
Fertilizer Application	0.25	0.18	0.18
Ratoon Stage	-0.12	-0.05	-0.12
Plowing Frequency	0.08	0.05	0.08
CV Classification			
Maturity: Not Mature	-0.20	-0.18	-0.22
Maturity: Mature	0.00	0.00	0.00
Maturity: Over Mature	-0.15	-0.22	-0.18

3.8 Automated Decision Support and Recommendation Engine

The backend doubles as an automated agronomic advisory tool, using decision support to compare predicted LKG/TC against an 85% threshold. If yields fall short, it analyzes penalty vectors to generate targeted interventions, such as chemical control alerts for severe RSSI or corrective fertilizer and weeding schedules. The Recommendation Engine also issues real-time harvest directives. Stalks classified as “Not Mature” prompt advisories to delay cutting to allow for optimal sucrose accumulation; “Mature” classifications trigger recommendations to finalize immediate harvest and transport logistics; and “Over Mature” results issue urgent alerts to expedite harvesting to mitigate further yield degradation caused by sucrose inversion.

4. Results

4.1 Overall Model Performance

Both implemented classifiers demonstrated high performance during the documented training procedure. ResNet-18 attained a best validation accuracy of 97.69% and a final test

accuracy of 97.54%. The YOLOv8 classification model achieved a maximum validation accuracy of 98.18% and a final test accuracy of 97.68%.

Both models were evaluated using 3,409 testing images and nine artifact categories. The results demonstrate that both classifiers performed strongly on the prepared VISCANE image classification dataset, with YOLOv8 achieving a slightly higher final test accuracy and ResNet-18 delivering comparably strong performance.

Table 5 Overall Classification Performance

Model	Best Validation Accuracy	Test Accuracy	Testing Images	Number of Classes
ResNet-18	97.69%	97.54%	3,409	9
YOLOv8 Classification	98.18%	97.68%	3,409	9

4.2 Variety and Maturity Accuracy

The diagnostic evaluation distinguished between variety-recognition and maturity-recognition accuracy independently from the exact combined-label outcome. This distinction clarified whether the models effectively learned the variety component, the maturity component, or only the joint class label.

For ResNet-18, the diagnostic accuracy specific to variety accomplishments reached 99.88%, whereas the diagnostic accuracy exclusive to maturity was 97.54%. For YOLOv8, both the variety-specific and maturity-specific diagnostic accuracies were 97.68%. These findings show that both models effectively captured the visual patterns essential for the recognition of variety and maturity within the refined dataset.

Table 6 Diagnostic Accuracy by Evaluation Category

Model	Exact Combined-Label Accuracy	Variety-Only Accuracy	Maturity-Only Accuracy
ResNet-18	97.54%	99.88%	97.54%
YOLOv8 Classification	97.68%	97.68%	97.68%

4.3 Per-Class Performance

The ResNet-18 per-class results showed high performance across the nine classes. Eight classes attained an accuracy of at least 98.78%, and six classes achieved 100.00% accuracy. The only notably lower-performing class was MAURITIO RC888 / Mauritius RC888, Mature, which attained an accuracy of 82.31% on 441 test images.

The lower result for MAURITIO RC888 / Mauritius RC888, Mature, indicates that this class remained the primary source of residual error for ResNet-18. Most other variety-maturity categories were classified with minimal or no errors.

Table 7 ResNet-18 Per-Class Accuracy

Variety and Maturity Category	Accuracy	Test Images
VMC 84-524, Mature	98.78%	328
VMC 84-524, Not Mature	99.44%	357
VMC 84-524, Over Mature	100.00%	231
VMC 84-947, Mature	100.00%	433
VMC 84-947, Not Mature	100.00%	421
VMC 84-947, Over Mature	100.00%	461
MAURITIO RC888 / Mauritius RC888, Mature	82.31%	441
MAURITIO RC888 / Mauritius RC888, Not Mature	100.00%	381
MAURITIO RC888 / Mauritius RC888, Over Mature	100.00%	356

4.4 Classification Errors

The remaining confusion errors associated with ResNet-18 were primarily concentrated in the MAURITIO RC888 / Mauritius RC888, Mature category. The most significant misclassification occurred when images of MAURITIO RC888 / Mauritius RC888, Mature were predicted as

MAURITIO RC888 / Mauritius RC888, Not Mature, accounting for 58 instances. The second most frequent error involved predictions of MAURITIO RC888 / Mauritius RC888, Mature as MAURITIO RC888 / Mauritius RC888, Over Mature, with 18 instances.

Table 8 Major ResNet-18 Classification Errors

Actual Category	Predicted Category	Count
MAURITIO RC888 / Mauritius RC888, Mature	MAURITIO RC888 / Mauritius RC888, Not Mature	58
MAURITIO RC888 / Mauritius RC888, Mature	MAURITIO RC888 / Mauritius RC888, Over Mature	18
VMC 84-524, Mature	VMC 84-524, Not Mature	2
VMC 84-524, Mature	VMC 84-947, Not Mature	2
VMC 84-524, Not Mature	VMC 84-524, Mature	2
MAURITIO RC888 / Mauritius RC888, Mature	VMC 84-524, Over Mature	1
MAURITIO RC888 / Mauritius RC888, Mature	VMC 84-947, Not Mature	1

4.5 Dataset Quality and Diagnostic Findings

The dataset summary included all nine expected variety-maturity classes and did not generate any low-sample warnings at the specified threshold. Each class was represented by several hundred images within the training, validation, and test sets. This class coverage contributed to the stability of the results on a per-class basis.

Although the documented results were strong, split independence remains an important validation concern for image datasets collected from similar cane or stalk captures. Exact duplicate files were handled during preprocessing, but near-duplicate captures should still be reviewed using the split-audit output. This check is important because visually similar images across the training, validation, and test sets can inflate measured accuracy.

4.6 System Output

The output of the trained model was incorporated into the VISCANE decision-support workflow. The system used the predicted maturity status as one of the inputs for yield estimation and recommendation formulation. When the model classified a sample as Mature, the system provided harvest-readiness recommendations. When the model classified a sample as Not Mature, the system recommended delaying harvesting. When the model classified a sample as Over Mature, the system advised urgent harvesting to mitigate potential quality degradation.

The system also considered the agronomic inputs provided by the user. RSSI severity, farm size, weeding, fertilizer application, ratoon stage, and plowing frequency influenced the final estimated values of LKG/TC and LKG/HA. This enabled VISCANE to generate recommendations based on both visual maturity and field management conditions.

5. Discussion

The results demonstrate that the VISCANE prototype successfully implemented an end-to-end process for image-based sugarcane classification, maturity interpretation, yield estimation, and farmer recommendation. In the evaluation, both ResNet-18 and YOLOv8 classifiers attained high accuracy on the prepared dataset. YOLOv8 achieved the highest final test accuracy at 97.68%, whereas ResNet-18 attained 97.54%.

The diagnostic evaluation showed strong performance in both variety recognition and maturity recognition. ResNet-18 attained an accuracy of 99.88% for variety-only diagnostics and 97.54% for maturity-only diagnostics. Similarly, YOLOv8 achieved 97.68% accuracy across both diagnostic categories. These findings demonstrate that the dataset and training enabled both models to effectively learn the critical visual distinctions necessary for VISCANE's workflow.

The residual errors associated with ResNet-18 were concentrated in MAURITIO RC888 / Mauritius RC888, Mature. The majority of these inaccuracies involved predictions within the same

variety but a different maturity status, particularly Not Mature and Over Mature. This indicates that the remaining difficulty is not related to confusion among broad varieties but rather pertains to the distinction of fine-grained maturity levels within MAURITIO RC888 / Mauritius RC888.

The documented dataset included all nine expected variety-maturity classes. No low sample sizes were noted, and each class contained hundreds of test images. This supports the reliability of the reported performance metrics within the prepared dataset.

However, the high accuracy should be interpreted together with split-quality evidence. The presence of near-duplicate images from the same cane or stalk across training, validation, and testing datasets may result in the validation and testing performance metrics overestimating actual field generalization. Future research should incorporate cane- or stalk-level split auditing and, if possible, include an independent field-test dataset collected separately from the training images.

The implemented project also clarified the precise role of YOLOv8 within the system. In the version evaluated, YOLOv8 was trained specifically as an image-classification model rather than a detection model. Therefore, the present research findings should characterize YOLOv8 as a baseline for classification within the project. Should a future iteration incorporate sugarcane stalk detection or localization, that version should be evaluated separately using detection-specific outputs.

Overall, the project demonstrates that VISCANE can combine image classification with deterministic agronomic computation to support sugarcane quality assessment. The system workflow is functional, and the results show strong classification performance on the prepared dataset. Future research should focus on confirming split independence, validating the model on a separately collected field-test set, reviewing the remaining MAURITIO RC888 / Mauritius RC888 Mature confusion cases, validating maturity labels with domain experts, and standardizing field-image capture. For practical deployment, the system should also be tested across more farms, lighting conditions, camera devices, and sugarcane varieties before full-scale adoption.

6. Conclusion

The study designed and implemented VISCANE, an edge-based AI system for sugarcane quality grading, maturity detection, and yield estimation. The model evaluations showed excellent performance, with YOLOv8 reaching 97.68% accuracy and ResNet-18 close at 97.54%. The system's primary strength is its hybrid architecture, which integrates computer vision outputs with user-entered field parameters, such as disease severity, fertilizer use, plowing and weeding frequency, and ratoon stage to support real-time agronomic adjustments and harvest recommendations.

Although the overall results demonstrate high effectiveness, minor errors were observed, particularly in distinguishing subtle maturity variations within the MAURITIO RC888 variety, underscoring the inherent difficulty of identifying phenotypic similarities across growth stages. The high accuracy suggests a need for split-independence auditing to prevent inflated results from similar field captures. Future work should validate models against independent datasets, expand the dataset to resolve misclassifications, and include more local sugarcane varieties.

Overall, VISCANE represents a practical, transparent, and accessible tool that transitions crop assessment from subjective assumptions to data-driven analysis, thereby addressing vulnerabilities within the local sugar industry. Its offline functionality helps smallholder farmers improve harvest timing, reduce penalties, and increase yields, supporting economic resilience in agriculture.

Acknowledgments

This study was made possible by the guidance, support, and encouragement of many individuals and institutions to whom the researchers owe their deepest gratitude.

The researchers extend their profound appreciation to Mr. Lynol I. Ibarra for his invaluable mentorship, dedicated assistance, and commitment, spanning the initial planning stages through the full development of the study and system, and for providing clarity throughout the research process.

Special thanks are also extended to their thesis coordinator, Engr. Orville Balangue, MSCS, and to Mr. Raymart B. Abella, for their insights and constructive feedback that greatly enhanced the quality of this work, and to Dr. Mae B. Lodana, whose constant support and encouragement sustained the researchers in completing this endeavor.

The researchers are also equally grateful to Ms. Danica Duazo, Mr. Ariel Sumagaysay, MSCS, and Mr. Jerome Lontes for generously sharing their expertise and recommendations, which significantly refined and improved the study.

Heartfelt gratitude is given to the families, friends, and sources of inspiration of the researchers for their unwavering encouragement, understanding, and moral support, which provided strength and motivation throughout this academic journey.

Finally, the researchers also acknowledge the Sugar Regulatory Administration (SRA), PHILSURIN, and the various farmers of Isabela, Negros Occidental, for their cooperation, valuable contributions, and insights, that has offered essential perspectives to ground this study in practical relevance and ensured its alignment with the realities of the local sugarcane industry.

References

Briones, R., Galang, I. M., & Latigar, J. (2023). Transforming Philippine Agri-Food Systems with Digital Technology: Extent, Prospects, and Inclusiveness. In *Philippine Institute for Development Studies*. https://pidswebs.pids.gov.ph/CDN/document/pidsdps2329.pdf

Diyanah, S. M., Kozono, M., & Hazmi, A. (2024, December 29). Accelerating the digitalisation of the agriculture and food system in the ASEAN region. *Eria.org.* https://www.eria.org/research/accelerating-the-digitalisation-of-the-agriculture-and-food-system-in-the-asean-region

Food and Agriculture Organization of the United Nations. (2025). Sugar cane production. *Our World in Data.* https://ourworldindata.org/grapher/sugar-cane-production. Retrieved November 11, 2025.

Montesclaros, J. M. L., & Teng, P. S. (2023). Digital technology adoption and potential in Southeast Asian agriculture. *Asian Journal of Agriculture and Development, 20*(2), 7–30. https://doi.org/10.37801/ajad2023.20.2.2

Oñal, P., Juntilla, R., & Ortega, J. (2021). Degree of farming innovations and the level of productivity of sugarcane farmers in the Visayas, Philippines. *European Journal of Agricultural and Rural Education (EJARE),* 57–67. https://media.neliti.com/media/publications/382222-degree-of-farming-innovations-and-the-le-3875268d.pdf

Pantoja, B., Alvarez, J., & Sanchez, F. (2019). Implementing sugarcane block farming for increased farm income and productivity. *Philippine Institute for Development Studies.* https://pidswebs.pids.gov.ph/CDN/PUBLICATIONS/pidsrp0901.pdf

Rose, D. C., & Chilvers, J. (2018). Agriculture 4.0: Broadening responsible innovation in an era of smart farming. *Frontiers in Sustainable Food Systems, 2*(87). https://doi.org/10.3389/fsufs.2018.00087

Solomon, S., Khumla, N., Manimekalai, R., & Misra, V. (2024). Prospects of diversification for sustainable sugar bioenergy industries in ASEAN countries. *Sugar Tech, 26,* 951–971. https://link.springer.com/article/10.1007/s12355-024-01432-x

Sugar Regulatory Administration (SRA). (2019). Overview of the sugarcane industry. https://www.sra.gov.ph/storage/OVERVIEW-OF-THE-SUGARCANE-INDUSTRY_September-2019.pdf. Retrieved October 27, 2025.

Yuan, J., Fan, J., Sun, Z., Liu, H., Yan, W., Li, D., Liu, H., Wang, J., & Huang, D. (2025). Deployment of CES-YOLO: An Optimized YOLO-Based Model for Blueberry Ripeness Detection on Edge Devices. *Agronomy*, *15*(8), 1948. https://doi.org/10.3390/agronomy15081948

Sun, H., & Wang, R.-F. (2025). BMDNet-YOLO: A Lightweight and Robust Model for High-Precision Real-Time Recognition of Blueberry Maturity. *Horticulturae*, *11*(10), 1202. https://doi.org/10.3390/horticulturae11101202

Vamsi, K., Sumanth, M., Keerthi, K., Lakshmi, T. V., & Kishore, N. (2026). AI-Integrated Precision Agriculture Monitoring and Decision Support System. *Journal of Emerging Technologies and Innovative Research (JETIR)*, *13*(2). https://www.jetir.org/papers/JETIR2602473.pdf

Seo, J.-I., & Sim, H. (2024). *Integrated deep learning models for precise disease diagnosis in pepper crops.* http://koreascience.or.kr/journal/view.jsp?kj=KCTSAD&py=2024&vnc=v19n4&sp=79

AlistodDalang: An IoT-Driven, Solar-powered Fire Detection Sensor and Real-Time Alert System for the Remote Areas

Bryan O. Mislang*, Angel Aizy F. Madelo, Tristan D. Borromeo, Omar Mohammed Hussien Al-awlaqi
[1]Lyceum-Northwestern University
*Email : mislang.bryan.o@lyceum.edu.ph

Abstract

The increasing occurrence of fire incidents in remote and rural communities continues to pose a serious threat to lives, properties, and environmental safety, especially in areas where access to emergency infrastructure, electricity, and internet connectivity is limited. This challenge underscores the urgent need for a reliable and real-time fire detection system that can operate effectively in off-grid environments and provide immediate alerts to responders and community members. In response, the study titled AlistodDalang was developed using a Design Science Research approach to design, build, and evaluate an innovative solution tailored for such environments. The system integrates smoke and flame sensors with an Arduino-based microcontroller for continuous monitoring, and utilizes a GSM SIM800L module to send SMS and call notifications when fire hazards are detected, ensuring functionality even without internet access. A solar-powered energy system with battery storage supports continuous operation, making the device suitable for deployment in remote locations with unstable or unavailable power sources. To enhance usability and monitoring capability, a web-based platform was also developed to visualize real-time alerts, device status, and geolocation data. Evaluation of the system was conducted using the System Usability Scale (SUS) with respondents from local government units, the Bureau of Fire Protection, and barangay communities. Results revealed a high level of effectiveness and usability, with a mean SUS score of 89.24, interpreted as an Excellent rating and indicating strong user acceptance. Overall, the system provides a practical and sustainable solution for fire safety enhancement.

Keywords: IoT-based Fire Detection; Real-Time Alert System; Emergency Response; Solar-Powered Monitoring; Rural Community Safety

1. Introduction

Forest fires are one of the most destructive natural disasters, causing severe environmental damage, loss of biodiversity, and threats to human life and infrastructure. Detecting fires at an early stage is essential to prevent them from spreading and causing large-scale destruction. Recent technological advancements have introduced the use of satellite-based Internet of Things (IoT) systems for forest monitoring and early fire detection. In this approach, sensors placed on trees or on the forest floor measure environmental factors such as temperature, humidity, atmospheric pressure, and smoke levels to identify the initial signs of combustion. When abnormal conditions are detected, the sensors transmit alert messages through satellites to ground stations, enabling authorities to receive notifications within minutes and respond quickly. This technology is particularly useful in remote forest areas where terrestrial communication networks are limited or unavailable, allowing continuous monitoring and faster emergency response to wildfire outbreaks (Kinéis, 2023).

Fire incidents and emergencies can occur at any time and place, regardless of the precautions taken. For instance, on November 25, 2018, a fire in Seoul severely damaged KT's underground cable tunnels, cutting 168,000 telephone lines and disrupting hospitals, banks, and other institutions (Sensor,2021). On June 2, 2025, a residential fire in Las Piñas and Parañaque, Metro Manila displaced more than 150 residents and injured five individuals after a domestic accident involving hot cooking oil (Macababbad, 2025). On April 6, 2024, a forest fire in Aguilar and Bugallon, Pangasinan spread through inaccessible mountain areas where firefighting was hampered by poor road access, underscoring the dangers of fires in rural and forested regions (GMA News, 2024). These incidents show that fire hazards affect both urban and rural areas, with severe consequences for health, infrastructure, and community safety.

Although commercial fire detection systems are available, most are costly, heavily reliant on electricity, and dependent on internet connectivity. This makes them unsuitable for rural or off-grid communities where infrastructure is weak and power is unreliable. Moreover, many existing systems

do not integrate mobile communication features such as SMS alerts, which are vital for quick response in areas with limited resources. Consequently, communities remain vulnerable to delayed fire detection and slower emergency response. This situation highlights the urgent need for a low-cost, solar-powered, and IoT-enabled fire detection system that operates reliably even in underserved and remote environments (Grey, 2025).

This study supports several Sustainable Development Goals (SDGs). It contributes to SDG 3 (Good Health and Well-being) by reducing fire-related risks and protecting lives, and to SDG 7 (Affordable and Clean Energy) through the use of solar power. By integrating IoT technologies, it advances SDG 9 (Industry, Innovation, and Infrastructure), while also promoting safer and more resilient communities in line with SDG 11 (Sustainable Cities and Communities). Furthermore, the study supports SDG 17 (Partnerships for the Goals) by encouraging collaboration among local government units, fire protection agencies, and community leaders in implementing and sustaining the system. Overall, AlistodDalang promotes innovation, sustainability, and inclusive safety for vulnerable communities.

2. Objectives

This study aimed to design, develop, and evaluate the AlistodDalang solar-powered, IoT-driven fire detection and real-time alert system for remote areas and communities with available cellular signal coverage. Specifically, it analyzed the existing challenges in fire detection and emergency response in remote areas with limited yet available cellular connectivity. It also determined the required data inputs, hardware components, and communication technologies necessary for developing an IoT-based fire detection system suitable for off-grid and geographically isolated environments that can utilize cellular networks. Furthermore, the study designed and developed the AlistodDalang system integrating smoke and flame sensors, GSM-based alert mechanisms, solar power capability, and a web-based monitoring platform for real-time data tracking and alert management. In addition, it identified and implemented essential system features that ensured reliable automated alerts and real-time notifications, even in areas with weak or unstable cellular signals. Finally, the study evaluated the usability, functionality, reliability, and user acceptance of the developed system when deployed in selected remote and rural communities with cellular signal availability.

3. Materials and Methods

This study employed Design Science Research (DSR) as its overall research design, which focuses on developing and evaluating artifacts to solve real-world problems while contributing to knowledge (Brocke et al., 2020). DSR is an iterative approach that allows continuous refinement of a system through repeated cycles of design, development, and evaluation. The proponents selected this methodology to develop *AlistodDalang:* An IoT-Driven Fire Detection Sensor and Real-Time Alert System for Remote Areas and Rural Communities, as it supports the creation of a practical and effective safety solution tailored to underserved areas. Through DSR, the study followed a structured process consisting of problem awareness, suggestion, development, evaluation, and conclusion, ensuring that the system was systematically built, tested, and improved based on real-world conditions and user feedback.

Within the development phase of the DSR process, the Prototyping Model was utilized as the system development approach to operationalize the design and construction of the artifact. The Prototyping Model is a software development approach in which an initial version of the system is created to clarify and refine user requirements (GeeksforGeeks, 2025). In this study, the proponents used the Prototyping Model in developing *AlistodDalang*, allowing iterative feedback, continuous improvement, and enhancement of system functionality to ensure that user needs and project objectives were effectively met.

The process began with the Requirements phase, where system needs were identified and defined through interviews and consultations with end-users and stakeholders. Based on observations in remote communities, fire incidents were typically detected manually and reported through phone calls or direct visits to fire stations, often resulting in delayed response. To address this, consultations were conducted with the Bureau of Fire Protection (BFP) Aguilar and BFP Bugallon to gather both

functional and non-functional requirements, ensuring that the system aligned with actual fire monitoring and reporting practices.

In the Quick Design phase, a preliminary system design was developed to outline the structure and core functionalities of *AlistodDalang* before full implementation. This was followed by the Build Prototype phase, where a working prototype was created to demonstrate key features, validate design decisions, and prepare the system for user evaluation.

During the User Evaluation phase, the prototype was assessed by personnel from BFP Aguilar and BFP Bugallon. Their feedback focused on usability, accuracy of information, and relevance to fire monitoring operations, which helped identify areas for improvement. In the Refining Prototype phase, the system was enhanced based on user feedback, improving features, interface design, and overall performance to better meet operational needs.

Finally, in the Implement and Maintain phase, the finalized system was deployed and continuously maintained. Regular weekly testing, real-time monitoring, and scheduled monthly maintenance were conducted to ensure system reliability, stability, and sustained performance.

Through this integration, the Prototyping Model functioned as the tactical development mechanism embedded within the DSR framework, enabling iterative system realization while maintaining the methodological rigor of the research design.

4. Results

Status of the Current Fire Detection and Emergency Response

The existing fire detection and emergency response process in remote areas and communities reveals several critical gaps that hinder timely and effective action. A primary limitation is the heavy reliance on manual fire detection by constituents, which often results in delayed identification and reporting of incidents. This delay is further compounded by the lack of structured and reliable communication channels, especially in geographically isolated areas with limited infrastructure.

Another significant gap lies in the decision-making process at the barangay level, where the forwarding of reports to the Bureau of Fire Protection (BFP) is not always immediate or consistent. This introduces uncertainty and potential delays in escalation. Similarly, the BFP's response process involves additional verification and resource assessment, which, while necessary, may further prolong emergency response time in critical situations.

Moreover, the absence of an automated alert system limits real-time information dissemination among stakeholders, reducing coordination efficiency between constituents, barangay officials, and emergency responders. Although the Local Government Unit (LGU) performs documentation and post-incident recording, this occurs only after the event, indicating a gap in proactive monitoring and early intervention mechanisms.

Overall, these gaps highlight the need for a more efficient, automated, and technology-driven fire detection and alert system that minimizes human dependency, enhances communication, and ensures faster emergency response in remote and rural communities.

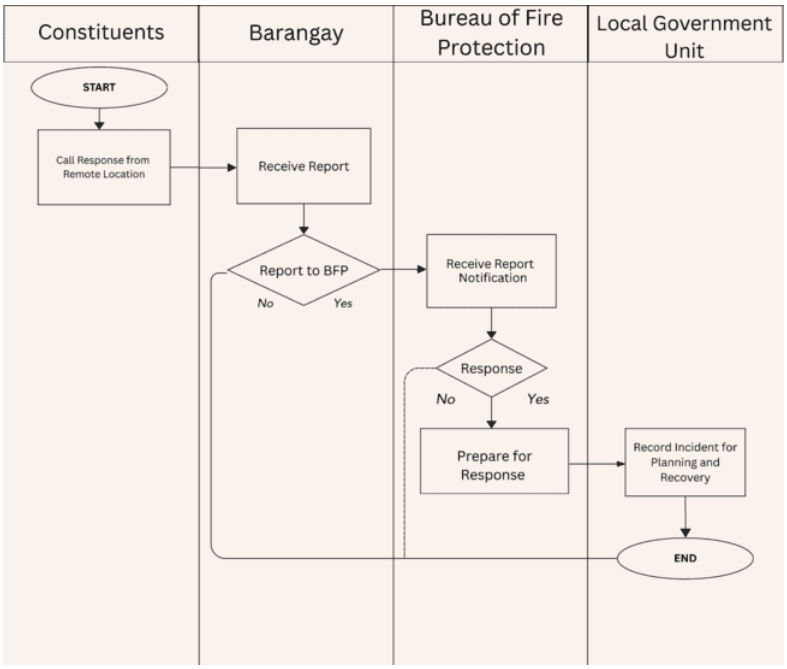

Figure 1. Current Challenges in Fire Detection Affecting Emergency Response in Remote and Rural Communities

B. Requirements in the System Design

Based on the developed proposed system, the researchers identified the following requirements that were employed in the existing AlistodDalang.

Input Requirements

Data inputs required included system-generated alerts triggered by abnormal sensor activity, providing details such as device type, hazard detected, and timestamp for immediate action. GPS-based device location data ensures accurate mapping and faster identification of fire incidents, while real-time sensor readings from smoke and flame sensors allows continuous environmental monitoring and early fire detection. Together, these inputs supports timely, accurate, and efficient emergency response.

Process Requirements

The process requires continuous collection, processing, transmission, and visualization of environmental data for timely fire detection and response. It begins with real-time data acquisition from smoke and flame sensors through an Arduino microcontroller, followed by threshold-based evaluation to identify potential fire hazards. Once abnormal conditions were detected, the system automatically generated alerts containing device information, detected hazard type, and timestamps.

These alerts are immediately communicated through a GSM module via SMS and call notifications, ensuring rapid dissemination even without internet connectivity. In parallel, sensor data are continuously transmitted to ThingSpeak for real-time logging and visualization, while alert records and system logs are stored in the Supabase backend for centralized data management and historical analysis. Finally, a monitoring dashboard integrates data from both platforms to display real-time sensor readings, alert notifications, device status, and location mapping, supporting efficient monitoring and informed emergency response.

Output Requirements

The output generated after data processing and analysis, provides essential information for monitoring and emergency response. The system produces geolocation mapping through the dashboard, which displayed device locations using predefined coordinates and data from ThingSpeak, enabling responders to quickly identify affected areas. It also generates real-time alerts when fire-related hazards are detected, showing details such as device ID, type of hazard, and time of occurrence, while simultaneously sending SMS and call notifications via the GSM module to ensure immediate dissemination of warnings. In addition, system logs and reports are stored in the Supabase backend, recording sensor readings, alerts, and device activities to support continuous monitoring, system evaluation, and future analysis.

Security Requirements

The security measures implemented to protect the AlistodDalang system's data and hardware components, ensures data integrity, reliability, and physical protection against environmental and unauthorized risks. Data integrity is maintained through secure storage of alerts and device logs in Supabase, supported by regular backups to prevent data loss and ensure system reliability. In addition, physical security is ensured by housing the devices in durable aluminum enclosures, which is protected the sensors and electronic components from physical damage, environmental exposure, and potential tampering.

Hardware Requirements

The system is composed of integrated hardware components that collectively enables fire detection, data processing, communication, and sustainable power management. The Arduino Uno functions as the main microcontroller, processing sensor inputs, executing fire detection logic, and controlling output devices such as the buzzer and GSM module. The buzzer provided a local audible alarm to immediately warn nearby individuals upon detection of fire or smoke.

For environmental monitoring, flame sensors detect infrared radiation emitted by flames, while smoke sensors measure smoke presence and concentration for early fire detection. The GSM SIM800L module enables wireless communication by sending SMS alerts and transmitting data to the ThingSpeak platform for real-time monitoring. Power is supplied through a solar panel, which provides renewable energy for continuous operation in remote areas, while a lithium battery stores the generated energy to ensure uninterrupted system performance. The charging module regulates battery charging with protection against overcharging, over-discharging, and short circuits, while the DC booster module stabilized and step-up voltage levels to meet system requirements. Jumper wires connects all components, ensuring proper integration and reliable hardware operation.

Software Requirements

The software tools and platforms support data visualization, communication, backend management, and web application development. Interactive charts are used to visualize historical smoke and fire data, alert frequency, and system performance trends, enabling users to gain actionable insights for data-driven decision-making. Leaflet is employed to implement interactive mapping features, displaying the geographical locations of fire detection devices and incident points to enhance situational awareness and emergency response coordination.

For backend services, Supabase function as the cloud database and authentication system, securely storing device information and alert records while enabling authorized access for monitoring and management. ThingSpeak serves as the IoT data ingestion and visualization platform, receiving real-time sensor readings and supporting time-series analysis of fire and smoke events. On the frontend, Vite and React are used to develop a fast, responsive, and modular web application for monitoring alerts, device status, and system activity, while Tailwind CSS provided a utility-first framework that ensured a clean, consistent, and responsive user interface across devices.

Communication Technologies Requirement

The integration of communication technologies ensures reliable data transmission, real-time monitoring, and rapid emergency notification. The GSM SIM800L module is used to send SMS-based alerts and initiate emergency calls directly to responders, LGUs, and barangay officials, ensuring fast and reliable communication even in rural areas with limited or unstable internet connectivity.

Supabase function as a cloud-based backend platform for storing and tracking alerts, which are then displayed on the system dashboard to support real-time monitoring and accessible incident information for administrators and responders. Meanwhile, the ThingSpeak IoT platform is utilized to transmit sensor readings and device status data for centralized monitoring, enabling real-time visualization, logging, and analysis of fire-related events that are integrated into the system dashboard.

C. Features of the System

The following were the features integrated into the system:

SMS and Call Alerts. This feature automatically sent real-time SMS and call notifications to registered contacts when the system detected fire indicators such as smoke or flame. Each SMS contained the device's current sensor readings, providing detailed information about detected smoke and flame levels. Using the SIM800L GSM module, the system ensured that alerts were delivered instantly, even without internet access. This enabled users and authorities to quickly assess the situation and take immediate action, enhancing response time and overall safety in remote and rural areas.

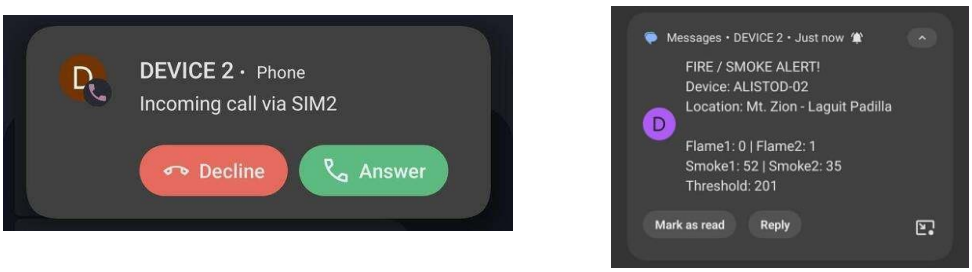

Figure 2. SMS and Call Alerts

Real-time Device Monitoring. This feature allowed users to continuously monitor the status and activity of all connected fire detection devices through the web-based platform. Sensor data such as smoke and flame levels were updated in real time, providing an accurate view of environmental conditions. Users were able to track each device's operational status, location, and alert history, enabling quick identification of potential fire threats.

Figure 3. Alert Detection and History Logging

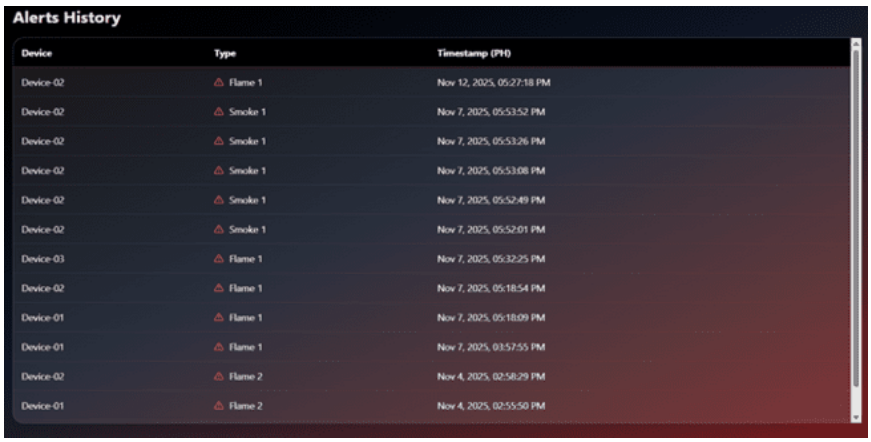

Geolocation Mapping. This feature visually displayed the exact locations of all deployed fire detection devices on an interactive map integrated into the web application. Each device marker showed real-time sensor readings, including smoke and flame levels, as well as the device name, latitude, longitude, and last update timestamp. When an alert was triggered, the corresponding device was highlighted on the map, allowing users to instantly identify where the incident occurred.

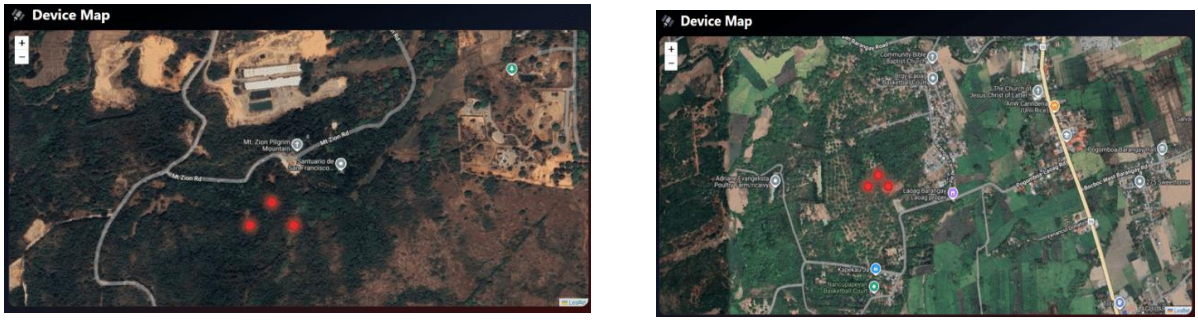

Figure 4. Geolocation Mapping of Two Areas: (1) Mt. Zion, Bugallon and (2) Brgy. Laoag, Aguilar

Solar-powered Operation. This feature enabled the entire fire detection system to operate using solar energy, ensuring continuous functionality even in areas without a stable power supply. Each device was equipped with a solar panel and rechargeable battery, allowing it to harvest and store energy during the day for uninterrupted operation at night or during power outages. This sustainable design made the system eco-friendly, cost-efficient, and highly reliable, particularly in remote and rural communities.

Figure 5: Solar-powered Operation

System Usability Scale Measurement of the System

The System Usability Scale (SUS) was developed by John Brooke in 1986 as a straightforward tool to assess the usability of virtually any system. Over nearly three decades, the SUS has demonstrated its reliability as a method for evaluating system usability, aligning well with established industry benchmarks.

The proponents conducted a face-to-face survey among 251 respondents from the LGU, BFP, and barangays in Bugallon and Aguilar. Additionally, the researchers demonstrated the developed system to these respondents to gather feedback on its functionality, usability, and relevance to community fire safety needs.

Table 1 Overall SUS Respondents Results

Respondents	Frequency	SUS Score	Adjective Rating
Aguilar (Residents)	135	92.30	Excellent
Bugallon (Residents)	84	85.45	Excellent
BFP	14	94.64	Excellent
Barangay Officials	18	95.83	Excellent
Total		**89.24**	**Excellent**

As summarized, the overall System Usability Scale (SUS) measurement presented in Table 2 indicates that the proposed system achieved a mean usability score of 89.23. This result suggests that the respondents are generally satisfied with the system's features and functionality. The obtained score falls within the "Excellent" usability range, implying that the system is easy to use, intuitive, and effective in supporting user tasks. Moreover, the result reflects a high level of user acceptance and demonstrates that the system is able to meet user expectations, although minor improvements may still be considered to further enhance overall usability.

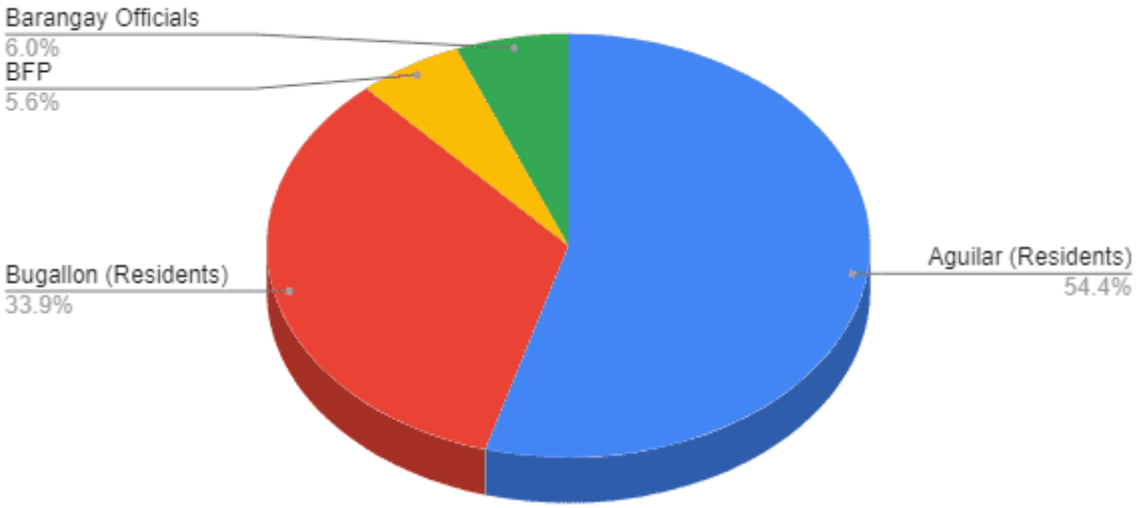

Figure 1 Respondent Frequency Percentage

The figure illustrates the distribution of respondents who participated in the usability evaluation of the AlistodDalang system. The largest proportion of respondents came from Aguilar (Residents), comprising 54.4% of the total participants, while Bugallon (Residents) accounted for 33.9%. In addition, BFP personnel represented 5.6% of the respondents, and Barangay Officials contributed 6.0%.

This distribution indicates that the evaluation was primarily influenced by end-users from Aguilar and Bugallon, which are the main deployment sites of the system. The dominance of resident respondents suggests that the SUS results strongly reflect the perspectives of community users who directly experience fire risks and system alerts in real-world conditions. Meanwhile, the inclusion of BFP personnel and barangay officials, although smaller in proportion, provides professional and administrative insights that strengthen the validity of the usability assessment.

Overall, the respondent distribution demonstrates that the SUS evaluation represents a multi-stakeholder perspective, with a strong emphasis on rural community users. This balanced participation ensures that the usability findings of the AlistodDalang system are grounded in both practical community experience and emergency response expertise, thereby enhancing the reliability and relevance of the overall assessment results.

5. Discussion

The study identified significant challenges in fire detection within remote and rural areas where only basic cellular signal coverage is available. These challenges include the absence of timely fire detection systems, limited access to reliable communication infrastructure, and delayed emergency response. Such conditions increase the risk of fire-related damage due to the lack of immediate and accessible alert mechanisms. These findings emphasized the need for an efficient, real-time, and practical fire detection solution capable of operating effectively in environments with limited connectivity, while still utilizing available cellular networks for emergency communication.

To address these issues, the developed AlistodDalang system implemented an integrated Input-Process-Output (IPO) framework. The system utilized real-time sensor readings (smoke and flame detection), GPS-based device location, and automated alert generation as key inputs. These

inputs were processed through continuous environmental monitoring, threshold-based analysis, and GSM-based communication protocols. This processing mechanism enabled the system to generate immediate alerts using cellular signal networks, ensuring functionality even in the absence of internet connectivity. The outputs of the system included real-time SMS and call alerts to responders, geolocation mapping of incidents, and system-generated logs, all of which contributed to faster decision-making and improved emergency response.

In the event of fire detection, the system initiates real-time alerts through the GSM module embedded in the sensor unit. Once smoke or flame is detected, the Arduino triggers the GSM module to send SMS notifications and place automated phone calls to pre-registered contact numbers. These contact numbers belong to authorized responders, particularly personnel from the Bureau of Fire Protection (BFP), whose mobile devices serve as the primary receivers of emergency alerts in off-grid or low-connectivity environments.

Upon receiving the alert, the responder's mobile device functions as a critical link between the remote sensor unit and the centralized monitoring system. These devices are typically located at the BFP station, positioned in the central area of the town where stable internet connectivity is available. When the responder's device is connected to the internet (via mobile data or Wi-Fi), it enables access to the system dashboard, allowing incident data to be captured, synchronized, and transmitted to cloud platforms such as Supabase and ThingSpeak.

Through this communication flow, sensor-generated data is initially transmitted via GSM to the responder's mobile device and subsequently relayed to the server/dashboard for storage, monitoring, and visualization. This ensures that immediate emergency alerts are delivered reliably even without internet access in remote deployment areas, while enhanced data logging, analysis, and real-time monitoring are achieved when connectivity becomes available at the BFP station.

Furthermore, the system's usability was evaluated using the System Usability Scale (SUS), with 251 respondents from various sectors. The system obtained a mean SUS score of 89.24, which falls under the "Excellent" category. This result indicates that the system is highly usable, efficient, and well accepted by users, although minor improvements may still be considered to further enhance user experience.

Overall, the system adopts a hybrid (dual-mode) architecture that clearly separates critical emergency functions from internet-dependent features. The core functionality—fire detection and alerting—operates entirely without internet connectivity, relying solely on GSM-based SMS and voice call alerts to ensure real-time notification. In contrast, internet connectivity is utilized only at the responder level, particularly at the BFP station where stable network access is available. At this stage, incident data is synchronized with cloud platforms using mobile data (GPRS) or internet connection, enabling secondary features such as data storage, historical logging, remote monitoring, and visualization.

This architectural approach ensures that life-critical alert mechanisms remain fully operational in disconnected environments, while still providing advanced monitoring and data management capabilities when connectivity is available. As a result, the system achieves both reliability and scalability, making it highly suitable for deployment in rural and remote communities.

6. Conclusion

Overall, the findings confirm that the AlistodDalang system is a feasible, reliable, and effective solution for fire detection and real-time alerting in remote and rural areas with cellular signal coverage. By utilizing sensor-based monitoring, GSM-based communication, GPS tracking, and solar-powered operation, the system successfully improves early fire detection and ensures timely delivery of alerts to respondents even without internet connectivity. Its strong usability rating further indicates that it is well-accepted and user-friendly. Ultimately, the system enhances situational awareness, supports faster emergency response, and strengthens fire disaster preparedness in underserved communities.

For future researcher and developers may focus on extending system coverage through alternative communication technologies (e.g., LoRaWAN or satellite), incorporating predictive analytics for proactive fire detection, and conducting large-scale deployments to validate scalability and interoperability within broader emergency response systems.

Acknowledgements

The researchers sincerely express their profound gratitude to Lyceum-Northwestern University (LNU) for providing the academic environment, resources, and support that made this study possible. Special appreciation is extended to the College of Information and Computing Studies (CICS) for its guidance, support, and valuable insights, and to thesis adviser, and the Dean for their continuous assistance, encouragement, and expertise throughout the development of this research. Their constructive feedback and academic direction greatly contributed to the improvement and successful completion of the study.

References

GeeksforGeeks. (2025, July 1 1). *Prototyping model – Software engineering*. Retrieved in Dec 2025 from https://www .geeksforgeeks.org/software-engineering-prototyping-model/

GMA Regional TV News (2024). *Forest fire hit mountains in Aguila , Pangasinan*. GMA Network. Retrieved on June 2025 from https://www .gmanetwork.com/regionaltv/ news/101296/forest-fire-hit-mountains-in-aguilar-pangasinan/story/

Grey , C. (2025). *Firefighting in remote areas. Fire Product Search*. Retrieved on June 2025 from https://www .fireproductsearch.com/firefighting-in-remote-areas/

Kinéis (2023). *The new approach of satellite Internet of Things in forest fires detection*. Retrieved on June 2025 from https://kineis.com/en/iot-satellite-forest-fire-detection/#:~:text=The%20aim%20of%20a%20fire,in%20these%20vast%20forest%20areas.

Macababbad, E. J. (2025, June 3). *5 hurt in fire crossing Las Piñas, Parañaque.* Retrieved on June 2025 from https://www.philstar.com/nation/2025/06/03/2447729/5-hurt-fire-crossing-las-pias-paraaque

Sensor , R. (2021, October 25). *Fire incidents occur frequently in the computer room. Is the computer room environmental monitoring system useful?* RIKA. Retrieved on June 2025 from https://www .rikasensor .com/fire-incidents-occur-frequently-in-the-computer-room-is-the-computer-room-environmental-monitoring-system-useful.html

Predictors of Adoption of an Automated Rice Monitoring and Management System Among Farmers in Pangasinan, Philippines

Febrey C. Lamsen
Program Head, Electronics and Computer Engineering Department
Email : Lyceum-Northwestern University

Abstract

Pangasinan's palay production faced a notable decline from 160,879 metric tons in 2018 to 158,805 metric tons in 2019, largely triggered by irrigation repairs in Sto. Tomas and Rosales. This research analyzes the predictors of technology adoption for an Automatic Rice Monitoring and Management System in Pangasinan, Philippines. Employing a descriptive-developmental design across 13 barangays, the study identifies Frequency of Agricultural Technology Use, Training Assistance, and Age as the primary determinants of adoption likelihood. Using a mixed-methods descriptive-developmental research design, data were collected from 301 rice farmers selected through proportionally allocated stratified random sampling across 13 barangays in Basista, Pangasinan through a validated survey questionnaire with agricultural stakeholders. Quantitative data were analyzed using descriptive statistics and predictive modeling techniques, while feature importance analysis was employed to identify the factors that most significantly influence farmers' willingness to adopt the proposed Automatic Rice Monitoring and Management System. Guided by the principles of the Technology Acceptance Model (TAM) and Diffusion of Innovations Theory, the study examines how individual experience, training support, and demographic factors influence farmers' willingness to adopt agricultural monitoring technologies. Findings indicate a strong willingness (74.1% of respondents) to adopt the Automatic Rice Monitoring and Management Systems, provided systems are mobile-compatible and cost-effective. Notably, experiential factors specifically prior tech exposure (importance score: 0.38) outperform traditional demographics like income or education as predictors. These findings contribute to the growing body of agricultural technology adoption research by demonstrating that prior technology exposure is a stronger predictor of adoption than traditional socioeconomic characteristics among rice farmers. This study provides a vital framework for designing user-centric, affordable precision tools, ensuring that digital interventions are contextually aligned with the technical capacities of local farmers to enhance regional food security.A limitation of this study is that the findings are based on farmers from selected barangays in Basista, Pangasinan and primarily reflect adoption intentions rather than actual long-term system use. Future research should validate the model across other rice-producing regions and through real-world deployments, while enhancing predictive capabilities using additional field data and advanced machine learning techniques to improve system effectiveness and scalability.

Keywords: Automatic Rice Monitoring; Smart Agriculture; Descriptive-Developmental Design; Technology Adoption; Pangasinan Rice Farming

1. Introduction

Rice serves as the primary staple food for a global majority, providing essential calories and protein, particularly within developing nations. To meet rising demands by 2025, global production must reach approximately 760 million tonnes, a 35% increase from 1996 levels. However, achieving this is fraught with difficulty as arable land in Asia, where 90% of the world's rice is produced and consumed, has largely been exhausted (Duwayri et al., 1999). Historically, consumption needs in the Asia-Pacific region were met through yield increases driven by improved varieties rather than land expansion (Khush, 1995). The contemporary challenge, therefore, is to increase annual production from 524 million to 700 million tonnes using fewer resources, such as water, labor, and pesticides, amidst the plateauing of irrigated areas due to salinity and water scarcity (Papademetriou et al., 2000).

Agricultural modernization is critically urgent as climate change and related disasters (CCRD) increasingly jeopardize food security in vulnerable economies (Tumbaga & Vargas, 2017). Inefficient water management continues to drive unpredictable productivity and systemic poverty (Haefele et al., 2016). Projections suggest that for every 1ºC rise in minimum temperature, rice yields may decline by 10%, largely offsetting potential gains from increased CO2 levels (Fahad et al., 2019).

In the Philippines, extreme climatic fluctuations like El Niño and typhoons caused over 80% of rice losses between 1970 and 1990 (Lansigan et al., 2000), with major storms further exposing the vulnerability of households where rice represents 20% of food expenses (Blanc & Strobl, 2016).

While the Green Revolution introduced high-yielding varieties, many farmers still struggle with optimal nutrient management due to technical and financial barriers (Balisacan & Sebastian, 2007; Sebastian et al., 1999). Precision agriculture remains largely inaccessible to resource-poor growers (Duwayri, 1999). However, mobile technology offers a promising bridge for diagnosing pests and diseases, which currently destroy 37% of annual rice crops (Eusebio et al., 2028). Integrating these digital tools is essential to mitigate losses and stabilize production amidst escalating environmental pressures.

In Pangasinan, the impact of these challenges is locally acute. Despite being a top economic performer in Philippine agriculture (Bernardino, 2024), the province frequently suffers from irrigation shortages, leading farmers to abandon rice for less water-intensive crops like corn (Gabriel-Galban, 2024). Extreme heat indices reaching 51^0C have forced laborers to work at night, exposing them to hazards like snake bites (Sotelo, 2024). Additionally, persistent infestations of rice black bugs (RBB) and rats continue to suppress yields in municipalities like Sta. Barbara and Basista (Pasion, 2018; Department of Agriculture, 2020). While the Unified Theory of Acceptance and Use of Technology (UTAUT) suggests that farmers are willing to adopt new tools if they perceive them as beneficial and user-friendly (Nguyen et al., 2023), many still rely on error-prone paper-based recording (Roslin et al., 2021).

This study aims to determine the critical predictors of technology adoption for an automated rice monitoring and management system among farmers in Basista, Pangasinan. By evaluating socio-demographic and behavioral factors, the research identifies how prior technological exposure and training assistance influence adoption likelihood. Ultimately, the study provides a data-driven framework for designing cost-effective, user-centric agricultural tools that bridge the gap between traditional practices and modern digital transformation.

2. Objectives

The primary objective of this study is to design an Automatic Rice Monitoring and Management System specifically engineered for the socio-economic and environmental landscape of Pangasinan. This research investigates the critical predictors of technology adoption including technological exposure, training assistance, and age to ensure the proposed system aligns with the actual technical capacities and financial constraints of local farmers. By addressing the regional decline in rice production, which fell from 160,879 metric tons to 158,805 metric tons in 2019 following a contraction in harvested area (Philippine Statistics Authority, 2019), this work provides a data-driven framework for precision agriculture. The study's significance lies in its ability to optimize pest control, water management, and nutrient distribution through accessible digital tools, ultimately enhancing productivity and ensuring food security in a region highly vulnerable to infrastructural and climatic shifts.

3. Materials and Methods

Research Design

This study employed a descriptive-developmental research design, an approach that bridges the gap between problem identification and solution engineering. The descriptive component focused on characterizing the demographic profiles, technical capabilities, and farmland specifications of rice farmers, while systematically documenting the specific monitoring challenges they encounter in the field. Simultaneously, the developmental component involved the iterative conceptualization and prototyping of the monitoring system. This methodology prioritized the actual working conditions and usability requirements of the farmers, ensuring that the technology developed is not only innovative but also practical for daily agricultural operations.

Locale of the Study and Data Sources

This study was centered in Basista, Pangasinan, a 4th class municipality spanning 2,400 hectares and serving as a key agricultural hub in the province's second district. With a population of 37,679 (2020 Census), the locale provided a critical environment for research, as approximately 80%

of its residents rely on agriculture, specifically across 1,110 hectares dedicated to lowland rice and corn. To capture the complexities of this sector, researchers integrated secondary data from the 171,643 farmers managing over 185,379 hectares province-wide with primary insights gathered from 301 local rice farmers across all 13 barangays. Conducted over a six-month period from November 2024 to April 2025, the study utilized a diverse sample to account for varied farm sizes ranging from smallholdings under 1 hectare to larger properties and differing levels of technological exposure, where 43.5% of respondents reported no prior use of agricultural technology. By synthesizing these quantitative benchmarks with qualitative expert perspectives, the research established a comprehensive baseline for designing an automated monitoring system tailored to the region's specific socio-economic and environmental needs.

Data Gathering Procedure

The data gathering process was executed through a rigorous protocol designed to build rapport with the community and maintain ethical standards. Initial coordination involved obtaining formal permissions from the Municipal Agricultural Office and the Cooperative and Farmer's Association Presidents of the 13 barangays. Participants were engaged through information sheets and consent forms provided in both English and Pangasinan to ensure transparency. Quantitative data were collected through structured questionnaires distributed during community meetings or direct farm visits, allowing for high response rates and immediate clarification of terms.

Research Instrument and Validation

The primary research tool was a custom-developed questionnaire, formulated through a systematic four-stage validation process. The conceptualization stage involved drafting items in English based on a thorough literature review of pest control, water resource management, and weather adaptation. This draft was then subjected to an expert review by a panel of specialists who evaluated the content for validity, clarity, and cultural relevance. To bridge the linguistic gap, the instrument was translated into Pangasinan and then back-translated to verify linguistic equivalence. Finally, a pilot testing phase was conducted with a small group of farmers in Basista. This crucial step allowed the researchers to identify and rectify any ambiguities in the questions, ensuring the final instrument was a reliable and valid tool for measuring technical capabilities and the farmers' readiness to adopt automated monitoring technologies.

4. Results

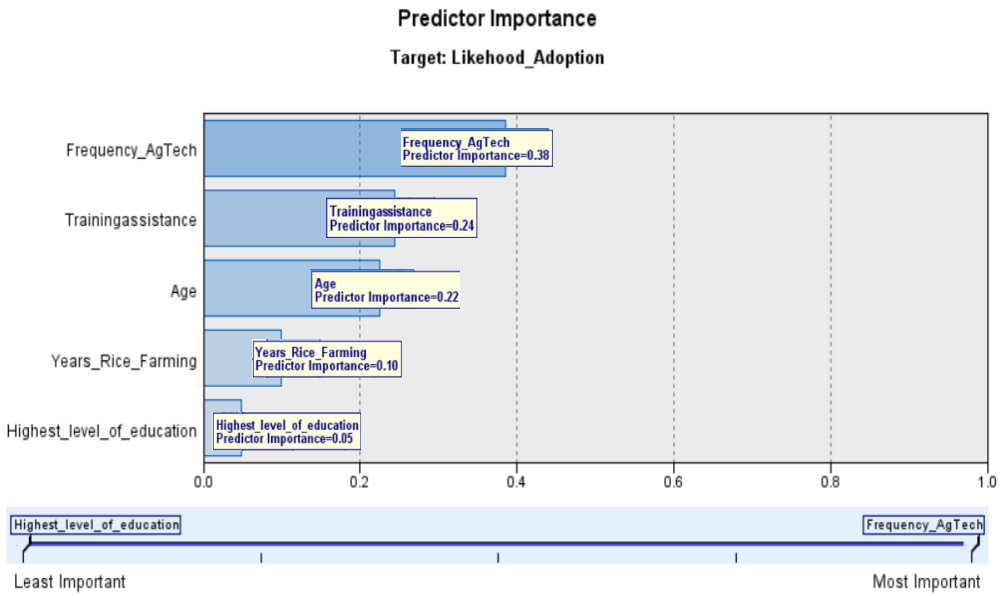

Figure 1. Predictor Importance of Likelihood of Adoption of the Proposed Model of Automatic Rice Monitoring Management System

The analysis of predictor importance reveals a clear hierarchy of factors influencing the adoption of an automatic rice monitoring and management system. The most dominant determinant is the Frequency of Agricultural Technology Use, which carries a substantial importance score of 0.38. In the classification tree model, importance scores represent the relative influence of each predictor on adoption outcomes, with higher scores indicating greater predictive contribution. This suggests that technological familiarity acts as a gateway; farmers already integrated into digital workflows possess a higher propensity for adopting advanced automated solutions. Following closely are Training Assistance (0.24) and Age (0.22), highlighting that both institutional support and generational perspectives are critical in shaping a farmer's readiness for innovation.

In contrast, traditional demographic and socio-economic markers showed significantly less influence. While Years Engaged in Rice Farming maintained a moderate impact (0.10), variables like Education (0.05), Sex, Farm Size, and Main Source of Income were found to be negligible predictors. These results shift the focus away from static profiles, indicating that adoption is driven by experiential and behavioral readiness. Consequently, successful implementation strategies should prioritize consistent technological exposure and hands-on training over targeting farmers based on income or landholdings.

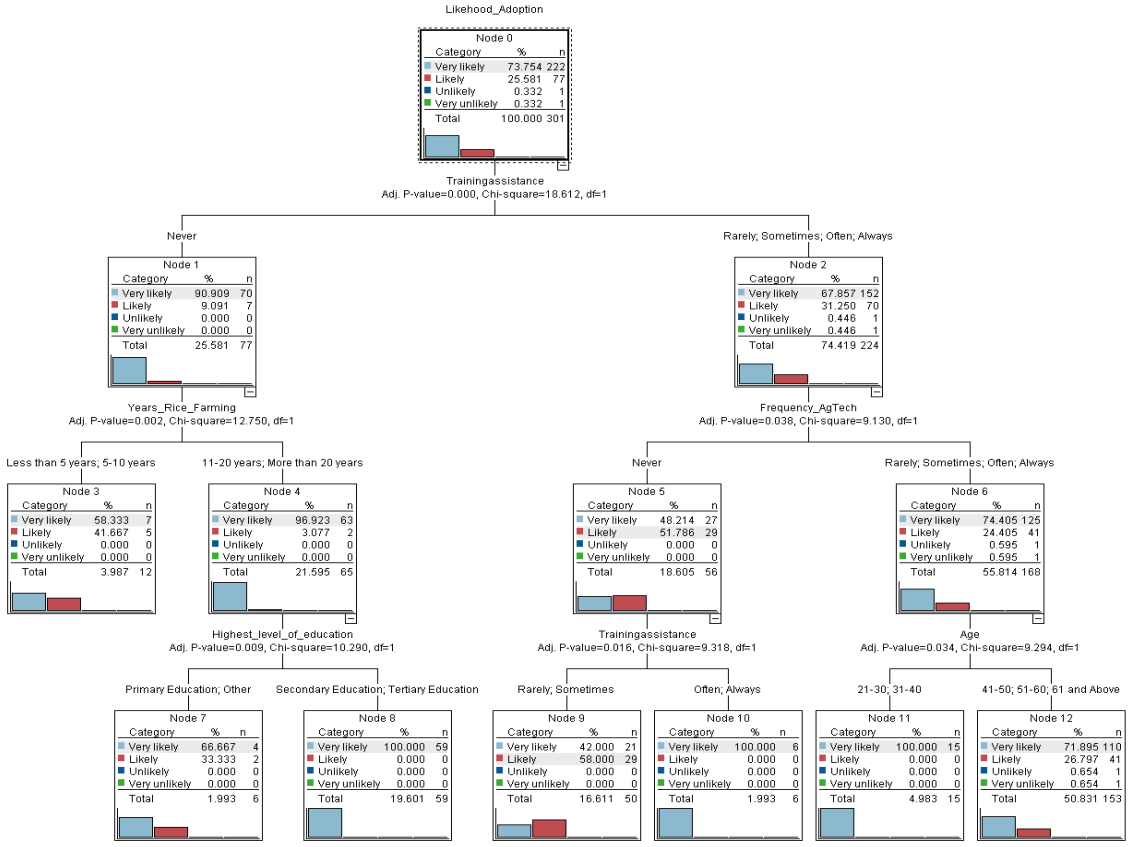

Figure 2. Classification Tree Model Describing the Relationship Between the Profile and Likelihood of the Adoption of the Proposed Model of Automatic Rice Monitoring Management System

The classification tree analysis identifies training assistance as the primary differentiating factor in predicting adoption likelihood, revealing a nuanced landscape for agricultural innovation. A notable initial split shows a counterintuitive trend: farmers who did not receive formal training exhibited higher adoption probabilities than those who did. This suggests that a lack of institutional support may drive independent, proactive behavior among farmers seeking to solve persistent field challenges. Within this "no-training" cohort, years of farming experience serves as the critical secondary splitter. Specifically, seasoned farmers with 11 to over 20 years of experience are the most

"very likely" to adopt the system, likely due to a deep-seated recognition of the limitations inherent in traditional, manual monitoring methods.

Conversely, for the branch that received training, the frequency of agricultural technology use becomes the strongest subsequent predictor, indicating that familiarity breeds readiness for advanced systems. Further differentiation in this group is influenced by educational attainment and age. The terminal nodes define the ideal adopter profile: well-trained, tech-savvy individuals within the 21–50 age bracket with at least a secondary education. This confirms that while experience motivates adoption, technical literacy and formal schooling provide the necessary framework for successful digital integration.

5. Discussion of Findings

The statistical analysis of farmer profiles identifies Frequency of Agricultural Technology Use as the primary predictor of adoption likelihood with a significant importance score of 0.38, followed by Training Assistance (0.24) and Age (0.22).The predictive modeling results are supported by the descriptive findings of the study. Farmers who frequently used agricultural technology were identified as the strongest predictors of adoption likelihood (importance score = 0.38), which is consistent with the observed openness toward technology, as 91.4% of respondents reported high to very high confidence in using technology and 99.4% expressed a likely or very likely intention to adopt the proposed system. Training Assistance (0.24) also emerged as a key predictor, aligning with the finding that 74.1% of farmers demonstrated high willingness to attend training programs. Age (0.22) was likewise found to influence adoption decisions, reflecting the predominance of middle-aged and older farmers in the study, with the 51–60 age group comprising 33.6% of respondents.

This suggests that while experienced farmers recognize the potential benefits of automated monitoring systems, adoption strategies should consider age-related differences in technological familiarity and learning preferences. Collectively, these findings indicate that technology adoption is influenced more by practical exposure, confidence, training support, and age-related experience than by traditional demographic characteristics such as educational attainment, income, or sex. This hierarchy suggests that prior engagement with digital tools is a critical determinant, as farmers already integrated into technological workflows are far more inclined to embrace automated monitoring solutions.

Conversely, the minimal impact of Highest Level of Education (0.05) and other static traits like sex and income implies that technology uptake is driven by experiential and behavioral factors rather than formal schooling or demographic status. The classification tree model reinforces this by establishing that well-trained, tech-savvy individuals serve as the "early adopters," highlighting a critical need for capacity-building initiatives that equip farmers with practical technical skills. Because age-related factors influence decision-making, adoption strategies should be tailored to generational preferences, potentially utilizing younger farmers as community influencers or pilot-testing user-interface (UI) modifications to enhance accessibility. Ultimately, these findings suggest that government policy and future research should prioritize "tech-exposure" programs and hands-on demonstrations over purely informational campaigns, ensuring that systems are contextually relevant and supported by the continuous training necessary for a successful digital transition in agriculture.

The finding that farmers without training assistance initially show a higher likelihood of adoption challenges conventional assumptions. This may suggest that these individuals are more proactive or independently motivated to seek technological solutions due to a lack of formal support systems, or it may indicate that the content of current training programs is not effectively engaging the most tech-inclined farmers. The role of extensive farming experience (11–20+ years) as a motivator suggests that seasoned farmers may have a deeper understanding of the limitations of traditional monitoring and thus perceive a higher value in automated solutions. For those within the formal support network, the importance of technology use frequency underscores how sustained engagement with digital tools builds the necessary readiness for further integration. The influence of age and education highlights the necessity of generational and cognitive accessibility in system design. Working-age farmers with secondary education appear more adaptable to data-driven approaches.

Furthermore, the strong preference for mobile and web-based platforms (68.1%), affordable system costs (54.2% preferred below Php 3,000), and real-time system adjustments (69.4%) reinforces the importance of designing accessible, user-centered technologies that address farmers'

operational needs. Collectively, these findings provide empirical support for prioritizing hands-on technology exposure, capacity-building initiatives, and affordable digital solutions to promote the successful adoption of automated rice monitoring and management systems. It should be noted that the study employed a classification tree model and feature importance analysis to determine the relative influence of predictor variables on adoption likelihood. As the analysis focused on predictive modeling rather than inferential regression, traditional statistical measures such as regression coefficients and significance tests were not generated. Nevertheless, the feature importance rankings provide valuable insights into the factors most associated with adoption behavior. Future studies may strengthen the predictive framework by incorporating logistic regression and additional model validation metrics, such as accuracy, precision, recall, and ROC-AUC, to further evaluate and compare predictive performance. Ultimately, the model suggests that while training is critical, its impact is nuanced and must be complemented by strategies that empower different experience groups and provide continuous exposure to agri-tech.

The identified predictors of adoption provide practical guidance for key stakeholders involved in agricultural modernization initiatives. For policymakers and local government units, the findings highlight the importance of investing in technology exposure programs, demonstration farms, and subsidized digital agriculture initiatives that allow farmers to gain hands-on experience with emerging technologies. Agricultural extension workers should prioritize continuous training, mentoring, and technical support, particularly for farmers with limited prior exposure to agricultural technologies. Meanwhile, technology developers should design affordable, mobile-compatible, and user-friendly systems that accommodate varying levels of digital literacy and farming experience.

Given the influence of age on adoption likelihood, implementation strategies should also incorporate age-sensitive approaches, such as simplified interfaces, localized training materials, and peer-learning mechanisms that encourage younger and more technologically experienced farmers to serve as technology champions within their communities. Through coordinated efforts among these stakeholders, the successful adoption and sustainability of automatic rice monitoring and management systems can be significantly enhanced.

6. Conclusion

This study provides critical insights into the readiness of Pangasinan rice farmers to transition from manual methods to an Automatic Rice Monitoring and Management System. The findings reveal an overwhelming inclination toward adoption, driven by a strong demand for real-time pest detection, data reporting, and automated system adjustments. Farmers expressed a distinct preference for mobile-compatible platforms and demonstrated significant price sensitivity, favoring cost-effective solutions. Crucially, the research identifies that technology adoption is governed more by behavioral and experiential factors than by traditional demographics. The Frequency of Agricultural Technology Use (0.38) and Training Assistance (0.24) emerged as the most significant predictors, indicating that familiarity and formal learning are essential for digital integration. While age (0.22) and farming experience (0.10), specifically the 11–20 year bracket, further refined adoption likelihood, variables such as sex, education, and farm size had minimal impact. This suggests that the local agricultural sector is primed for transformation, supported by a high degree of confidence in technology and a strong willingness (74.1% of respondents) to undergo training programs for the proposed technology. The classification tree analysis further nuances these findings, revealing that while training is a pivotal driver, a notable openness to innovation exists even among those currently underserved by technical support, potentially reflecting an urgent need for technological intervention. Ultimately, these results provide a strategic foundation for developing an accessible, user-centric, and affordable agricultural framework. Future research and implementation should move beyond demographic targeting, focusing instead on intensive training initiatives and enhancing technology exposure to bridge the gap between traditional practices and automated precision farming. Such efforts will ensure that the resulting systems are not only technically sound but also socially and economically viable for the Pangasinan farming community.

Acknowledgment

I want to take the time to express my deepest gratitude to all the people who provided me with the unwavering support and guidance throughout my thesis and academic journey. Your

encouragement, wisdom, and belief in me have been invaluable every step of the way. From lending an ear during moments of doubt to offering insightful advice and constructive feedback, your contributions have truly shaped my growth and success.

I am profoundly grateful for the time you've invested in me, whether through brainstorming sessions, reviewing manuscripts, or simply being a pillar of emotional support. Your belief in my abilities has inspired me to push myself further and achieve more than I thought possible.

Thank you once again for being a part of this significant chapter in my life. Your generosity and encouragement have made a lasting impact, and I look forward to carrying your wisdom with me as I continue to pursue my academic and professional aspirations.

References

Balisacan AM, Sebastian LS et al. 2007. Securing rice, reducing poverty: challenges and policy directions. Los Baños (Philippines): Southeast Asian Regional Center for Graduate Studies and Research in Agriculture (SEARCA), Philippine Rice Research Institute (PhilRice) and Department of Agriculture-Bureau of Agricultural Research (DA-BAR), College, Los Baños, Laguna. 352 p

Bernardino, R.R. (2024, April 4). Pangasinan, Philippines' 3rd Leading Agricultural Area. Pangasinan Information and Media Relations Office. https://www.pangasinan.gov.ph/pangasinan-philippines-3rd-leading-agricultural-area/

Blanc, E., and E. Strobl, 2016: Assessing the Impact of Typhoons on Rice Production in the *Philippines. J. Appl. Meteor. Climatol., 55*, 993–1007, https://doi.org/10.1175/JAMC-D-15-0214.1.

Duwayri, M., Tran, D. V., & Nguyen, V. N. (1999). Reflections on yield gaps in rice production. *International Rice Commission Newsletter, 48*, 13-26.

Eusebio L. Mique and Thelma D. Palaoag. 2018. Rice Pest and Disease Detection Using Convolutional Neural Network. In Proceedings of the 1st International Conference on Information Science and Systems (ICISS '18). Association for Computing Machinery, New York, NY, USA, 147–151. https://doi.org/10.1145/3209914.3209945

Fahad S., Adnan M., Noor M., Arif M., Alam M., Khan I.A., Ullah H., Wahid F., Mian I.A., Jamal Y., Basir A., Hassan S., Saud S., Amanullah, Riaz M., Wu C., Khan M.A., Wang D. (2019). Chapter 1-Major Constraints for Global Rice Production. https://doi.org/10.1016/B978-0-12-814332-2.00001-0 on December 18, 2024.

Gabriel-Galban, J. (2024, August 9). Over 800 farms in Pangasinan struggle due to lack of irrigation. GMA Regional TV. https://www.gmanetwork.com/regionaltv/news/103378/over-800-farms-in-pangasinan-struggle-due-to-lack-of-irrigation/story/

Haefele S.M., Kato Y., Singh S. (2016). Climate ready rice: Augmenting drought tolerance with best management practices. https://www.sciencedirect.com/science/article/abs/pii/S0378429016300168 on December 16, 2024.

Khush, G.S. 1995. Modern varieties. *Geojournal 35* (3): 275 - 284. Their real contribution to food supply and equity.

Lansigan, F. P., De Los Santos, W. L., & Coladilla, J. O. (2000). Agronomic impacts of climate variability on rice production in the Philippines. *Agriculture, ecosystems & environment, 82*(1-3), 129-137.

Nguyen L.L.H., Khuu D.T., Halibas A.S., Nguyen T.Q. (2023). Factors That Influence the Intention of Smallholder Rice Farmers to Adopt Cleaner Production Practices: An Empirical Study of Precision Agriculture Adoption. https://pubmed.ncbi.nlm.nih.gov/37678818 on December 12, 2024.

Papademetriou, M. K., Dent, F. J., & Herath, E. M. (Eds.). (2000). Bridging the rice yield gap in the Asia-Pacific Region (Vol. 222). Bangkok, Thailand: FAO Regional Office for Asia and the Pacific. https://coin.fao.org/coin-static/cms/media/9/13171760277090/2000_16_high.pdf on December 18, 2024.

Pasion, A. (2018, January 4). Harvest drops in Pangasinan due to rice black bug, rats. Philippine News Agency. https://www.pna.gov.ph/articles/1020430

Philippine Statistics Authority. 2019, September 19. Ilocos Region's Palay and Corn Outputs decline in 2nd quarter 2019. https://rsso01.psa.gov.ph/statistics/cps/node/55268 on April 11, 2025.

Roslin N.A., Ismail M.R., Che'ya N.N., Rosle R. (2021). Smartphone Application Development for Rice Field Management Through Aerial Imagery and Normalised Difference Vegetation Index (NDVI) Analysis. https://doi.org/10.47836/pjst.29.2.07 on December 22, 2024.

Sebastian LS, Alviola IV PA, Francisco SR. 1999. Bridging the rice yield gap in the Philippines. http://www.fao.org/docrep/003/x6905e/x6905e00.htm. February 5, 2016.

Sotelo, Y. (2024, August 18). In Pangasinan, farm time shifts amid climate change. Inquirer.net. https://newsinfo.inquirer.net/1973937/in-pangasinan-farm-time-shifts-amid-climate-change

Tumbaga J. R. A. and Vargas D.S. (2017). Farmers' Resilience towards Climate Change Related Disasters (CCRDs): The Case of Barangay Mabalbalino, San Carlos City, Pangasinan. https://clsu-ijst.org/index.php/ijst2/article/view/30/0 on December 16, 2024.

HealGuide: Bridging Community Health Gaps Through Digital Symptom Guidance and Affordable Home Remedies

Precilda C. Blaza
Department of Natural Sciences, Lyceum Northwestern University, Dagupan City, Pangasinan, Philippines
Email: blaza.precilda.c@lyceum.edu.ph

Abstract

Coastal and remote communities face significant health disparities due to geographic isolation and limited infrastructure. While mobile Health (mHealth) tools offer promise, most are designed for stable urban environments, leaving a gap for platforms addressing acute ailments through culturally relevant home remedies. This study developed and evaluated a user-centered web application for mothers in remote coastal areas to manage common symptoms using scientifically validated remedies. A total of 50 mothers were recruited through community leaders using voluntary collaboration and informed consent protocols. Data were collected via a structured questionnaire which demonstrated high internal reliability (Cronbach's $\alpha = 0.88$). Findings revealed strong perceived usability and satisfaction wherein respondents strongly agreed on the clarity of remedies ($M = 4.42$) and ease of navigation ($M = 4.24$). While performance scores ($M = 4.20$) indicated a need for further optimization, the app was also perceived to effectively promote health awareness ($M = 4.46$). The application demonstrates potential as a context-sensitive tool to reduce health disparities and empower caregivers, though longitudinal evidence of clinical outcomes is required.

Keywords: web-based app, mobile health, mothers, remote area

1. Introduction

Mobile health (mHealth) applications have been increasingly recognized as transformative tools for healthcare delivery, particularly in rural and coastal communities where access to clinical services remains limited. Globally, mHealth has demonstrated potential to enhance disease management, promote health education, and facilitate timely medical interventions, while empowering patients through remote monitoring and self-management tools (McCool, Det al., 2021; Abaza & Marschollek, 2017; Liew et al., 2018). Evidence from Southeast Asia and the Philippines indicates that mHealth applications have been increasingly recognized as transformative tools for healthcare delivery where rural and coastal communities continue to face persistent barriers to access such as infrastructural and literacy constraints (Okolo, et al., 2024; Emeihe et al. 2024).Their potential lies in expanding coverage, supporting self-management, and strengthening public health systems through digitalization, which simultaneously enhances patient safety, improves satisfaction, and ensures that population health statistics remain current for providers. Evidence demonstrates that mHealth platforms have been deployed for reminders, monitoring, screening, remote consultations, and outbreak response, with notable applications during Ebola, Zika, and COVID-19 emergencies (McCool, et al., 2021; Abaza & Marschollek, 2017; Wood et al., 2019). In the Philippines, mobile health clinics and SMS-based interventions have shown promise in improving chronic disease management and maternal health outcomes, yet adoption remains uneven across rural barangays due to infrastructural and literacy constraints (Okolo, et al., 2024; Abaza & Marschollek, 2017).

Despite this promise, a significant implementation gap persists. The digital health market now comprises more than 325,000 applications, yet only a small fraction undergo peer-reviewed evaluation of usability or effectiveness, raising concerns about their real-world impact. Dropout rates of up to 50% in internet-based interventions illustrate the difficulty of sustaining user engagement (Smith et al., 2025). Functional hurdles such as visually complex interfaces and lengthy text blocks contribute to disengagement, while infrastructural barriers—including intermittent internet connectivity, unreliable electricity, and limited ICT infrastructure—undermine adoption in remote and coastal barangays (Pognon et al., 2025; Perski & Short, 2021; Hui et al., 2022). Furthermore, most applications are designed for urban populations with stable infrastructure and high digital literacy, leaving marginalized and geographically isolated communities underserved (Islam et al., 2020; Alruwaili et al., 2023; Emeihe et al., 2024). Content specificity also remains limited, as many platforms emphasize chronic conditions while neglecting common acute ailments such as fever, flu, or

headache, and fail to integrate scientifically validated, affordable home remedies. Users frequently report that general web-based health information is unsettling or unreliable, underscoring the need for medically validated sources to foster patient autonomy (Kaihlanen et al., 2022; Smith & Magnani, 2019).

The effectiveness of existing platforms is constrained by assumptions of stable internet connectivity, adequate device availability, and user proficiency. In low-bandwidth contexts, electricity and internet service are unreliable, interoperability is weak, and skilled labor is scarce, leading to systemic exclusion of rural users, women, and older adults (Hui et al., 2022; Hepburn, Williams, & McCann, 2025). Moreover, digital health platforms often demand higher levels of digital, health, and language literacy than general consumer applications, creating a mismatch between design and user capacity. Studies in Southeast Asia highlight that even regular internet users struggle with health applications when interfaces are overly complex, navigation is unintuitive, and content is written above recommended reading levels (Kaihlanen et al., 2022; Smith & Magnani, 2019). Philippine evidence further underscores that older adults and marginalized populations with low literacy are consistently identified as high-risk groups, with repeated observations of difficulty in navigating mHealth apps and reliance on external assistance (Alharthi, 2025). Usability reviews also report poor navigation, dense wording, and task complexity as recurring barriers for patients and clinicians, with older adults specifically struggling due to cognitive, visual, and dexterity limitations (Giebel et al., 2022; Alzghaibi, 2025; Wildenbos, et al., 2019).

In Southeast Asia, country coverage remains thin in Brunei, Cambodia, Laos, Myanmar, Timor-Leste, and Vietnam (Okolo et al., 2024), while clinical areas such as palliative care remain severely understudied, with only a handful of eligible studies identified (Wood et al., 2019). In the Philippines, the lack of equity-specific reporting and interventions tailored to low-bandwidth and low-literacy environments demonstrates why existing platforms fail as they are built for ideal users and ideal infrastructure rather than the realities of rural and marginalized communities. Addressing these gaps requires the integration of literacy support, simplified interfaces, and low-bandwidth optimization into platform design. Evidence further shows that none of 131 reviewed digital health interventions assessed all six domains of the eHealth literacy model, and only 5.3% covered both health and digital literacy, underscoring the undermeasurement of skills users actually need (Benny, et al., 2020). Ensuring that digitalization fulfills its promise of equitable healthcare delivery across diverse Southeast Asian populations requires alignment with Sustainable Development Goals (SDG 3: good health and well-being, SDG 10: reduced inequalities) and the National Unified Health Research Agenda (NUHRA), emphasizing evidence-based, inclusive, and context-sensitive mHealth strategies that strengthen health equity in the region.

This study is guided by the Technology Acceptance Model (TAM), which explains user adoption of mobile health (mHealth) applications through the constructs of perceived usefulness and perceived ease of use. Derived from the Theory of Reasoned Action, TAM posits that these perceptions shape attitudes and behavioral intentions, ultimately influencing usage (Malatji, 2020; Zaineldeen, 2020; Park, 2025). Foundational studies demonstrated that perceived usefulness consistently exerts a stronger effect on adoption than ease of use, with longitudinal evidence showing its predictive power over time (Davis, 1989, 1993). Later extensions incorporated social and contextual variables, yet the two original constructs remain central (Venkatesh, 2000; Rahimi, 2018). In the Philippine and Southeast Asian context, where low bandwidth, limited digital literacy, and infrastructural constraints hinder mHealth adoption, TAM provides a relevant framework: perceived usefulness reflects the extent to which users believe mHealth improves access and outcomes, while perceived ease of use captures the challenges of navigating platforms in low-literacy and resource-limited settings (Okolo, Babawarun, & Olorunsogo, 2024; Hui et al., 2022; Hepburn, Williams, & McCann, 2025). This conceptual grounding ensures that the study addresses regional evidence gaps while situating findings within a well-established theoretical model.

2. Objective

To develop and implement a web-based application that delivers health education and self-management tools for common acute ailments and their scientifically validated home-based remedies, specifically targeting mothers in coastal and remote communities underserved by traditional healthcare infrastructure.

The study is guided by the following specific objectives:

1. Design a simple and intuitive user interface that accommodates varied levels of digital literacy.
2. Evaluate the acceptance, usability, and satisfaction of the platform among mothers in remote and coastal communities.
3. Identify strengths and areas for optimization in the application's performance, contextual quality, and effectiveness in low-bandwidth settings.

The primary objective of this study is to develop and implement a web-based application designed to provide health education and self-management tools for common acute ailments and their scientifically validated home-based remedies. This intervention specifically targets coastal and remote communities that are often underserved by traditional healthcare infrastructure due to geographic isolation and limited professional personnel.

The study is guided by the following specific objectives:

1. To design a simple, intuitive user interface that accommodates users with varied levels of digital literacy, guided by the TAM constructs of perceived ease of use and perceived usefulness.
2. To evaluate the acceptance, usability, and satisfaction of the platform among 50 mothers in remote and coastal communities, as measured by a validated structured questionnaire.
3. To identify strengths and areas for optimization in the application's performance, quality context, and effectiveness for low-bandwidth settings.

3. Materials and Methods

Technical Web Development

The health application was developed within the Base44 environment to ensure the creation of a responsive and high-performance web interface. The platform was hosted online and made accessible through a dedicated website link, requiring an active internet connection for the initial session and subsequent data synchronization. Core digital remedies were integrated into the design, including a Symptom Tracking module, which was utilized to record family health status and facilitate early disease detection, and a Knowledge Education repository, which was employed to provide information on common ailments and affordable home remedies using readily available household items. To enhance reliability and safeguard user trust, the application was constructed within a "privacy-first" framework and technically optimized for low-bandwidth environments typical of remote regions, thereby ensuring accessibility and functionality in resource-constrained settings.

Survey Analysis

Inclusion criteria required participants to be mothers residing in remote or geographically isolated areas, serving as the primary managers of family health, and capable of accessing the platform through a provided web link. Recruitment was facilitated through community leaders using voluntary collaboration and informed consent protocols.

A total of 50 respondents were recruited for this study. Inclusion criteria required participants to be mothers residing in remote or geographically isolated areas, serving as the primary managers of family health, and capable of accessing the platform through a provided web link. Recruitment was facilitated through community leaders using voluntary collaboration and informed consent protocols. Of the total approached, 55 mothers were invited, yielding a response rate of 90.9%". A power analysis was not conducted due to the exploratory and development-oriented nature of the study; however, a sample of 50 is consistent with similar usability evaluation studies in mHealth (Hajesmaeel-Gohari et al., 2022).

The primary data collection instrument was a structured Application Questionnaire employing a five-point Likert scale. Respondents were asked to rate positive statements ranging from "Strongly Agree" (5) to "Strongly Disagree" (1). The questionnaire was organized into three domains: Quality Context, which evaluated the clarity of remedies, helpfulness of information, and appropriateness of suggested household items; Usability, which measured ease of learning, navigation efficiency, and

visual design appeal; and Effectiveness, which assessed the impact on digital health literacy and confidence in managing family health.

Procedures followed a standardized workflow. Participants were first provided with the web link and a brief orientation regarding the study's purpose and data privacy measures. Respondents then completed designated tasks on the platform, such as tracking a family member's symptoms and identifying specific home remedies.

Data analysis was conducted using descriptive statistics, including mean, standard deviation, and variance. Mean satisfaction scores were calculated for each domain. These findings were intended to guide iterative refinement of the Base44-based platform, ensuring improved usability, contextual adaptability, and effectiveness in remote health management.

4. Results

Table 1. Usability

Indicator	**AWM**	**REMARKS**
The app interface is easy to understand.	4.34	Strongly Agree
Searching symptoms is simple and fast.	4.44	Strongly Agree
Navigation between pages is user-friendly.	4.24	Strongly Agree
The design is attractive and organized.	4.3	Strongly Agree
The app works smoothly on my device.	4.2	Agree

The usability domain yielded mean scores ranging from M = 4.20 to M = 4.44, all falling within the "Agree" to "Strongly Agree" range with participants consistently agreeing that the app was easy to use. The highest-rated indicator was the simplicity and speed of symptom searching (M = 4.44), while the lowest was smooth device operation (M = 4.20). This suggests that while the interface design and navigation are well-received, device compatibility and performance under low-bandwidth conditions remain areas for optimization.

Table 2. Quality Context

Indicators	**AWM**	**REMARKS**
The remedies are clear and understandable.	4.42	Strongly Agree
Instructions are step-by-step and easy to follow.	4.38	Strongly Agree
The information provided is helpful.	4.36	Strongly Agree
Remedies use affordable/common household items.	4.24	Strongly Agree
The warning/disclaimer section is clear.	4.24	Strongly Agree

Within the quality context domain, ratings were uniformly high, reflecting strong confidence in the clarity and practicality of the remedies provided. The top strengths were the clear presentation of remedies and step-by-step instructions, which suggest that the app effectively supports comprehension and usability. Minor weaknesses were noted in the affordability of household items and the clarity of disclaimers, though these still received favorable ratings, pointing to a need for slight adjustments rather than major redesign.

Table 3. Effectivity

Indicators	**AWM**	**REMARKS**
The app helps me find remedies quickly.	4.16	Agree
The app can be useful in emergencies or minor illnesses.	4.2	Agree
The app promotes health awareness.	4.46	Strongly Agree
I would recommend this app to others.	4.22	Strongly Agree
Overall, I am satisfied with the application.	4.26	Strongly Agree

Effectiveness scores revealed that the app was perceived primarily as an educational and awareness-building tool. The strongest outcome was its ability to promote health awareness, which exceeded other indicators and highlights its role in empowering users with knowledge. The weakest area was the speed of finding remedies, suggesting that while the app is effective in fostering awareness and satisfaction, its utility as a rapid-response tool in emergencies requires further enhancement.

5. Discussions

The usability results indicate that the strongest feature of the application was the simplicity and speed of symptom searching, which directly supports the TAM construct of perceived ease of use. This is consistent with the study of Emeihe et al (2024) and Manzano-Monfort et al (2024), emphasizing that mobile Health applications for rural areas must prioritize simple, intuitive interfaces to accommodate varied levels of digital literacy. This finding reinforces prior evidence that intuitive navigation and minimal text are critical for users with limited digital literacy in rural contexts. Research suggests that features such as clear instructions and minimal text are essential for users with limited technological experience (Safi et al. 2019 & Hajesmaeel-Gohari et al 2022). However, the weakest area was smooth device operation, reflecting persistent challenges with connectivity and compatibility in low-bandwidth environments (Emeihe et al. 2024 & Fan et al 2024). This suggests that while interface design is well-received, technical optimization remains essential to sustain long-term engagement.

The quality context evaluation (Table 2) indicates that the application successfully provides clear, step-by-step instructions (M = 4.38) for scientifically validated home remedies (M = 4.42). Goetz et al (2017) and Baumel and Kane (2018) highlights a critical "knowledge gap" where users often find web-based health information unsettling or unreliable unless it comes from medically validated sources. By focusing on affordable household items (M = 4.24), the application circumvents the high costs of medical interventions that often exclude remote populations (Emeihe et al. 2024). This practical approach fosters patient autonomy, empowering residents to manage common symptoms independently when access to professional care is delayed by geographic isolation. This context demonstrates consistent strengths, particularly in the clarity of remedies and step-by-step instructions, which align with recommendations that medically validated and comprehensible content fosters trust and autonomy among underserved populations (Goetz et al., 2017; Baumel & Kane, 2018). Minor weaknesses were observed in affordability and disclaimers, though these still achieved favorable ratings, indicating only incremental improvements are needed.

The application's high effectiveness in promoting health awareness (M = 4.46) and high levels of overall satisfaction (M = 4.26) reflect positive trends in mHealth adoption seen in other underserved regions. Pognon et al. (2024) suggests that end-user satisfaction is driven by the perception that a digital tool provides immediate, actionable health knowledge. The strong willingness of participants to recommend the app (M = 4.22) suggests it has achieved "social proof," a critical shortcut for selecting digital interventions that peers find acceptable (Hajesmaeel-Gohari et al 2022 & Emeihe et al 2024). These findings indicate that participants perceived the platform as a reliable bridge to healthcare, reducing disparities by providing immediate guidance for minor illnesses like the flu and fever in areas where traditional clinical infrastructure is sparse (Lv et al 2019). Effectiveness results highlight health awareness promotion as the strongest outcome, suggesting that the application is perceived more as an educational tool than as a rapid-response intervention. This aligns with findings that satisfaction in mHealth is often driven by access to actionable health knowledge rather than emergency utility (Pognon et al., 2024). The weakest indicator was speed in finding remedies, which points to the need for further streamlining of search functions to enhance responsiveness.

While the overall satisfaction ratings are encouraging, sustainability and user retention remain critical concerns in mHealth interventions. Prior studies have reported dropout rates of up to 50% in internet-based health interventions (Smith et al., 2025), and engagement often declines after initial novelty effects wear off (Perski & Short, 2021). The slightly lower score for smooth device operation (M = 4.20) may signal an early attrition risk: if technical frustrations persist, users may abandon the platform despite appreciating its content. Future iterations should incorporate offline functionality, push notifications for medication or health reminders, and periodic content updates to sustain engagement over time.

Findings from this study align with mHealth usability research conducted in other rural Asian contexts, revealing consistent patterns in adoption and design requirements. In Bangladesh, Islam et al. (2020) reported that interface simplicity and content clarity were key predictors of acceptance, underscoring the importance of intuitive navigation for populations with limited digital literacy. Similarly, Liew et al. (2019) emphasized that health applications serving low-literacy groups in Southeast Asia must employ minimal text and prioritize visual-first design, principles reflected in HealGuide's video-based remedy format. The application's emphasis on validated remedies and accessible instructions further addresses the "knowledge gap" identified in prior studies, ensuring that health information is both comprehensible and medically reliable. Unlike urban-focused platforms evaluated in China (Lv et al., 2019), HealGuide specifically targets coastal and geographically isolated communities, thereby extending the evidence base to more resource-constrained settings. By demonstrating that TAM-aligned design principles—particularly perceived ease of use and perceived usefulness—can be successfully adapted to marginalized populations, this study advances equity in digital health delivery across diverse socio-economic and geographic contexts.

6. Conclusions

The study concludes that the HealGuide web application was perceived by 50 mothers in remote and coastal communities as usable, satisfactory, and contextually appropriate for managing common acute ailments. Consistently high mean scores for usability (M = 4.34) and quality context (M = 4.42) indicate strong alignment with the Technology Acceptance Model (TAM) constructs of perceived ease of use and perceived usefulness. By providing scientifically validated home-based remedies using affordable items, the application was viewed as empowering residents and reducing reliance on local clinical resources. However, these findings reflect user perceptions at a single point in time and do not establish clinical effectiveness; longitudinal studies with larger and more diverse samples are needed to assess sustained impact and health outcomes.

The results highlight several design and policy implications for mHealth development in underserved regions. First, offline functionality should be prioritized to ensure continuity of access in low-bandwidth and unstable network environments. Second, digital literacy training programs for mothers in coastal and rural communities are essential to maximize usability and adoption. Third, clear regulatory standards for data privacy and security must be established to safeguard user trust and protect sensitive health information. Beyond these priorities, bridging the knowledge gap through medically validated content remains critical to counter unreliable sources and foster patient autonomy.

Future research should explore sustainability and attrition risks, given that mHealth interventions often face declining engagement after initial use. Incorporating features such as push notifications, periodic content updates, and AI-driven personalized feedback may help sustain user retention. Longitudinal studies are also recommended to evaluate the application's long-term impact on clinical visits, health outcomes, and equity in healthcare access, particularly among marginalized and low-literacy populations who are frequently excluded from conventional app development.

References

Abaza, H., & Marschollek, M. (2017). mHealth application areas and technology combinations: A comparison of literature from high and low/middle income countries. *Methods of Information in Medicine, 56*(Suppl. 1), e105–e122. https://doi.org/10.3414/ME16-02-0042

Alharthi, S. A. (2025). Bridging the Digital Divide in Health for Older Adults: A Repeated Cross-Sectional Study of mHealth in Saudi Arabia. *IEEE Access, 13*, 63757-63773. https://doi.org/10.1109/access.2025.3558368

Alruwaili, M. M., Shaban, M., & Ramadan, O. M. E. (2023). Digital health interventions for promoting healthy aging: A systematic review of adoption patterns, efficacy, and user experience. *Sustainability*, *15*(23), 16503. https://doi.org/10.3390/su152316503.

Alzghaibi, H. (2025). Healthcare Practitioners' Perceptions of mHealth Application Barriers: Challenges to Adoption and Strategies for Enhancing Digital Health Integration. *Healthcare, 13*. https://doi.org/10.3390/healthcare13050494

Baumel, A., & Kane, J. M. (2018). Examining predictors of real-world user engagement with self-guided eHealth interventions: Analysis of mobile apps and websites using a novel dataset. *Journal of Medical Internet Research*, *20*(12), e11491. http://www.jmir.org

Benny, M. E., Kabakian-Khasholian, T., El-Jardali, F., & Bardus, M. (2020). Application of the eHealth Literacy Model in Digital Health Interventions: Scoping Review. *Journal of Medical Internet Research, 23*. https://doi.org/10.2196/23473

Davis, F. D., Bagozzi, R., & Warshaw, P. R. (1989). User Acceptance of Computer Technology: A Comparison of Two Theoretical Models. *Management Science, 35*, 982-1003. https://doi.org/10.1287/mnsc.35.8.982

Davis, F. D. (1993). User Acceptance of Information Technology: System Characteristics, User Perceptions and Behavioral Impacts. *Int. J. Man Mach. Stud., 38*, 475-487. https://doi.org/10.1006/imms.1993.1022

Emeihe, E. V., Nwankwo, E. I., Ajegbile, M. D., Olaboye, J. A., & Maha, C. C. (2024). Mobile health applications for disease management in rural areas: A systematic review. *International Journal of Applied Research in Social Sciences*, *6*(8), 1725–1746. https://www.fepbl.com/index.php/ijarss

Fan, S., Jain, R. C., & Kankanhalli, M. S. (2024). A comprehensive picture of factors affecting user willingness to use mobile health applications. *ACM Transactions on Computing for Healthcare*, *5*(1), Article 2. https://doi.org/10.1145/3626962.

Giebel, G. D., Speckemeier, C., Abels, C., Plescher, F., Börchers, K., Wasem, J., Blase, N., & Neusser, S. (2022). Problems and Barriers Related to the Use of Digital Health Applications: Scoping Review. *Journal of Medical Internet Research, 25*. https://doi.org/10.2196/43808

Goetz, M., Müller, M., Matthies, L. M., Hansen, J., Doster, A., Szabo, A., Pauluschke-Fröhlich, J., Abele, H., Sohn, C., Wallwiener, M., & Wallwiener, S. (2017). Perceptions of patient engagement applications during pregnancy: A qualitative assessment of the patient's perspective. *JMIR mHealth and uHealth*, *5*(5), e73. http://mhealth.jmir.org.

Hajesmaeel-Gohari, S., Khordastan, F., Fatehi, F., Samzadeh, H., & Bahaadinbeigy, K. (2022). The most used questionnaires for evaluating satisfaction, usability, acceptance, and quality outcomes of mobile health. *BMC Medical Informatics and Decision Making*, *22*, 22. https://doi.org/10.1186/s12911-022-01764-2.

Hepburn, J., Williams, L., & McCann, L. (2025). Barriers to and Facilitators of Digital Health Technology Adoption Among Older Adults With Chronic Diseases: Updated Systematic Review. *JMIR Aging, 8*. https://doi.org/10.2196/80000

Hui, C., Abdulla, A., Ahmed, Z., Goel, H., Habib, G. M. M., Hock, T. T., Khandakr, P., Mahmood, H., Nautiyal, A., Nurmansyah, M., Panwar, S., Patil, R., Rinawan, F. R., Salim, H., Satav, A., Shah, J., Shukla, A., Tanim, C. Z. H., Balharry, D., & Pinnock, H. (2022). Mapping national information and communication technology (ICT) infrastructure to the requirements of potential digital health interventions in low- and middle-income countries. *Journal of Global Health, 12*. https://doi.org/10.7189/jogh.12.04094

Islam, M. N., Karim, M. M., Inan, T. T., & Islam, A. K. M. N. (2020). Investigating usability of mobile health applications in Bangladesh. *BMC Medical Informatics and Decision Making*, *20*, 22. https://doi.org/10.1186/s12911-020-1033-3.

Kaihlanen, A., Virtanen, L., Buchert, U., Safarov, N., Valkonen, P., Hietapakka, L., Hörhammer, I., Kujala, S., Kouvonen, A., & Heponiemi, T. (2022). Towards digital health equity - a qualitative study of the challenges experienced by vulnerable groups in using digital health services in the COVID-19 era. *BMC Health Services Research, 22*. https://doi.org/10.1186/s12913-022-07584-4

Liew, M. S., Zhang, J., See, J., & Ong, Y. L. (2019). Usability challenges for health and wellness mobile apps: Mixed-methods study among mHealth experts and consumers. *JMIR mHealth and uHealth*, *7*(1), e12160. https://mhealth.jmir.org/2019/1/e12160/.

Lv, Q., Jiang, Y., Qi, J., Zhang, Y., Zhang, X., Fang, L., Tu, L., Yang, M., Liao, Z., Zhao, M., Guo, X., Qiu, M., Gu, J., & Lin, Z. (2019). Using mobile apps for health management: A new health care mode in China. *JMIR mHealth and uHealth*, *7*(6), e10299. https://mhealth.jmir.org/2019/6/e10299/.

Malatji, W., Eck, R. V., & Zuva, T. (2020). Understanding the usage, Modifications, Limitations and Criticisms of Technology Acceptance Model (TAM). *Advances in Science, Technology and Engineering Systems Journal, 5*, 113-117. https://doi.org/10.25046/aj050612

Manzano-Monfort, G., Paluzie, G., Díaz-Gegúndez, M., & Chabrera, C. (2023). Usability of a mobile application for health professionals in home care services: A user-centered approach. *Scientific Reports*, *13*, 2964. https://doi.org/10.1038/s41598-023-29640-7.

McCool, J., Dobson, R., Whittaker, R., & Paton, C. (2021). Mobile health (mHealth) in low- and middle-income countries. *Annual Review of Public Health, 43*, 525–539. https://doi.org/10.1146/annurev-publhealth-090820-111743

Okolo, C. A., Babawarun, O., & Olorunsogo, T. O. (2024). Mobile health (mHealth) innovations for public health feedback: A global perspective. *International Medical Science Research Journal*. 10.51594/imsrj.v4i3.915

Park, J. H., Lee, C.-W., & C. (2025). Examining Users' Acceptance Intention of Health Applications Based on the Technology Acceptance Model. *Healthcare, 13*. https://doi.org/10.3390/healthcare13060596

Perski, O., & Short, C. E. (2021). Acceptability of digital health interventions: Embracing the complexity. *Translational Behavioral Medicine*, *11*(7), 1473–1480. https://doi.org/10.1093/tbm/ibab048.

Pognon, P. R., Boima, F., & Mekonnen, Z. A. (2025). Health workers' acceptance and satisfaction on the usability of the digital health goods, in Kono District, Sierra Leone. *Journal of Multidisciplinary Healthcare*, *18*, 1067–1079. https://doi.org/10.2147/JMDH.S509441.

Rahimi, B., Nadri, H., Afshar, H., & Timpka, T. (2018). A Systematic Review of the Technology Acceptance Model in Health Informatics. *Applied Clinical Informatics, 09*, 604 - 634. https://doi.org/10.1055/s-0038-1668091

Safi, S., Danzer, G., & Schmailzl, K. J. (2019). Empirical research on acceptance of digital technologies in medicine among patients and healthy users: Questionnaire study. *JMIR Human Factors*, *6*(4), e13472. http://humanfactors.jmir.org

Smith, B., & Magnani, J. (2019). New technologies, new disparities: the intersection of electronic health and digital health literacy. *International journal of cardiology, 292*, 280 - 282. https://doi.org/10.1016/j.ijcard.2019.05.066

Smith, L., Simpson, G., Holt, S., & Dambha-Miller, H. (2025). Digital applications to support self-management of multimorbidity: A scoping review. *medRxiv*. https://doi.org/10.1101/2025.04.14.25325811.

Wood, C. S., Thomas, M. R., Budd, J., Mashamba-Thompson, T., Herbst, K., Pillay, D., Peeling, R. W., Johnson, A. M., McKendry, R. A., & Stevens, M. M. (2019). Taking connected mobile-health diagnostics of infectious diseases to the field. *Nature, 566*(7745), 467–474. https://doi.org/10.1038/s41586-019-0956-2

Wildenbos, G., Jaspers, M., Schijven, M., & Dusseljee-Peute, L. W. (2019). Mobile health for older adult patients: Using an aging barriers framework to classify usability problems. *International journal of medical informatics, 124*, 68-77 . https://doi.org/10.1016/j.ijmedinf.2019.01.006

Venkatesh, V., & Davis, F. D. (2000). A Theoretical Extension of the Technology Acceptance Model: Four Longitudinal Field Studies. *Management Science, 46*, 186-204. https://doi.org/10.1287/mnsc.46.2.186.11926

Zaineldeen, S., Li, H., Koffi, A. L., & Hassan, B. (2020). Technology Acceptance Model' Concepts, Contribution, Limitation, and Adoption in Education. *Universal Journal of Educational Research, 8*, 5061-5071. https://doi.org/10.13189/ujer.2020.081106

Designing a Citizen-Centric Transparency Platform for Government Project Monitoring in the Philippines: A Conceptual Framework

Christel Joy D. Verania*, John Quinn Agonace, Larcen Emmanuel D. Belangel, Julian Curt J. Flores, Keane Chandre Guadarama, Justine Blaire Suarez
School of Basic Education, STI West Negros University
*Email : agonacejohnquinn@gmail.com

Abstract

This study proposes a citizen-centric transparency platform for government project monitoring in the Philippines by developing a conceptual framework and evaluating a non-functional interface prototype grounded in Task–Technology Fit (TTF), E-Governance Theory, and Transparency and Accountability Theory. Existing digital governance systems often suffer from fragmented information, limited accessibility, weak citizen participation, and insufficient real-time transparency, reducing the effectiveness of public monitoring and accountability mechanisms. Using a Design Science Research (DSR) approach, the study synthesized findings from literature, policy documents, and transparency initiatives to identify key governance and usability gaps. Based on these findings, a conceptual framework and UI/UX prototype named YUHOM were designed to support project monitoring, financial transparency, progress tracking, and citizen feedback reporting. The prototype was evaluated by 35 respondents from academic institutions, governance-related sectors, IT professionals, and potential citizen-users using a TTF-based evaluation instrument. Results revealed positive user perceptions across Task Characteristics (M = 3.60), Technology Characteristics (M = 3.50), Task–Technology Fit (M = 3.45), and User Perceived Performance Impact (M = 3.44), all interpreted as "Agree." Findings indicate that the proposed platform demonstrates functional viability and moderate alignment between citizen monitoring tasks and technological capabilities. The study contributes to the growing discourse on digital governance by presenting a theoretically grounded and citizen-oriented transparency framework that promotes accessibility, participation, accountability, and public trust in government infrastructure monitoring. The findings further suggest that citizen-centered digital platforms can strengthen participatory governance and improve transparency practices in developing countries.

Keywords: Citizen-Centric Transparency Platform; E-Governance; Government Project Monitoring; Task–Technology Fit (TTF); Transparency and Accountability.

1. Introduction

Transparency and accountability are important for the public to have access to information on the use of public resources. On an international scale, digital governance and open data programs are key approaches to enhancing government transparency, efficiency, and trust. E-government platforms are increasingly being embraced by governments around the world as part of digital transformation initiatives to enhance public service delivery and governance efficiency (Hansson, Belkacem, & Ekenberg, 2021). However, while these efforts are underway, problems persist, including accessibility issues, digital exclusion, lack of real-time information, and low citizen involvement (Twizeyimana & Andersson, 2022). Digital transformation in government is not just a technological revolution but also a structural and participatory issue that impacts citizens' engagement with government (Hansson et al., 2021; Twizeyimana & Andersson, 2022). This means that many governments are not yet fully realizing transparent, accessible, and participatory digital systems.

Globally, many nations have adopted open government and digital transparency systems supported by open data systems and e-government innovations. These platforms seek to provide greater public access to government data via digital dashboards, data portals, and monitoring systems. These systems use digital technologies such as online dashboards, databases, cloud-based systems, and application programming interfaces (APIs) that allow government data to be stored, managed, and shared efficiently across platforms. These tools help present public information such as budgets, projects, and services in a more organized and accessible way. Research indicates that open government data initiatives enhance transparency and accountability but are dependent on openness, data quality, and citizen participation (Safarov, Meijer, & Grimmelikhuijsen, 2021). Moreover,

research shows that digital government platforms need to progress from information dissemination to interaction, participation, and feedback (Porumbescu, 2022). Similarly, digital transformation and government innovation using tools such as social media have been acknowledged as a means to enhance communication and transparency between government and citizens (Criado, Sandoval-Almazán, & Gil-Garcia, 2020). However, there are still global challenges in promoting continuous public participation and the effective implementation of open data systems in various countries (Attard et al., 2020).

In the Philippines, transparency and accountability in governance are supported by national digital transformation programs and global open government initiatives. Although the Philippines is increasingly adopting e-government systems in line with global standards, there are implementation issues. These include Article II, Section 28 of the 1987 Philippine Constitution, which ensures public disclosure of government transactions; Republic Act No. 9184 or the Government Procurement Reform Act, which promotes transparency in government procurement processes; and Republic Act No. 10173 or the Data Privacy Act, which protects personal data in digital systems. The country also participates in the Open Government Partnership and continues to develop e-government services through agencies such as the Department of Information and Communications Technology (DICT). However, studies show that developing nations, such as the Philippines, have challenges with system integration, data access, and efficiency of digital infrastructure (Safarov et al., 2021). These limitations impact the success of transparency programs and limit citizens' access to up-to-date government data. At a micro level, such as in cities in the Philippines like Bacolod, citizens may experience disjointed access to data on government projects and are forced to access information from different sources. This is a symptom of problems in digital governance systems, where information is not consolidated, interactive, or dynamic.

The existing literature on digital governance and open data systems indicates that while many governments have implemented transparency platforms, most of these systems are still based on a "publish-only" approach, meaning they only present information without allowing users to interact and provide feedback (Criado et al., 2020). Moreover, open data systems still have issues with usability, accessibility, and citizen participation, which limit their effectiveness in improving government accountability (Attard et al., 2020). There are also few studies on mobile-based, citizen-centered systems for real-time monitoring of government projects, particularly in developing nations such as the Philippines. This suggests the need for a system that enables not only information sharing but also interactivity, participation, and feedback.

This study will design a conceptual framework of a Citizen-Centric Transparency Platform for Government Project Monitoring for enhancing government monitoring of projects in the Philippines. This framework seeks to provide features based from needs of the users and established theories to produce a design for an ideal prototype feature.

2. Objectives

The general objective of this study is to design a citizen-centric transparency platform for government project monitoring in the Philippines through the development of a conceptual framework grounded in Task-Technology Fit (TTF), E-Governance, and Transparency and Accountability Theory, and to develop and evaluate a non-functional interface prototype (UI/UX mockups) that enhances public access, participation, transparency, and accountability in government projects.

1. To examine the existing challenges, limitations, and citizen needs in government project monitoring and transparency practices in the Philippines through a comprehensive literature review.
2. To develop a conceptual framework for a citizen-centric transparency platform based on Task-Technology Fit (TTF), E-Governance, and Transparency and Accountability Theory.
3. To design a non-functional interface prototype (UI/UX mockups) of the proposed transparency platform that visually represents how citizens can access project information, monitor project implementation, and submit feedback or reports.
4. To evaluate the perceived Task-Technology Fit (TTF) of the proposed interface prototype in terms of task characteristics, technology characteristics, and overall task-technology alignment for citizen engagement in government project monitoring.

2.1 Theoretical Framework

The three theories are interconnected and collectively establish the foundation of the proposed platform. Task-Technology Fit Theory (Goodhue et al., 1995) ensures that the system is usable and aligned with citizen monitoring tasks. E-Governance Theory (Lubis et al., 2024) positions the platform within the broader context of digital public administration and participatory governance. Transparency and Accountability Theory (Lourenço, 2023) ensures that the system fosters openness, trust, and institutional responsibility. The integration of these theories suggests that a successful citizen-centric transparency platform must satisfy three essential conditions: it must be functionally aligned with user needs, digitally accessible and participatory, and capable of promoting transparency that leads to accountability. Through this integrated theoretical perspective, YUHOM is conceptualized as more than a technological solution. It is designed as a governance mechanism that empowers citizens, improves public trust, and strengthens oversight in government project implementation. The theoretical framework guides the development of the conceptual model, the design of the non-functional interface prototype, and the evaluation of the platform's perceived effectiveness in supporting citizen engagement. Ultimately, the study proposes that the successful implementation of YUHOM can contribute to improved transparency, stronger accountability, increased citizen participation, and enhanced trust in government project monitoring systems in the Philippines.

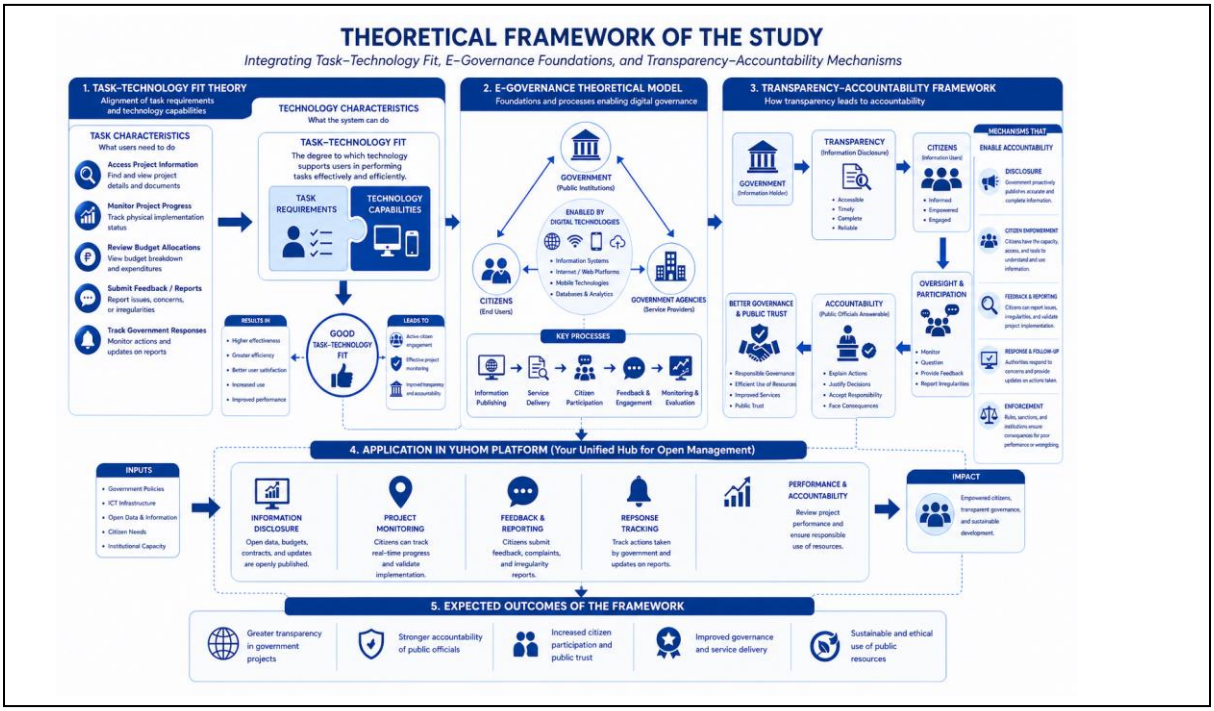

Figure 1 Theories used for designing the proposed prototype and conceptual framework.

3. Materials and methods

3.1 Research Design

This study employed a Design Science Research (DSR) approach using a prototyping method to design and evaluate a citizen-centric transparency platform for government project monitoring in the Philippines. The study focused on developing a conceptual framework anchored on Task-Technology Fit (TTF), E-Governance Theory, and Transparency and Accountability Theory. These theories served as the foundation for designing the proposed platform and ensuring that the interface aligns with citizen needs, promotes transparency, and strengthens accountability in government project implementation. Since the study aimed to produce a design artifact rather than a fully functional system, a non-functional interface prototype in the form of UI/UX mockups was developed.

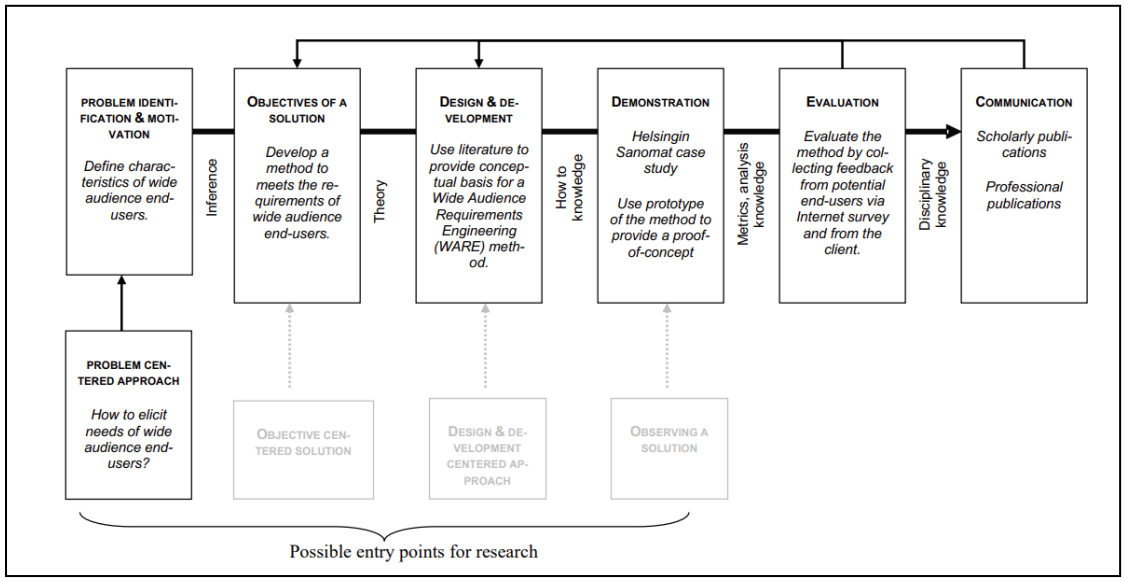

Figure 2 Research Design

3.2 Research Locale

The study was conducted within the context of public governance and government project monitoring in the Philippines. It focused on transparency initiatives and digital governance practices that influence citizen participation in monitoring government projects. Since the study is conceptual and prototype-based, the research locale was not limited to a specific local government unit but instead covered the broader Philippine governance setting where transparency and accountability remain significant concerns. The evaluation of the interface prototype involved selected respondents from academic institutions, government offices, IT professionals, governance practitioners, and potential citizen-users who possess relevant knowledge in digital systems, transparency mechanisms, and public service monitoring.

3.3 Data Sources

The study utilized both secondary and primary sources of data. Secondary data were gathered from published journal articles, government reports, policy documents, laws related to transparency and accountability, and previous studies on e-governance and public sector monitoring systems. Existing government transparency platforms were also reviewed to identify system gaps and design opportunities. These sources provided the theoretical and practical foundation for the development of the conceptual framework and the interface prototype. Primary data were collected during the prototype evaluation stage using a Task-Technology Fit (TTF)-based questionnaire, expert validation forms, and user perception assessments. These primary data were used to determine the perceived effectiveness and acceptability of the proposed interface design.

3.4 Data Processing

The study adopts a structured four-phase research procedure to ensure the development of a theory-driven and citizen-centered transparency platform. The first phase critically examines existing challenges in government project monitoring by synthesizing recent literature, policy frameworks, and stakeholder insights. Key issues identified include limited access to project information, delayed updates, weak citizen engagement, and inadequate accountability mechanisms, highlighting a significant transparency gap in current governance systems. The second phase focuses on the development of a conceptual framework grounded in Task-Technology Fit (TTF), E-Governance Theory, and Transparency–Accountability Theory. This integration establishes a coherent foundation that aligns citizen tasks with technological capabilities, promotes participatory digital governance, and reinforces mechanisms for openness and accountability. In the third phase, these theoretical foundations are translated into a non-functional interface prototype. The design emphasizes core features such as project monitoring dashboards, transparency displays, and citizen feedback modules,

reflecting the identified user needs and governance requirements. Finally, the fourth phase evaluates the prototype using the TTF framework, focusing on users' perceived alignment between system features and monitoring tasks. The findings provide evidence on the platform's potential to enhance transparency, accountability, and citizen participation.

3.5 Data Analysis

The study used both qualitative and quantitative methods of data analysis. Qualitative analysis was applied during the literature review, conceptual framework development, and interpretation of expert comments and suggestions. This helped identify major transparency gaps and improve the prototype design based on theoretical and practical insights. Quantitative analysis was used during the prototype evaluation stage, based on responses collected from the TTF questionnaire. The researcher used a weighted mean and descriptive analysis to assess respondents' perceptions of the interface prototype. This allowed the study to determine the level of perceived Task-Technology Fit and the overall acceptability of the proposed transparency platform design.

3.6 Prototype Evaluation

The prototype was evaluated using the Task–Technology Fit (TTF) framework, focusing on three key constructs: task characteristics, technology characteristics, and perceived task–technology fit. The evaluation instrument was contextualized to reflect the requirements of a citizen-centric government project monitoring system, ensuring its relevance to public sector applications. To establish content validity, the instrument was reviewed by experts in information systems and e-governance prior to its deployment. Each construct was measured using a five-point Likert scale to capture users' perceptions of system effectiveness. To standardize interpretation, the mean scores were converted into percentage values ranging from 0 to 100 through a linear transformation. This approach enabled a clearer and more consistent evaluation of usability levels across respondents. The resulting scores were interpreted using a heuristic classification scale, which categorizes user responses from "Strongly Disagree" to "Strongly Agree," reflecting varying degrees of perceived usefulness and effectiveness of the platform.

Table 1 Usefulness Dimension Table of Interpretation.

Range (%)	Mean Score	Interpretation
81 – 100	4.21 – 5.00	Strongly Agree
61 – 80	3.41 – 4.20	Agree
41 – 60	2.61 – 3.40	Neutral
21 – 40	1.81 – 2.60	Disagree

3.7 Ethical Consideration

Ethical considerations were observed throughout the study to ensure responsible research practices. All secondary sources used in the literature review were properly cited to avoid plagiarism and maintain academic integrity. Respondents involved in the evaluation stage were informed of the study's purpose, and their participation was strictly voluntary. Confidentiality of responses was maintained, and all collected data were used solely for academic and research purposes. Informed consent was also secured before the evaluation process to ensure transparency and respect for participants' rights.

4. Results

4.1 Finding on Existing Challenges and Transparency

The findings reveal persistent challenges in accessing timely, clear, and usable government information, which continue to limit effective transparency and citizen engagement. Although e-governance systems are in place, data is often not presented in a user-friendly manner, making it difficult for citizens to monitor government projects and participate in accountability processes (Alam et al., 2023; Afiyah, 2024). In the Philippine context, this reflects a transparency gap where information exists but is not fully accessible or actionable for public use. This indicates that transparency is constrained not by data availability, but by issues of usability and citizen-centered system design (Cao, 2024). Overall, these findings highlight the need for a more accessible, user-

focused digital platform to improve public understanding, engagement, and oversight of government projects.

Table 2 Extracted results from literature review.

Theme	Key Authors	Extracted Findings and Results
Challenges in Project Monitoring	Lourenço (2023); Hossain et al. (2016)	Transparency often fails due to administrative overload and policy accumulation. There is a persistent supply-side bias where data is uploaded but remains fragmented and difficult for citizens to monitor.
Citizen Engagement	Cegarra-Navarro et al. (2014); Al Araby (2024); Attard et al. (2015); Alam et al. (2023); Afiyah (2024)	Technology knowledge (T-knowledge) is a primary determinant of engagement. Systems must move toward a "Smart Citizen" model of co-production, as passive data receipt leads to low participation and awareness.
Task-Technology Fit (TTF)	Goodhue & Thompson (1995)	A system is only effective if its functional capabilities match the user's specific tasks. High complexity and a lack of fit for local digital literacy levels cause users to abandon platforms.
Transparency and Accountability	Sari & Muslim (2023); Pujari & Joshi (2024); Pratiwi et al. (2024); Meijer (2009); Bertot et al. (2010)	Transparency is a prerequisite for accountability. Legal frameworks like the RTI Act empower citizens, but real accountability requires financial reporting to be clear, governed, and accessible to discourage mismanagement.
Citizen-Centric Interface Design	Putra et al. (2023); Nam (2012); Ruijer et al. (2020); Cao (2024)	Design must focus on user habits and Human-Centered Design (HCD) rather than government hierarchy. Interactive visualizations act as the essential bridge to transform static text into usable information.

4.2 Conceptual Framework of the Citizen-Centric Transparency Platform

The conceptual framework of this study was developed based on the findings of the conducted survey, which revealed that respondents strongly demand accessible information on budget allocation, project progress, and regular updates regarding government infrastructure projects in the Philippines. They also highlighted the need for real-time updates, simplified data visualization tools, and interactive features that allow feedback submission and issue reporting. Guided by these findings, the framework is structured using an input–process–output–outcome approach, where government data sources serve as the input. These data are then processed through a data integration and visualization layer that transforms complex information into simplified, user-friendly, and visually presented formats. The processed information is delivered through a citizen-centric transparency platform that includes key features such as a project information dashboard, project progress monitoring, access to transparency information, and citizen feedback and reporting mechanisms, all supported by user-friendly navigation. The framework is further grounded in Task-Technology Fit Theory, Transparency and Accountability Theory, and E-Government Theory. Task-Technology Fit Theory emphasizes aligning visualization tools and system features with users' information needs to improve usability and effectiveness, while E-Government Theory supports the use of digital platforms for efficient public service delivery and information dissemination. Meanwhile, Transparency and Accountability

Theory underpin the expected outcomes of the framework, where improved access to information and citizen participation are expected to enhance government transparency, strengthen accountability, increase citizen engagement, and improve the monitoring of infrastructure projects.

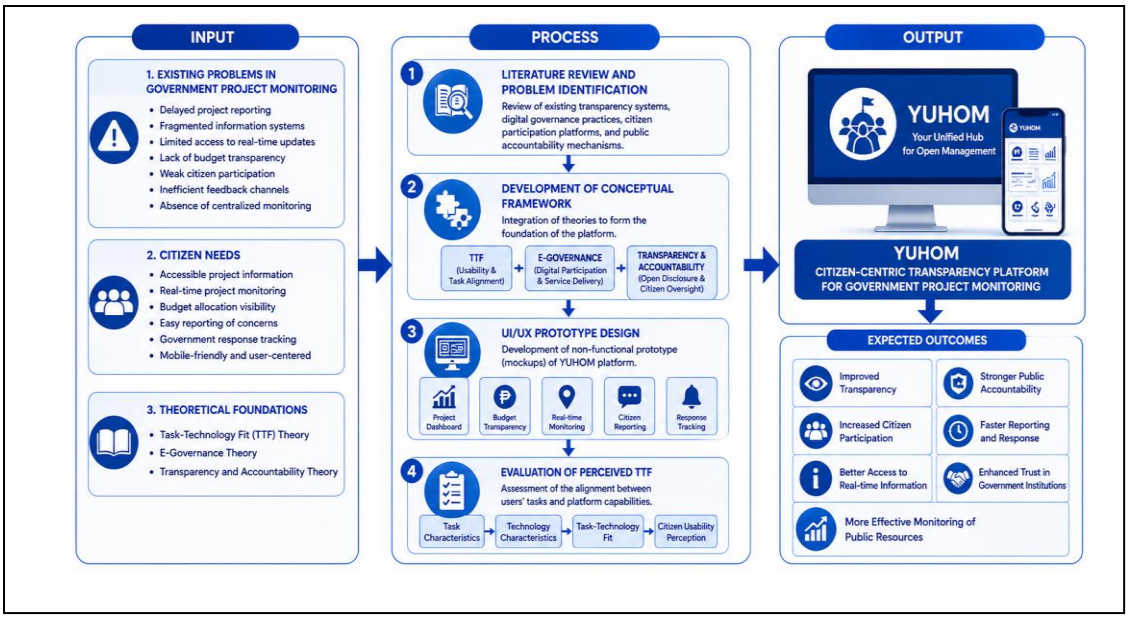

Figure 3 Conceptual framework for designing a citizen-centric transparency platform.

4.3 Interface Prototype Development

The system interface consists of five functional components aligned with a citizen-centric transparency platform: the Project Information Dashboard, Project Status Monitoring Interface, Transparency View Screens, Citizen Feedback and Reporting Interface, and Navigation Structure. These components collectively demonstrate strong Task-Technology Fit (TTF) by ensuring that system functionalities directly support users' tasks in accessing, monitoring, and engaging with government infrastructure project information. In particular, the system improves task performance by providing relevant and easily accessible information, enabling timely project updates, simplifying data interpretation through visual interfaces, and facilitating efficient user interaction through intuitive navigation and feedback mechanisms. This alignment between user tasks and system features ensures improved usability, reduced effort in information retrieval, and more effective citizen engagement with government project monitoring.

4.3.1 Project Information Dashboard

Figure 4(a) The interface displays a project details view where users can monitor government initiatives. It includes key information such as project title, status, budget, location, and description, along with a progress bar and budget utilization indicator. A "Report Issue" feature is also provided to allow users to submit feedback or concerns related to the project. Figure 4(b) The interface shows an issue reporting and tracking view, focusing on a specific reported problem. It presents details such as the issue title, description, date, and image evidence, along with a mapped location and status updates. This enables users to track reported concerns and stay informed about their resolution progress.

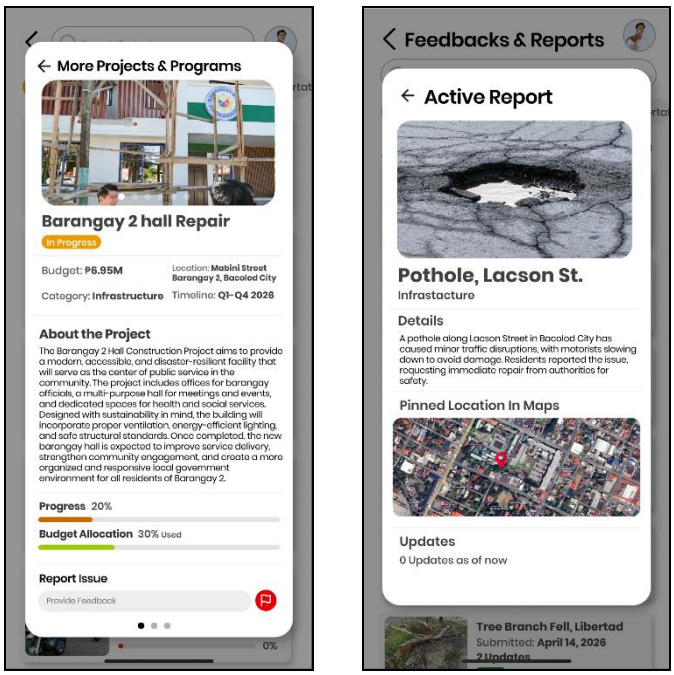

(1) (2)

Figure 4 (a) Project details interface; 4 (b) Reporting and Tracking

4.3.2 Project Status Monitoring Interface

Figure 5 presents the different interfaces of the mobile-based project monitoring system designed to enhance transparency and citizen engagement. Figure 5(a) depicts the Financial Breakdown Interface, which visualizes the allocation of the project budget across different components using a pie chart, allowing users to easily understand how resources are distributed. Figure 5(b) illustrates the Projects and Programs List Interface, where users can browse multiple projects categorized by sector, with summarized details such as budget and progress indicators. Figure 5 (c) displays the Project Progress Tracking Interface, highlighting the timeline of project phases (e.g., conceptualization, design, procurement) and their current status, as well as accountability information.

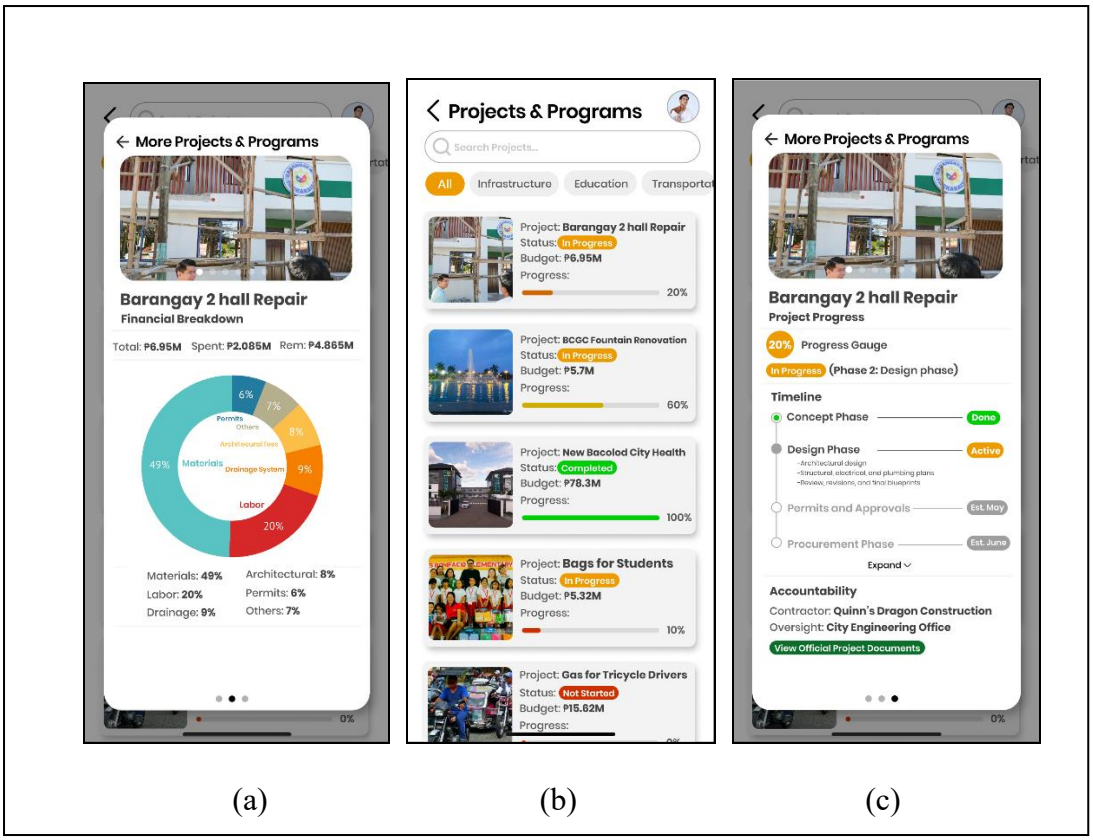

(a) (b) (c)

Figure 5 (a) Financial breakdown; 5(b) Project and program list interface; 5(c) Project progress tracking interface

4.3.3 Transparency View Screens

Figure 5 presents the interfaces of the system's Feedback and Issue Reporting module, which enables users to conveniently submit and manage community concerns. Figure 5(a) illustrates the New Report Form Interface, where users can create a report by selecting a category (e.g., infrastructure, education, transportation, services, or citizen concerns), entering a title and description, and uploading supporting images. The interface also includes a "Pin Location" feature and an option to submit reports anonymously, ensuring accessibility and encouraging wider participation. Figure 5(b) shows the Category Selection Interaction, highlighting the dropdown menu that allows users to classify their reports accurately. This feature supports proper categorization and routing of issues to the appropriate authorities, improving response efficiency and organization within the system. Figure 5(c) presents the Location Pinning Interface, where users can visually identify and confirm the exact location of the reported issue through an interactive map. This functionality enhances the accuracy of reports and facilitates quicker validation and response from concerned agencies.

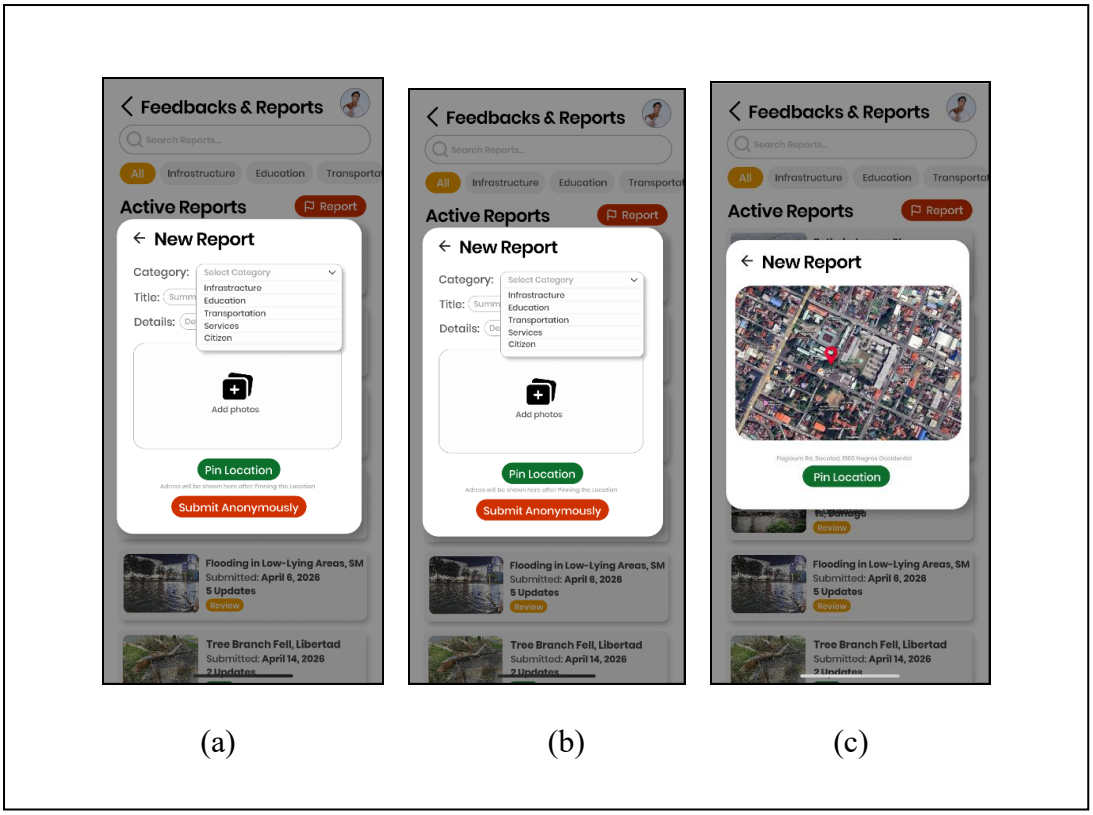

Figure 5 (a) Destination overview 13(b) Destination details; 13(c) Dining location for added feature

4.3 Prototype Evaluation

This section presents the analysis and interpretation of data collected from 35 respondents to evaluate the alignment between citizen monitoring tasks and the proposed technological solution. The study adopted the Task–Technology Fit (TTF) framework, assessing four key constructs: Task Characteristics, Technology Characteristics, Task–Technology Fit, and User Perceived Performance Impact. All indicators were measured using a **5-point Likert scale**, and results are presented using mean scores, standard deviations, and corresponding interpretations

4.3.1 Task Characteristics (Citizen Monitoring Tasks)

The results for Task Characteristics (Overall Mean = 3.60, Agree) indicate that respondents generally recognize the importance of engaging in citizen monitoring activities. The relatively higher ratings across most indicators suggest that participants perceive tasks such as verifying project progress, monitoring implementation, and understanding project updates as relevant and necessary. However, the neutral rating observed in one item (Q1) implies that while respondents acknowledge the importance of monitoring, this need may not yet be fully internalized as a consistent behavior. This reflects a gap between awareness and active engagement, which is common in early-stage civic technology adoption. From a prototype evaluation perspective, this finding confirms that the system addresses real and meaningful user needs, validating the relevance of the problem domain. At the same time, it highlights the need for the prototype to incorporate features that not only support tasks but also encourage sustained user participation.

Table 3 Task Characteristics Result

Code	Mean	SD	Interpretation
Q1	3.40	1.38	Neutral
Q2	3.60	1.41	Agree
Q3	3.80	1.33	Agree
Q4	3.63	1.33	Agree
Q5	3.57	1.37	Agree
Overall Mean	3.60	1.36	Agree

4.3.2 Technology Characteristics (Platform Features)

The evaluation of Technology Characteristics (Overall Mean = 3.50, Agree) suggests that the prototype is perceived as generally usable and functionally adequate. Respondents expressed agreement across all indicators, indicating that the system successfully delivers its core features, such as providing accessible information, presenting budget data clearly, and enabling user interaction. Notably, higher ratings associated with information clarity and feedback mechanisms suggest that users value transparency and participatory features within the platform. However, the absence of higher mean scores (e.g., above 4.0) indicates that while the prototype meets basic usability expectations, it has not yet achieved a level of excellence or strong user satisfaction. In the context of prototype evaluation, this implies that the system is functionally acceptable but still in a developmental stage, requiring enhancements in interface design, interactivity, and overall user experience to improve engagement and perceived quality.

Table 4 Technology Characteristics Result

Code	Mean	SD	Interpretation
Q1	3.42	1.33	Agree
Q2	3.49	1.33	Agree
Q3	3.54	1.36	Agree
Q4	3.49	1.32	Agree
Q5	3.54	1.38	Agree
Overall Mean	3.50	1.34	Agree

4.3.3 Task-Technology Fit (Platform Features)

The results for Task–Technology Fit (Overall Mean = 3.45, Agree) reveal a moderate level of alignment between user needs and system capabilities. While several indicators were rated positively, the presence of neutral responses (Q1 and Q4) suggests that the prototype does not yet fully support users in performing monitoring tasks effectively, nor does it clearly outperform traditional methods. This indicates that although the system facilitates access to information and improves understanding, its impact on actual task performance remains limited. From a prototype evaluation standpoint, this is a critical finding, as it highlights that the system is useful but not yet transformative. The prototype demonstrates potential but requires further refinement to strengthen its ability to enhance efficiency, reduce user effort, and provide clear advantages over existing approaches. This stage reflects a typical condition in early prototypes, where functionality exists but optimization and performance enhancement are still evolving.

Table 5 Task-Technology Fit

Code	Mean	SD	Interpretation
Q1	3.29	1.33	Neutral
Q2	3.57	1.35	Agree
Q3	3.54	1.33	Agree
Q4	3.29	1.29	Neutral
Q5	3.54	1.28	Agree
Overall Mean	3.45	1.32	Agree

4.3.4 User Perceived Performance Impact

The User Perceived Performance Impact results (Overall Mean = 3.44, Agree) indicate that respondents generally perceive the prototype as having a positive influence on their awareness, decision-making, and participation in government project monitoring. Higher ratings in areas related to awareness and informed opinion formation suggest that the system effectively contributes to knowledge dissemination. However, the neutral responses in items related to transparency and overall usefulness reveal that users are not yet fully convinced of the system's broader impact. This suggests that while the prototype demonstrates potential benefits, its value proposition has not been fully realized or experienced by users. In terms of prototype evaluation, this finding implies that the system is promising but still requires validation in more realistic or extended usage contexts. Enhancing system credibility, improving feature depth, and demonstrating tangible outcomes may help strengthen users' perception of its effectiveness.

Table 5 User Perceive Performance Impact

Code	Mean	SD	Interpretation
Q1	3.54	1.33	Agree
Q2	3.54	1.33	Agree
Q3	3.29	1.25	Neutral
Q4	3.54	1.25	Agree
Q5	3.29	1.27	Neutral
Overall Mean	3.44	1.29	Agree

4.3.4 Summary of Findings

The results reveal a clear pattern in which user need exceeds system impact. Task Characteristics obtained the highest mean (3.60), indicating that respondents strongly recognize the importance of monitoring government projects. In contrast, the lower mean scores for Task–Technology Fit (3.45) and User Perceived Performance Impact (3.44) suggest that the prototype has not yet fully translated this recognized need into corresponding outcomes. This disparity implies that while the system is relevant to users, its capacity to effectively support and enhance task performance remains limited. Furthermore, the findings indicate that the prototype is functional but not yet transformative. The Technology Characteristics score (3.50) reflects general acceptance of the system's features and usability. However, the absence of higher ratings suggests that the system does not yet provide a significantly improved or superior user experience. Although respondents perceive the system as useful, it is not yet viewed as a tool that substantially changes or enhances existing monitoring practices. The relatively lower score for Task–Technology Fit highlights a critical limitation. While the system supports user tasks at a basic level, it does not sufficiently improve efficiency or reduce effort compared to traditional methods. This suggests that the prototype currently functions more as an informational support tool rather than a performance-enhancing system, which is central to the Task–Technology Fit framework. Similarly, the lower mean for User Perceived Performance Impact indicates that respondents are not fully convinced of the system's overall effectiveness. Although users acknowledge its potential benefits, these remain largely perceived rather than experienced, likely due to the prototype's early stage of development. This underscores the need to demonstrate clearer, tangible benefits, such as improved transparency, faster access to information, and increased citizen participation. Overall, the computed mean of 3.50 indicates that the prototype is generally acceptable and positively perceived, albeit at a moderate level. While the system meets basic user expectations in terms of relevance and usability, it has not yet achieved a level of performance that strongly reinforces its effectiveness. These findings suggest that the prototype is functionally viable but requires further refinement, particularly in enhancing user engagement, improving task support, and delivering measurable performance outcomes that can elevate user perception from acceptance to strong endorsement.

Table 6 Summary of TTF Evaluation Results

Construct	Overall Mean	SD	Interpretation
Task Characteristics	3.60	1.36	Agree
Technology Characteristics	3.50	1.34	Agree
Task–Technology Fit	3.45	1.32	Agree
User Perceived Performance Impact	3.44	1.29	Agree

5. Discussion

The findings provide a structured evaluation of the proposed citizen-centric transparency platform using the Task–Technology Fit (TTF) framework. Overall, the results indicate that while the system is relevant and functionally adequate, its impact on user performance and engagement remains moderate, reflecting its prototype stage. The high score for Task Characteristics (M = 3.60) confirms that users recognize the importance of monitoring government projects, validating the relevance of the problem domain. However, the presence of neutral responses suggests a gap between awareness and actual engagement, indicating the need for features that actively promote participation. The Technology Characteristics (M = 3.50) results show that the system is generally usable and capable of delivering its intended functions. While respondents acknowledge its clarity and accessibility, the moderate rating suggests that the prototype meets baseline expectations but lacks a more refined and engaging user experience. The Task–Technology Fit (M = 3.45) indicates that alignment between user needs and system capabilities exists but is not fully optimized. The system supports information access but does not significantly enhance efficiency or outperform traditional methods, suggesting it functions primarily as an informational support tool. Similarly, the User Perceived Performance Impact (M = 3.44) reflects that users recognize the system's potential benefits, particularly in increasing awareness, but these benefits remain largely perceived rather than experienced. Overall, the results demonstrate a progression from strong task relevance to moderate system impact, indicating that the prototype has established a solid foundation but requires further refinement to enhance performance, strengthen task–technology alignment, and deliver measurable outcomes.

6. Conclusion

The proposed citizen-centric transparency platform is relevant, functional, and theoretically grounded, but remains in a developmental stage in terms of performance and impact. The integration of Task–Technology Fit Theory, E-Government Theory, and Transparency and Accountability Theory provided a strong conceptual foundation for designing a system that addresses real-world challenges in government project monitoring. The developed conceptual framework effectively translates user needs into system design by integrating data accessibility, visualization, and interactive features. The prototype interface further operationalizes this framework, demonstrating the feasibility of delivering a user-centered platform that supports transparency and citizen engagement. The evaluation results confirm that the system is acceptable and usable, as reflected in the overall mean of 3.50. However, the findings also reveal that the system has not yet fully achieved its intended purpose of enhancing task performance and delivering significant impact. The moderate ratings in Task–Technology Fit and User Perceived Performance Impact indicate that while the system supports user needs, it does not yet provide a clear advantage over existing methods. The study establishes that the prototype is functionally viable and holds strong potential for real-world application, particularly in improving access to government information and promoting citizen participation. However, further refinement is necessary to enhance system effectiveness, improve user experience, and deliver measurable performance benefits. Strengthening these aspects will be essential in transforming the system from a functional prototype into a fully effective transparency platform capable of supporting accountability and participatory governance.

Acknowledgements

The researchers would like to express their sincere gratitude to all individuals and institutions who contributed to the completion of this study. Special thanks are extended to Bobby A. Rodriguez III for his guidance, supervision, and valuable research insights, and to Ivan Patricio for his support and assistance in the development and implementation of the system. The researchers also thank their families for their unwavering support and encouragement, and their friends for providing valuable insights and motivation throughout the study. Appreciation is likewise extended to the College of Information and Communications Technology (CICT) and STI West Negros University for supporting the researchers and providing opportunities for learning and academic growth. Above all, the researchers give their deepest gratitude to God Almighty for His guidance, wisdom, and countless blessings throughout this journey.

References

Attard, J., Orlandi, F., Scerri, S., & Auer, S. (2015). A systematic review of open government data initiatives. *Government Information Quarterly, 32*(4), 399–418. https://doi.org/10.1016/j.giq.2015.07.006

Al Araby, M. A. A. (2024). Transforming citizen engagement in e-governance framework: A conceptual analysis. *Jurnal Analisis Kebijakan & Pelayanan Publik, 10*(2), 213–235. https://doi.org/10.31947/jakpp.v10i2.35497

Ansari, B., Barati, M., & Martin, E. G. (2022). Enhancing the usability and usefulness of open government data: A comprehensive review of the state of open government data visualization research. Government Information Quarterly, 39(1), 101657. https://doi.org/10.1016/j.giq.2021.101657

Belkhiria, F., & Thongpapanl, N. (2025). Importance of technology–job fit on the sustained use of e-government. *Journal of Global Information Management, 33*(1), 1–20. https://doi.org/10.4018/JGIM.394260

Bertot, J. C., Jaeger, P. T., & Grimes, J. M. (2010). Using ICTs to create a culture of transparency: E-government and social media as openness and anti-corruption tools for societies. Government Information Quarterly, 27(3), 264–271. https://doi.org/10.1016/j.giq.2010.03.001

Cucciniello, M., Porumbescu, G. A., & Grimmelikhuijsen, S. (2021). 25 years of transparency research: Evidence and future directions. *Public Administration Review, 81*(1), 32–44. https://doi.org/10.1111/puar.13229

Gonzalez-Zapata, F., & Heeks, R. (2015). The multiple meanings of open government data: Understanding different stakeholders and their perspectives. Government Information Quarterly, 32(4), 441–452. https://doi.org/10.1016/j.giq.2015.09.001

Goodhue, D. L., & Thompson, R. L. (1995). Task–technology fit and individual performance. MIS Quarterly, 19(2), 213–236. https://doi.org/10.2307/249688

Hossain, M. A., Dwivedi, Y. K., & Rana, N. P. (2016). State-of-the-art in open data research: Insights from existing literature and a research agenda. *Journal of Organizational Computing and Electronic Commerce, 26*(1–2), 14–40. https://doi.org/10.1080/10919392.2015.1124007

Lourenço, R. P. (2023). Government transparency: Monitoring public policy accumulation and administrative overload. *Government Information Quarterly, 40*(1), Article 101762. https://doi.org/10.1016/j.giq.2022.101762

Lubis, M. A., et al. (2024). Electronic governance in advancing sustainable development goals: A systematic literature review. Discover Global Society. https://doi.org/10.1007/s44282-024-00102-3

Meijer, A. (2009). Understanding modern transparency. International Review of Administrative Sciences, 75(2), 255–269. https://doi.org/10.1177/0020852309104175

Nam, T. (2012). Suggesting frameworks of citizen-sourcing via Government 2.0. Government Information Quarterly, 29(1), 12–20. https://doi.org/10.1016/j.giq.2011.07.005

OECD. (2022). Government at a glance 2021/2022: Accountability and transparency in the public sector. OECD Publishing. https://doi.org/10.1787/1c258f55-en

Pratiwi, R. I., Haliah, & Kusumawati, A. (2024). The influence of transparency, governance, and financial accountability in managing financial reporting in the public sector. International *Journal of Educational and Life Sciences, 2*(10), 1165–1180. https://doi.org/10.59890/ijels.v2i10.2571

Pujari, R., & Joshi, P. (2024). Transparency in public sector governance: The role of the Right to Information Act. ShodhKosh: *Journal of Visual and Performing Arts, 5*(6), 187–196. https://doi.org/10.29121/shodhkosh.v5.i6.2024.3817

Putra, R. R., Putra, E., & Handayani, S. (2023). User interface design for citizen data grouping information system using human-centered design method. SITEKIN: *Jurnal Sains, Teknologi dan Industri, 20*(2). http://dx.doi.org/10.24014/sitekin.v20i2.21450

Ruijer, E., Grimmelikhuijsen, S., van den Berg, J., & Meijer, A. (2018). Open data work: Understanding open data usage from a practice lens. International Review of Administrative Sciences, 86(1), 3–19. https://doi.org/10.1177/0020852317753068

Sari, R., & Muslim, M. (2023). Accountability and transparency in public sector accounting: A systematic review. Amkop *Management Accounting Review, 3*(2), 90–106. https://doi.org/10.37531/amar.v3i2.1440

Suradi, A., Purnomo, H. D., & Hendry. (2026). A user-centred e-government service design framework. *Engineering, Technology & Applied Science Research, 16*(1), 31852–31862. https://doi.org/10.48084/etasr.14851

United Nations Department of Economic and Social Affairs. (2024). United Nations e-government survey 2024. https://publicadministration.un.org/egovkb/en-us/Reports/UN-E-Government-Survey-2024

Valle, J. S., et al. (2024). Impact of e-government technologies on citizen engagement. *International Journal of Multidisciplinary: Applied Business and Education Research, 5*(11), 4577–4591. https://doi.org/10.11594/ijmaber.05.11.24

World Bank. (2023). GovTech maturity index 2023: GovTech—Putting people first. https://www.worldbank.org/en/topic/governance/brief/govtech-putting-people-first

Zhang, L., & Chen, X. (2023). Online civic engagement in smart cities. *Computers in Human Behavior, 143*, 107682. https://doi.org/10.1016/j.chb.2023.107682.

Enhanced phosphate removal using chemically activated eggshell derived CaO

Punnawat Pengthong[1], Chitawan Daolert[1], Kornkanok Srisarat[2], Chanokchon Anukul[3], Sakdinun Nuntang[3*]

[1]Montfort College, Chiang Mai, 50000, Thailand
[2]The Prince Royal's College, Chiang Mai, 50000, Thailand
[3]Industrial Chemistry Innovation Program, Faculty of Science, Maejo University, Chiang Mai 50290, Thailand
*Sakdinun.nt@gmail.com

Abstract

This study investigates the development of a low-cost adsorbent derived from chicken eggshell waste for phosphate removal from aqueous solutions. Activated eggshell adsorbents were prepared using different chemical activating agents, including H_3PO_4, NaOH, and $ZnCl_2$, followed by thermal treatment. The physicochemical properties of the synthesized materials were characterized using X-ray diffraction and nitrogen adsorption–desorption analysis. Batch adsorption experiments were conducted to evaluate the effects of adsorbent type, contact time, initial phosphate concentration, adsorbent dosage, and solution pH. The results revealed that chemical activation significantly enhanced the surface properties and adsorption performance compared to raw eggshell. Among the prepared materials, $ZnCl_2$-eggshell adsorbent exhibited the highest adsorption capacity (67.20 mg/g), which was attributed to the combined effect of increased surface area and the presence of CaO active phases. The adsorption process reached equilibrium within 120 min, and the maximum adsorption capacity increased with increasing adsorbent dosage but decreased at higher initial phosphate concentrations. The adsorption efficiency was also influenced by solution pH, with optimal performance observed under mildly acidic conditions. The removal mechanism was mainly governed by the interaction between CaO and phosphate ions, involving both surface adsorption and chemical precipitation.

Keywords: Eggshell waste; Activated eggshell; Phosphate removal; Adsorption; Calcium-based adsorbent

1. Introduction

Phosphorus (P) is an essential nutrient for biological systems; however, its excessive release into aquatic environments has become a critical environmental concern. Phosphate originating from domestic wastewater, agricultural runoff, and urban discharge can be transported into natural water bodies through precipitation and surface flow. Elevated phosphate levels stimulate the rapid proliferation of phytoplankton, ultimately leading to eutrophication, a process that severely disrupts aquatic ecosystems. This phenomenon is associated with oxygen depletion, deterioration of water quality, and significant losses in biodiversity, posing long-term ecological and public health risks (Smith et al., 2016; Schindler et al., 2016). In addition, harmful algal blooms can produce toxins that accumulate along the food chain, increasing the risk of human exposure (Paerl & Otten, 2018). It has been reported that eutrophication may occur when phosphate concentrations exceed approximately 0.02 mg/L in freshwater systems, emphasizing the need for strict regulation and efficient removal strategies (Carpenter, 2020).

Various technologies have been developed to remove phosphorus from wastewater, including chemical precipitation, ion exchange, biological treatment, membrane filtration, and electrochemical processes (Yeoman et al., 2017; Nguyen et al., 2019). Despite their effectiveness, these methods often suffer from high operational costs, energy demand, and the generation of secondary waste such as sludge, which requires further treatment and disposal (Loganathan et al., 2014; Wang et al., 2021). These challenges highlight the need for alternative approaches that are both economically viable and environmentally sustainable.

Among the available techniques, adsorption has gained considerable attention due to its simplicity, cost-effectiveness, and high removal efficiency. Recent studies have focused on developing adsorbents derived from natural minerals, synthetic materials, and industrial by-products (Zhang et al., 2019; Li et al., 2022). However, mineral-based and engineered adsorbents are often limited by production costs and scalability, while some waste derived materials, such as fly ash or sludge, may introduce secondary contamination through leaching of hazardous components (Gao et

al., 2020). Therefore, identifying safe, low-cost, and efficient adsorbents remains a key research priority.

Recently, calcium rich materials have emerged as promising candidates for phosphate removal due to their strong affinity for phosphate ions through precipitation and surface complexation mechanisms. Moreover, phosphate-loaded calcium materials can potentially be repurposed as fertilizers, contributing to resource recovery and circular economy strategies (Kumar et al., 2018; Xie et al., 2020). This dual functionality offers a sustainable pathway for both wastewater treatment and nutrient recycling.

The chicken eggshell waste is particularly attractive due to its abundance, low cost, and high calcium carbonate ($CaCO_3$) content. Eggshells are primarily composed of $CaCO_3$, with minor fractions of calcium phosphate, magnesium carbonate, and organic matter (King'ori, 2019). Prior research has demonstrated their applicability in various environmental applications, including heavy metal removal, catalyst development, and adsorption processes (Cho et al., 2017; Al-Ghouti & Da'ana, 2020). These findings suggest that eggshell-derived materials have strong potential as value-added adsorbents.

To further enhance adsorption performance, chemical activation is commonly employed to modify the physicochemical properties of biomass-derived materials. Activating agents such as phosphoric acid (H_3PO_4), sodium hydroxide (NaOH), and zinc chloride ($ZnCl_2$) have been shown to significantly improve porosity, surface area, and functional group distribution, thereby enhancing adsorption capacity (Ioannidou & Zabaniotou, 2017; Tran et al., 2021). Nevertheless, studies that systematically compare the effects of different chemical activating agents on eggshell-derived materials for phosphate removal remain limited.

Therefore, this study aims to develop and evaluate activated material derived from chicken eggshell waste using different chemical activation strategies. The synthesized materials were characterized in terms of their structural and surface properties using X-ray diffraction (XRD) and nitrogen adsorption–desorption analysis. The adsorption performance toward phosphate was investigated through batch experiments, and phosphate concentrations were quantified using UV–visible spectrophotometry. This work is expected to provide new insights into the utilization of eggshell waste as a sustainable, low-cost adsorbent for efficient phosphate removal from aqueous systems.

2. Materials and methods

2.1 Preparation of activated eggshell adsorbent (Act.-ES)

Eggshells were cleansed and desiccated in sunlight for one day. Grind the powder into a fine consistency. The powdered eggshell was thoroughly combined with a 4:1 ratio of an activating agent (H_3PO_4, NaOH, and $ZnCl_2$: AR grade: Sigma-Aldrich) to eggshells. Agitate the solution for one hour. Allow the solution to rest for 24 hours to facilitate the activation process. Subsequently, the mixture was activated at 400 °C for 3 hours in a muffle furnace. The activated eggshell adsorbent was then washed to neutrality and dried at 100 °C for one hour. The activated eggshell adsorbent utilizing activating agents H_3PO_4, NaOH, and $ZnCl_2$ were designated as Act.-*ES*-H_3PO_4, Act.-*ES*-NaOH, and Act.-*ES*-$ZnCl_2$, respectively.

2.2 Characterization of adsorbents

The structural information of the activated eggshell adsorbent was obtained using power X-ray diffraction (XRD) analysis on a Empyrean 3 Panalytical dif-fractometer employing Cu Kα radiation and an X-ray power of 40 kV and 40 mA. N_2 adsorption-desorption measurement was conducted at -196 ºC using an Anton Paar Nova 600 to obtain the textural properties of the materials. The weight of the sample used (initially around 40 mg) was measured exactly after pretreatment at 100 ºC for 2 h.

2.3 Adsorption study

In a batch system, the adsorption studies of phosphate on activated eggshell adsorbent were performed using 50-mL Erlenmeyer flasks containing phosphate solution and dried absorbents. All batch experiments were carried out in 50 mL glass-stoppered, Erlenmeyer flasks containing a fixed amount of adsorbent with 15 mL phosphate solution at a known initial concentration. The flasks were

agitated at a constant speed of 120 rpm in an incubator shaker at room temperature. The type of adsorbents, initial phosphate concentrations, time, solid/liquid ratio and pH were evaluated in this study.

Phosphate concentration in aqueous samples was determined using the molybdenum blue method according to the standard procedures described by American Public Health Association (APHA, 2017). Briefly, an appropriate 5 mL sample solution was mixed with the freshly prepared colorimetric reagent (0.8 mL). The reaction mixture was allowed to stand for 10 min at room temperature to ensure complete color development. The absorbance of the resulting, blue-colored complex was then measured at a wavelength (λ_{max}) of 830 nm using a UV–visible spectrophotometer (Jasco V-7 3 0) as show in Fig. 1. The colorimetric reagent used for phosphate determination was prepared by mixing four stock solutions: 5 N sulfuric acid (H_2SO_4), 5% (w/v) ammonium molybdate tetrahydrate ($(NH_4)_6Mo_7O_{24}\cdot 4H_2O$: AR grade: Sigma-Aldrich), 1.76% (w/v) L-ascorbic acid ($C_6H_8O_6$: AR grade: RCI Labscan), and 0.3 % (w/v) potassium antimony tartrate trihydrate ($K(SbO)C_4H_4O_6\cdot 3H_2O$: AR grade: Sigma-Aldrich). These solutions were combined in a volumetric ratio of 50:5:30:1, respectively, to obtain the working reagent. The amount of phosphate removal and adsorption capacity was calculated according to a mass balance on the phosphate concentration using Eq (1) and Eq. (2), respectively:

$$\% \text{ Phosphate removal} = \frac{(C_o - C_e)}{C_o} \times 100 \quad (1)$$

$$\text{Adsorption capacity: } q_e = \frac{(C_o - C_e)V_i}{W} \quad (2)$$

where Q_e is adsorption capacity at adsorption equilibrium (mg/g, dried adsorbent); C_o is the initial phosphate concentration (mg/L); C_e is the equilibrium phosphate concentration in solution (mg/L); V_i is the volume of initial solution (L); W is the weight of dried adsorbent (g). All the experiments were performed duplicate and the average value from results was taken. All measurements were performed in triplicate (n = 3), and the results are reported as mean ± standard deviation.

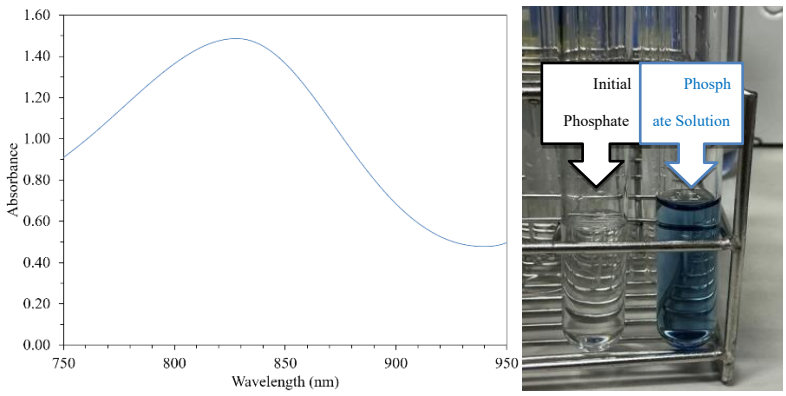

Fig. 1. UV-Vis data of phosphate spectrum (λ_{max} = 830 nm).

3. Results and discussion

3.1 Characterization of adsorbents

The crystalline characteristics of raw eggshell and chemically activated eggshell-derived carbons were investigated using X-ray diffraction (XRD), as shown in Fig. 2. The diffraction pattern of the untreated eggshell exhibited a dominant peak at $2\theta \approx 29.5°$, which is attributed to the calcite phase ($CaCO_3$), confirming that calcium carbonate is the primary constituent of the raw material. After chemical activation followed by thermal treatment, the diffraction patterns of all modified samples revealed the emergence of CaO-related phases, accompanied by a noticeable reduction in

calcite peak intensity. This observation indicates that $CaCO_3$ was partially decomposed and transformed into CaO during the activation process. Such phase transformation has been widely reported for calcium-rich biomaterials subjected to high-temperature treatment (Cho et al., 2017; King'ori, 2019).

Among the different activating agents, the sample treated with phosphoric acid exhibited the most significant structural alteration, as evidenced by the reduced calcite peak and the increased intensity of CaO-related reflections. This behavior can be explained by the chemical interaction between H_3PO_4 and $CaCO_3$, leading to the formation of calcium phosphate intermediates, which subsequently decompose into CaO upon calcination. In contrast, NaOH and $ZnCl_2$ mainly act as pore forming agents and do not significantly react with $CaCO_3$ prior to thermal treatment (Gao et al., 2020; Tran et al., 2021).

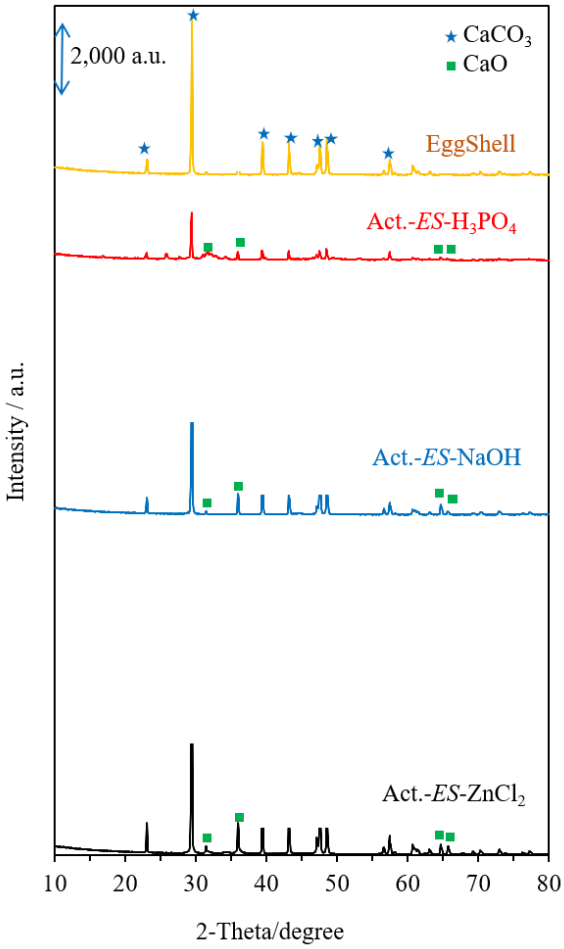

Fig. 2. XRD analysis of Eggshell, Act.-*ES*-H_3PO_4, Act.-*ES*-NaOH, and Act.-*ES*-$ZnCl_2$.

The textural properties of the materials are summarized in Table 1. The pristine eggshell exhibited a negligible BET surface area, reflecting its non-porous structure. In contrast, all activated samples showed a considerable increase in surface area, confirming the effectiveness of chemical activation. The surface area followed the order: H_3PO_4 > $ZnCl_2$ > NaOH, which is consistent with previous findings that phosphoric acid promotes both micropore and mesopore formation through bond cleavage and structural rearrangement mechanisms (Li et al., 2022). These results clearly demonstrate that the choice of activating agent plays a crucial role in determining both the mineral composition and pore structure, which are key factors governing adsorption performance.

Table 1. Textural properties of the eggshell and activated eggshell adsorbent.

Sample	*Specific surface area* (S_{BET}) ($m^2\ g^{-1}$)
Eggshell	0.15
Act.-*ES*-H_3PO_4	6.74
Act.-*ES*-NaOH	2.98
Act.-*ES*-$ZnCl_2$	6.30

3.2 Adsorption behavior for phosphate removal

The influence of adsorbent type on phosphate removal is illustrated in Fig. 3. All activated samples exhibited significantly higher removal efficiency compared to raw eggshell, highlighting the importance of surface modification and pore development. Among them, the $ZnCl_2$-activated sample showed the highest adsorption capacity (67.20 mg/g), which can be attributed to its relatively high surface area combined with a significant CaO content.

The enhanced performance of this material is mainly associated with the chemical interaction between CaO and phosphate ions, leading to the formation of insoluble calcium phosphate ($Ca_3(PO_4)_2$). This indicates that the removal mechanism involves both surface adsorption and chemical precipitation, which is consistent with previous studies on calcium-based adsorbents (Kumar et al., 2018; Xie et al., 2020). Therefore, the Act.-*ES*-$ZnCl_2$ adsorbent was selected for further investigation.

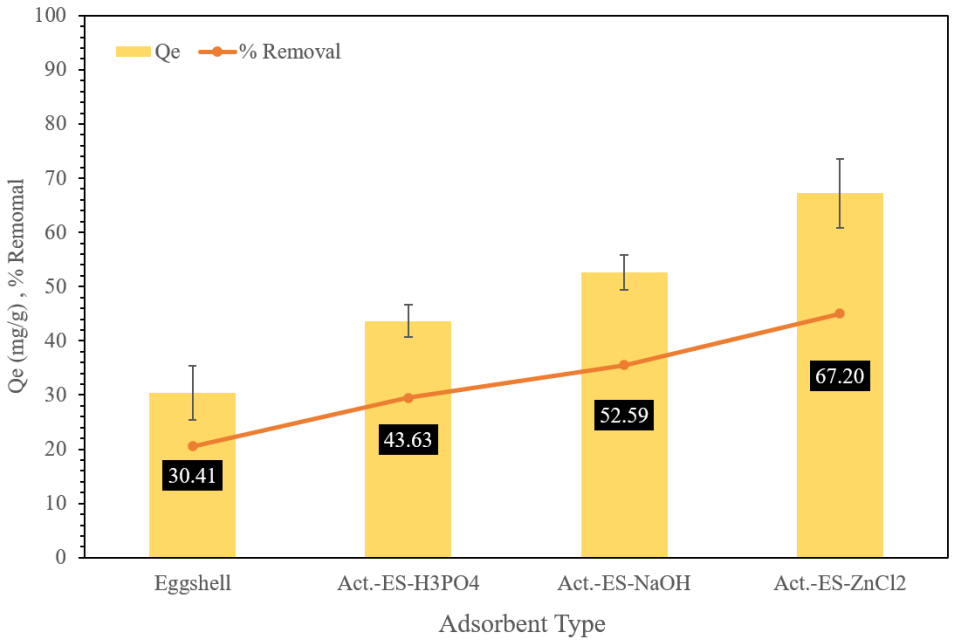

Fig. 3. Effect of type of adsorbents on phosphate removal.

The adsorption kinetics of phosphate onto the selected adsorbent are presented in Fig. 4. A rapid uptake of phosphate was observed during the initial stage (within 100 min), followed by a slower adsorption rate until equilibrium was reached at approximately 120 min. The initial rapid adsorption can be attributed to the availability of abundant active sites on the adsorbent surface. As the adsorption process proceeds, these sites become progressively occupied, resulting in a decrease in adsorption rate. This behavior is typical for adsorption systems involving heterogeneous surfaces and has been widely reported in phosphate adsorption studies (Wang et al., 2021).

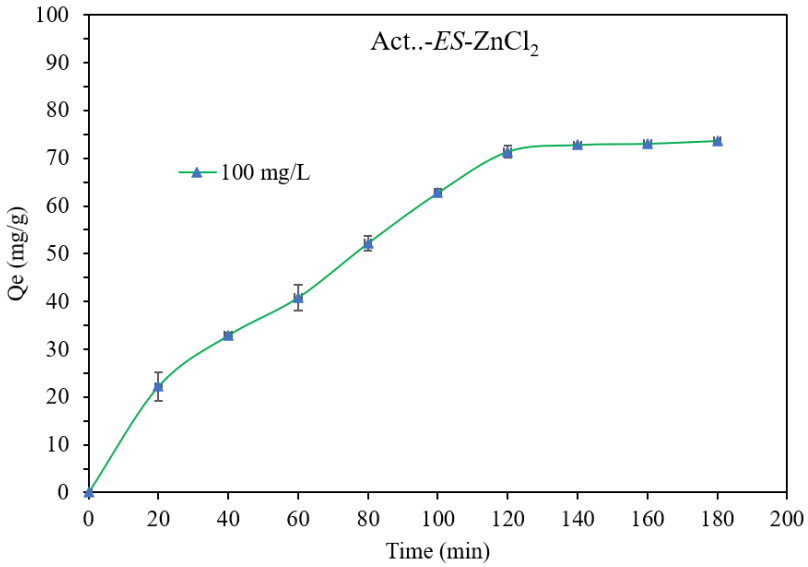

Fig. 4 Effect of contact time on phosphate removal.

The effect of initial phosphate concentration on adsorption capacity is shown in Fig. 5. The adsorption capacity decreased from 71.40 to 57.88 mg/g as the initial concentration increased from 100 to 150 mg/L. The decrease in adsorption capacity at higher phosphate concentrations was not consistent with the behavior typically observed in conventional adsorption systems, where increasing initial concentration generally enhances adsorption capacity due to a stronger concentration gradient. In the present study, phosphate removal was governed not only by surface adsorption but also by calcium phosphate precipitation involving CaO species derived from calcined eggshells. At elevated phosphate concentrations, rapid formation of calcium phosphate precipitates may occur on the adsorbent surface, blocking accessible active sites and limiting further phosphate diffusion into the porous structure. This phenomenon could reduce the effective utilization of adsorption sites and consequently lower the measured adsorption capacity. Similar behavior has been reported for calcium-based adsorbents where surface precipitation becomes the dominant removal mechanism under high phosphate loading conditions. (Nguyen et al., 2019).

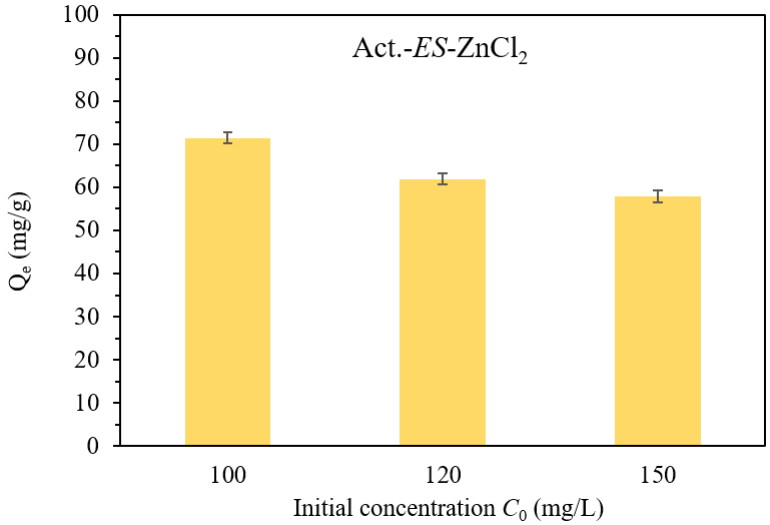

Fig. 5 Effect of initial concentration on phosphate removal.

The influence of adsorbent dosage on phosphate removal is presented in Fig. 6. The adsorption capacity increased from 71.40 to 88.90 mg/g when the dosage was increased from 0.01 to 0.03 g per 15 mL solution. This improvement can be attributed to the increased availability of active sites, including both surface functional groups and CaO phases. A higher dosage provides more adsorption sites and enhances

the probability of interaction between phosphate ions and the adsorbent surface. Similar observations have been reported for other calcium-rich adsorbents used in phosphate removal (Zhang et al., 2019).

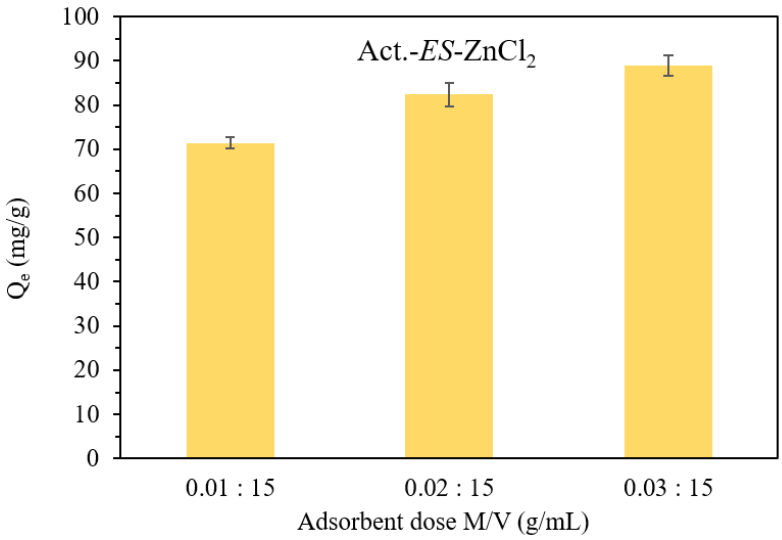

Fig. 6 Effect of adsorbent dose on phosphate removal.

The effect of solution pH on phosphate adsorption is shown in Fig. 7. The adsorption capacity decreased as the pH increased from 5 to 9, with a maximum value of 70.80 mg/g observed under mildly acidic conditions. The pH dependent behavior can be explained by the speciation of phosphate ions and the surface charge of the adsorbent. Under acidic conditions, the presence of $H_2PO_4^-$ species and positively charged surface sites favors electrostatic attraction and ion exchange. As the pH increases, the dominant species shift toward HPO_4^{2-} and PO_4^{3-}, while the surface becomes less positively charged, reducing adsorption efficiency. Furthermore, previous studies have reported that phosphate removal by calcium-based materials is governed by both ion exchange and precipitation mechanisms at pH < 8.5, whereas precipitation becomes dominant at higher pH values (Blanco et al., 2016). The results obtained in this study suggest that precipitation plays a significant role in phosphate removal, particularly due to the presence of CaO in the adsorbent.

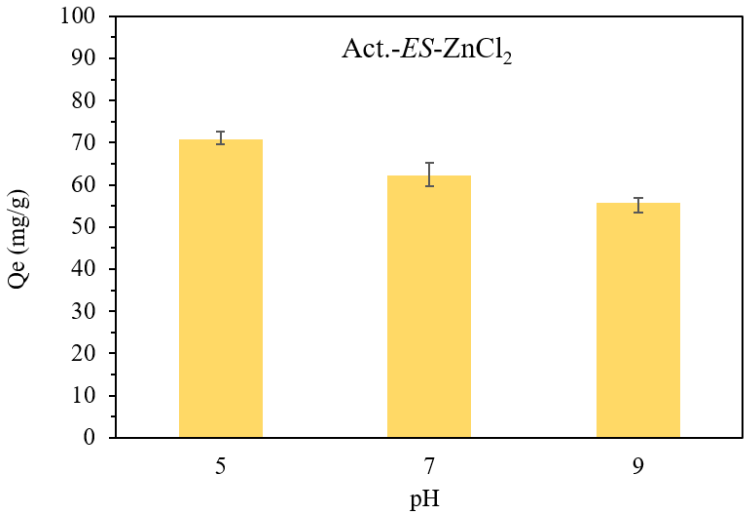

Fig. 7 Effect of pH on phosphate removal.

4. Conclusion

In this study, activated eggshell adsorbent was successfully synthesized using different chemical activating agents and applied for phosphate removal from aqueous solutions. The results demonstrated that chemical activation significantly improved both the structural and adsorption properties of the materials. Among the prepared adsorbents, the $ZnCl_2$-activated sample exhibited superior performance due to its higher surface area and the presence of CaO phases, which played a

key role in phosphate removal. The adsorption process was strongly influenced by operational parameters, including contact time, initial concentration, adsorbent dosage, and solution pH. Equilibrium was achieved within 120 min, and higher adsorption capacity was obtained at lower initial phosphate concentrations and higher adsorbent dosages. The adsorption behavior was found to be pH-dependent, with improved performance under mildly acidic conditions. The removal mechanism was attributed to a combination of surface adsorption and precipitation reactions between calcium species and phosphate ions.

References

American Public Health Association (APHA), American Water Works Association (AWWA), Water Environment Federation (WEF). (2017). Standard Methods for the Examination of Water and Wastewater (23rd ed.). Washington, DC.

Blanco, I., Molle, P., de Miera, L. E. S., Ansola, G. (2016). Basic oxygen furnace steel slag aggregates for phosphorus treatment: Evaluation of its potential use as a substrate in constructed wetlands. *Water Research*, 89, 355–365.

Carpenter, S. R. (2020). Eutrophication of aquatic ecosystems: Bistability and soil phosphorus. *Proceedings of the National Academy of Sciences*, 117(7), 3330–3332.

Cho, Y., Seo, D., Lee, H., Kim, J. (2017). Application of eggshell waste as an adsorbent for removing heavy metals from aqueous solutions. *Journal of Environmental Chemical Engineering*, 5(3), 2561–2568.

Gao, Y., Yue, Q., Gao, B., Li, A. (2020). Insight into activated carbon from different kinds of chemical activating agents: A review. *Science of the Total Environment*, 746, 141094.

King'ori, A. M. (2019). A review of the uses of poultry eggshells and shell membranes. *International Journal of Poultry Science*, 10(11), 908–912.

Kumar, R., Sharma, R. K., Singh, A. P. (2018). Phosphorus recovery from wastewater using calcium-based adsorbents: A review. *Journal of Environmental Chemical Engineering*, 6(3), 3525–3534.

Li, R., Wang, J. J., Zhou, B., Awasthi, M. K., Ali, A., Zhang, Z. (2022). Enhancing phosphate adsorption by modified biochar: A review. *Science of the Total Environment*, 812, 152536.

Nguyen, T. A. H., Ngo, H. H., Guo, W. S., Nguyen, T. V., Li, J., Liang, S. (2019). Phosphorus elimination from wastewater using adsorption processes: A critical review. *Journal of Environmental Management*, 236, 386–402.

Paerl, H. W., Otten, T. G. (2018). Harmful cyanobacterial blooms: Causes, consequences, and controls. *Microbial Ecology*, 65(4), 995–1010.

Schindler, D. W., Hecky, R. E., McCullough, G. K. (2016). The rapid eutrophication of Lake Winnipeg: Greening under global change. *Journal of Great Lakes Research*, 42(1), 6–13.

Smith, V. H., Joye, S. B., Howarth, R. W. (2016). Eutrophication of freshwater and marine ecosystems. *Limnology and Oceanography*, 61(S1), S1–S14.

Tran, H. N., You, S. J., Hosseini-Bandegharaei, A., Chao, H. P. (2021). Mistakes and inconsistencies regarding adsorption of contaminants from aqueous solutions: A critical review. *Water Research*, 120, 88–116.

Wang, J., Chen, Y., Liu, Y. (2021). Advanced materials for phosphorus removal from wastewater: A review. *Chemical Engineering Journal*, 406, 126788.

Xie, F., Wu, F., Liu, G., Mu, Y., Feng, C., Wang, H. (2020). Phosphate recovery from wastewater by calcium-based materials and its reuse as fertilizer. *Journal of Cleaner Production*, 265, 121782.

Yeoman, S., Stephenson, T., Lester, J. N., Perry, R. (2017). The removal of phosphorus during wastewater treatment: A review. *Environmental Pollution*, 49(3), 183–233.

Zhang, M., Song, G., Gelardi, D. L., Huang, L., Khan, E., Carroll, K. C., et al. (2019). Evaluating biochar and its modifications for the removal of ammonium, nitrate, and phosphate in water. *Water Research*, 148, 1–19.

Synthesis of amine functionalized rice husk silica for enhanced purification of anthocyanins from butterfly pea (*Clitoria ternatea*)

Ponpomkwan Chanhom[1], Natcha Vanichchagorn[2], Natthanai kosaiyakanont[3], Tummatida Kittitirapong[4], Nichaphat Chansai[5], Sakdinun Nuntang[5*]

[1]Chiang Mai University Demonstration School, Chiang Mai, 50000, Thailand
[2]Chiang Mai International School, Chiang Mai, 50000, Thailand
[3]Montfort College, Chiang Mai, 50000, Thailand
[4]Bunyawat Witthayalai School, Lampang, 52000, Thailand
[5]Industrial Chemistry Innovation Program, Faculty of Science, Maejo University, Chiang Mai 50290, Thailand
*Sakdinun.nt@gmail.com

Abstract

This study investigates the synthesis of amine-functionalized rice husk silica (RHS–NH_2) for the purification of anthocyanins from butterfly pea (*Clitoria ternatea*) extract. Rice husk silica (RHS) was prepared via acid treatment and calcination, followed by surface modification using (3-aminopropyl)triethoxysilane through a post-grafting method. The obtained materials were characterized by FTIR and N_2 adsorption–desorption analysis, confirming the successful introduction of amine functional groups and the preservation of mesoporous structure. Anthocyanins were extracted using an aqueous system under controlled conditions, and the effects of extraction time, adsorption, and desorption were systematically evaluated. The results showed that increasing extraction time enhanced anthocyanin yield, reaching optimal conditions at 2 h. The RHS–NH_2 adsorbent exhibited significantly higher adsorption performance compared to pristine RHS, despite its lower surface area, due to the presence of amine groups that promote electrostatic interactions and hydrogen bonding with anthocyanin molecules. Desorption studies revealed that a water to ethanol mixture (50:50, v/v) provided the highest recovery of anthocyanins from RHS–NH_2. The overall findings demonstrate that amine-functionalized rice husk silica is an effective and low-cost adsorbent for improving anthocyanin purification, with potential for application in food and pharmaceutical industries.

Keywords: anthocyanin; butterfly pea; rice husk silica; amine functionalization; adsorption–desorption.

1. Introduction

Butterfly pea (*Clitoria ternatea*) is a widely cultivated perennial plant recognized for its adaptability, low cultivation cost, and contribution to soil enrichment. Its flowers have attracted increasing attention due to their rich phytochemical profile and versatile applications in food, pharmaceutical, and biomedical fields. In particular, butterfly pea extracts are commercially available in various forms, including dried powders, concentrations, and encapsulated products, owing to their stability under refrigerated conditions and ease of processing. These extracts are especially valued as natural colorants and bioactive ingredients, driven by growing demand for plant-derived compounds with functional health benefits.

Anthocyanins are the bioactive constituents in butterfly pea flowers, predominantly present as polyacylated derivatives that exhibit remarkable color stability in neutral to mildly acidic conditions. Beyond their coloring properties, anthocyanins possess strong antioxidants, anti-inflammatory, and potential therapeutic activities, making them promising candidates for medical and nutraceutical applications (Khoo et al., 2017; He & Giusti, 2015). Butterfly pea is particularly notable among anthocyanin sources because it produces a distinct blue pigment, which is relatively rare in nature and highly desirable for food and pharmaceutical formulations (Escher et al., 2020; Chayaratanasin et al., 2021).

Conventional extraction techniques, such as aqueous extraction at moderate temperatures (50–60 °C), have been widely employed due to their simplicity, safety, and compatibility with food-grade processing (Prabawati et al., 2019; Pham et al., 2020). However, these approaches typically yield crude extracts containing complex mixtures of anthocyanins, sugars, organic acids, and other phenolic compounds. Advanced separation technologies, including membrane filtration (ultrafiltration

and nanofiltration) and osmotic concentration, have been explored to enrich anthocyanin content; nevertheless, these methods are often limited to concentration rather than true purification, resulting in products of insufficient purity for high-value applications (Cassano et al., 2018; Li et al., 2022).

Adsorption-based purification has emerged as an effective strategy for isolating anthocyanins due to its operational simplicity, scalability, and cost efficiency. Macroporous resins, such as Amberlite XAD series, have been extensively used for anthocyanin recovery from plant matrices (Sun et al., 2018; Zhang et al., 2019). Despite their effectiveness, these materials present several drawbacks, including high cost, limited chemical stability under prolonged operation, and reduced mechanical durability, which restrict their large-scale application.

In recent years, biogenic silica derived from agricultural waste, particularly rice husks, has gained attention as a sustainable and low-cost alternative adsorbent. Rice husk silica (RHS) can be produced through acid leaching followed by controlled thermal treatment, yielding a high-purity amorphous silica with a large specific surface area and tunable pore structure (Kalapathy et al., 2015; Shen et al., 2021). The abundant availability and environmentally friendly nature of rice husks further enhance the attractiveness of this material for green processing applications. To improve adsorption performance, surface functionalization of silica has been widely investigated. Among various modifications, amine functionalization has proven particularly effective due to the introduction of positively charged active sites, which can promote electrostatic interactions, hydrogen bonding, and π–π interactions with anthocyanin molecules (Tran et al., 2017; Wang et al., 2020). Such interactions are crucial for enhancing both adsorption capacity and selectivity, especially in complex plant extracts. Consequently, amine-functionalized silica materials have shown significant potential in the purification of bioactive compounds, including phenolics and pigments, under mild and controllable conditions.

Previous studies have demonstrated that amine-functionalized silica materials can effectively adsorb various phenolic compounds, dyes, and bioactive molecules due to the presence of amino groups, which enhance specific interactions with these compounds. Similarly, rice husk-derived silica has been widely investigated as a sustainable adsorbent because of its high silica content, low cost, and environmental friendliness. However, most reported studies have focused on pollutant removal, metal ion adsorption, or general adsorption applications. In contrast, the use of amine-functionalized rice husk silica (RHS–NH_2) for anthocyanin purification has received very limited attention.

To the best of our knowledge, no previous study has systematically investigated the adsorption–desorption behavior of anthocyanins from butterfly pea extract using RHS–NH_2 as an adsorbent. Therefore, the present work aims to bridge this gap by developing a low-cost and sustainable adsorbent derived from agricultural waste for anthocyanin purification and evaluating its adsorption and desorption performance under different operating conditions.

2. Materials and methods

2.1 Preparation of amine-functionalized rice husk silica (RHS–NH_2)

First, 40 g of rice husk was submerged for 4 h in 1M HCl. The solid was rinsed multiple times with DI water and dried in a 110 ºC oven for 2 days. The material was generated into rice husk silica by heat-treating in a muffle furnace for 6 h at 700 ºC using ceramic crucibles. The rice husk treated with acid was designated as RHS.

Amine-functionalized rice husk silicas were prepared via post grafting method. The silanol groups on the silica surface were substituted with amino silanes under reflux conditions. Firstly, 5 g of RHS was refluxed in toluene (100 mL) at 70 ºC for 2 hours. Subsequently, 4 g of (3-Aminopropyl)-triethoxysilane (APTES) was added slowly using a dropper. The mixture underwent continuous reflux for a duration of 24 hours. The solid was filtered, washed twice with ethanol and dichloromethane, and allowed to dry at room temperature. The samples were designated as RHS-NH_2.

2.2 Characterization of amine-functionalized rice husk silica (RHS–NH_2)

Standard procedures were used to characterize the prepared physical and chemical properties of the adsorbents. N_2 adsorption-desorption measurements were carried out at -196 °C using a BEL Japan BELSORP-mini II instrument to determine the material's textural characteristics. All samples were pre-treated at 150 °C for 2 h and then measured for exact weight prior to the adsorption. The

specific surface area (S_{BET}) was calculated according to Brunauer–Emmett–Teller (BET) theory using adsorption data at relative pressures (P/P_0) of 0.02–0.2. The total pore volume (V_t) was evaluated at a relative pressure of about 0.99. The pore diameter was calculated from the desorption branches using the Barrett–Joyner–Halenda (BJH) method. The presence of functional groups was determined using Fourier-transform infrared (FTIR) spectra (Perkin Elmer spectrum two: 900–4000 cm^{-1} in transmittance mode by KBr pellet technique).

2.3 Butterfly pea extraction

Dry butterfly pea flower was extracted with deionized water using a mass (g)/volume(mL) ratio of dried butterfly pea to water of 1:20 for 0.5, 1 and 2 h at 60 °C. The extraction procedure was repeated three times, until the extract was colorless. The extracts were combined and filtered through a filter paper, then concentrated under reduced pressure with a rotary evaporator (R-100 BUCHI Rotavapor, Switzerland) and then kept at 4 °C until used.

2.4 Determination of Anthocyanin Content

Data indicated that the absorption maximum of the water extract of butterfly pea anthocyanins was found to be at wavelength of 520 nm as reported by Bani et. al. The butterfly pea anthocyanin content was determined by the pH differential method. A JASCO V-730 UV−vis spectrophotometer was used for spectral measurements at 5 2 0 and 7 00 nm, respectively, using deionized water as a blank. Anthocyanin content analysis follows the procedure by Bani et al. First, dilution factors were determined by diluting samples in KCl buffer (pH 1.0) till absorbance at λ_{max} (520 nm) is within linear reading range of spectrophotometer. Sample must be less than 20 % of total volume. Spectrophotometer was zeroed by using distilled water at λ_{max} and 700 nm. Two samples were prepared based on the dilution factor, one with KCl buffer (pH 1.0) and the other with sodium acetate buffer (pH 4.5). These dilutions were left to equilibrate for 15 min. Absorbance of each solution was measured at λ_{max} and 700 nm against a blank cell filled with distilled water. The monomeric anthocyanin pigment concentration was calculated by using the following eq (1):

$$\text{Total Anthocyanin (TAC)} \left(\frac{\text{mg}}{\text{L}}\right) = \frac{[(\lambda_{max} - \lambda_{700})_{pH\,1.0} - (\lambda_{max} - \lambda_{700})_{pH\,4.5}] \times MW \times DF \times 100(}{\varepsilon \times 1} \quad (1)$$

MW is molecular weight of predominant anthocyanin in sample, DF is dilution factor, ε is the molar absorptivity of the anthocyanin. The formula is based on a pathlength of 1 cm, which is equal to the cuvette width. To compare between literature, anthocyanin concentration in this paper is expressed as cyanidin-3-glucoside (MW = 449.2 and ε = 26,900).

2.5 Adsorption Experiments

The performance of pure-silica RHS and RHS-NH_2 materials in anthocyanin adsorption was evaluated through static adsorption at room temperature. Typically, 10 mL of extract solution was mixed with 0.1 g of a dried adsorbent in a 50 mL Erlenmeyer flask. The flask was sealed tightly and shaken on an incubation orbital shaker at 120 rpm for 12 h to ensure adsorption equilibrium. Subsequently, the solution was filtered to remove the adsorbent (Fig. 1) and subjected to UV-vis analysis and determined by the pH differential method. The amount of anthocyanin adsorption capacity was calculated according to Eq (2):

$$\text{Adsorption capacity: } q_e = \frac{(C_0 - C_e)V_i}{W} \quad (2)$$

where Q_e is adsorption capacity at adsorption equilibrium (mg/g, dried adsorbent); C_o is the initial anthocyanin concentration (mg/L); C_e is the equilibrium anthocyanin concentration in solution (mg/L); V_i is the volume of initial solution (L); W is the weight of dried adsorbent (g). All the experiments were performed duplicate and the average value from results was taken. All measurements were performed in triplicate (n = 3), and the results are reported as mean ± standard deviation.

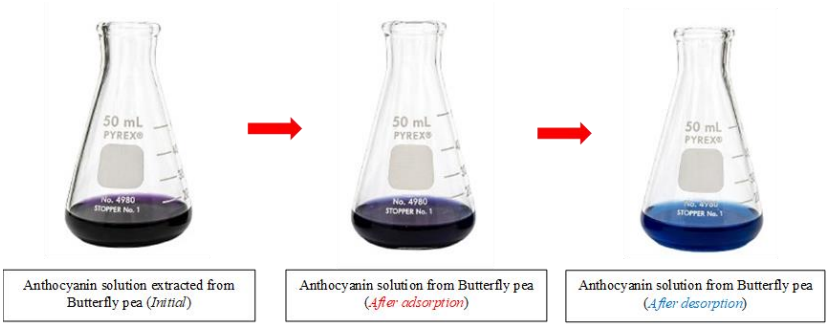

Fig.1 Anthocyanin solution from butterfly pea in each step of adsorption-desorption study.

2.6 Desorption Experiments

A static desorption test of the spent adsorbents (RHS and RHS-NH_2) was performed after the equilibrium of anthocyanin adsorption was reached. Ethanol/deionized water solutions with various (v/v) ratios were used as solvents (H_2O: EtOH = 100:0, 50:50 and 0:100), and the solid:liquid ratio was maintained at 1 g: 50 mL. The flasks were continually shaken at 120 rpm for 12 h at room temperature. The anthocyanin contents of the desorbed solutions as shown in Fig.1 were analyzed by UV-vis analysis and determined by the pH differential method. The recovery efficiency was calculated according to Eq (3):

$$\text{Recovery Efficiency (\%)} = \frac{C_{des}}{C_0 - C_e} \times 100 \qquad (3)$$

where C_0 is the initial anthocyanin concentration, C_e is the equilibrium anthocyanin concentration after adsorption, and C_{des} is the anthocyanin concentration recovered during desorption.

3. Results and discussion

3.1 Characterization of adsorbents

The structural and chemical properties of the synthesized adsorbents were investigated using Fourier transform infrared spectroscopy (FTIR) and nitrogen adsorption–desorption analysis. As shown in Fig. 2, both RHS and amine-functionalized RHS (RHS–NH_2) exhibited a broad absorption band in the range of 2800–3700 cm^{-1}, which is attributed to the stretching vibrations of hydroxyl groups (–OH) and silanol groups (Si–OH). A strong band observed at ~ 1100 cm^{-1} corresponds to the asymmetric stretching vibration of siloxane bonds (Si–O–Si), confirming the silica framework structure.

After functionalization, additional peaks appeared at around 2940 and 2866 cm^{-1}, which are assigned to C–H stretching vibrations of methylene groups introduced by organosilane moieties. Furthermore, the bands detected in the region of 1465–1642 cm^{-1} are associated with N–H bending vibrations, indicating the successful grafting of amine functional groups onto the silica surface. These findings are consistent with previous studies reporting amine-functionalized silica materials for adsorption applications (Tran et al., 2017; Wang et al., 2020). Further characterization using XPS, CHN elemental analysis, or thermogravimetric analysis is recommended in future studies to quantitatively determine the amine loading on RHS-NH_2.

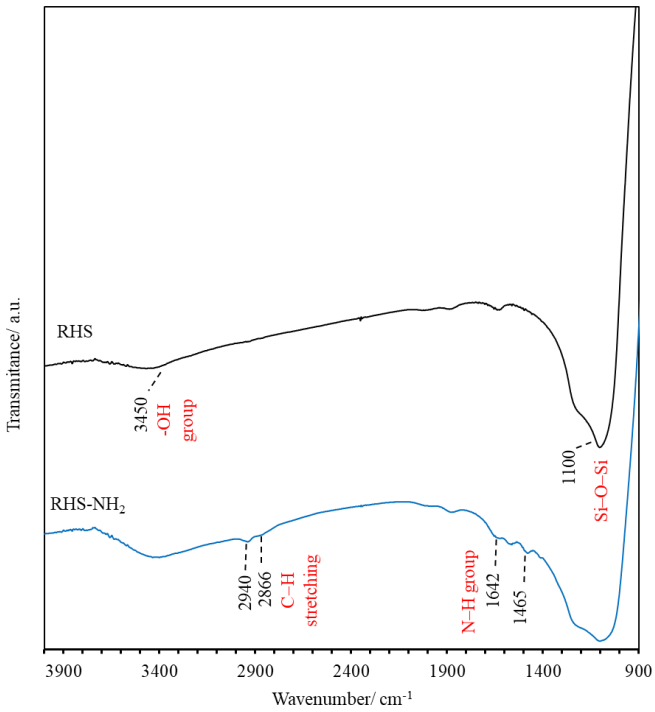

Fig. 2 FTIR spectra of RHS and RHS-NH_2 adsorbents.

The textural properties of the materials were further analyzed using nitrogen adsorption–desorption isotherms (Fig. 3A). Both samples exhibited type IV isotherms according to IUPAC classification, indicating the presence of mesoporous structures. The pore size distribution (Fig. 3B) revealed an average pore diameter in the range of 3–4 nm, confirming mesoporosity.

As summarized in Table 1, pristine RHS exhibited a relatively high specific surface area (136 $m^2\ g^{-1}$), along with a pore volume of 0.34 $cm^3\ g^{-1}$. After amine functionalization, a noticeable decrease in surface area (44 $m^2\ g^{-1}$), pore diameter, and pore volume was observed. This reduction can be attributed to the incorporation of amine-containing silane groups within the pore channels, partially blocking the pore structure. Similar trends have been reported for functionalized mesoporous silica, where surface modification enhances chemical functionality at the expense of textural properties (Shen et al., 2021).

Table 1 Textural properties of the adsorbents

Sample[a]	S_{BET}[b] ($m^2\ g^{-1}$)	D_p[c] (nm)	Vt[d] ($cm^3\ g^{-1}$)
RHS	136	3.71	0.34
RHS-NH_2	44	3.28	0.20

[a] Dried samples
[b] BET surface area
[c] Pore diameter calculated using BJH method
[d] Total pore volume

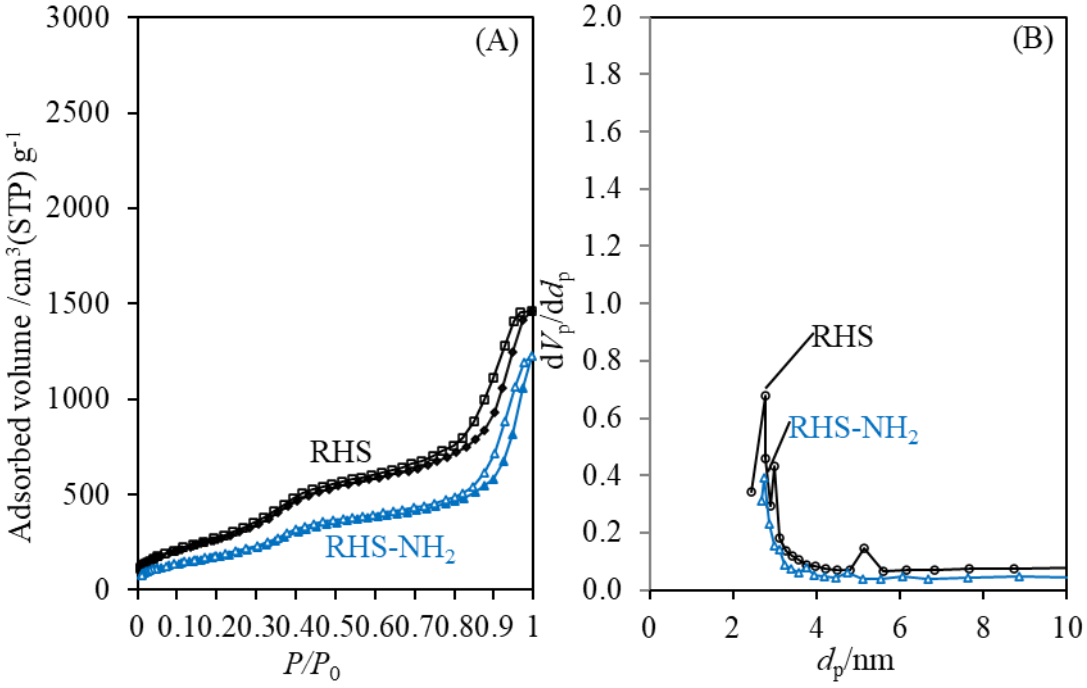

Fig. 3 N_2 adsorption-desorption isotherms (A) and BJH pore size distribution (B) of RHS and RHS-NH_2 adsorbents.

3.2 Effect of extraction time on anthocyanin yield

The influence of extraction time on total anthocyanin content (TAC) was evaluated under controlled conditions (60 °C, solid-to-liquid ratio of 1:20). As shown in Table 2, the TAC increased from 31.73 to 33.61 mg L^{-1} when extraction time was extended from 0.5 to 2 h. This trend indicates that prolonged extraction facilitates the diffusion of anthocyanins from plant matrices into the solvent, thereby enhancing extraction efficiency.

The observed behavior can be explained by mass transfer mechanisms, where the concentration gradient between plant tissue and solvent drives the release of bioactive compounds. However, the increase in TAC beyond 1 h was relatively moderate, suggesting that equilibrium was gradually approached. In addition, the relatively small increase in TAC observed between 1 and 2 h indicates that mass transfer equilibrium was approached under the selected extraction conditions. This observation is in correspondence with previous studies on anthocyanin extraction, which reported diminishing returns at longer extraction times due to saturation effects and possible degradation of heat-sensitive compounds (Prabawati et al., 2019; Pham et al., 2020). Therefore, an extraction time of 2 h was selected as the optimal condition to maximize anthocyanin yield while maintaining process efficiency.

Table 2 The change of anthocyanin properties under different extraction conditions

Condition	Temperature (°C)	Dried butterfly pea to water ratio	Extraction time (hour)	TAC [a] (mg/L)
A	60	1:20	0.5	31.73 ± 0.004
B	60	1:20	1.0	32.88 ± 0.010
C	60	1:20	2.0	33.61 ± 0.007

[a] Values are expressed as mean ± STD.

3.3 Adsorption study

The adsorption performance of RHS and RHS–NH_2 was evaluated using butterfly pea extract obtained under optimal extraction conditions. As presented in Table 3, the residual anthocyanin

concentration after adsorption decreased more significantly in the presence of RHS–NH_2 compared to pristine RHS. This indicates a higher adsorption efficiency for the functionalized material.

The adsorption mechanism can be further explained by considering the pH-dependent behavior of anthocyanins and the surface chemistry of RHS–NH_2. Anthocyanins predominantly exist as flavylium cations under strongly acidic conditions, whereas quinoidal base and anionic forms become increasingly dominant as pH increases. During the adsorption process, the butterfly pea extract was expected to remain in a mildly acidic environment due to the presence of naturally occurring organic acids and anthocyanins. Under these conditions, amino groups introduced by APTES can be protonated to form $–NH_3^+$ species. The enhanced adsorption performance of RHS–NH_2 may therefore be attributed to a combination of electrostatic interactions, hydrogen bonding between hydroxyl groups of anthocyanins and surface amino groups, and additional intermolecular interactions. These synergistic interactions increase the affinity of anthocyanins toward the functionalized silica surface compared with pristine RHS. (Wang et al., 2020; Li et al., 2022).

Although the surface area of RHS–NH_2 was lower than that of pristine RHS, its adsorption capacity was significantly higher, highlighting the dominant role of surface chemistry over textural properties in this system. Similar observations have been reported in functionalized adsorbents designed for selective adsorption of phenolic compounds (Sun et al., 2018). The adsorption capacity obtained in this work (9.26 mg g^{-1}) is within the range reported for low-cost silica-based adsorbents used for the purification of phenolic compounds. Although some commercial adsorbents may exhibit higher adsorption capacities, RHS–NH_2 offers several advantages, including low-cost preparation, utilization of agricultural waste, and environmental sustainability. These characteristics demonstrate the potential of RHS–NH_2 as an alternative adsorbent for anthocyanin purification.

Table 3 The amount of anthocyanin after adsorption.

Adsorbents	Temperature (°C)	Solid/Liq. Ratio (g/mL)	Adsorption time (hour)	TAC [a] (mg/L)	Adsorption Efficiency (%)
RHS	Room Temp.	1:100	12	27.39 ± 0.48	18.5
RHS-NH_2	Room Temp.	1:100	12	24.35 ± 0.79	27.6

[a] Values are expressed as mean ± STD.

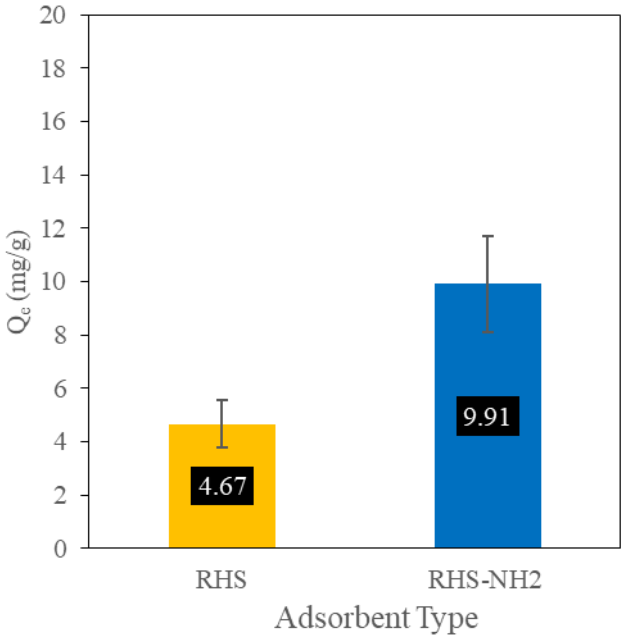

Fig. 4 Effect of type of adsorbents on anthocyanin adsorption.

3.4 Desorption study

Desorption studies were conducted using different water to ethanol mixtures to evaluate the recovery of anthocyanins from the adsorbent surface. As shown in Table 4, solvent polarity played a crucial role in the desorption process. For pristine RHS, the highest desorption efficiency was achieved using pure water, which can be attributed to its high polarity and ability to disrupt weak physical interactions between anthocyanins and the silica surface. In contrast, RHS–NH_2 exhibited maximum desorption efficiency at a water to ethanol ratio of 50:50, yielding a TAC of 5.57 mg L^{-1}.

This behavior suggested that anthocyanins adsorbed on RHS–NH_2 were bound through stronger interactions, including hydrogen bonding and electrostatic forces. The addition of ethanol reduces solvent polarity and enhances the solubility of anthocyanins, facilitating their release from the functionalized surface. This synergistic effect of mixed solvents has been widely reported in desorption processes involving phenolic compounds (Cassano et al., 2018; Li et al., 2022).

The higher recovery efficiency of RHS in pure water (51.93%) suggests that anthocyanins were mainly adsorbed through relatively weak physical interactions, which could be readily disrupted by water molecules. In contrast, anthocyanins adsorbed on RHS–NH_2 were more strongly retained due to hydrogen bonding and electrostatic interactions associated with the grafted amino groups. Consequently, pure water was insufficient to effectively desorb the adsorbed anthocyanins. The use of a water–ethanol mixture (50:50, v/v) significantly improved desorption efficiency (60.15%), likely because ethanol reduced solvent polarity and enhanced anthocyanin solubility, thereby facilitating the disruption of adsorbate–adsorbent interactions and promoting anthocyanin recovery.

Table 4 The amount of anthocyanin after desorption.

Adsorbents	Solvent (H_2O:EtOH)	Temperature (°C)	Solid/Liq. Ratio (g/mL)	Desorption time (hour)	TAC [a] (mg/L)	Recovery Efficiency (%)
RHS	100 : 0	Room Temp.	1:50	12	3.23 ± 0.58	51.9
	50 : 50				2.22 ± 0.62	35.7
	0 : 100				0.95 ± 0.32	15.3
RHS-NH_2	100 : 0	Room Temp.	1:50	12	2.44 ± 0.49	26.4
	50 : 50				5.57 ± 0.28	60.2
	0 : 100				2.50 ± 0.44	27.0

[a] Values are expressed as mean ± STD.

4. Conclusion

In this work, amine-functionalized rice husk silica (RHS–NH_2) was successfully synthesized and applied as an adsorbent for the purification of anthocyanins from butterfly pea extract. The characterization results confirmed the successful incorporation of amine groups onto the silica surface, while maintaining a mesoporous structure suitable for adsorption processes. The extraction study indicated that anthocyanin yield increased with extraction time, with optimal performance achieved at 2 h. In the adsorption study, RHS–NH_2 demonstrated superior performance compared to pristine RHS, highlighting the importance of surface functional groups in enhancing adsorption efficiency. The improved performance was attributed to specific interactions between anthocyanins and amine groups, including electrostatic attraction and hydrogen bonding. The desorption results showed that solvent polarity plays a key role in anthocyanin recovery, with a 50:50 (v/v) water to ethanol mixture providing the highest desorption efficiency for RHS–NH_2. These findings suggest that the adsorption–desorption system can be effectively tuned for improved purification performance. The developed approach offers potential for further optimization and scale-up toward practical applications in natural product processing.

References

Bani, O., Taslim, Iriany, Sinaga, M., Violleta, S. (2024). Extraction, concentration, and storage of butterfly pea anthocyanin for commercialization. *Case Studies in Chemical and Environmental Engineering*, 10, 100860.

Cassano, A., Conidi, C., Drioli, E. (2018). Clarification and concentration of pomegranate juice by membrane processes. *Separation and Purification Technology*, 195, 324–331.

Chayaratanasin, P., Barbieri, M. A., Suanpairintr, N., Adisakwattana, S. (2021). Clitoria ternatea: A review of phytochemistry and pharmacology. *Journal of Ethnopharmacology*, 272, 113887.

Escher, G. B., Wen, M., Zhang, L., Rosso, N. D. (2020). Stability of anthocyanins in food systems: A review. *Trends in Food Science & Technology*, 105, 1–16.

He, J., Giusti, M. M. (2015). Anthocyanins: Natural colorants with health-promoting properties. *Annual Review of Food Science and Technology*, 6(1), 163–187.

Kalapathy, U., Proctor, A., Shultz, J. (2015). A simple method for production of pure silica from rice hull ash. *Bioresource Technology*, 85(3), 285–289.

Khoo, H. E., Azlan, A., Tang, S. T., Lim, S. M. (2017). Anthocyanidins and anthocyanins: Colored pigments as food, pharmaceutical ingredients. *Food & Nutrition Research*, 61(1), 1361779.

Li, X., Wu, X., Chen, J., Huang, Y. (2022). Advances in anthocyanin purification technologies: A review. *Food Chemistry*, 374, 131673.

Pham, T. N., Le, V. V. M., Vo, H. P. (2020). Optimization of aqueous extraction of anthocyanins from butterfly pea flowers. *Journal of Food Processing Engineering*, 43(6), e13411.

Prabawati, E. K., Sari, B. L., Kurniawan, A. (2019). Extraction of anthocyanins from butterfly pea (*Clitoria ternatea L.*). *Food Chemistry*, 295, 326–334.

Shen, Y., Zhao, P., Shao, Q. (2021). Porous silica and carbon derived from rice husk pyrolysis: Preparation and applications. *Materials Today Sustainability*, 11–12, 100046.

Sun, Y., Liu, J., Kennedy, J. F. (2018). Adsorption and desorption of anthocyanins using macroporous resins. *Journal of Food Engineering*, 223, 1–10.

Tran, H. N., You, S. J., Hosseini-Bandegharaei, A., Chao, H. P. (2017). Mistakes and inconsistencies regarding adsorption of contaminants from aqueous solutions. *Chemical Engineering Journal*, 325, 128–141.

Wang, J., Guo, X. (2020). Adsorption kinetic models: Physical meanings, applications, and solving methods. *Journal of Hazardous Materials*, 390, 122156.

Zhang, Z., Kou, X., Fugal, K., McLaughlin, J. (2019). Comparison of anthocyanin purification by macroporous resins. *Industrial Crops and Products*, 134, 129–138.

Development of a Simple, Low-Cost, and Portable In-House Air Sampling Device for Heavy Metal Contamination in Airborne

Apinya Navakhun*, Natnicha Seeladlao
Department of Chemistry, Faculty of Science, Burapha University, Chonburi, Thailand
*Email: apinyan@go.buu.ac.th

Abstract

Airborne particulate matter (PM) contaminated with heavy metals poses a significant environmental and public health concern, particularly in urban and industrial areas. This study aimed to design and develop a simple, low-cost, and portable in-house particulate matter sampling device capable of separating airborne particles into different size fractions for heavy metal analysis. The fabricated device consisted of three layers of filter paper with pore sizes of 10, 2.5, and 1.2 μm, enabling the collection of particles in the size ranges of >10 μm, 10–2.5 μm, and 2.5–1.2 μm, respectively. A total of 189 particulate matter samples were collected in Saensuk Subdistrict, Mueang Chonburi District, Chonburi Province, Thailand. The collected samples were analyzed for lead (Pb), copper (Cu), and cadmium (Cd) concentrations using Atomic Absorption Spectrometry (AAS). The results revealed that Cd was the predominant heavy metal detected in both indoor and outdoor particulate matter samples, followed by Pb and Cu, respectively. Heavy metal concentrations were generally higher in indoor environments, suggesting the accumulation of particulate pollutants in enclosed spaces with limited air circulation. The findings demonstrate that the developed PM sampling device can serve as an effective and economical tool for particulate matter monitoring and heavy metal assessment.

Keywords: in-house particulate matter sampler; particulate matter (PM); heavy metal analysis; Atomic Absorption Spectrometry (AAS)

1. Introduction

Fine particulate matter (PM), particularly PM10 and PM2.5, refers to airborne particles with aerodynamic diameters smaller than 10 and 2.5 micrometers, respectively (Xian & Jones, 2022). These particles have become major environmental and public health concerns worldwide (Goodarzi et al., 2023). Due to their extremely small size, especially PM2.5 particles, they can penetrate deeply into the respiratory system and enter the bloodstream, leading to various adverse health effects, including respiratory diseases, cardiovascular disorders, neurological complications, and cancer (Matei, 2025). The toxicity of PM is influenced not only by particle concentration but also by the chemical substances adsorbed onto the particle surface (Wang et al., 2024). Among the various chemical constituents associated with PM, heavy metals are considered particularly hazardous because of their toxicity, persistence, bioaccumulation potential, and carcinogenic properties (Abdulaziz et al., 2022). Metals such as lead (Pb), cadmium (Cd), chromium (Cr), nickel (Ni), arsenic (As), and mercury (Hg) are commonly detected in atmospheric particulate matter originating from anthropogenic activities, including industrial emissions, fossil fuel combustion, vehicular exhaust, waste incineration, and construction activities (Park et al., 2024). In addition, these metals were selected because they can serve as useful tracers for identifying potential emission sources in the environment. Lead (Pb) is commonly associated with industrial activities, metal processing operations, battery manufacturing and recycling, and legacy contamination from historical use of leaded fuels. Copper (Cu) is frequently used as an indicator of non-exhaust traffic emissions, particularly those arising from brake pad wear, tire wear, and road dust resuspension. Cadmium (Cd), on the other hand, is often linked to fossil fuel combustion, waste incineration, metallurgical industries, and other high-temperature industrial processes. Consequently, the simultaneous determination of Pb, Cu, and Cd in particulate matter can provide valuable information regarding both the level of environmental contamination and the potential sources contributing to atmospheric particulate pollution. Such information is essential for developing effective air quality management strategies and mitigating human exposure to toxic particulate-bound metals (Pant & Harrison, 2013; Amato et al., 2014; Fahim et al., 2026). However, conventional PM sampling instruments are often expensive, bulky, and difficult to transport, limiting their application in field investigations and

localized environmental monitoring (Aziz & Zaman, 2025). Most commercial air sampling systems are designed for stationary monitoring stations and require substantial financial investment, technical expertise, and continuous maintenance. Consequently, collecting samples from remote areas or specific locations of interest may be impractical, particularly in resource-limited settings. Therefore, the development of a low-cost, in-house PM sampling device has become increasingly important. A portable and affordable sampling system can facilitate flexible field sampling and enable researchers to collect particulate matter samples efficiently in targeted areas. In addition, low-cost samplers may improve accessibility for environmental studies, educational purposes, and community-based air quality monitoring programs. Such systems also provide opportunities to expand the spatial coverage of PM monitoring, particularly in areas lacking permanent air quality monitoring stations (Matos-Espinosa et al., 2025).

Therefore, the primary objective of this study was to design and develop a low-cost, portable, and self-constructed PM sampling device for particulate matter collection. In addition, heavy metal concentrations associated with the collected PM samples were analyzed to evaluate potential environmental and health impacts. Heavy metals, including lead (Pb), cupper (Cu), and cadmium (Cd) were quantified using Atomic Absorption Spectrometry (AAS). Furthermore, this study demonstrates the practicality and reliability of an affordable PM sampling system for environmental monitoring, particularly in areas where conventional monitoring systems are inaccessible or unaffordable.

2. Objectives

The objectives of this study were to design and develop a low-cost, portable, and self-constructed particulate matter (PM) sampling device for environmental monitoring applications, to collect PM samples from selected sampling locations using the developed device, and to determine the concentrations of heavy metals, including lead (Pb), cupper (Cu), and cadmium (Cd) associated with the collected PM samples using Atomic Absorption Spectrometry (AAS).

3. Materials and methods

Instruments, Materials, and Chemicals

An Atomic Absorption Spectrophotometer (AAS) (PinAAcle 900F, PerkinElmer, USA) was used for the determination of heavy metals in particulate matter (PM) samples. A sample preconcentrator (TT-200-VSC, Hercuvan Lab System, Malaysia) was employed for sample digestion. Glass fiber filter papers (1.2 μm pore size) and cellulose filter papers (2.5 and 10 μm pore sizes) manufactured by Whatman were used in the PM sampling device. All chemicals used were of analytical reagent grade, including copper (II) sulfate pentahydrate obtained from VWR International (USA), lead (II) nitrate from Ajax Finechem (Australia), cadmium standard solution (Cd, 1000 ppm) from Fisher Scientific (USA), and 65% w/w nitric acid from Merck Group (Germany).

Heavy Metal Digestion and Analysis

Particulate matter samples collected on filter papers were prepared by cutting the filters into small pieces and placing them into glass vials. Subsequently, 5 mL of 5% v/v nitric acid was added, and the samples were digested using a sample preconcentrator at 150 °C for 5 min. After cooling, the solutions were filtered through cotton packed in a dropper tube into a 25 mL volumetric flask and diluted to volume with deionized water to obtain a final nitric acid concentration of 1% v/v. The digested sample solutions were then analyzed for lead (Pb), copper (Cu), and cadmium (Cd) using the AAS under the optimized operating conditions shown in Table 1. To minimize potential contamination during sample preparation and analysis, procedural blanks were included in the study. The sampling devices were placed in a sealed enclosure for 24 h and subsequently subjected to the same preparation and analytical procedures as the actual samples. The concentrations obtained from the procedural blanks were used to correct the measured values by subtracting the background contribution from the corresponding sample results.

Table1 Atomic Absorption Spectrometer conditions

condition	Elements		
	Pb	Cu	Cd
Wavelength (nm)	283.31	324.75	228.80
Type of flame	Air-C_2H_2	Air-C_2H_2	Air-C_2H_2
Fuel flow (L/min)	2.5	2.5	2.0
Burner (cm)	10	10	10
Slit	0.7	0.7	0.7
Lamp Current (mA)	440	15	4
Linear Range (ppm)	10	1.6	1.0

Preparation of the Sampling Device and Sample Collection

The sampling device was prepared using filter papers with pore sizes of 10, 2.5, and 1.2 μm and a diameter of 47 mm. The filters were arranged in a three-layer configuration with a spacing of 1 cm between each layer. The device was designed to allow air to flow sequentially through the first, second, and third filter layers. Particulate matter (PM) samples were collected from both indoor and outdoor environments in Saensuk Subdistrict, Mueang Chonburi District. The sampling devices were installed at various sampling locations, as presented in Table 2 and Figure 1, and secured using adhesive tape. The sampling sites were divided into two areas based on their surrounding characteristics. Stations A–C were in residential areas characterized by clustered high-rise buildings and regular vehicular traffic, including cars and motorcycles. Among these sites, Stations B and C were situated near major transportation routes and were frequently affected by traffic congestion during certain periods of the day. In contrast, Stations D–F were located in the educational area and were characterized by the presence of mature trees and. Although vehicular movement was present in these areas, traffic volume was considerably lower than that observed at Stations A–C. Sampling was conducted in triplicate simultaneously at each location for 24 h under ambient temperatures ranging from 20 to 35 °C. After the sampling period, each filter layer was separated and individually stored in zip-lock plastic bags prior to further analysis.

Figure 1 Geographic locations of the sampling stations displayed using both a road map and satellite map.

Table 2 Characteristics and locations of particulate matter sampling stations

Sampling station	Characteristics of sampling area
Station A (13.29115° N, 100.92972° E)	A condominium surrounded by other buildings and located far from traffic routes. The area had continuous airflow. Sampling was conducted on the 4th floor.
Station B (13.28656° N, 100.92380° E)	A high-rise building located near a main traffic route opposite shopping mall. Sampling was conducted on the 3rd floor.
Station C (13.28616° N, 100.92759° E)	A five-story building located near a traffic route with continuous airflow throughout the area. Sampling was conducted on the 5th floor.
Station D (13.28146° N, 100.92562° E)	A three-story building in which the room was obstructed by adjacent rooms, resulting in limited airflow. Sampling was conducted on the 3rd floor.
Station E (13.28148° N, 100.92553° E)	An area located near traffic routes and a parking lot in front of the building, with continuous airflow. Trees surrounded the rear side of the building. Sampling was conducted on the 1st floor.
Station F (13.28131° N, 100.92443° E)	An area with a traffic route in front of the building and continuous airflow, while the rear side was obstructed by nearby buildings. Sampling was conducted on the 6th floor.

4. Results and Discussion

Fabrication of the In-House Particulate Matter Sampling Device

An in-house particulate matter (PM) sampling device was fabricated using filter papers with pore sizes of 10, 2.5, and 1.2 µm and a diameter of 47 mm, arranged in a three-layer configuration with a spacing of 1 cm between each layer, as shown in Figure 2. The 10 µm filter was used to collect particles larger than 10 µm, whereas the 2.5 µm filter collected particles in the size range of 10–2.5 µm, and the 1.2 µm filter collected particles in the size range of 2.5–1.2 µm. The device was designed to allow air to flow sequentially through the first, second, and third filter layers, respectively. Unlike conventional PM sampling methods, such as direct-reading instruments, pump-based filtration systems, or direct particle collection techniques, the in-house sampling device was developed as a simple and cost-effective alternative. The proposed device offers several advantages, including low cost, ease of material procurement, compact size, and portability. A limitation of this study is that only three heavy metals were analyzed, providing preliminary information on metal contamination associated with PM. The developed sampler collects particulate matter based on the filter pore size, while the types and concentrations of metals associated with the collected particles are primarily determined by the emission sources and environmental conditions rather than the sampler itself. Although the collected PM was subsequently subjected to metal extraction and analysis, future studies could employ multi-element techniques such as ICP-OES or ICP-MS to simultaneously quantify a broader range of trace metals and provide a more comprehensive characterization of PM-associated metal contamination.

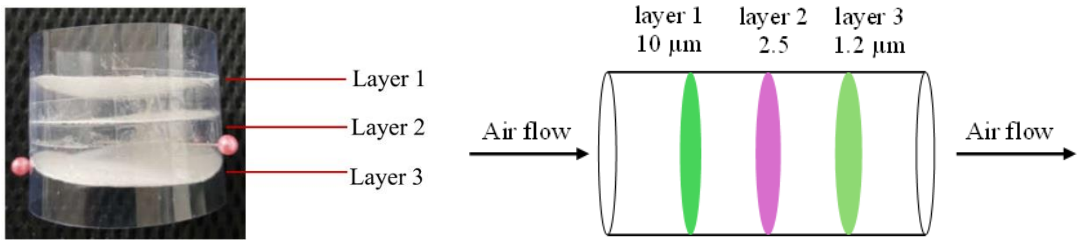

(a) (b)

Figure 2 (a) The fabricated in-house particulate matter sampling device

(b) Schematic diagram illustrating airflow through the sampling device.

Determination of heavy metals in Particulate Matter

Standard calibration curves for the determination of lead (Pb), copper (Cu), and cadmium (Cd) were prepared using standard solutions in the concentration range of 0.1000–0.5000 mg/L, with each concentration analyzed in triplicate. The calibration results are presented in Table 3. The correlation coefficients (R^2) of the calibration curves for Pb, Cu, and Cd were 0.9950, 0.9995, and 0.9981, respectively, indicating good linearity for all three metals. In quantitative analysis, an R^2 value greater than 0.99 is generally considered acceptable; therefore, the obtained calibration curves were suitable for quantitative determination. The limits of detection (LOD) and limits of quantification (LOQ) were determined by analyzing the blank solution (1% v/v nitric acid) 15 times and calculated using the equations LOD = 3SD/Slope and LOQ = 10SD/Slope where SD represents the standard deviation of blank and slope corresponds to the slope of the calibration curve. The obtained LOD and LOQ values for Pb, Cu, and Cd are also summarized in Table 3. However, the relatively high LOD and LOQ values indicate that the method could be further improved. Increasing the concentration factor during sample preparation, for example by reducing the final solution volume from 25 mL to 10 or 5 mL, may enhance detection sensitivity. In addition, the use of larger filter diameters than the 47-mm filters employed in the in-house PM sampler could increase particle collection surface area, while extending the sampling duration (e.g., to 48 h) could increase particulate mass loading and improve the detectability of trace elements. A limitation of the present study is that method accuracy was not evaluated. Future work should include accuracy assessment through recovery studies (% recovery) and/or analysis of Certified Reference Materials (CRMs) to further validate the analytical method and ensure the reliability of the measured concentrations.

Table 3 Linear calibration equations, correlation coefficients (R^2), limits of detection (LOD), and limits of quantification (LOQ) for lead, copper, and cadmium

Parameters	**Pb**	**Cu**	**Cd**
Linear equation	y = 0.0275x + 0.0004	y = 0.2078x + 0.0006	y = 0.5347x + 0.0045
R^2	0.9950	0.9995	0.9981
LOD (mg/L)	0.0327	0.0043	0.0028
LOQ (mg/L)	0.1091	0.0144	0.0094

Particulate matter samples were collected from Saensuk Subdistrict, Mueang Chonburi District, Chonburi Province, Thailand. A total of 189 samples were obtained from 5 indoor sampling points and 7 outdoor sampling stations. The collected particulate matter was classified into three particle size fractions: particles larger than 10 µm, particles between 10–2.5 µm, and particles between 2.5–1.2 µm. The samples were subsequently analyzed for three heavy metals, namely lead (Pb), copper (Cu), and cadmium (Cd). The analytical results are showed in Table 4 and summarized in Table 5. The analysis of lead (Pb), copper (Cu), and cadmium (Cd) concentrations in indoor and outdoor particulate matter samples revealed no statistically significant differences between indoor and outdoor environments. However, among the heavy metals detected, Cd exhibited the highest concentrations, followed by Pb and Cu, respectively. The determination of heavy metals in particulate matter fractions larger than 10 µm, 10–2.5 µm, and 2.5–1.2 µm showed that Cd concentrations were consistently higher than those of Pb and Cu in all particle size fractions. In addition, indoor sampling points placed directly inside rooms exhibited lower heavy metal concentrations than sampling points located near air-conditioning vents and behind electric fans, particularly in the 10–2.5 µm particle size fraction. This difference may be attributed to uncontrolled airflow conditions at passive indoor sampling points, which may have allowed fine particles to bypass the second filter layer, whereas air-conditioning and fan-assisted sampling locations provided more controlled airflow and improved particle collection efficiency. No statistically significant differences in heavy metal concentrations were observed among the sampling sites, including residential areas characterized by dense high-rise buildings, locations adjacent to major traffic routes, and areas with greater vegetation cover. This finding is consistent with previous studies reporting that particulate matter (PM) and PM-associated heavy metals can be transported over considerable distances through atmospheric processes, resulting

in relatively homogeneous spatial distributions within a limited geographic area. The spatial distribution of PM-bound metals is influenced not only by local emission sources but also by meteorological conditions, air-mass movement, and long-range atmospheric transport. Consequently, nearby sampling locations may exhibit similar metal concentrations despite differences in local land use and environmental characteristics. Since the sampling sites in the present study were located within a relatively small area, atmospheric mixing and particle dispersion may have reduced spatial variability, resulting in the absence of significant differences among sampling stations (Li et al. (2013) and Wu et al. (2021).

Table 4 lead (Pb), copper (Cu), and cadmium (Cd) in particulate matter samples collected from indoor and outdoor environments at different sampling stations

Station	Sampling Location	Particle Size Fraction (μm)	Average Metal Concentration (mg/L)		
			Pb	Cu	Cd
A	Indoor	>10	trace**	N.D.*	0.1674±0.0131
		10–2.5	trace	N.D.	0.1679±0.0010
		2.5–1.2	trace	N.D.	0.1619±0.0054
	Outdoor	>10	trace	N.D.	0.1629±0.0261
		10–2.5	N.D.	N.D.	0.1653±0.0012
		2.5–1.2	trace	N.D.	0.1695±0.0152
B	Indoor	>10	0.1449±0.0356	N.D.	0.1661±0.0254
		10–2.5	0.3587±0.1064	N.D.	0.1920±0.1005
		2.5–1.2	trace	N.D.	0.1623±0.0854
	Outdoor	>10	N.D.	N.D.	0.1627±0.1052
		10–2.5	N.D.	N.D.	0.1664±0.0568
		2.5–1.2	trace	N.D.	0.1608±0.0254
C	Indoor	>10	0.2364±0.1356	N.D.	0.1666±0.1242
		10–2.5	0.1152±0.0956	trace	0.1690±0.0854
		2.5–1.2	1.6000±0.0912	N.D.	0.1632±0.0985
	Outdoor	>10	N.D.	trace	0.1650±0.0025
		10–2.5	N.D.	trace	0.1661±0.1985
		2.5–1.2	trace	N.D.	0.1610±0.1854
D	Indoor	>10	trace	trace	0.1557±0.0535
		10–2.5	0.2222±0.1211	trace	0.1581±0.0895
		2.5–1.2	0.2141±0.1081	trace	0.1549±0.1254
	Outdoor	>10	N.D.	N.D.	0.1529±0.1451
		10–2.5	N.D.	N.D.	0.1555±0.0981
		2.5–1.2	N.D.	N.D.	0.1504±0.0981
E	Indoor	>10	0.1855±0.0680	trace	0.1501±0.1451
		10–2.5	trace	trace	0.1540±0.2541
		2.5–1.2	trace	trace	0.1486±0.1541
	Outdoor	>10	N.D.	N.D.	0.1540±0.0985
		10–2.5	N.D.	N.D.	0.1486±0.1254
		2.5–1.2	N.D.	N.D.	0.1537±0.0985
F	Outdoor (Front of Building)	>10	trace	trace	0.1625±0.1441
		10–2.5	1.4545±0.1653	trace	0.1652±0.2541
		2.5–1.2	trace	N.D.	0.1607±0.0874
	Outdoor (Back of Building)	>10	0.3685±0.2044	N.D.	0.1633±0.0789
		10–2.5	N.D.	trace	0.1660±0.1155
		2.5–1.2	0.4885±0.2532	trace	0.1596±0.1251

* *N.D. = Not Detected.*
** *trace = Below LOQ*

Table 5 Summary of heavy metal analysis in particulate matter samples

Heavy Metal	Number of Samples	Indoor Heavy Metal Concentration (mg/L)			Outdoor Heavy Metal Concentration (mg/L)		
		Detected Samples	Minimum	Maximum	Detected Samples	Minimum	Maximum
Pb	189	23	trace	1.6000	67	trace	1.4545
Cu	189	8	trace	trace	11	trace	trace
Cd	189	63	0.1486	0.1920	126	0.1486	0.1695

The results presented in Table 5 indicate that most of the lead (Pb) concentrations measured in this study were either below the detection limit or below the quantification limit (LOQ). This may be attributed to the relatively high LOD and LOQ values for Pb compared with those of the other analyzed metals, limiting the ability of the method to detect and quantify Pb at low environmental concentrations. Consequently, the Pb dataset was incomplete, and further methodological improvements and investigations are required to obtain more comprehensive information on Pb contamination in PM. For Cadmium (Cd), the most prominent heavy metal detected in particulate matter samples collected from both indoor and outdoor environments. Cd was detected in 63 indoor samples and 126 outdoor samples, with concentration ranges of 0.1486–0.1920 mg/L and 0.1486-0.1695 mg/L, respectively. The highest Cd concentration was observed in indoor samples, suggesting that indoor environments may facilitate the accumulation of airborne particles due to limited ventilation and continuous exposure to indoor pollutant sources. The widespread detection of Cd suggests that this metal may be broadly distributed in ambient particulate matter and could originate from multiple environmental sources, such as fuel combustion, industrial emissions, and waste incineration. In contrast, copper (Cu) was detected in only a limited number of samples, specifically 8 indoor samples and 11 outdoor samples, with trace concentrations.

Overall, the findings demonstrate that heavy metal contamination was more frequently detected and generally more concentrated in indoor particulate matter compared with outdoor particulate matter. This observation may be attributed to reduced air circulation indoors, allowing particulate matter and associated heavy metals to accumulate over time. Furthermore, the detection of Pb, Cu, and Cd in fine particulate matter raises concerns regarding long-term human exposure, as fine particles can penetrate deeply into the respiratory system and potentially contribute to adverse health effects. These findings highlight the importance of continuous air quality monitoring and the implementation of pollution control measures to reduce heavy metal contamination in airborne particulate matter. According to the Pollution Control Department (2023), Pb concentrations should not exceed 0.0005 mg/L, Cd concentrations should not exceed 0.1000 mg/L, and Cu concentrations should not exceed 0.0001 mg/L. The concentrations detected in this study exceeded the recommended limits, indicating the potential risk of long-term adverse health effects associated with heavy metal exposure.

Nevertheless, this study was conducted as a preliminary investigation and may contain certain limitations, particularly regarding airflow control during passive indoor sampling. Therefore, future studies should improve sampling efficiency by incorporating an exhaust fan system into the sampling device and should further validate the findings using additional analytical techniques, such as scanning electron microscopy (SEM).

5. Conclusion

An in-house particulate matter (PM) sampling device was successfully developed using three layers of filter paper with pore sizes of 10, 2.5, and 1.2 μm to classify airborne particles into three size fractions (>10 μm, 10–2.5 μm, and 2.5–1.2 μm). The device provided a simple, low-cost, compact, and portable alternative for particulate matter collection and environmental monitoring. Using this device, 189 particulate matter samples were collected from indoor and outdoor environments in Saensuk Subdistrict, Mueang Chonburi District, Chonburi Province, Thailand, and analyzed for lead

(Pb), copper (Cu), and cadmium (Cd). The results showed that Cd was the predominant heavy metal detected, followed by Pb and Cu, with higher concentrations generally observed in indoor environments than outdoor environments. The presence of these heavy metals in fine particulate matter suggests contamination from anthropogenic sources such as vehicle emissions, industrial activities, fuel combustion, and chemical waste. Therefore, continuous air quality monitoring and effective pollution control strategies are necessary, while further studies using improved sampling systems and additional analytical techniques are recommended to enhance the accuracy and reliability of the results.

Acknowledgements

The authors would like to express their sincere gratitude to the Department of Chemistry, Faculty of Science, Burapha University, for providing laboratory facilities, instruments, and equipment for this research. The authors also acknowledge the support from the Scientific Instrumentation and Innovation Service Unit (SIF-IN-61030210) for providing scientific equipment and instrumental services throughout this study.

References

Abdulaziz, M., Alshehri, A., & Badri, H. (2022). Concentration level and health risk assessment of heavy metals in PM2.5 in ambient air of Makkah City, Saudi Arabia. Polish Journal of Environmental Studies, 31(5), 3991–4003.

Amato, F., Cassee, F. R., van der Gon, H. A. C. D., Gehrig, R., Gustafsson, M., Hafner, W., Harrison, R. M., Jozwicka, M., Kelly, F. J., Moreno, T., Prevot, A. S. H., Schaap, M., Sunyer, J., Querol, X., & Alastuey, A. (2014). Urban air quality: The challenge of traffic non-exhaust emissions. *Journal of Hazardous Materials, 275*, 31–36.

Aziz, S., & Zaman, S. U. (2025). Comprehensive analysis of heavy metals in indoor PM2.5: Source identification and health risk assessment in Dhaka, Bangladesh. Environmental Challenges, 18, 101234.

Fahim, Y. A., Boughdady, H. M., Othman, W. A., Mostafa, S. M., Helmi, L. M., Elsayed, A. A., Hamouda, O. S., Gad, O. M., & Sallam, R. M. (2026). *Heavy metal air pollution: Human health effects and nanomaterial strategies for monitoring and remediation*. *Biological Trace Element Research*. Advance online publication. https://doi.org/10.1007/s12011-026-05019-3

Goodarzi, B., Mohammadi, M. J., Alidadi, H., Salmanzadeh, M., Ehrampoush, M. H., & Khorsandi, H. (2023). Investigating PM2.5 toxicity in highly polluted urban and industrial areas. Scientific Reports, 13, 45052.

Li, H., Qian, X., Hu, W., Wang, Y., & Gao, H. (2013). Heavy metals in atmospheric particulate matter: A comprehensive understanding is needed for monitoring, risk assessment, and control. *Environmental Science & Technology, 47*(23), 13210–13211.

Matei, E. (2025). Heavy metals in particulate matter—Trends and impacts on human health. Atmosphere, 16(2), 215.

Matos-Espinosa, C., Hernández-Mena, L., García-Rico, L., & Torres-Rodríguez, M. (2025). Heavy metal concentrations in particulate matter: A case study. Atmosphere, 16(11), 1236.

Pant, P., & Harrison, R. M. (2013). Estimation of the contribution of road traffic emissions to particulate matter concentrations from field measurements: A review. *Atmospheric Environment, 77*, 78–97.

Park, S., Kim, J., Lee, H., & Choi, Y. (2024). PM2.5 and heavy metals in urban and agro-industrial areas. Discover Environment, 4, 112.

Pollution Control Department. (2023). *Thailand ambient air quality standards*. Ministry of Natural Resources and Environment, Thailand.

Wang, J., Liu, Y., Zhang, X., Chen, H., & Li, Q. (2024). Characteristics and health risks of PM2.5-bound metals. Aerosol and Air Quality Research, 24(6), 230456.

Wu, P. C., Lee, C. T., Liu, S. C., & Chou, C. C. K. (2021). Tracing local sources and long-range transport of PM10 using lead isotopic compositions and chemical characteristics. *Scientific Reports, 11*, 6605

Valorization of Waste Mango Leaves into Sustainable Bio-sorbents for Removal of Malachite Green Dye from Aqueous Solutions

Payuporn Pramuansuk[1], Ratiwun Suwattanamala[2], Akapong Suwattanamala[1*]
[1,]Department of Chemistry, Faculty of Science, Burapha University, Chonburi 20131, Thailand
[2]Division of Environmental Health, Faculty of Public Health, Burapha University, Chonburi 20131, Thailand
*Email: akapong@go.buu.ac.th

Abstract

Open burning is a common disposal method for fallen leaves and contributes to environmental pollution through the release of particulate matter (PM2.5), CO, and CO_2, posing significant risks to both environmental and human health. This study investigated the potential of fallen mango leaves as a low-cost bio-sorbent for the removal of malachite green *(*MG*)* dye from aqueous solutions. The mango leaves were chemically pretreated using 0.5 M NaOH and sieved to obtain particle sizes ranging from 0.300 to 0.355 mm, namely MLP. Batch adsorption experiments were performed to evaluate the effects of adsorption parameters and determine the optimum conditions. The highest removal efficiency of approximately 99.5% was achieved using 0.250 g of adsorbent with a contact time of 90 min at initial dye concentration of 20 mg L^{-1}. The adsorption kinetics were best described by the pseudo-second-order model, while the equilibrium data were well fitted by the Freundlich isotherm model, indicating multilayer adsorption on a heterogeneous surface. Thermodynamic analysis revealed Gibbs free energy (ΔG°) values ranging from −11.38 to −13.56 kJ mol^{-1}, with enthalpy (ΔH°) and entropy (ΔS°) values of 21.61 kJ mol^{-1} and 108.56 J $mol^{-1}K^{-1}$, respectively, confirming that the adsorption process was spontaneous and endothermic. The adsorption of MG onto MLP was primarily attributed to physical interactions, including hydrogen bonding, dipole force and π–π interactions between the dye molecules and the bio-sorbent surface. These findings demonstrate that fallen mango leaves can be effectively valorized into a sustainable and efficient bio-sorbent for dye-contaminated wastewater treatment.

Keywords*:* mango leaves; malachite green; adsorption; bio-sorbent; biomass

1. Introduction

Adsorption has been extensively employed for wastewater treatment because of its operational simplicity, mild treatment conditions, and high removal efficiency (Liu *et al*., 2021). The effectiveness of the adsorption process largely depends on the properties of the adsorbent, particularly its surface area and porous structure. Biomass-derived carbon materials produced through pyrolysis under oxygen-limited conditions (Sharma *et al.*, 2019; Gao, 2022; Abewaa *et al.*, 2023) and biochar (Ali *et al.*, 2023) have attracted significant interest as sustainable and cost-effective adsorbents. Owing to their abundant availability and low production cost, various biomass wastes have been widely utilized as precursors for carbon material synthesis. Biomass carbon activation methods are generally classified into physical and chemical activation (Tsai *et al*., 2022; Yusop, Abdullah, and Ahmad, 2023). Physical activation typically employs steam, carbon dioxide, or mixed gases as activating agents, whereas chemical activation utilizes reagents such as NaOH, KOH, H_3PO_4, and $ZnCl_2$. Although physical activation is considered more environmentally favorable due to reduced chemical usage and lower equipment corrosion, it often requires higher temperatures and longer processing times, while producing carbons with less-developed pore structures. Therefore, the development of biomass-derived carbon materials with enhanced surface area and adsorption performance remains a significant challenge.

Malachite green (MG) is a cationic synthetic dye widely used in textile and related aquaculture industries due to its strong affinity for negatively charged functional groups in materials such as silk, wool, cotton, polyester, and nylon. However, the extensive use of MG has raised significant environmental and health concerns because of its cytotoxic, genotoxic, mutagenic, and potentially carcinogenic effect. In addition, the discharge of MG-contaminated wastewater can adversely affect aquatic ecosystems by reducing light penetration, decreasing dissolved oxygen levels, and disrupting aquatic plant and animal life (Raval *et al.*, 2017). Therefore, effective treatment of MG-containing wastewater prior to environmental discharge is essential.

Thailand is one of the world's major mango-producing countries, with annual production exceeding one million tonnes (FAOSTAT, 2024). The cultivation and maintenance of mango orchards generate considerable quantities of pruning residues and fallen leaves, which require appropriate management. In many agricultural regions, biomass residues are still disposed of through open-field burning, contributing to greenhouse gas emissions and fine particulate matter (PM2.5) pollution. Prolonged exposure to PM2.5 is associated with respiratory and cardiovascular diseases, as well as increased cancer risk (Chen *et al*., 2017). Therefore, the valorization of abundant mango leaf waste into bio-sorbents offers a sustainable alternative to open burning disposal. Mango leaves are classified as lignocellulosic biomass consisting primarily of cellulose, hemicellulose, lignin, extractives, and inorganic minerals. The relative proportions of these components depend on cultivar, environmental conditions, and analytical methods. Owing to the presence of these compounds, mango leaf biomass contains functional groups capable of interacting with dye molecules through adsorption mechanisms.

This study focuses on the utilization of fallen mango leaves as a bio-sorbent for malachite green removal from aqueous solutions. The proposed approach provides an alternative to open burning and high-temperature carbonization processes, while promoting the conversion of agricultural waste into a value-added material. Consequently, this strategy not only addresses dye-contaminated wastewater but also supports sustainable biomass utilization and environmentally conscious waste management practices.

2. Objectives

This study aimed to characterize the physicochemical properties of a bio-sorbent prepared from fallen mango leaves and to evaluate its adsorption performance for the removal of malachite green dye from aqueous solutions. In addition, the adsorption behavior of malachite green onto the bio-sorbent surface was systematically investigated through kinetic, isotherm, and thermodynamic analyses to better understand the adsorption mechanism and process feasibility.

3. Materials and methods

Materials

All used chemicals were of Analytical Grade without further purification. Malachite green (MG) and sodium hydroxide (NaOH) were supplied by Loba Chemie PVT. LTD. and Ajax Finechem, respectively. A stock solution of MG dye of 100 mg/L was prepared by accurate weight dissolving in double-distilled water. The further solution with desired concentration was prepared by prior dilution the stock solution to use.

Bio-sorbent preparation

Fallen leaves of the Nam Dok Mai mango cultivar (*Mangifera indica* L. cv. Nam Dok Mai) from a home garden tree were collected from Chanthaburi Province, Thailand, in December 2024 and subsequently used as the raw material for bio-sorbent preparation. The collected sample was washed with tap water to remove impurities and dust particles. The sample was sundried for 24 h and then placed in an oven at 70^{o}C for 24 h to remove the remaining moisture. The dried mango leaves were crushed and then sieved using stainless sieve mesh to obtain a powder particle size of approximately 300-355 μm (50 mesh), as noted RMLP. The RMLP modification was performed by treating 1.0 g of RMLP with 20 mL of 0.5 M NaOH and then followed by heating at 70^{o}C for 5 h to eliminate colored component. The bio-sorbent produced was washed several times with distilled water to remove excess NaOH from its surface until its pH reached neutral. The bio-sorbent obtained from modified mango leaf powder, as called MLP, was dried in the oven at 70^{o}C overnight. Finally, the dried MLP was sealed in a zip-lock plastic bag and placed in a desiccator prior to the adsorption experiments.

Characterization technique

Attenuated Total Reflectance Fourier Transform Infrared Spectroscopy (PerkinElmer, ATR-FTIR -2000 type) in scanning wavenumber range of 4000-500 cm^{-1} was applied to identify functional group of RMLP and MLP. Scanning Electron Microscope (LEO, SEM-LEO 1450 VP type) was applied to determine of porous surface morphology of MLP bio-sorbent. UV-VIS Spectrophotometer

(Agilent, UV-VIS-Agilent Cary 3500 Multicell type) was used to determine of malachite green dye concentration after adsorption.

Batch adsorption experiments for malachite green dye removal

The efficiency adsorption of bio-sorbents for malachite green (MG) dye removal from aqueous solutions was carried out by batch method. Batch adsorption experiments were conducted by the series of 125 mL conical flasks containing desired MLP dosage and 50 mL of MG dye solution, using a shaker water bath at 80 rpm keeping constant 30 ºC and initial pH solution = 6.5-7.0. Optimum conditions were determined by performing batch adsorption experiments in the adsorbent dosage range of 0.025-0.275 g, in the dye concentration range of 10-100 mg L^{-1}, and in the contact time range of 0–120 min. The ranges of these operating parameters were followed by the previous studies of MG adsorption onto the other adsorbents (Sharma *et al.*, 2019; Krishna Murthy *et al.*, 2019; Abewaa *et al.*, 2023; Vara *et al*., 2024). The adsorption isotherms, thermodynamic and kinetic studies were performed for the specific duration of contact time in the temperature range of 30-50ºC to obtain the parameters. After the desired contact time, the solutions were filtered by filter paper and the residual dye concentration in the filtrate part was determined by absorbance measurements in a UV-Visible Spectrophotometer at a maximum wavelength of 618 nm. After verifying Beer-Lambert 's law via calibration curve, the starting and residual dye concentrations (before and after adsorptions) were used to calculate the amount of adsorbed material and the percentage of removal ability. The adsorption capacity and the removal percentage (% removal) were determined by the following formula :

$$q_e = \frac{(C_0 - C)}{m} V \qquad (1)$$

$$\%\, removal = \frac{(C_0 - C)}{C_0} \times 100\ \% \qquad (2)$$

q_e (mg g^{-1}) is the adsorption capacity at equilibrium where C_o, and C (mg L^{-1}) are the initial and final dye concentration, V (L) is the volume of the reaction solutions, m(g) is the mass of the bio-sorbent used.

4. Results and Discussion

Characterization of bio-sorbent

The FT-IR spectra were analyzed to identify the functional groups presented on the adsorbent surface, as shown in Figure 1. A broad peak at 3304 cm^{-1} was observed in all samples, corresponding to the O–H stretching vibration of hydrogen-bonded hydroxyl groups in cellulose, lignin, and hemicellulose of biomass architecture. The peak at 2850 cm^{-1} was assigned to the aliphatic C–H stretching vibrations of $–CH_2$ and $–CH_3$ groups in lignocellulosic components. The absorption band at 1735 cm^{-1} corresponded to the C=O stretching vibration of ester and carboxyl groups, mainly associated with hemicellulose and lignin structure. The band at 1607 cm^{-1} was assigned to aromatic C=C stretching vibrations of lignin, whereas the peak at 1316 cm^{-1} was attributed to C–O stretching vibrations of lignocellulosic components. The FT-IR spectra of raw mango leaf powder (RMLP) and modified mango leaf powder (MLP) showed similar functional groups; however, MLP exhibited relatively higher peak intensities, suggesting an increased abundance of hydroxyl and carboxyl functional groups after modification. The characteristic peaks at 1607 and 1316 cm^{-1} indicate the possible contribution of aromatic and oxygen-containing functional groups in the adsorption of malachite green (MG) dye through hydrogen bonding and π-π interactions. The spectrum of modified mango leaf powder after adsorption (MLPA) showed noticeable changes compared with that of MLP. The intensity of the O–H band at 3304 cm^{-1} slightly decreased, indicating possible interactions between hydroxyl groups and dye molecules. A reduction in the peak intensity at 1735 cm^{-1} may be associated with the participation of carboxylic groups during the adsorption process. In addition, the

decreased intensity at 1607 cm^{-1} may be associated with interactions between aromatic lignin groups and dye molecules. Slight changes at 1316 cm^{-1}, together with a minor shift at 1032 cm^{-1} corresponding to C–O–C stretching vibrations may indicate interactions between lignocellulosic functional groups and the positively charged MG molecules through hydrogen bonding and dipole-dipole related interactions. These findings are consistent with previous studies reported by Vara *et al.* (2024), confirming that mango leaf biomass contains suitable functional groups for MG adsorption.

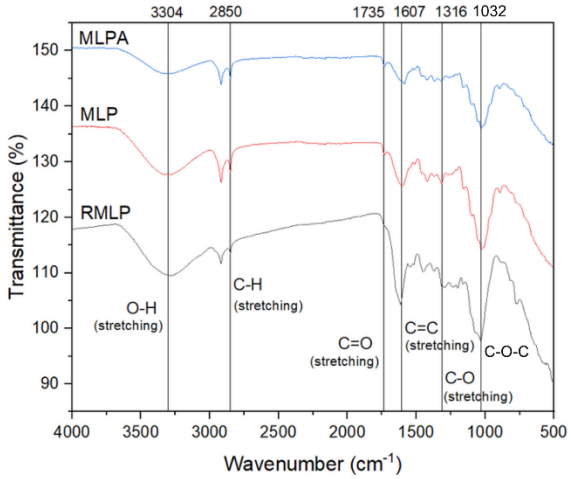

Figure 1 FT-spectra for raw mango leaf powder (RMLP), modified mango leaf powder (MLP) and modified mango leaf powder after adsorption (MLPA).

Figure 2 presents the SEM images of the bio-sorbent derived from MLP at a magnification of 1000× with a scale bar of 10 µm, revealing a heterogeneous surface morphology with pore-like cavities and irregular surface features. The MLP bio-sorbent exhibited both relatively smooth and rough regions distributed throughout the structure. The development of these porous features is likely associated with the extraction and modification processes during adsorbent preparation. Such morphological characteristics may enhance surface accessibility and facilitate the diffusion of malachite green molecules into the porous structure, thereby potentially improving the adsorption performance of the bio-sorbent.

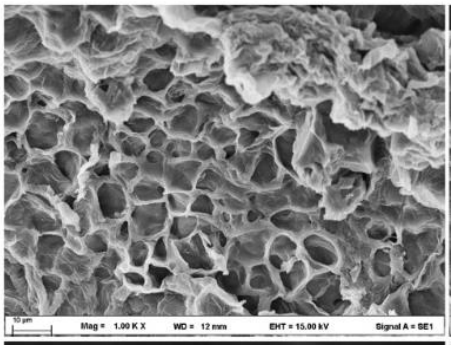

Figure 2 SEM image of modified mango leaf powder (MLP) with magnification level of 1000x .

Effect of operating parameters

The effect of contact time on the adsorption process was investigated over a contact time range of 0–105 min, as shown in Figure 3a-3b, while the other parameters, including bio-sorbent dosage (0.250 g), temperature (30 °C), and initial dye concentration (60 mg L^{-1}), were kept constant. As shown in Figure 3a, the removal efficiency increased rapidly during the initial stage of adsorption, particularly within the first 5–10 min, which may be attributed to the abundance of available active sites and the high concentration gradient between the adsorbate and adsorbent surface. As the contact time increased, the adsorption rate gradually decreased due to the progressive occupation of active sites and possible diffusion limitations. The adsorption system approached equilibrium after approximately 15 min, with only minor changes observed thereafter. To ensure that adsorption

equilibrium was attained across all investigated initial dye concentrations, a contact time of 90 min was employed in all subsequent experiments.

The effect of the initial concentration of MG dye ranging from 10 to 100 mg L^{-1} on the adsorption performance is presented in Figure 3c. The adsorption experiments were conducted under constant conditions of 0.250 g bio-sorbent dosage, 30 °C temperature, and 90 min contact time. The adsorption capacity (q_t) increased progressively with increasing initial dye concentration, which may be attributed to the enhanced concentration gradient and increased mass transfer driving force between the liquid and solid phases. As a result, a greater number of dye molecules could interact with the available adsorption sites on the bio-sorbent surface. In contrast, the percentage removal exhibited a slight decrease at higher dye concentrations, likely due to the progressive saturation of available adsorption sites relative to the increasing number of dye molecules in solution. Nevertheless, the removal efficiency remained higher than 98% over the investigated concentration range, indicating the high adsorption affinity of the bio-sorbent toward MG dye. Furthermore, MLP exhibited removal efficiency comparable to those of biomass-derived activated carbons reported in the literature (Sharma *et al.*, 2019; Abewaa *et al.*, 2023; Yusop, Abdullah, and Ahmad, 2023). Its simple preparation without thermal activation reduces energy and chemical demands while maintaining effective dye removal performance. In addition, the conversion of fallen mango leaves into a value-added bio-sorbent supports agricultural waste valorization and the principles of a circular economy.

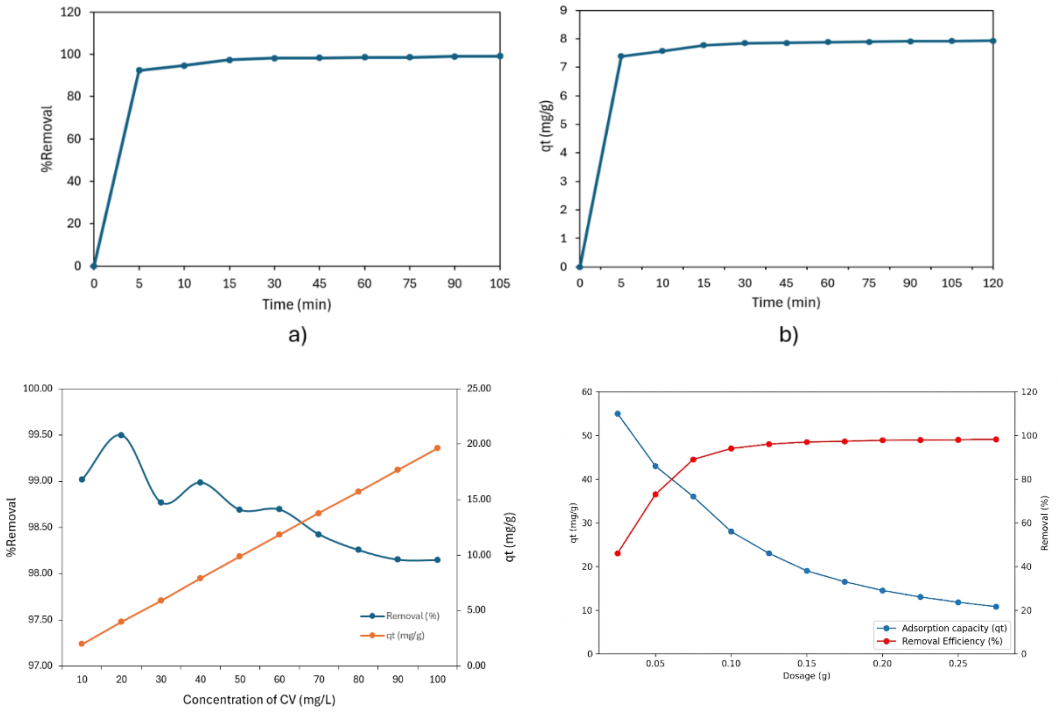

Figure 3 Effect of operating parameters om MG adsorption: a)-b) contact time c) initial dye concentration d) dosage.

The effect of bio-adsorbent dosage on the removal efficiency and adsorption capacity of MG dye was investigated to determine the optimum dosage for cost-effective treatment while the other parameters, including temperature (30 °C), contact time (90 min) and initial dye concentration (60 mg L^{-1}) were maintain constant. As illustrated in Figure 3d, an increase in adsorbent dosage from 0.025g to 0.275 g led to a significant enhancement in the MG removal percentage. The removal efficiency reached 98.47 % with a dosage of 0.250 g. This positive correlation is attributed to the increased availability of active surface area and vacant binding sites at higher dosages, facilitating greater dye-adsorbent interaction. However, beyond 0.250 g, the removal efficiency reached a plateau, suggesting that this dosage is optimal for maximizing removal while minimizing adsorbent consumption and operational costs. Conversely, the adsorption capacity (q_t) exhibited a downward trend as the adsorbent dosage increased. This phenomenon can be explained by the relative abundance of

adsorption sites compared to the fixed number of dye molecules in the system, resulting in the underutilization of available sites. Furthermore, high adsorbent dosage may lead to particle aggregation and overlapping of active sites, which increases the diffusion path length and creates physical interference between particles, consequently reducing the q_t values. Similar behavior with the acid treated coffee husk as adsorbent on MG removal has been reported by Krishna Murthy *et al.* (2019).

Kinetics of Adsorption

Two common kinetic models, namely pseudo-first-order and pseudo-second-order were employed to investigate the adsorption kinetics of MG dye on to MLP. The pseudo-first-order kinetic model is described by the following Lagergren equation:

$$\ln(q_{e,obs} - q_t) = \ln q_{e,cal} - k_1 t \quad (3)$$

where q_e and q_t (mg/g) represent the amounts of MG dye adsorbed at equilibrium and at contact time t (min), respectively and k_1(min^{-1}) is the pseudo-first-order rate constant. The calculated equilibrium adsorption capacity ($q_{e,cal}$) and k_1 values were obtained from the slope and intercept of the linear plot of ln (q_e - q_t) versus t, as summarized in Table1. The results showed that the calculated adsorption capacities ($q_{e,cal}$) were not in close agreement with the experimental values ($q_{e,obs}$). This discrepancy suggests that the adsorption behavior of MG onto MLP was not adequately described by the pseudo-first-order kinetic model.

The pseudo-second-order kinetic model was further applied to evaluate the adsorption kinetics of MG dye onto MLP. This model is expressed as follows:

$$\frac{t}{q_t} = \frac{1}{k_2 q_e^2} + \frac{t}{q_e} \quad (4)$$

where k_2 (g mg $^{-1}$ min^{-1}) is the pseudo-second-order rate constant. The values of k_2 and q_e were calculated from the slopes and intercepts of the corresponding plot, as summarized in Table 1. The calculated equilibrium adsorption capacities obtained from the pseudo-second-order model showed good agreement with the experimental values. In addition, the correlation coefficient (r^2) values exceeded 0.999 for all initial MG concentrations, indicating an excellent fit to the experimental data. Therefore, the adsorption of MG onto MLP is better described by the pseudo-second-order kinetic model. These findings are consistent with previous studies reporting MG adsorption onto various adsorbents (Sharma *et al.*, 2019; Gao, 2022; Tsai *et al.*, 2022; Abewaa *et al.*, 2023).

Table 1 Kinetic parameters of pseudo-first and pseudo-second-order models for the adsorption of MG dye onto MLP at various concentration.

Concentration (mg/L)	$q_{e\,(exp)}$ (mg g^{-1})	$q_{e\,(cal)}$ (mg g^{-1})	k	r^2
Pseudo-first-order model				
20	3.99	0.08	1.1x10^{-3}	0.9959
40	7.94	0.04	3.3x10^{-3}	0.5837
60	11.87	0.00	6.6x10^{-3}	0.7463
Pseudo-second-order model				
20	3.99	3.99	0.87	0.9995
40	7.94	7.95	0.28	0.9999
60	11.87	11.92	0.13	0.9997

Adsorption Isotherm

Three adsorption isotherm models, namely Langmuir, Freundlich, Temkin, were applied to investigate the equilibrium adsorption behavior of MG dye onto MLP. The Langmuir isotherm model assumes monolayer adsorption on a homogeneous adsorbent surface, whereas the Freundlich isotherm model describes adsorption on heterogeneous surfaces containing diverse functional groups and

adsorption sites. The Langmuir, Freundlich and Temkin isotherm models are described by the following equation, respectively :

$$\frac{C_e}{q_e} = \frac{1}{q_m K_L} + \frac{C_e}{q_m} \quad (5)$$

$$\ln q_e = \ln K_F + \frac{1}{n} \ln c_e \quad (6)$$

$$q_e = \frac{RT}{b_T} \ln A_T + \frac{RT}{b_T} \ln c_e \quad (7)$$

where q_m (mg g^{-1}) is the maximum adsorption capacity, n is the Freundlich constant, K_L is the Langmuir constant, K_F is the Freundlich constant. In addition, the constant b_T of Temkin is associated with adsorption heat and A_T is the Temkin constant. The slope and the intercept of each linear plot were used to obtain Langmuir, Freundlich and Temkin parameters, as summarized in Table 2.

Table 2 Isotherm parameters for the adsorption of MG dye onto MLP.

Model	Temperature (°C)		
	30	40	50
Langmuir			
q_{max} (mg/g)	149.14	379.80	1931.28
K_L	0.06	0.19	1.98
r^2	0.1021	0.0262	0.0006
Freundlich			
K_F	19.59	24.88	30.35
n	1.07	0.96	0.97
r^2	0.97	0.98	0.97
Temkin			
A_T	10.52	9.96	12.34
b_T	0.34	0.30	0.30
B	7.18	9.96	12.34
r^2	0.86	0.91	0.93

The adsorption equilibrium data of MG onto MLP were described by the Freundlich isotherm model, as demonstrated by the high R^2 values obtained from the linear regression analysis (Table 2). This result suggests heterogeneous surface adsorption and the possible formation of multiple adsorption layers. These findings are consistent with previous studies reporting MG adsorption onto various adsorbents (Gao, 2022; Yusop, Abdullah, and Ahmad, 2023).

Thermodynamic Studies

The Van't Hoff equation was used to determine the three essential parameters, namely enthalpy change (ΔH°), entropy change (ΔS°) and Gibbs free energy (ΔG°) by the following equations :

$$\Delta G^0 = -RT \ln K_c \quad (8)$$

$$\ln K_c = -\frac{\Delta H^0}{R}\left(\frac{1}{T}\right) + \frac{\Delta S^0}{R}$$

where, R is the universal gas constant (8.314 J mol^{-1} K^{-1}), K_C represents the thermodynamic constant, and T is the absolute temperature (K). The values of ΔH° and ΔS° were determined from the slope and intercept of the linear plot of ln K_C versus 1/T, respectively. The thermodynamic

parameters for the adsorption of MG onto the bio-adsorbent were evaluated, and the results are summarized in Table 3.

Table 3 Thermodynamic parameters for the adsorption of MG dye onto MLP.

Temperature (ºC)	ΔG° (kJ mol^{-1})	ΔH° (kJ mol^{-1})	ΔS° (J mol^{-1} K^{-1})
30	-11.38	21.61	108.56
40	-12.22		
50	-13.56		

The Gibbs free energy change (ΔG^o) was found to be negative across all investigated temperatures (30, 40, and 50°C), with values decreasing from -11.38 to -13.56 kJ mol^{-1} as the temperature increased. These negative values confirm that the adsorption process is thermodynamically spontaneous and becomes more favorable at higher temperatures. The positive enthalpy change (ΔH^o) of +21.61 kJ mol^{-1} indicates the endothermic nature of the adsorption process. This suggests that the adsorption efficiency improves with increasing temperature, which is consistent with the experimental findings. Furthermore, the magnitude of $\Delta H^o < 40$ kJ mol^{-1} suggests that the interaction between the MG molecules and the adsorbent surface is primarily governed by physisorption. The entropy change (ΔS^o) was recorded as +108.56 J mol^{-1} K^{-1}. The positive value of ΔS^o reflects an increase in the randomness at the solid-liquid interface during the adsorption process. This increase in disorder can be attributed to the displacement of water molecules previously coordinated around the MG ions; as the dye molecules transition from the bulk solution to the adsorbent surface, the dehydration of the dye ions releases a significant number of water molecules back into the solution, thereby increasing the overall entropy of the system. Similar results have been reported for the MG adsorption onto the other adsorbents (Krishna Murthy *et al.*, 2019; Gao, 2022; Abewaa *et al.*, 2023).

Adsorption mechanism The adsorption of MG dye onto MPA is likely governed by interactions between MG molecules and the lignocellulosic components of the bio-sorbent, including cellulose, hemicellulose, and lignin. MG contains aromatic tertiary amine groups that may interact with oxygen-containing functional groups, particularly hydroxyl and carboxylic groups present on the lignocellulosic surface. These interactions may involve hydrogen bonding and dipole-related interactions between the positively charged dye molecules and electron-rich oxygen-containing groups on the bio-sorbent surface. In addition, the adsorption process may also be influenced by π–π interactions between the aromatic rings

of MG molecules and the aromatic structures of lignin within the lignocellulosic matrix. Such intermolecular interactions could contribute to the stabilization of dye molecules on the bio-sorbent surface and enhance the adsorption performance. The proposed adsorption mechanism is illustrated in Figure 4. Previous FT-IR analysis of MLP and MLPA showed noticeable changes in the bands associated with hydroxyl, carbonyl, aromatic, and C–O functional groups, suggesting the involvement of hydrogen bonding, oxygen-containing functional groups, and π–π interactions during the adsorption of MG onto the lignocellulosic bio-sorbent surface.

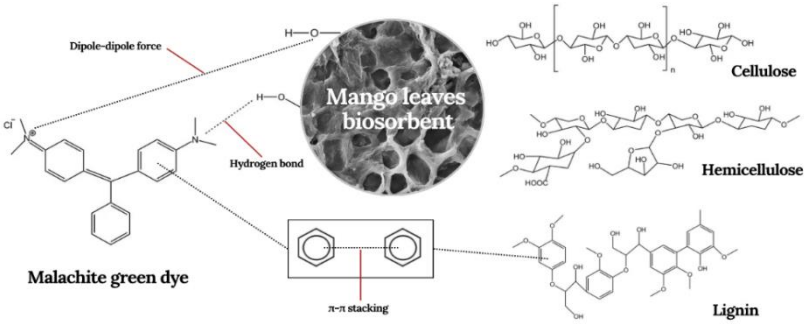

Figure 4 The possible interaction between MG and MLP during adsorption.

5. Conclusion

The present work highlights the potential of fallen mango leaves as a sustainable feedstock for the development of bio-sorbent for removal MG from aqueous solutions. The proposed approach provides

an environmentally responsible pathway for converting an abundant agricultural residue into a value-added material, thereby contributing to waste valorization and circular resource management. Owing to its simple preparation process and minimal resource requirements, the developed bio-sorbent offers potential as a sustainable alternative for MG dye-contaminated wastewater treatment applications. Future research should focus bio-sorbent regeneration, performance under realistic wastewater conditions, and techno-economic viability to facilitate large-scale and long-term implementation.

Acknowledgements

This work was partially funded by research grant from Department of Chemistry, Faculty of Science, Burapha University.

References

Abewaa, M., Mengistu, A., Takele, T., Fito, J., & Nkambule, T. (2023). Adsorptive removal of malachite green dye from aqueous solution using *Rumex abyssinicus*-derived activated carbon. *Scientific Reports, 13*, 14701.

Ali, Y. A. E. H., Ahrouch, M., Lahcen, A.A., Abdellaoui, Y., & Stitou, M. (2023). Recent advances and prospects of biochar-based adsorbents for malachite green removal: A comprehensive review. *Chemistry Africa, 6*(3), 579–608.

Chen, J., Li, C., Ristovski, Z., Milic, A., Gu, Y., Islam, M. S., Wang, S., Hao, J., Zhang, H., He, C., Guo, H., Fu, H., Miljevic, B., Morawska, L., Thai, P., Lam, Y. F., Pereira, G., Ding, A., Huang, X., & Dumka, U. C. (2017). A review of biomass burning: Emissions and impacts on air quality, health and climate in China. *Science of the Total Environment, 579*, 1000–1034.

Food and Agriculture Organization of the United Nations. (nd). FAOSTAT 2024. Retrieved June 10, 2024, from https://www.fao.org/faostat/en/#home

Gao, W. (2022). Porous biomass carbon derived from *Clivia miniata* leaves via NaOH activation for removal of dye. *Material*s, *15*, 1285.

Krishna Murthy, T. P., Gowrishankar, B. S., Chandra Prabha, M. N., Kruthi, M., & Hari Krishna, R. (2019). Studies on batch adsorptive removal of malachite green from synthetic wastewater using acid treated coffee husk: Equilibrium, kinetics and thermodynamic studies. *Microchemical Journal, 146*, 192–201.

Liu, M., Li, L., Tang, M., Hong, L., Sun, S., & Xing, W. (2021). Multi-component separation of small molecular/ionic pollutants with smart pH-gating membranes. *Chemical Engineering Science, 245*, 116854.

Raval, N. P., Shah, P. U., & Shah, N. K. (2017). Malachite green "a cationic dye" and its removal from aqueous solution by adsorption. *Applied Water Science, 7*, 3407–3445.

Sharma, G., Sharma, S., Kumar, A., Naushad, M., Du, B., Ahamad, T., Ghfar, A. A., Alqadami, A. A., & Stadler, F. J. (2019). Honeycomb structured activated carbon synthesized from *Pinus roxburghii* cone as effective bioadsorbent for toxic malachite green dye. *Journal of Water Process Engineering, 32*, 100931.

Tsai, C.-Y., Lin, P.-Y., Hsieh, S.-L., Kirankumar, R., Patel, A. K., Singhania, R.-R., Dong, C.-D., Chen, C.-W., & Hsieh, S. (2022). Engineered mesoporous biochar derived from rice husk for efficient removal of malachite green from wastewaters. *Bioresource Technology, 347*, 126749.

Vara, D., Jha, S., Bisht, S., Shahabuddin, S., Gaur, R., Suhas, & Tyagi, I. (2024). Sustainable bio-based adsorbents for simultaneous and efficient removal of hazardous dyes from aqueous solutions. *Toxics, 12*, 266.

Yusop, M. F. M., Abdullah, A. Z., & Ahmad, M. A. (2023). Malachite green dye adsorption by jackfruit based activated carbon: Optimization, mass transfer simulation and surface area prediction. *Diamond and Related Materials, 136*, 109991.

Ai-Act Development of an Ai-Driven Aviation Communication Trainer for WCC ATC Binalonan

Hazel Mae C. Labador*, Tatiana Trisha T. Francisco, Jhon Clarence Kabigting, Adrian John A. Gonzales, Clark John Moore R. Tiu, Aeron Dave T. Tayaban, Mackenzie Nicole D. Cuaresma, Joey Aldrich T. Almanza
WCC Aeronautical and Technological College
*Email : avt.hazelmaelabadort@gmail.com

Abstract

Effective aviation communication is critical to flight safety, yet traditional lecture-based training often fails to provide students with sufficient real-time practical exposure to standard phraseology. This study focused on the development and evaluation of the AI-ACT (AI-Integrated Aviation Communication Trainer) system for WCC ATC Binalonan. The system aimed to enhance the communication proficiency of students from the College of Aviation, Avionics Technology, and Aircraft Maintenance Technology programs by simulating real-time interactions among pilots, air traffic controllers, and maintenance personnel across four flight stages: pre-flight, taxi, flight, and landing

This study focused on the development and evaluation of the AI-ACT (AI-Driven Aviation Communication Trainer) for WCC ATC Binalonan. The system enhanced aviation communication proficiency by providing AI-driven, real-time phraseology feedback. It used Automatic Speech Recognition (ASR) to simulate pilot, ATC, and maintenance personnel interactions across pre-flight, taxi, flight, and landing stages. Quantitative evaluation from 176 respondents and expert evaluators yielded an overall functional suitability mean of 4.81 (Highly Functional) and Cronbach's Alpha of 0.897, indicating high reliability. Expert ratings confirmed functional completeness (4.60), correctness (4.54), and appropriateness (4.66). The AI core logic achieved the highest accuracy (4.86) in identifying phraseology errors. The system effectively bridged classroom theory and practical radio communication.

Keywords: AI-ACT; AI in Aviation Education; AI-Enhanced Training; Aviation Training Simulation Technology; Communication Trainer

INTRODUCTION

Air traffic control constituted a complex global network of facilities and procedures designed to organize and manage aircraft movements within controlled airspace to guarantee safe and efficient air traffic operations. As the aviation industry evolved, technology became an integral part of aviation safety. The integration of modern technology was specifically critical in ensuring the precision of operations during the phases of pre-flight, taxi, flight, and landing.

The International Civil Aviation Organization (2025) highlighted that Artificial intelligence (AI) is revolutionizing the aviation industry, optimizing processes and improving efficiency in key areas such as air traffic management (ATM), predictive maintenance and safety. Its ability to process large volumes of data, including weather information, flight plans and transfers, and to detect patterns, permits route optimization, congestion prediction and risk anticipation, improving safety and efficiency in the use of airspace. This strategic reliance on technological advancement strongly aligns with the United Nations Sustainable Development Goal 9 regarding Industry, Innovation, and Infrastructure by promoting resilience and cutting-edge technology systems.

According to Bautista, J. E. (2025), such errors were mostly due to failures or a lack of communication. One research discovered that 70% to 80% of accidents in the world sector are attributed to poor communication. Hayes (2020) further found that in the workplace, over 30% of operational mistakes related to poor teamwork and communication fidelity were directly attributed to such failures.

Within the WCC Aeronautical and Technological College, previous researchers addressed the training need through the project titled "Control Tower and Pilot Communication Simulation System" (CTAPSS). Carpio (2022) focused the study on the development of a hardware-based console

designed to replicate an actual ATC workstation. The project aimed to provide students with a hands-on tool to practice basic communication procedures and phraseologies across four stages of flight, including pre-flight, taxi, flight, and landing. The AI-ACT project presented a unique evolution of the earlier concept by shifting the focus from hardware replication to intelligent software integration. Unlike the precursor by Carpio (2022), the AI-ACT system utilized Artificial Intelligence and Automatic Speech Recognition to generate dynamic and unscripted scenarios.

The AI-ACT system was built upon the Intelligent Agent Model presented in Russell and Norvig (2021), a conceptual framework in artificial intelligence design that established the operational logic of rational agents operating in dynamic environments. This theory differs from classic game rules since it explains the self-contained character of the model without considering external factors such as users. However, the theory describes simulated behavior in relation to users. Rationality in the agent function means that the actions chosen will optimize the performance measures of the system based on perception results.

Objectives

The objective of this study was to develop the AI-ACT system to improve radio communication training for WCC ATC, Binalonan. The design of the system provides an interactive training platform that simulates real-time communication among pilots, air traffic controllers, and maintenance personnel. Through the system, students practiced standard aviation phraseology to improve their ability to communicate effectively under pressure. AI was used to give instant feedback and help users correct mistakes.

The project aimed to:

A. Conduct problem evaluation and needs analysis to identify gaps in existing radio communication training in terms of realism, feedback mechanisms, and student engagement.

B. Design and develop the system with the following software requirements:

a. simulation software;
b. AI integration; and
c. 3D user interface.

C. Test the software system based on user acceptability in terms of:

a. functionality;
b. performance;
c. compatibility;
d. interaction capability;
e. reliability;
f. security; and
g. maintainability.

D. Assess the level of acceptability and system effectiveness by evaluating the simulation software in terms of:

a. functional completeness;
b. functional correctness; and
c. functional appropriateness.

MATERIALS AND METHODS

The researchers used appropriate research design and data gathering approaches in the development of the AI-ACT system. This included the review of related studies regarding the implementation of artificial intelligence, aviation communication training, and simulation-based systems. Questionnaires and surveys were utilized to test the accuracy and reliability of the system and to assess whether user satisfaction was achieved. The evaluation was based on functionality, performance, compatibility, interaction capability, reliability, security, and maintainability.

The study employed a quantitative research design to evaluate the effectiveness of the AI-ACT system as an aviation communication training tool. It followed the Design Science Research Methodology (DSRM), which focused on the development and evaluation of a technological solution

to address existing problems in aviation communication training. The WCC ATC Binalonan Campus was the setting of the research. In the AI-ACT system, the researchers simulated the Binalonan Aerodrome environment to replicate real-world aviation communication scenarios and to familiarize students with actual communication procedures used in the aerodrome. The system incorporated visual perspectives such as the pilot point of view (cockpit view) and the air traffic controller point of view (control tower view), allowing students to experience role-based interactions in a realistic setting. The participants in the study were students from WCC ATC Binalonan enrolled in the College of Aviation (COA), Avionics Technology (AVT), and Aircraft Maintenance Technology (AMT) programs, for a total of 176 respondents. These students were selected because they were directly involved in aviation communication training, making them suitable for evaluating how the AI-ACT system supported the development of their radio communication skills.

The AI-ACT system utilized user accounts where each participant had a personal account to access the application. The system also included recorded session history, which allowed the super administrator and system administrator to monitor and review user performance for evaluation and training purposes.

The system development process followed Waterfall Methodology, a structured and sequential approach consisting of five major phases: requirements, design, implementation, testing, and deployment, as shown in Figure 1. After development, the system underwent testing to evaluate its performance, identify errors, and ensure that it met the required standards and objectives. Necessary revisions and improvements were made based on the results of the testing phase. Finally, in the deployment phase, the completed system was implemented and made available for use by the intended users, allowing them to utilize the AI-ACT system for aviation communication training.

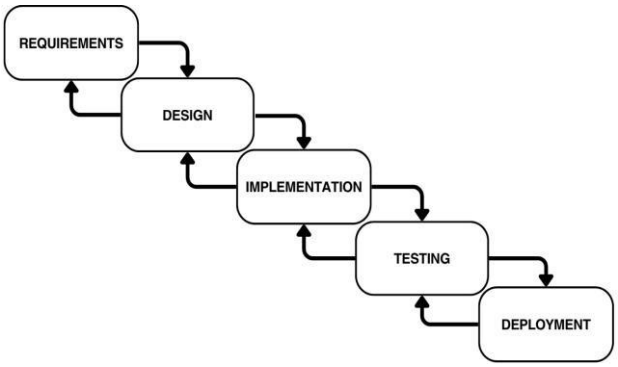

Figure 1 Waterfall Methodology

A comprehensive overview, presented in Table 1, was provided of the materials essential to the development and functionality of the AI-ACT for WCC ATC. Each component was carefully chosen to serve specific functions, contributing to the system's overall design and performance. The materials selected for the AI-ACT system were integrated to optimize training effectiveness in aviation communication.

Table 1 Materials to be Used in the Study

Name	Specification
Computer	• Processor: AMD Ryzen or Intel Core i3 or higher • RAM: At least 4 GB (8 GB recommended) • Storage: Minimum 128 GB • Operating System: Windows 10
Headset with Microphone	• Type: Over-ear or on-ear headset • Microphone: Built-in microphone • Connectivity: USB or 3.5mm audio jack
Mouse	• Type: Optical mouse • Connectivity: USB or wireless
Keyboard	• Type: Standard QWERTY keyboard • Connectivity: USB or wireless

The researcher's project progress is presented in the Table 2. This includes project design, programming, research planning, and final documentation. The researchers conducted the study planning process, including identifying the project's development needs, collecting the required documents, and reviewing related studies. Project design, programming, and final documentation necessary for the development of the application are also part of the research process.

Table 2 Gantt Chart of the Study

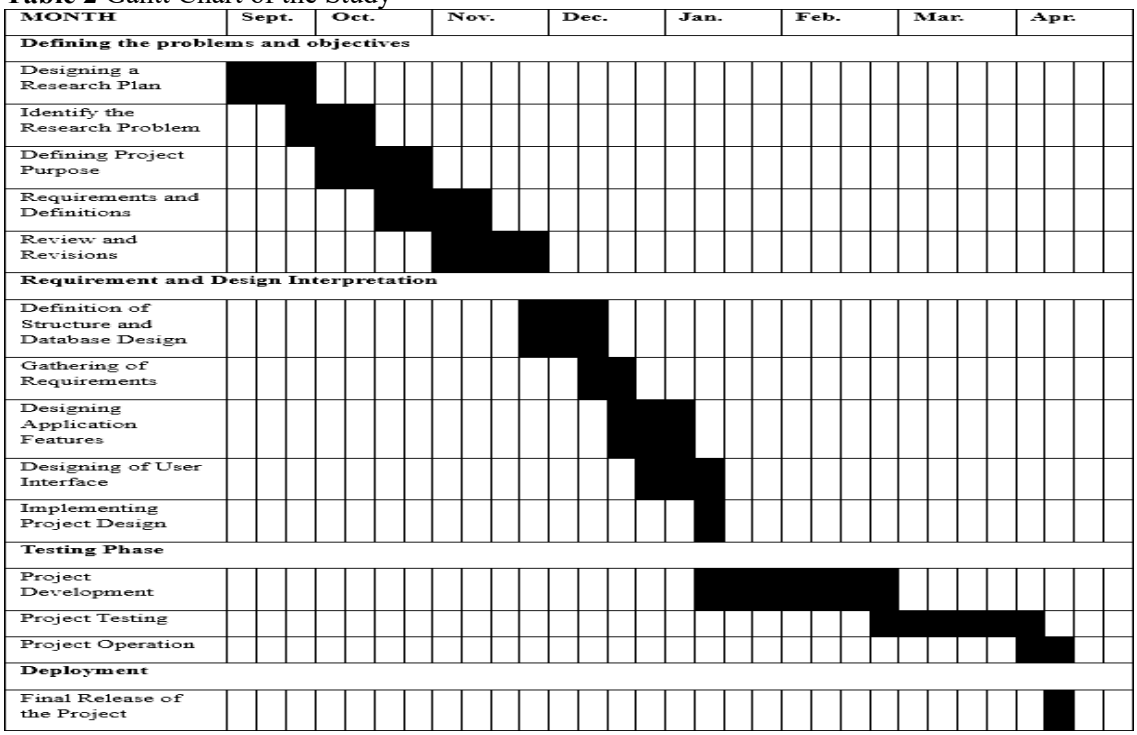

The AI-ACT system was developed as an aviation communication training application through the collaboration of the researchers and a programmer who assisted in coding the system. The goal was to create a tool that is easy to use, functional, and helpful for students, instructors, and maintenance personnel. The system integrated Artificial Intelligence and Automatic Speech Recognition to support communication training.

The system was used by instructors as an additional learning tool for teaching aviation communication to students enrolled in programs such as COA, AVT, and AMT. It provided a

controlled environment where students could practice radio communication using proper aviation phraseology.

The study utilized three (3) evaluation instruments to gather measurable data and assess the effectiveness of the AI-ACT system as an aviation communication training tool. The first instrument was the needs analysis assessment (see Table 3 for the Internal Consistency description), which was administered to Aviation professional respondents to determine the limitations of existing aviation communication training methods.

Table 3 Cronbach's Alpha Scale for Needs Analysis

Cronbach's alpha	**Internal Consistency**
$\alpha \geq 0.9$	Excellent
$0.9 > \alpha \geq 0.8$	Good
$0.8 > \alpha \geq 0.7$	Acceptable
$0.7 > \alpha \geq 0.6$	Questionable
$0.6 > \alpha \geq 0.5$	Poor
$0.5 > \alpha$	Unacceptable

The second instrument was the software evaluation instrument (see Table 4 for the 5-point Likert Scale for the evaluation of results), which was administered to expert evaluators and guided by ISO/IEC 25010 standards. This instrument assessed the AI-ACT system in terms of functional completeness, functional correctness, and functional appropriateness.

Table 4 5-Point Likert Scale for Software Requirement

Scale	**Range**			**Descriptive Equivalents**
5	4.21– 5.00	Highly Functional	Highly Accurate	Highly Appropriate
4	3.41 – 4.20	Moderately Functional	Moderately Accurate	Moderately Appropriate
3	2.61 – 3.40	Functional	Accurate	Appropriate
2	1.81 – 2.60	Least Functional	Least Accurate	Least Appropriate
1	1.00 – 1.80	Not Functional	Not Accurate	Not Appropriate

The third instrument was the user acceptability survey (see Table 5 for the 5-point Likert Scale for the evaluation of results), which was administered to student respondents after interacting with the AI-ACT system and was also guided by ISO/IEC 25010 standards. This instrument evaluated the system based on multiple software quality characteristics, including functional suitability, performance efficiency, compatibility, interaction capability, reliability, security, maintainability, and safety.

Table 5 5-Point Likert Scale for User Acceptability

		Functionality	**Efficiency**	**Compatibility**
Scale	**Range**			**Descriptive Equivalent**
5	4.21– 5.00	Highly Functional	Highly Efficient	Highly Compatible
4	3.41 – 4.20	Moderately Functional	Moderately Efficient	Moderately Compatible
3	2.61 – 3.40	Functional	Efficient	Compatible
2	1.81 – 2.60	Least Functional	Least Efficient	Least Compatible
1	1.00 – 1.80	Not Functional	Not Efficient	Not Compatible

		Capability	Reliability	Security
Scale	**Range**			**Descriptive Equivalent**
5	4.21– 5.00	Highly Capable	Highly Reliable	Highly Secured
4	3.41 – 4.20	Moderately Capable	Moderately Reliable	Moderately Secured
3	2.61 – 3.40	Capable	Reliable	Secured
2	1.81 – 2.60	Least Capable	Least Reliable	Least Secured
1	1.00 – 1.80	Not Capable	Not Reliable	Not Secured

		Maintainability	Safety
Scale	**Range**	**Descriptive Equivalent**	
5	4.21– 5.00	Highly Maintainable	Highly Safe
4	3.41 – 4.20	Moderately Maintainable	Moderately Safe
3	2.61 – 3.40	Maintainable	Safe
2	1.81 – 2.60	Least Maintainable	Least Safe
1	1.00 – 1.80	Not Maintainable	Not Safe

The researchers designed a survey with closed-ended questions using a Likert scale to gather feedback from participants after they interacted with the software system. The questions were developed based on research in aviation communication training and technology integration and were reviewed by professionals to ensure clarity and relevance. The researchers examined the quantitative data using appropriate statistical tools to evaluate the effectiveness of the AI-ACT system in enhancing aviation radio communication skills. Attention was given to assessing the system's functionality, usability, and overall performance in supporting learning and user interaction. The results of the analysis helped determine whether the system achieved its intended purpose as a training tool for aviation students and professionals. In addition, the findings provided insights into user experiences and perceived learning outcomes, which were used to further assess the system's effectiveness.

Results

This chapter presented the results of the study together with the corresponding analysis and interpretation of the data gathered. The findings were based on the responses obtained from the needs analysis assessment, software evaluation, and user acceptability survey administered to student respondents and expert evaluators. The collected data were organized, tabulated, and analyzed using appropriate statistical tools. The results were then discussed in relation to the objectives of the study to determine the effectiveness, performance, and acceptability of the AI-ACT system as an aviation communication training tool.

This section presented the results of the needs analysis conducted among student respondents to determine the current state of aviation communication training. The data gathered were analyzed to assess the effectiveness of existing instructional methods, particularly lecture-based approaches, and to identify the challenges faced by students in applying standard aviation phraseology in practical situations. The results provided a clearer understanding of the gaps in current training practices, including limitations in hands-on experience, communication confidence, and role-based interaction. These findings served as a foundation for the development of the AI-ACT system, which aimed to address the identified needs and improve overall learning experience in aviation communication training.

The data in Table 6 reveal a strong consensus among respondents regarding the inadequacy of existing training methods in developing effective aviation communication skills. The overall average weighted mean of 4.63, interpreted as Strongly Agree, indicates that learners consistently experience gaps in opportunities for practical application, real-time interaction, and skill reinforcement. This suggests a pressing need to enhance current instructional strategies through more advanced and responsive training systems.

Table 6 Actual Needs and Challenges as to AI-Driven Aviation Communication Trainer

No.	Indicators	MEAN	DE
1	Classroom lecture alone is not sufficient for me to practice aviation radio communication effectively.	4.44	Strongly Agree
2	Without an actual simulation or demonstration, it is difficult for me to apply proper aviation phraseology.	4.53	Strongly Agree
3	Theoretical discussion alone does not give me enough opportunity to practice real-time communication exchanges.	4.67	Strongly Agree
4	Classroom discussion does not fully prepare me for the pressure of real aviation communication scenarios	4.49	Strongly Agree
5	I find it hard to develop correct radio communication habits through lecture-based instruction alone.	4.65	Strongly Agree
6	I learn communication protocols more effectively when I can repeatedly practice them in interactive scenarios.	4.78	Strongly Agree
7	I understand aviation phraseology better when I am allowed to practice it in a simulated environment.	4.62	Strongly Agree
8	A simulation-based trainer would help me gain confidence in communicating as a pilot , air traffic controller, or maintenance personnel.	4.58	Strongly Agree
9	Current training methods do not adequately address the communication needs of maintenance personnel.	4.67	Strongly Agree
10	I need more training opportunities that cover communication across all roles, including pilot, ATC, and maintenance.	4.69	Strongly Agree
11	I would benefit from receiving immediate and specific feedback on my use of aviation phraseology during practice.	4.71	Strongly Agree
12	A system that provides real-time corrections during communication practice would improve the quality of my training.	4.62	Strongly Agree
13	A training system that uses artificial intelligence would help bridge the gap between classroom learning and actual aviation communication.	4.67	Strongly Agree
AVERAGE WEIGHTED MEAN		**4.63**	**STRONGLY AGREE**

The initial view presented to the user upon launching the AI-ACT software was the Registration and Login UI, designated as Figure 1. This interface functioned as the primary access point where students entered their unique nicknames and passwords to begin a training session.

Figure 1 Log in/ Register page

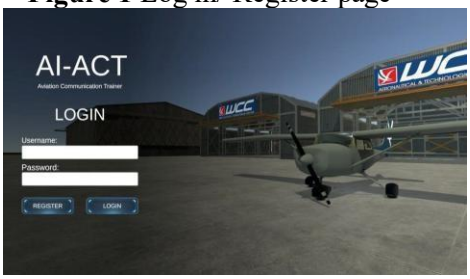

The Main Menu UI, presented as Figure 2, appeared immediately after the student successfully authenticated their credentials. This interface maintained the consistent visual theme of the airfield environment while it provided the primary navigation options for the application. The menu was structured as a vertical list of four main options: START SIMULATION, PROFILE, SETTINGS, and LOGOUT.

Figure 2 AI-ACT Menu Page

The Role Selection UI, shown in Figure 3, illustrated the critical stage where the user picked the specific training role they wished to utilize. The screen prominently displayed the prompt "SELECT YOUR ROLE" at the top, along with instructions to hover the mouse for further details.

Figure 3 Role Selection

Figure 4 showed the user management section, which was accessible only to the super admin. The next figure displayed all the accounts and what the super admin could do.

Figure 4 Super Admin Selection (User Management)

DATA FLOW DIAGRAM

The AI-ACT system showed in Figure 5, shows how data moved between the user, system processes, and databases. It explained the step-by-step flow of information from user login to the final performance result.

Figure 5 Data Flow diagram of AI-ACT

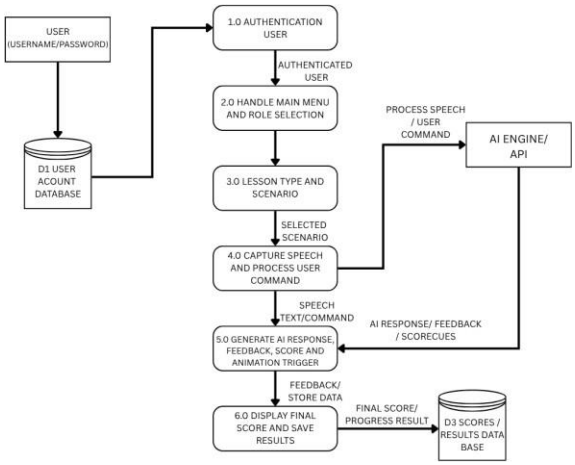

USER CASE DIAGRAM

Figure 6 visualized the functional interactions and data flow within the AI ACT system; an integrated training platform focused on aircraft communication proficiency. This closed loop process comprising user selection, AI driven detection, and multimedia feedback was designed to bridge the gap between theoretical knowledge and practical communication proficiency in high pressure aviation environments.

Figure 6 Use Case Diagram Visualization

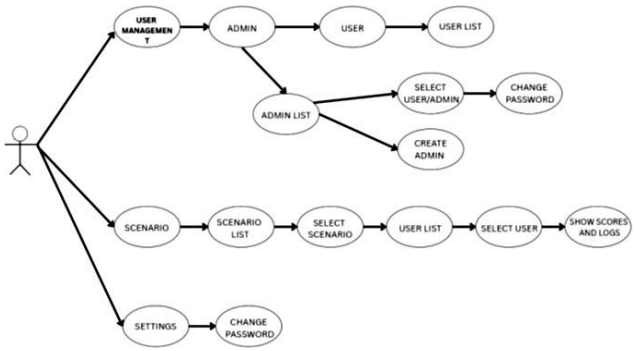

FINAL OUTPUT PERSPECTIVE

After conducting a series of tests and system demonstrations, the researchers observed that the AI-ACT system experienced minor delays in performance, particularly during real-time communication processing and simulation rendering. Verification, validation, and testing were carried out to ensure that the AI-ACT system performed correctly and produced reliable results. The researchers made sure that the system followed the specified requirements and functioned according to its intended design.

Based on Table 7, the development of the AI-ACT for WCC ATC Binalonan cost a total of ₱150,000. The main expenses included hiring experts for coding, building the AI system, and designing the visuals. These costs covered everything needed to make the software work correctly for student training.

Table 7 Project Cost

Item	Estimated Cost (in Peso)	Details
Software Development and Licenses	PHP 35,000	Licenses for AI tools include all features enhance realism.
Miscellaneous Expenses	PHP 25,000	Materials for testing, printing, project presentations, and other unforeseen costs.
Programmer assistance fee	PHP 90,000	Software development
TOTAL	**PHP 150,000**	

The team calculated a ₱60,000 markup based on a 40% profit margin applied to the documented ₱150,000 total development cost. This produces a final recommended selling price of ₱210,000. The valuation reflects the AI-ACT's transformation from research prototype to institutional-ready aviation communication trainer for WCC ATC Binalonan.

SURVEY RESULTS AND DISCUSSIONS

This section discusses the results of the testing and evaluation of the AI-ACT System based on the ISO/IEC 25010 as assessed by experts as to various aspects such as functional completeness, functional correctness, and functional appropriateness.

The table 8 reading for Functional Completeness shows an overall average weighted mean of 4.60, which the manuscript classifies as “Highly Functional”, while Functional Appropriateness shows an overall average weighted mean of 4.66, classified as “Highly Appropriate.”

Table 8 Experts’ Evaluation as to Functional Completeness and Functional Correctness

INDICATOR	MEAN	DESCRIPTIVE EQUIVALENT
FUNTIONAL COMPLETENESS	4.60	Highly Functional
FUNTIONAL CORRECTNESS	4.60	Highly Appropriate

LEVEL OF ACCEPTABILITY

This section contains the level of acceptability of an AI Integrated Aviation Communication Trainer as evaluated based on the International Organization for Standardization (ISO) 25010: 2023 for software quality models. Table 9 presents the level of acceptability of our developed AI-ACT in terms of functional suitability. The researchers recorded an overall average weighted mean of 4.81, which carries a descriptive equivalent of highly functional.

Table 9 Functional Suitability

INDICATOR	WEIGHTED MEAN	DESCRIPTIVE EQUIVALENT
FUNCTIONAL COMPLETENESS	4.91	Highly Functional
FUNCTIONAL CORRECTIONS	4.84	Highly Functional
FUNCTIONAL APPROPRIATENESS	4.67	Highly Functional
AVERAGE WEIGHTED	**4.81**	**Highly Functional**

Based on table 10 the researchers found that the AI-ACT system performed exceptionally well across all tested parameters, establishing it as a robust and well-integrated solution. Every category evaluated, from performance efficiency to safety, consistently earned a "Highly" positive rating, with average weighted means ranging from 4.56 to 4.64. The system proved that it could simultaneously uphold stringent security and maintainability standards while remaining highly efficient and user-friendly. Specifically, these results confirmed that the AI-ACT system successfully achieved its design goals, proving itself to be a stable, secure, and reliable tool ready for practical application.

Table 10 Overall Results from the Survey

Indicator	Average Weighted Mean	Descriptive Equivalent
Compatibility	4.60	Highly Compatible
Interaction Capability	4.63	Highly Capable
Reliability	4.59	Highly Reliable
Security	4.64	Highly Secured
Maintainability	4.64	Highly Maintainable
Safety	4.60	Highly Safe
Performance Efficiency	4.56	Highly Efficient

DISCUSSION

The researchers successfully fulfilled all project objectives by developing the AI-ACT system, a software simulator that utilized Unity 3D and the OpenAI API to facilitate dynamic, unscripted aviation communication training. The system demonstrated exceptional functional suitability, achieving an overall average weighted mean of 4.81 and a robust Cronbach’s Alpha value of 0.897, which confirmed its reliability in measuring student proficiency across all flight stages. Furthermore, expert evaluations validated the platform's core dimensions, awarding high ratings of

4.60 for functional completeness, 4.54 for functional correctness, and 4.66 for functional appropriateness, with both the AI core logic and the administrative dashboard securing impressive individual ratings of 4.86.

Student feedback reinforced these findings, as participants consistently rated the system as "Highly" effective across all tested ISO/IEC 25010 quality characteristics, with the highest mark reaching 4.91 for functional completeness. By providing precise, real-time feedback on standard aviation phraseology, the AI-ACT system effectively bridged the gap between theoretical classroom instruction and practical radio operation. These results confirmed that the platform successfully addressed the students identified need for interactive, repetitive practice, ultimately proving itself to be a stable and reliable training solution that prepared users for the high-pressure demands of professional aviation operations.

Conclusion

The study successfully developed and validated the AI-ACT system as a highly effective aviation communication training tool, consistently achieving an overall weighted mean of 4.81 for functional suitability and a high Cronbach's Alpha value of 0.897. By implementing role-based interactions for pilots, air traffic controllers, and maintenance personnel, the system directly addressed critical training gaps identified during the initial needs analysis. Furthermore, the AI-driven real-time feedback mechanism proved highly reliable, earning a 4.86 accuracy rating for its core logic, which significantly bolstered student proficiency by providing immediate, corrective guidance on standard aviation phraseology.

The researchers fulfilled all primary project objectives, successfully transitioning from the initial problem evaluation to the delivery of a sophisticated simulation platform that operationalized the Intelligent Agent Model. By bridging the divide between theoretical classroom instruction and the high-pressure demands of professional aviation operations, the AI-ACT system demonstrated both significant theoretical and practical contributions. Ultimately, these results confirmed that the platform provided a stable, accessible, and intelligent training solution that effectively prepared students for the complexities of real-world aviation communication.

Acknowledgements (if any)

The researchers wish to acknowledge and express their sincere gratitude to the following people and institutions, who were essential in completing this research project:

To God Almighty, who provided constant guidance, wisdom, and patience for the team.

Dr. Joey Aldrich T. Almanza, the Dean of the College of Avionics Technology, generously gave his expertise and technical skills to the research.

The members of the Panel of Examiners, Dr. Roger A. Martinez Jr., Dr. Rosalie Sheryll T. Rosales, Ms. Cathleen Faith D. Martinez, and Dr. Diosdado Caronongan, whose thoughtful feedback and excellent suggestions improved the quality of the study.

The dedicated instructors and students of the Avionics Technology Department shared their ideas and knowledge, which helped in the project's development.

References

Bautista, J. E. S. (2025). A human factors analysis and classification system of unsafe acts in Philippine general aviation accidents. Iconic Research and Engineering Journals, 9(6), 1072–1078.

Carpio, J. K. N., De Vera, R. J. K. G., Macabontoc, L. A., Racelis, G. Z. A., Santua,

J. & Valente, C. D. D. (2022). Control tower and pilot communication simulation system (CTAPSS) for air traffic control in the avionics department (Unpublished undergraduate thesis). WCC Aeronautical and Technological College.

Hayes, J. (2020). Teamwork and communication in high-risk industries

International Civil Aviation Authority (2024). The Impact of Artificial Intelligence On The Aviation Sector. Assembly - 42nd Session.

Russell, S. J., & Norvig, P. (2021). Artificial intelligence: A modern approach (4th ed.). Pearson.